

WATER SOLUBLE, LOW MIGRATION AND VISIBLE LIGHT PHOTOINITIATORS  
FOR GREENER PHOTOPOLYMERIZATION

by

Tuğçe Nur Eren Mert

B.S., Chemistry, Boğaziçi University, 2013

M.S., Chemistry, Boğaziçi University, 2015

Submitted to the Institute for Graduate Studies in  
Science and Engineering in partial fulfillment of  
the requirements for the degree of  
Doctor of Philosophy

Graduate Program in Chemistry

Boğaziçi University

2021

*Dedicated to my family...*

## ACKNOWLEDGEMENTS

I would wish to express my gratitude and warmest thanks to my supervisor Prof. Duygu Avcı Semiz for her valuable guidance, advice, suggestions, attention and encouragement throughout this study. It was a great pleasure to do research under her guidance.

I would like to express my appreciation to Prof. Jacques Lalevée for welcoming me in the Institut of Materials Science of Mulhouse – National Center for Scientific Research (IS2M - CNRS) for the collaboration within the scope of TUBITAK France PIA (Programme of Integrated Actions) Bosphorous project. I benefited greatly from his guidance and advice. I also want to thank his group members for their help and friendship.

I want to express my thanks to my committee members Prof. Nilhan Kayaman Apohan, Prof. Funda Yağcı Acar, Ersin Acar and Fırat İlker for politely sparing their valuable time for reviewing the final manuscript and for their constructive interpretations and recommendations.

I wish to extend my thanks to my current and former labmates Türkan, Seçkin, Melek, Betül, Sesil, Fulya and Belgin for their valuable friendship, support and giving me such an enjoyable working environment. Furthermore, I would like to thank all members of Chemistry Department for their help.

I would also like to thank Dr. Ayla Türkecul Bıyık for structural characterization of my samples through NMR; Prof. Dr. A. Neren Ökte, Duygu Tuncel for their help in UV-vis absorption analyses; Prof. Dr. Funda Yağcı Acar and Gözde Demirci for their contribution in cytotoxicity studies.

I want to express my gratitude to my family for their endless love, support and encouragement through my entire life.

I would also like to give my special thanks to my husband for his love, support and understanding. I am very grateful that he always wants the best for me whatever it takes; also for his faith in me to do the best in every step of my life.

Finally, I would like to acknowledge The Scientific and Technological Research Council of Turkey (TÜBİTAK) [117Z622] and Bogazici University Research Fund (20B05D1/16741) for their financial support for my research.

## ABSTRACT

### WATER SOLUBLE, LOW MIGRATION AND VISIBLE LIGHT PHOTOINITIATORS FOR GREENER PHOTOPOLYMERIZATION

In this work, novel monomeric, polymeric and mesomeric (high enough molecular weight to provide lower migration but not high enough to be called a macromolecule) photoinitiators (PIs) were synthesized with the aim of achieving the “green” properties of migration stability, water solubility, biocompatibility and visible light absorption. Their properties and performances were examined in terms of photophysical and photochemical aspects. In the third chapter, the first cyclopolymerizable monomeric PI in the literature (TXdMA) was produced by introducing both TX chromophore and hydrogen donating tertiary amine functionality on its structure. The fourth chapter reports two water soluble mesomolecule photoinitiators (TXBP and BPBP), synthesized by the substitution of biocompatible bisphosphonic acid functional groups into TX and benzophenone (BP); the first such PIs in the literature. In the fifth chapter, a water soluble mesomolecule photoinitiator (TXBP2) was fabricated through bisphosphonate functionalization of TX. The sixth chapter reports synthesis of a TX-based water soluble polymeric photoinitiator (PAA-TX) from the aza-Michael reaction of a poly(amido amine) to 9-oxo-9H-thioxanthen-2-yl acrylate. The last chapter describes the syntheses of two novel water soluble multifunctional polymeric photoinitiators (PEI-I2959-Ts and PEI-I2959) through incorporation of I2959 into branched poly(ethyleneimine) ( $M_w = 1800$  g/mol).

## ÖZET

### DAHA YEŞİL FOTOPOLİMERİZASYON İÇİN SUDA ÇÖZÜNÜR, SIZMASI DÜŞÜK VE GÖRÜNÜR IŞIK KULLANAN FOTOBASLATICILAR

Bu çalışmada, yeni monomerik, polimerik ve mezomerik (molekül ağırlığı düşük sızma sağlamak için yeterince yüksek olan, ancak makromolekül olarak adlandırılmasına yetecek kadar yüksek olmayan) fotobaşlatıcılar, migrasyon kararlılığı, suda çözünürlük, biyoyumluluk ve görünür ışık absorpsiyonu gibi yeşil özellikler elde edilmesi amacı ile sentezlendi. Özellikleri ve performansları fotofiziksel ve fotokimyasal açılarından incelendi. Üçüncü bölümde, literatürdeki ilk siklopolimerleşebilen fotobaşlatıcı (TXdMA), yapısına hem TX kromoforu hem de hidrojen verici tersiyer aminin katılması ile üretildi. Dördüncü bölüm, biyoyumlu bisfosfonik asit fonksiyonel gruplarının, TX ve benzofenon'a (BP) ikame edilmesi ile sentezlenen iki suda çözünür mezomolekül fotobaşlatıcıyı (TXBP ve BPBP) rapor eder; bunlar literatürde bu türdeki ilk PI'lardır. Beşinci bölümde, suda çözünür bir mezomolekül fotobaşlatıcı (TXBP2), TX'in bisfosfonat ile fonksiyonlandırılması ile üretildi. Altıncı bölüm, poli(amido amin)'in 9-okso-9H-tiyokzanten-2-il akrilat'a aza-Michael reaksiyonundan, TX-bazlı suda çözünür polimerik fotobaşlatıcı (PAATX)'in sentezini rapor eder. Son bölüm, I2959'un dallanmış poli(etilenimin)'e ( $M_w = 1800$  g/mol) dahil edilmesiyle, iki yeni suda çözünür multifonksiyonel polimerik fotobaşlatıcının (PEI-I2959-Ts and PEI-I2959) sentezini betimler.

**TABLE OF CONTENTS**

ACKNOWLEDGEMENTS .....	iv
ABSTRACT .....	vi
ÖZET .....	vii
TABLE OF CONTENTS .....	viii
LIST OF FIGURES.....	xiv
LIST OF TABLES.....	xxiii
LIST OF SYMBOLS.....	xxv
LIST OF ACRONYMS/ ABBREVIATIONS .....	xxvii
1. INTRODUCTION: PHOTOPOLYMERIZATION .....	1
1.1. Photoinduced Free Radical Polymerization.....	1
1.2. Free Radical Photoinitiators.....	3
1.2.1. Type I Photoinitiators .....	5
1.2.2. Type II Photoinitiators .....	6
1.3. Desiderata for Greener Photoinitiators .....	7
1.4. Low Migration Photoinitiators.....	9
1.4.1. Monomeric Photoinitiators.....	9
1.4.2. Polymeric Photoinitiators.....	11
1.4.3. Hyperbranched/Dendrimeric Photoinitiators .....	14
1.4.4. Dual-curable Photoinitiators.....	17
1.5. Water Soluble Photoinitiators .....	19
1.6. Visible Light Photoinitiators .....	21
1.7. Monomers .....	24
1.8. Light Sources .....	26

2. OBJECTIVES AND SCOPE .....	29
3. THIOXANTHONE BASED MONOMERIC PHOTOINITIATOR WITH 1,6-HEPTADIENE STRUCTURE .....	31
3.1. Introduction .....	31
3.2. Experimental .....	32
3.2.1. Materials and Methods.....	32
3.2.2. Synthesis of 2,2'-(((9-oxo-9H-thioxanthen-2-yl)azanediyl)bis(methylene)) diacrylic acid (TXdMA) .....	32
3.2.3. Computational Procedure.....	33
3.2.4. Photochemical Analyses .....	33
3.2.4.1. Steady State Photolysis Experiments.....	33
3.2.4.2. Fluorescence Experiments. ....	33
3.2.4.3. Laser Flash Photolysis.....	34
3.2.4.4. Cyclic Voltammetry.....	34
3.2.5. Photopolymerization Experiments.....	34
3.2.6. Migration Study .....	35
3.3. Results and Discussion .....	35
3.3.1. Synthesis and Characterization of TXdMA .....	35
3.3.2. Light Absorption.....	37
3.3.3. Photochemical Mechanisms.....	40
3.3.3.1. Steady State Photolysis. ....	40
3.3.3.2. Fluorescence Quenching, Laser Flash Photolysis (LFP), Cyclic Voltammetry Experiments.....	42
3.3.4. Photopolymerization.....	46
3.3.5. Migration Stability.....	49
3.4. Conclusions .....	50

4. WATER-SOLUBLE BISPHOSPHONIC ACID-FUNCTIONALIZED TYPE-II PHOTOINITIATORS.....	51
4.1. Introduction .....	51
4.2. Experimental .....	51
4.2.1. Materials and Methods.....	51
4.2.2. Syntheses of PIs: General Procedure for the Synthesis of BPBP and TXBP.....	52
4.2.3. Photochemical Analyses .....	53
4.2.3.1. UV-vis Spectroscopy Experiments.....	53
4.2.3.2. Fluorescence Experiments.....	53
4.2.3.3. Laser Flash Photolysis.....	53
4.2.3.4. ESR Spin Trapping (ESR-ST) Experiments. ....	53
4.2.4. Photoinitiating Activity Measurements .....	54
4.3. Results and Discussion .....	54
4.3.1. Syntheses of BPBP and TXBP .....	54
4.3.2. Light Absorption Properties .....	57
4.3.3. Photochemical Mechanisms.....	59
4.3.3.1. Steady-state Photolysis.....	59
4.3.3.2. Fluorescence Quenching, Laser Flash Photolysis (LFP), Electron Spin Resonance (ESR).....	61
4.3.4. Photopolymerization.....	65
4.4. Conclusions .....	68
5. A WATERBORNE BISPHOSPHONATE FUNCTIONALIZED THIOXANTHONE-BASED PHOTOINITIATOR.....	69
5.1. Introduction .....	69
5.2. Experimental .....	70
5.2.1. Materials and Methods.....	70
5.2.2. Synthesis of TXBP2.....	70

5.2.3. Photochemical Analyses .....	71
5.2.3.1. UV-vis Spectroscopy Experiments.....	71
5.2.3.2. Fluorescence Experiments.....	71
5.2.3.3. Laser Flash Photolysis Experiments.....	71
5.2.4. Photoinitiating Activity Measurements .....	71
5.2.4.1. Photo-DSC.....	71
5.2.4.2. Photoreactor.....	72
5.2.5. 3D Printing Experiments.....	72
5.3. Results and Discussion .....	72
5.3.1. Synthesis of TXBP2.....	72
5.3.2. Light Absorption Properties .....	74
5.3.3. Photochemical Mechanisms.....	75
5.3.3.1. Steady-State Photolysis.....	75
5.3.4. Photopolymerization.....	82
5.3.5. Laser Write Experiments using TXBP2/Iod .....	85
5.4. Conclusions.....	86
6. A WATER SOLUBLE THIOXANTHONE FUNCTIONALIZED POLYMERIC PHOTOINITIATOR WITH A DUAL CURING ABILITY.....	87
6.1. Introduction .....	87
6.2. Experimental .....	88
6.2.1. Materials and Methods.....	88
6.2.2. Synthesis of PAATX.....	89
6.2.3. Photochemical Analyses .....	89
6.2.3.1. UV-vis Spectroscopy Experiments.....	89
6.2.3.2. Fluorescence Experiments.....	89
6.2.3.3. Laser Flash Photolysis.....	90

6.2.4. Photopolymerization Experiments.....	90
6.2.4.1. FTIR.....	90
6.2.4.2. Photo-DSC.....	91
6.2.4.3. Photoreactor.....	91
6.2.5. Migration Study.....	92
6.3. Results and Discussion .....	92
6.3.1. Synthesis of PAATX.....	92
6.3.2. Light Absorption Properties.....	95
6.3.3. Photochemical Mechanisms.....	96
6.3.3.1. Steady-State Photolysis.....	96
6.3.3.2. Fluorescence Quenching, Laser Flash Photolysis (LFP).....	97
6.3.4. Photopolymerization.....	100
6.3.5. Migration Stability.....	102
6.4. Conclusions .....	104
<b>7. BRANCHED POLY(ETHYLENEIMINE) AND I2959 BASED WATER SOLUBLE POLYMERIC PHOTOINITIATORS.....</b>	<b>106</b>
7.1. Introduction.....	106
7.2. Experimental .....	108
7.2.1. Materials and Methods.....	108
7.2.2. Characterization and Methods.....	108
7.2.3. Syntheses of Photoinitiators .....	109
7.2.3.1. PEI-I2959.....	109
7.2.3.2. PEI-I2959-Ts.....	109
7.2.4. RT-FTIR Measurements .....	109
7.2.4.1. Michael Addition/Photo Studies.....	109
7.2.4.2. Aqueous Photopolymerization.....	110

7.2.5. Photo-DSC Measurements .....	110
7.2.6. Migration Study .....	111
7.2.7. Cytotoxicity Studies.....	111
7.2.8. Statistical Analysis.....	112
7.3. Results and Discussion .....	112
7.3.1. Synthesis and Characterization of PEI-I2959 & PEI-I2959-Ts .....	112
7.3.2. Light Absorption Properties .....	118
7.3.3. Michael Addition and Photopolymerization .....	119
7.3.4. Migration Stability.....	128
7.3.5. Cell Viability .....	129
7.4. Conclusion.....	130
8. CONCLUDING REMARKS.....	132
REFERENCES .....	134
APPENDIX A: COPY RIGHT LICENCES.....	172

## LIST OF FIGURES

Figure 1.1.	General representation of a photoinduced polymerization. Reproduced with permission from [3] American Chemical Society, Copyright (2010), (Figure A.1). .....	2
Figure 1.2.	Stages of a photoinduced free radical polymerization. Reproduced with permission from [7] John Wiley and Sons, Copyright (2019), (Figure A.2). .....	2
Figure 1.3.	Photophysical processes involved in the excited state of a photoinitiator. Reproduced with permission from [5] Elsevier, Copyright (2001), (Figure A.3). .....	4
Figure 1.4.	Different distributions of the electrons (configurations) in the three available MOs. Reproduced with permission from [1] John Wiley and Sons, Copyright (2012), (Figure A.4). .....	5
Figure 1.5.	General Type I photoinitiation mechanism [9]. .....	5
Figure 1.6.	Some examples of Type I photoinitiators. Reproduced with permission from [10] John Wiley and Sons, Copyright (2012), (Figure A.5). .....	6
Figure 1.7.	General Type II photoinitiation mechanism of benzophenone [9]. .....	7
Figure 1.8.	Some examples of Type II photoinitiators. Reproduced with permission from [1] John Wiley and Sons, Copyright (2012), (Figure A.4). .....	7
Figure 1.9.	Novel polymerizable thioxanthone photoinitiators. Reproduced with permission from [34] John Wiley and Sons, Copyright (2017), (Figure A.6). .....	10

Figure 1.10.	Alkyne functional hydroxy alkyl phenone (PI-4) and monoacyl phosphine oxide (PI-9) based low migration photoinitiators. Reproduced with permission from [22], Elsevier, Copyright (2016), (Figure A.7). ....	11
Figure 1.11.	Structural characteristics of different types of polymeric photoinitiators; In-chain linear polymeric PPIs (LPPIs) or side-chain LPPIs. Reproduced with permission from [102] Elsevier, Copyright (2019), (Figure A.8). ....	12
Figure 1.12.	PU-Type one component polymeric photoinitiators containing side chain benzophenone and coinitiator amine. Reproduced with permission from [89] John Wiley and Sons, Copyright (2007), (Figure A.9). ....	13
Figure 1.13.	One component TX or BP functionalized polymeric photoinitiators [18, 68]. ....	14
Figure 1.14.	Structural sketch of hyperbranched photoinitiators. Reproduced with permission from [102] Elsevier, Copyright (2019), (Figure A.8). ....	15
Figure 1.15.	Illustrative representation for supramolecular polymeric photoinitiators. Reproduced with permission from [114] Royal Society of Chemistry, Copyright (2020), (Figure A.10). ....	15
Figure 1.16.	Structure of hyperbranched PPI containing TX and PEO chain. Reproduced with permission from [116] Elsevier, Copyright (2009), (Figure A.11). ....	16
Figure 1.17.	Schematic representation of a dual-curing process [131]. ....	17
Figure 1.18.	Structure of piperazine functionalized benzophenone [129]. ....	18
Figure 1.19.	Properties of bifunctional hydroxyketone based photoinitiator compared with I2959. Reproduced with permission from [148] John Wiley and Sons, Copyright (2017), (Figure A.12). ....	20
Figure 1.20.	Structures of MAPO and BAPO salts. Reproduced with permission from [149] John Wiley and Sons, Copyright (2015), (Figure A.13). ....	21

Figure 1.21.	Scheme for the synthesis of charge transfer complex of a sulfonium salt as visible light PI. Reproduced with permission from [211] John Wiley and Sons, Copyright (2019), (Appendix A14).....	23
Figure 1.22.	Structure of different tetraacylgermanes and their photoinitiation mechanism. Reproduced with permission from [220] John Wiley and Sons, Copyright (2017), (Figure A.15).....	24
Figure 1.23.	Examples of basic acrylate monomers [4]. .....	25
Figure 1.24.	Emission spectra of mercury arc lamp and UV LEDs [239].....	27
Figure 3.1.	Synthesis route for the novel photoinitiator TXdMA.....	36
Figure 3.2.	<sup>1</sup> H and <sup>13</sup> C NMR spectra of TXdMA.....	37
Figure 3.3.	(A) UV-visible absorption spectra of TXdMA in different solvents (1.3x10 <sup>-4</sup> M); (B) Frontier orbitals (HOMO-LUMO) calculated on the B <sub>3</sub> LYP/6-31 G* level for TXdMA.....	39
Figure 3.4.	(A) Fluorescence spectra of TXdMA in different solvents (1.3x10 <sup>-4</sup> M) λ <sub>exc</sub> = 355 nm; (B) Absorption (solid lines) and corrected emission (dashed lines) spectra of TXdMA dissolved in acetonitrile. Solutions were excited at λ <sub>exc</sub> = 355 nm. Absorption spectrum was multiplied by the indicated factor. The concentration of TXdMA is 1.3 × 10 <sup>-4</sup> M.....	40
Figure 3.5.	Photolysis of TXdMA (2.78 x 10 <sup>-4</sup> M) in acetonitrile in the presence (A) and absence (B) of EDB (1.38 x 10 <sup>-3</sup> M). .....	42
Figure 3.6.	(A) The fluorescence quenching of TXdMA in acetonitrile solution (1.32 x 10 <sup>-4</sup> M) with different concentration of Iod; (B) Stern-Volmer plot; (C) The fluorescence quenching of TXdMA in acetonitrile solution (1.32 x 10 <sup>-4</sup> M) with different concentration of EDB; (D) kinetic for TXdMA in LFP experiments (laser excitation for t = 5μs); (E) Oxidation potential determination of TXdMA in acetonitrile. ....	45

Figure 3.7.	(A) Rate-time and conversion-time plots for the photopolymerization of TMPTA under nitrogen at 30 °C, $\lambda = 320\text{-}500$ nm in the presence of TXdMA, TXdMA/EDB, TXdMA/Iod, TX, TX/EDB and TX/Iod and (B) laser write experiments using a laser diode @405 nm.....	48
Figure 3.8.	Rate-time and conversion-time plots for the photopolymerization of PEGDA under nitrogen at 30 °C, $\lambda = 320\text{-}500$ nm in the presence of TXdMA/EDB, TXdMA/Iod, TX/EDB and TX/Iod. ....	49
Figure 3.9.	UV-vis absorption spectra of TX and TXdMA extracted with MeOH from the PEGDA polymer samples.....	50
Figure 4.1.	Syntheses of BPBP and TXBP.....	55
Figure 4.2.	$^1\text{H}$ NMR spectra of BPBP and TXBP.....	57
Figure 4.3.	A) UV-Vis absorption spectra of BPBP ( $4 \times 10^{-5}$ M) (inset: $2 \times 10^{-3}$ M in methanol) and B) TXBP ( $2 \times 10^{-4}$ M) in different solvents. ....	58
Figure 4.4.	Corrected absorption (black line) and emission (dashed line) spectra of TXBP in methanol. The solution was excited at $\lambda_{\text{exc}} = 396$ nm. ....	60
Figure 4.5.	Photolysis of TXBP in methanol ( $2 \times 10^{-4}$ M) in the presence A) and absence B) of Iod ( $1 \times 10^{-3}$ M), and in the presence of EDB ( $1 \times 10^{-3}$ M) C) using a 385 nm LED. ....	61
Figure 4.6.	A) The fluorescence quenching of TXBP in methanol solution ( $4.5 \times 10^{-5}$ M) with different concentrations of Iod; B) The Stern-Volmer plot of A; C) The fluorescence quenching of TXBP in methanol solution ( $4.5 \times 10^{-5}$ M) with different concentrations of EDB; D) The Stern-Volmer plot of C; E) Fluorescence lifetime measurement of TXBP dissolved in methanol. .	62
Figure 4.7.	Parameters characterizing the reactivity of the PIs.....	63
Figure 4.8.	Triplet state decay traces observed after laser excitation of A) BPBP and B) TXBP at 355 nm. Laser excitation for $t = 20$ $\mu\text{s}$ .....	64

Figure 4.9.	ESR spectra of the radicals generated in BPBP irradiated by LED@365 nm exposure and trapped by PBN in tert -butylbenzene. PBN radical adducts obtained are: $a_N = 13.6$ G, $a_H = 1.9$ G; and $a_N = 14.0$ G, $a_H = 5.3$ G. ....	65
Figure 4.10.	Rate-time and conversion-time plots for the photopolymerization of PEGDA-Water (80:20 wt%) under nitrogen at 25 °C, $\lambda = 320$ -500 nm in the presence of BPBP, BPBP/EDB, BPBP/Iod. ....	67
Figure 4.11.	Rate-time and conversion-time plots for the photopolymerization of PEGDA-Water (80:20 wt%) under nitrogen at 25 °C, $\lambda = 320$ -500 nm in the presence of TXBP, TXBP/EDB, TXBP/Iod. ....	67
Figure 5.1.	Structure of the novel photoinitiator TXBP2. ....	69
Figure 5.2.	Synthesis scheme of TXBP2. ....	73
Figure 5.3.	$^1\text{H}$ NMR spectrum of TXBP2. ....	74
Figure 5.4.	(A) UV–Vis absorption spectra of TXBP2 ( $1.5 \times 10^{-4}$ M) in THF, MeOH, $\text{CHCl}_3$ and $\text{H}_2\text{O}$ . (B) Corrected absorption (black line) and emission (red line) spectra of TXBP2 in $\text{CHCl}_3$ . The solution was excited at $\lambda_{\text{exc}} = 396$ nm. ....	75
Figure 5.5.	Photolysis of TXBP2 in chloroform ( $2 \times 10^{-4}$ M) in the absence (A) and presence (B) of EDB ( $1 \times 10^{-3}$ M), and in the presence of Iod ( $1 \times 10^{-3}$ M) (C) using a 385 nm LED. ....	76
Figure 5.6.	The fluorescence quenching of TXBP2 in chloroform solution with different concentrations of Iod (A) and EDB (C). The Stern-Volmer plot of TXBP2/Iod (B) of TXBP2/EDB (D). Fluorescence life time measurement of TXBP2 in chloroform. ....	78
Figure 5.7.	Photooxidation mechanism of TXBP2 with Iod. ....	79
Figure 5.8.	Photoreduction mechanism of TXBP2 with EDB. ....	80

Figure 5.9.	Triplet state decay traces observed after laser excitation of TXBP2 in chloroform at 355 nm, kinetic traces recorded at 600 nm under N <sub>2</sub> : A) in different Iod concentrations; B) in different EDB concentrations, Stern–Volmer plot for quenching of <sup>3</sup> [TXBP2]* C) by Iod and D) by EDB. $\lambda_{exc} = 355$ nm. ....	81
Figure 5.10.	Rate-time and conversion-time plots for the photopolymerization of TMPTA under nitrogen at 25 °C, $\lambda = 320$ -500 nm in the presence of TX, TX/EDB, TX/Iod and TXBP2, TXBP2/EDB, TXBP2/Iod.....	84
Figure 5.11.	Rate-time and conversion-time plots for the photopolymerization of PEGDA under nitrogen at 25 °C, $\lambda = 320$ -500 nm in the presence of TXBP2, TXBP2/EDB, TXBP2/Iod. ....	84
Figure 5.12.	Free radical photopolymerization experiments for 3D printing upon laser diode irradiation @405 nm: characterization of the patterns by numerical optical microscopy; TXBP2/Iod (0.1/1 wt%) in PEGDA.....	86
Figure 6.1.	Dual curing of HEMA/PEGDA formulations using PAATX.....	88
Figure 6.2.	The synthesis of PAATX. ....	93
Figure 6.3.	<sup>1</sup> H NMR and FTIR spectrum of PAATX.....	94
Figure 6.4.	(A) UV–vis absorption spectrum of PAATX ( $9.4 \times 10^{-5}$ M) in MeOH. (B) Absorption (black line) and emission (red line) spectra of PAATX in methanol. The solution was excited at $\lambda_{exc} = 402$ nm.....	95
Figure 6.5.	Photolysis of PAATX in methanol ( $9.4 \times 10^{-5}$ M) in the presence (A) and absence (B) of EDB ( $1 \times 10^{-3}$ M), and in the presence of Iod ( $1 \times 10^{-3}$ M) (C) using a 385 nm LED. ....	96
Figure 6.6.	(A) The fluorescence quenching of PAATX in methanol solution with different concentrations of Iod; (B) The Stern-Volmer plot of A; (C) The fluorescence quenching of PAATX in methanol solution with different	

	concentrations of EDB; (D) The Stern-Volmer plot of C, (E) Fluorescence life-time measurement of PAATX dissolved in methanol.....	98
Figure 6.7.	Triplet state decay trace observed after laser excitation of PAATX. Laser excitation was for $t = 20 \mu\text{s}$ . .....	100
Figure 6.8.	A) FTIR spectra for formulation 1 and B) Conversion (%) for formulations 1 and 6 monitored during the aza-Michael (10 min) and photopolymerization (5 min) reactions. ....	103
Figure 6.9.	A) Rate-time and B) Conversion-time plots of formulations 1-6 in Photo-DSC.....	104
Figure 6.10.	UV-vis absorption spectra of PAATX and TX extracted with methanol from the HEMA/PEGDA (75/25 wt%) polymer samples.....	104
Figure 7.1.	Dual Curing of HEMA/PEGDA formulations using PEI-I2959.....	107
Figure 7.2.	Syntheses scheme of PEI-I2959-Ts and PEI-I2959.....	113
Figure 7.3.	$^1\text{H}$ -NMR spectra of PEI-I2959 and PEI-I2959-Ts.....	115
Figure 7.4.	$^{13}\text{C}$ -NMR spectrum of PEI-I2959-Ts.....	116
Figure 7.5.	FTIR spectra of PEI-I2959-Ts and PEI-I2959. ....	116
Figure 7.6.	A) $T_g$ and B) TGA spectra of PEI-I2959-Ts and PEI-I2959.....	117
Figure 7.7.	UV-vis absorption spectra of A) PEI-I2959 ( $2 \times 10^{-5}$ M) (inset: ( $1 \times 10^{-4}$ M)) and B) PEI-I2959-Ts ( $2 \times 10^{-5}$ M) (inset: ( $1 \times 10^{-4}$ M)) in different solvents. ....	119
Figure 7.8.	Conversion-time plots for HEMA:PEGDA (50:50 wt%) mixtures containing 0.3 wt% PEI-I2959-Ts or PEI-I2959 monitored during the aza-Michael (20 min) and photopolymerization (15 min) reactions.....	120

- Figure 7.9. A) Rate-time and B) Conversion-time plots for HEMA containing PEI-I2959-Ts (0.1 wt%) (1), PEI-I2959 (0.1 wt%) (2), I2959 (0.1 wt%) (3), PEI (0.3 wt%) (4), C) Rate-time and D) Conversion-time plots for HEMA containing PEI-I2959-Ts/Iod (0.1/1 wt%) (1'), PEI-I2959/Iod (0.1/1 wt%) (2'), I2959/Iod (0.1/1 wt%) (3'), PEI/Iod (0.3/1 wt%) (4'). All photopolymerizations under UV-vis light (320-500 nm) irradiation in photo-DSC.....122
- Figure 7.10.  $R_p$  vs time and Conversion (%) vs time plots of BAPO (0.1 wt%) and BAPO (0.5 wt%) under visible light irradiation, I184 (0.1 wt%) under UV light irradiation at 25 °C.....123
- Figure 7.11. A) Rate-time and B) Conversion-time plots for HEMA containing PEI-I2959-Ts (0.1 wt%) (1), PEI-I2959 (0.1 wt%) (2), PEI-I2959-Ts (0.5 wt%) (1a), PEI-I2959 (0.5 wt%) (2a), C) Rate-time and D) Conversion-time plots for HEMA containing PEI-I2959-Ts/Iod (0.1/1 wt%) (1'), PEI-I2959/Iod (0.1/1 wt%) (2'), PEI-I2959-Ts/Iod (0.5/1 wt%) (1a'), PEI-I2959/Iod (0.5/1 wt%) (2a'), PEI/Iod (0.3/1 wt%) (4'). All photopolymerizations under visible light irradiation in photo-DSC. ....125
- Figure 7.12. Absorption spectra of A) PEI-I2959-Ts/Iod (0.1/1 wt%), PEI-I2959-Ts (0.1 wt%) and Iod (1 wt%) and B) PEI-I2959/Iod (0.1/2 wt%), PEI-I2959/Iod (0.1/1 wt%), PEI-I2959 (0.1 wt%) and Iod (1 wt%) in HEMA. ....126
- Figure 7.13. Conversion-time plots for AAm:water (40:60 wt%) mixture containing PEI-I2959 (0.1 mol%), PEI-I2959-Ts (0.1 mol%), I2959 (0.3 mol%) or I2959 (0.1 mol%). All photopolymerizations under UV irradiation in air depleted atmosphere in RT-FTIR. ....127
- Figure 7.14. Proposed mechanism for the photoinitiation with the PPIs ( $Ar_2I^+$  denotes the iodonium salt). ....128
- Figure 7.15. UV-vis absorption spectra of PEI-I2959-Ts and I2959 extracted with methanol from the HEMA/PEGDA (50/50 wt%) polymer samples. ....129

Figure 7.16.	Cytotoxicity assay with I2959, PEI-I2959-Ts and PEI-I2959 for 24 hours on NIH/3T3 and L929 cells. Statistical significance: $p < 0.0332$ (*), $p < 0.0021$ (**), $p < 0.0002$ (***), and $p < 0.0001$ (****).0.0001(****). Dashed lines show the 80% and 50% viabilities. ....	130
Figure A.1.	Permission from [3] American Chemical Society, Copyright (2010). ....	172
Figure A.2.	Permission from [7] John Wiley and Sons, Copyright (2019).....	173
Figure A.3.	Permission from [5] Elsevier, Copyright (2001).....	174
Figure A.4.	Permission from [1] John Wiley and Sons, Copyright (2012).....	175
Figure A.5.	Permission from [10] John Wiley and Sons, Copyright (2012).....	176
Figure A.6.	Permission from [34] John Wiley and Sons, Copyright (2017).....	177
Figure A.7.	Permission from [22], Elsevier, Copyright (2016). ....	178
Figure A.8.	Permission from [102] Elsevier, Copyright (2019).....	179
Figure A.9.	Permission from [89] John Wiley and Sons, Copyright (2007). ....	180
Figure A.10.	Permission from [114] Royal Society of Chemistry, Copyright (2020)..	181
Figure A.11.	Permission from [116] Elsevier, Copyright (2009). ....	182
Figure A.12.	Permission from [148] John Wiley and Sons, Copyright (2017).....	183
Figure A.13.	Permission from [149] John Wiley and Sons, Copyright (2015). ....	184
Figure A.14.	Permission from [211] John Wiley and Sons, Copyright (2019). ....	185
Figure A.15.	Permission from [220] John Wiley and Sons, Copyright (2017). ....	186

## LIST OF TABLES

Table 1.1.	Effects of the functionality of acrylates on their performance [239].	26
Table 3.1.	Solubilities of TXdMA and TX.	36
Table 3.2.	Absorption characteristics of TXdMA in selected solvents.	39
Table 3.3.	Photophysical/photochemical and electrochemical	46
Table 3.4.	Parameters characterizing the chemical mechanisms associated with the TXdMA/Iod system in acetonitrile.	46
Table 4.1.	The solubility of BPBP and e TXBP.	56
Table 4.2.	Photoinitiated polymerization of AAm at room temperature at $\lambda=365$ nm.	68
Table 5.1.	Absorption characteristics of TXBP2 ( $1.5 \times 10^{-4}$ M) in different solvents.	75
Table 5.2.	Parameters characterizing the singlet excited state reactivity of the TXBP2.	82
Table 5.3.	Parameters characterizing the triplet excited state reactivity of the TXBP2.	82
Table 5.4.	Photoinitiated polymerization of AAm in aqueous media at 25 °C at $\lambda=365$ nm for 15 minutes.	85
Table 6.1.	The solubility of PAATX.	93
Table 6.2.	Parameters characterizing the reactivity of the PAATX.	99
Table 6.3.	Compositions of the formulations.	101
Table 7.1.	The solubilities of PEI-I2959 and PEI-I2959-Ts.	114

Table 7.2.	Absorption characteristics of PEI-I2959 and PEI-I2959-Ts in different solvents. ....	119
------------	--	-----

## LIST OF SYMBOLS

$\Delta H_p$	Heat released per mole of double bonds reacted
$\Delta G_{et}$	Free energy change for electron transfer between PI and the additive
$\varepsilon$	Extinction coefficient
$I_a$	Intensity of absorbed light
$\lambda_{max}$	The wavelengths for maximum absorption
$\lambda_{em}$	The wavelengths for maximum emission
$\lambda_{exc}$	Excitation wavelength of the solution in fluorescence experiments
$\tau_0$	The singlet excited state lifetime of the PI
$\Phi$	Number of propagation chains initiated per light photon absorbed
$A_0$	The area under the absorbance peak at $815\text{ cm}^{-1}$ at time 0
$A_t$	The area under the absorbance peak at $815\text{ cm}^{-1}$ (C=C deformation) at time t (curing time)
$C$	Electrostatic interaction energy
CTC	Charge transfer complex
$E_{red}$	Reduction potential
$E_{ox}$	Oxidation potential
$E_S$	Excited singlet state energy
$E_T$	Excited triplet state energy
$I$	Fluorescence intensity of PI in the presence of the quencher
$I_0$	Fluorescence intensity of PI in the absence of the quencher
[I]	Concentration of the initiator
IPN	Interpenetrated polymer network
$k_q$	The fluorescence quenching rate constant
$K_{sv}$	Stern–Volmer quenching coefficient
$m$	The molar mass of the monomer

$M_n$	The number average molecular weight
$n$	The number of double bonds per monomer molecule
PI	Photoinitiator
PPI	Polymeric photoinitiator
Q/s	Heat flow per second
$R_{pmax}$	The maximum rate of polymerization
$R_p$	Rate of polymerization
$t_{max}$	The time until the highest heat flow is reached
BPBP	((3-benzoylphenyl)(hydroxy)methylene)bis(phosphonic acid)
PAATX	Thioxanthone functionalized poly(amido) amine
PEI-I2959	I2959 functionalized poly(ethylene imine)
PEI-I2959-Ts	I2959 and tosylate counteranion functionalized poly(ethylene imine)
TXBP	(1-hydroxy-2-((9-oxo-9H-thioxanthen-2-yl)oxy)ethane-1,1-diyl)bis(phosphonic acid)
TXBP2	octaethyl (((2-((9-oxo-9H-thioxanthen2yl)oxy)ethyl)azanediyl)bis(ethane-2,1,1-triyl))tetrakis(phosphonate)
TXdMA	2,2'-(((9-oxo-9H-thioxanthen-2-yl)azanediyl)bis(methylene))diacrylic acid

**LIST OF ACRONYMS/ ABBREVIATIONS**

AAm	Acrylamide
AP	Acetophenone
AQ	Anthraquinone
BAPO	Bisacylphosphine oxide
Bis-GMA	(2,2-Bis-[4-(2-hydroxy-3-methacryloyloxypropoxy)phenyl]propane
BP	Benzophenone
Bz	Benzil
CHO	Cyclohexene oxide
CMAC	2-(chloromethyl)acryloyl chloride
CO <sub>2</sub> Cl <sub>2</sub>	Oxalyl chloride
CQ	Camphorquinone
CV	Cyclic voltammetry
DABCO	1,4-Diazabicyclo[2.2.2]octane
DCM	Dichloromethane
D <sub>3</sub> DMA	Decanediol dimethacrylate
DMA	<i>N,N</i> -dimethyl aniline
DMAEM	<i>N,N</i> -dimethylaminoethyl methacrylate
DMF	Dimethylformamide
DSC	Differential Scanning Calorimetry

EDB	Ethyl 4-(dimethylamino)benzoate
ESR	Electron Spin Resonance
FT-IR	Fourier Transform Infrared Spectroscopy
GPC	Gel Permeation Chromatography
HDDA	Hexane-1,6-diol diacrylate
HEMA	2-hydroxyethyl methacrylate
hPEA	Hyperbranched poly(ether amine)
hPEI	Hyperbranched poly(ethylene imine)
IBVE	Isobutyl vinyl ether
I2959	2-Hydroxy-1-[4-(2-hydroxyethoxy)phenyl]-2-methyl-1-Propanone
Iod	Bis-(4-tert-butylphenyl)-iodonium hexafluorophosphate
ITX	2-Isopropylthioxanthone
K <sub>2</sub> CO <sub>3</sub>	Potassium Carbonate
LFP	Laser Flash Photolysis
MAPO	Monoacylphosphine oxide
MDEA	Methyl diethanolamine
MeOH	Methanol
MMA	Methyl methacrylate
NAM	<i>N</i> -acryl-morpholine
NMR	Nuclear Magnetic Resonance spectroscopy
NVP	<i>N</i> -vinyl pyrrolidine

PBN	Phenyl- <i>N-tert</i> -butylnitron
PAA	Poly(amido amine)
PEG	Poly(ethylene) glycol
PEGDA	Poly(ethylene glycol) diacrylate
PEO	Poly(ethylene) oxide
PPI	Poly(propylene imine)
PU	Poly(urethane)
PVA	Poly(vinyl) alcohol
RHMA	Alkyl $\alpha$ -hydroxymethacrylate
St	Styrene
TBBr	<i>Tert</i> -butyl $\alpha$ -bromomethacrylate
TBHMA	<i>Tert</i> -butyl $\alpha$ -hydroxymethacrylate
TXCH <sub>2</sub> COOH	2-((9-oxo-9H-thioxanthen-2-yl)oxy)acetic acid
TXDB	9-oxo-9H-thioxanthen-2-yl acrylate
TEA	Triethylamine
TEGDMA	Triethyleneglycol dimethacrylate
TEGDVE	Triethylene glycol divinylether
T <sub>g</sub>	Glass transition temperature
THF	Tetrahydrofuran
TFA	Trifluoroacetic acid
TMPTA	Trimethylolpropane triacrylate
TPO-L	Ethyl (2,4,6-trimethylbenzoyl) phenylphosphinate

TXOH	2-Hydroxy-9H-thioxanthen-9-one
TXNH <sub>2</sub>	2-aminothioxanthone
TX	Thioxanthone
UDMA	1,6-bis-[2-methacryloyloxyethoxycarbonylamino]- 2,4,4-trimethylhexane

## **1. INTRODUCTION: PHOTOPOLYMERIZATION**

Photoinduced polymerization science and technology provides many advantages over thermal curing process in terms of performance-based, economical and ecological aspects having the properties of high curing speed, low necessity of energy, low emission of volatile compounds, enhanced product durability, high surface quality for coatings and low costs of material, production process. These environmentally friendly characteristics of photoinduced polymerization makes it a green technology. UV curing technology has been widely used in many application areas such as protective coatings for various substrates such as concrete, metal, ceramic, glass, plastic, composites and textiles, varnishes, paints, printing inks, adhesives, microelectronics, photoresists, 3D printing and bioapplications such as, tissue engineering, dentistry and ophthalmology [1-5].

A photocurable resin (monomer/oligomer matrix), a photoinitiator or a photoinitiating system and a light source are the essential components of a photocurable formulation. A photoinitiating system which takes a major role in this process, although its volume in the resin is lowest, absorbs the light energy and provides the penetration of incident light into the sample and initiates the polymerization reaction by forming reactive species; radicals, cations and in some cases, anions or weak bases and forms linear or crosslinked polymer networks at the end (Figure 1.1). Even if it gives the name to whole process, light serves just as an initiating tool, do not interfere with the other stages of polymerization reaction. A photoinitiating system may affect rate of polymerization, yellowing and cost [6].

### **1.1. Photoinduced Free Radical Polymerization**

Photoinitiated free radical polymerization technique has a broad range of application areas in industry. It is more often used than cationic photopolymerization mainly due to the availability of a wider range of monomers and photoinitiators [3]. The photoinduced free radical polymerization is composed of four different steps of photoinitiation, propagation, chain transfer and termination as seen in Figure 1.2.

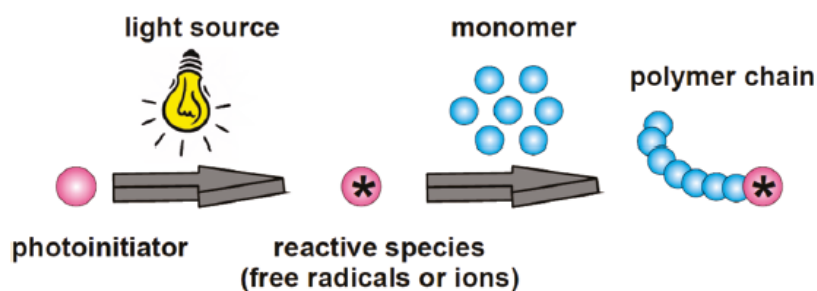
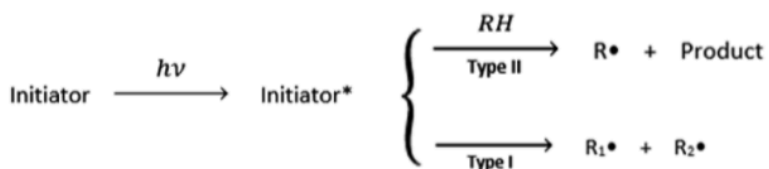


Figure 1.1. General representation of a photoinduced polymerization. Reproduced with permission from [3] American Chemical Society, Copyright (2010), (Figure A.1).

### Photoinitiation



### Propagation



### Chain-Transfer



### Termination



Figure 1.2. Stages of a photoinduced free radical polymerization. Reproduced with permission from [7] John Wiley and Sons, Copyright (2019), (Figure A.2).

The formation of free radicals which occurs through photoreactions of initiator molecules via Type I or Type II mechanism is the first step to synthesize macromolecules by free radical chain polymerization of monomers. In the propagation step, the polymer chain grows as the macroradical which is formed in the first step continues to react with other monomers. Chain transfer reaction is a radical displacement reaction which the free radical site of a growing polymer chain is transferred to another molecule by a hydrogen transfer from different species present in the system (e.g. unreacted monomer, initiator or solvent) and the newly formed radicals then initiate another polymer chain. In termination stage, radicals interact each other and polymer chain stops growing by a coupling or a disproportionation mechanism [7].

## 1.2. Free Radical Photoinitiators

Photoinitiators or photoinitiating systems are the key components in a photopolymerizable matrix which provides the communication between a light source and the monomer/oligomer resin. An ideal photoinitiating system must have the properties of no generation of yellowing products, good storage stability, good solubility and compatibility in the photocurable resin, low price, no odor or toxicity and biocompatibility. Some properties of photoinitiating systems such as, superior light absorption and photochemical reactivity, low sensitivity to oxygen and high chemical reactivity of the initiating species, determines the reactivity of a photosensitive system [1].

When a photoinitiator absorbs light energy, series of energetic processes which is depicted by a Jablonski diagram occur (Figure 1.3). Firstly, a photoinitiator is in ground state ( $S_0$ ), then it absorbs light energy and goes to singlet excited state (singlet state  $S_1, S_2, \dots S_n$ ). Transition from  $S_1$  to  $T_1$  excited state occurs through intersystem crossing but this transition is in competition with the fluorescence (emission of a photon) which is a deactivation path from  $S_1$  to  $S_0$  state by internal conversion. In  $T_1$  state, deactivation processes may also occur through phosphorescence (emission of a photon), oxygen or monomer quenching.

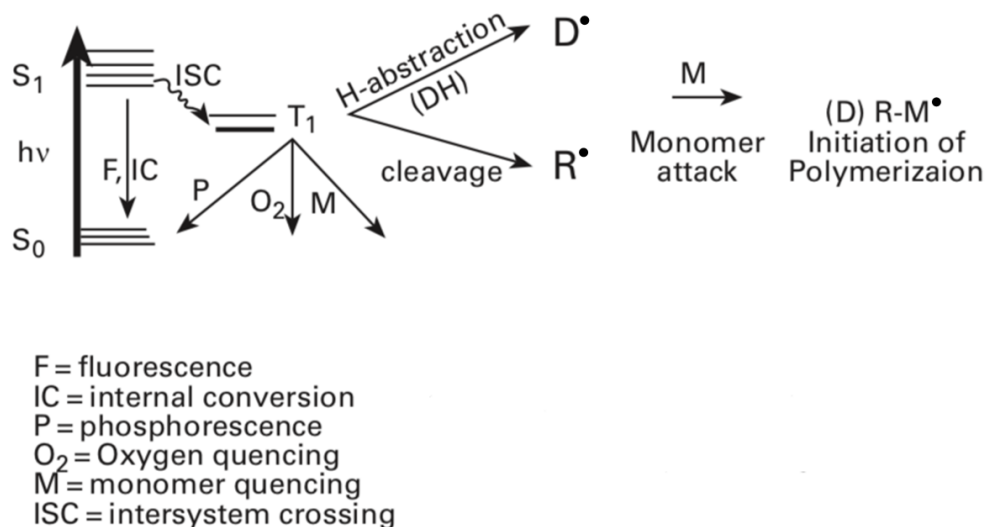


Figure 1.3. Photophysical processes involved in the excited state of a photoinitiator. Reproduced with permission from [5] Elsevier, Copyright (2001), (Figure A.3).

All the mentioned energetic processes so far are defined as photophysical as no chemical change appears in the structure of the photoinitiator. However, generation of an initiating radical at the singlet or triplet excited states is a photochemical process since a chemical modification takes place in the structure of the photoinitiator and new photoproducts are formed. Then, the initiating species react with a monomer to synthesize a macromolecular chain.

Two main types of electronic transitions:  $n-\pi^*$  or  $\pi-\pi^*$  transitions are seen in photopolymerization reactions which proceed in UV-Vis spectrum range.  $n-\pi^*$  transitions appear generally in the range of 300-380 nm and have low absorption properties.  $\pi-\pi^*$  transitions are seen usually in the short wavelengths and have high absorption properties (Figure 1.4) [1].

The formation of initiating species from singlet or triplet excited states occur through two different mechanisms; Type I or Type II.

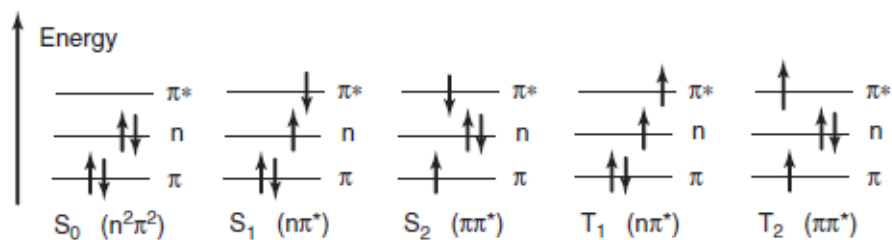


Figure 1.4. Different distributions of the electrons (configurations) in the three available MOs. Reproduced with permission from [1] John Wiley and Sons, Copyright (2012), (Figure A.4).

### 1.2.1. Type I Photoinitiators

In Type I photoinitiation which is a mono-molecular type initiation process, after excitation of the photoinitiator molecule by absorbing light energy, a homolytic cleavage reaction occurs from the  $\alpha$ -position (major) or  $\beta$ -position (minor) of carbonyl group depending on their bond strengths and two different radicals which are both capable of initiating a polymerization reaction are formed. Light energy is sufficient to be able to break the CO-C bond in Type I photoinitiators. The general photoinitiating mechanism of Type I photoinitiators were given in Figure 1.5 [8, 9]. Some examples of Type I photoinitiators can be seen in Figure 1.6.

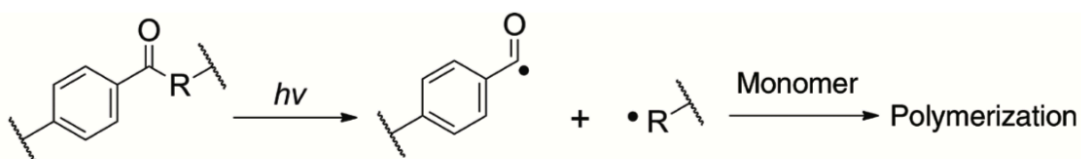


Figure 1.5. General Type I photoinitiation mechanism [9].

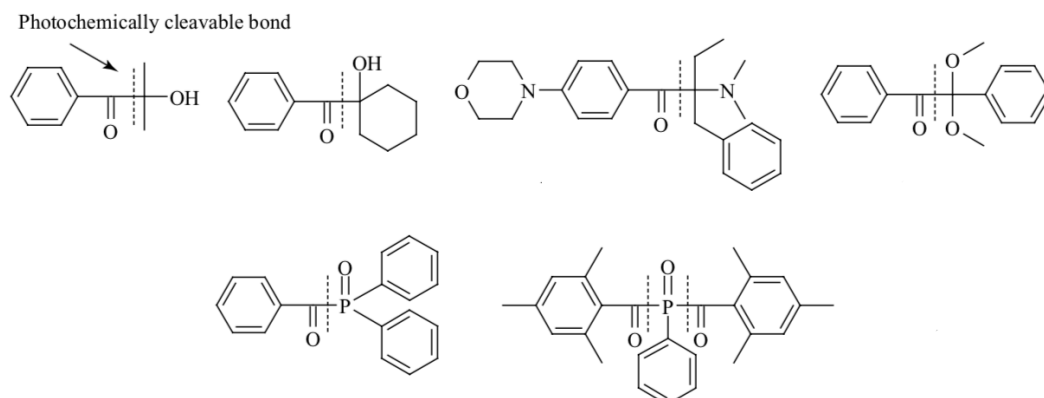


Figure 1.6. Some examples of Type I photoinitiators. Reproduced with permission from [10] John Wiley and Sons, Copyright (2012), (Figure A.5).

### 1.2.2. Type II Photoinitiators

Type II photoinitiators can not generate active radicals spontaneously, because UV light energy is insufficient to break the high energy of CO-aryl bonds. Therefore, Type II photoinitiators require a co-initiator which is capable of hydrogen donation such as amines, alcohols, thiols and ethers. Type II photoinitiators can generate longer-lived triplet excited state compared to Type I photoinitiators after absorption of light energy. Hence, a bimolecular reaction which is an electron transfer and a following proton transfer can occur between the photoinitiator and a hydrogen donor molecule and then, an aminoalkyl and a ketyl radical forms. As seen in Figure 1.7, while aminoalkyl radical is reactive in a photopolymerization reaction, ketyl radical can just take a role in termination processes by giving coupling reactions [8, 9]. Some examples of Type II photoinitiators (anthraquinones, ketocoumarins, benzophenones, thioxanthenes, camphorquinones and benzils) can be seen in Figure 1.8.

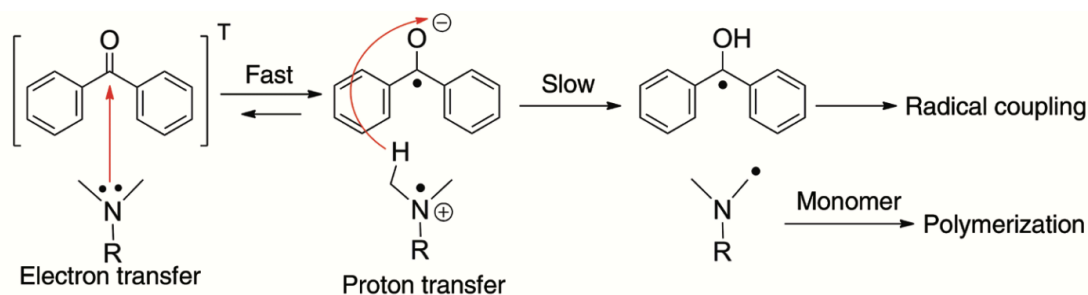


Figure 1.7. General Type II photoinitiation mechanism of benzophenone [9].

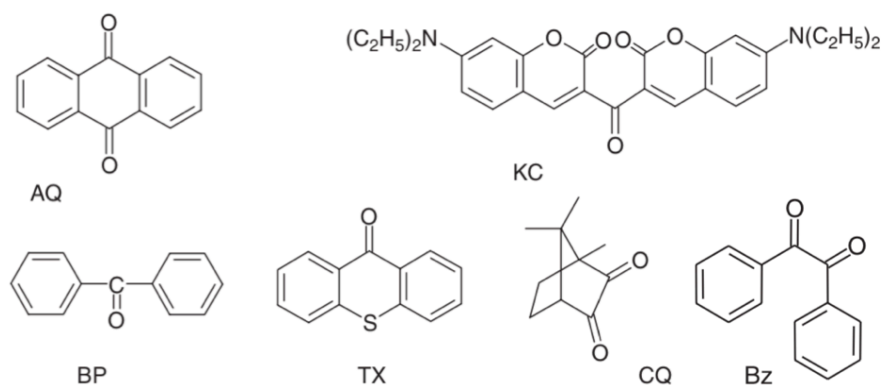


Figure 1.8. Some examples of Type II photoinitiators. Reproduced with permission from [1] John Wiley and Sons, Copyright (2012), (Figure A.4).

### 1.3. Desiderata for Greener Photoinitiators

Photopolymerization science and technology is continuously developing and finds many application areas in industry [10]. As discussed above, photoinitiators are the key components in every photocuring processes. Therefore, the continuity in the growth of radical photopolymerization is tied to new developments in the design of photoinitiators which will eliminate some drawbacks of this technology, in particular, make it more environmentally friendly.

One of the major disadvantages in a photocurable system is the migration of the unreacted photoinitiators, co-initiators (for Type II PIs) and the other photoproducts, especially when UV curable formulations are used in food packaging, toys, health care, e.g.

dental applications, and other materials which are used in everyday life by people [11]. In last decades, many notifications about migration of PIs from food packaging have been reported by the Rapid Alert System for Food and Feed (RASFF). In 2005, isopropylthioxanthone (ITX) was detected in baby milk [12-14]. In 2009, benzophenone and 4-methylbenzophenone were notified in foodstuffs (breakfast cereals, breakfast bars and milk). The carcinogenic effect of benzophenone and its photoproducts were demonstrated with the current studies (List of IARC (International Agency for Research on Cancer) Group 2B carcinogens) [15]. Therefore, there is a need for photoinitiators with improved migration stability to inhibit the problems associated with the leaching of photoinitiators or the photofragments from the cured coating such as toxicity, odor, and darkening of the cured films.

Photoinitiating systems able to work in aqueous conditions are also of great interest, since using water instead of any organic solvent has many obvious “green” advantages such as low emission of volatile organic compounds; the fact that water is easily available, cheap and non-flammable; contribution to the reduction of migration of residual monomers by the virtue of the reduction in the use of reactive diluents; easy control of rheology; no odor and toxicity problems due to leaching of solvent [16], [17]. Water soluble systems are preferred especially in biological and medical applications such as dental materials, 3D fabrication of pharmaceutical tablets, and fabrication of complex 3D structures for tissue engineering.

The light used to trigger the photopolymerization reaction is also of consequence: The ultraviolet light (UV) used in many photopolymerization systems is carcinogenic due to higher energy of its photons. Therefore such systems are unusable in biological and medical applications, some of which have been mentioned above. Furthermore, sources of visible light are widely available and much cheaper (e.g. ordinary lamps) than UV sources, possibly free in some contexts (e.g. sunlight). The UV sources’ light can also constitute a hazard for people involved, as can toxic materials (e.g. mercury) that some such sources contain. For these reasons the development of PIs that can work with visible light is strongly desired. To sum up, a “greener” PI should have as many as possible of the properties of migration stability, water solubility and visible-light operation. We next discuss each of these desiderata in turn.

## 1.4. Low Migration Photoinitiators

One of the parameters that has to be enhanced on the track of greener photoinitiators is the migration stability, as it is mentioned in Section 1.3. The idea behind the solution to the migration problem of PIs must be the immobilization of the PI into the polymer network. Low molecular weight photoinitiators can not meet this demand, because, they are usually not blocked into a cured composition, thoroughly. Therefore, there have been many undergoing research in designing new photoinitiators that will be less prone to be leached from the polymer network. Monomeric, polymeric, hyperbraced/dendrimeric and dual-curable photoinitiators are mostly studied to develop in accordance with the purpose of reduced migration properties [2].

### 1.4.1. Monomeric Photoinitiators

Polymerizable photoinitiators containing ethilenically unsaturated groups are one way of solution to the migration issue. By the virtue of the ethenically unsaturated unit, polymerizable photoinitiators can be covalently bonded to the cured composition which minimizes the extraction tendency of the photoinitiator.

Many monomeric photoinitiator containing Type I ( $\alpha$ -hydroxy ketones [18-22], acetophenones [21], acyl phosphine oxides [22]) and/or Type II (benzophenones [18, 21], [23-32], thioxanthenes [33-42]) or other photoinitiator units such as benzylidene cyclano dyes [43], naphthalimide derivatives [44] were designed so far. In the case of Type II photoinitiators, a coinitiator is also required. Generally, tertiary amines are preferred as coinitiators because of their high reactivity and oxygen inhibition ability. However, the use of low molecular weight amine molecules can cause toxicity and yellowing in the cured films which is detrimental to public health, especially when it is used in food packaging, biomedical applications and any item that can come into contact with a human. As a solution to this issue, one component monomeric photoinitiators which are manufactured through covalent attachment of coinitiator units into the photoinitiator structure were built up [23, 24, 33-35, 37, 41].

Three different one component polymerizable thioxanthone photoinitiators (TX-EA, TX-BDA and TX-PA) were reported [34] (Figure 1.9). The photoinitiation activities of the photoinitiators were tested in the photopolymerization of 1,6-hexanediol diacrylate (HDDA). While TX-BDA shows highest reactivity, TX-EA and TX-PA follow TX-BDA in the order of reactivity, respectively. When the hydrogen donor *N*-methyl-diethanolamine (MDEA) was added to the formulation, photopolymerization rate was increased in each case with the same order of the reactivity. Migration stability of the photoinitiators were very high and the order in the migration stability between these three PIs follows the trends in the photoreactivity order.

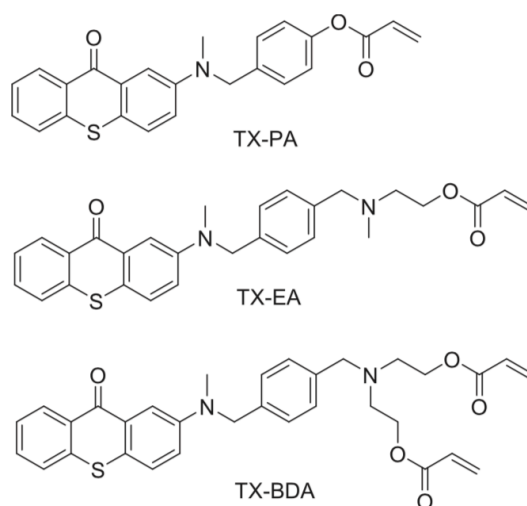


Figure 1.9. Novel polymerizable thioxanthone photoinitiators. Reproduced with permission from [34] John Wiley and Sons, Copyright (2017), (Figure A.6).

Hydroxyalkyl phenone (PI-4) and monoacyl phosphine oxide (PI-9) based photoinitiators containing alkyne functional groups were synthesized (Figure 1.10) [22]. Their photoreactivities were investigated in the polymerization of biocompatible vinyl carbonate/thiol resins in comparison with the reference photoinitiators, Irgacure 2959 (I2959) and non-functionalized acyl phosphine oxide derivative ethyl (2,4,6-trimethylbenzoyl) phenylphosphinate (TPO-L). Although PI-4 showed a lower efficiency compared to I2959 in the initiation of the polymerization of vinyl carbonate/thiol resin, PI-4 exhibited a better migration stability than I2959, the concentration of PI-4 in the extracted EtOH solution of the polymer was even below the detection limits. The high migration

stability of PI-4 is contributed to its immobilization into the polymer structure. PI-9 displayed a similar photoinitiation performance with TPO-L in the polymerization of vinyl carbonate/thiol resin. Migration stability of PI-9 was also higher compared to TPO-L. Thus, these novel photoinitiators have the potential to be used in applications where low migration is required.

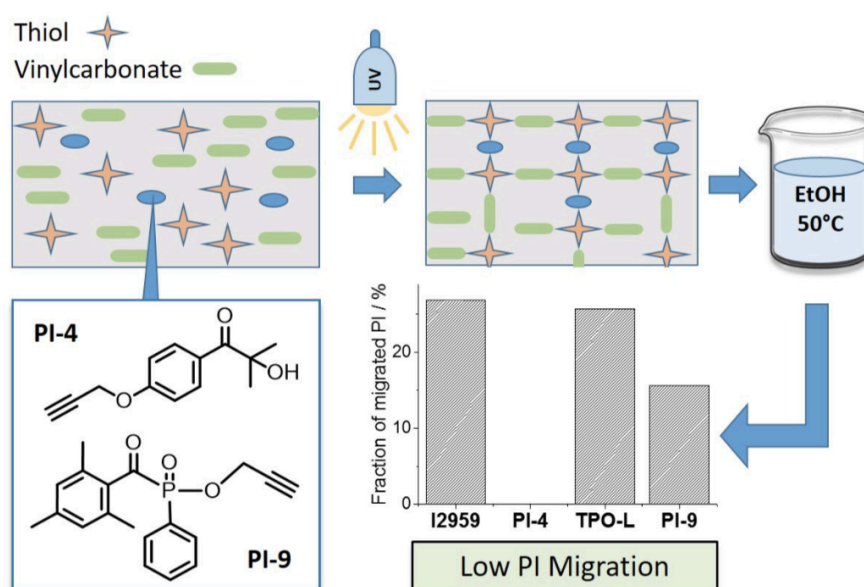


Figure 1.10. Alkyne functional hydroxy alkyl phenone (PI-4) and monoacyl phosphine oxide (PI-9) based low migration photoinitiators. Reproduced with permission from [22], Elsevier, Copyright (2016), (Figure A.7).

#### 1.4.2. Polymeric Photoinitiators

Another alternative way in designing novel photoinitiators with reduced migration properties is to form higher molecular weight photoinitiators which increases the probability of the photoinitiator to be trapped in the cured product through physical entanglements. The higher inherent viscosity of the higher molecular weight photoinitiators also hinders the diffusion of the PIs from the cured films. In addition to the low migration property of high molecular weight photoinitiators, they are also more compatible in the photocurable compositions rather than low molecular weight photoinitiators. For such reasons, many different polymeric photoinitiators including Type I or Type II chromophoric units such as,

( $\alpha$ -hydroxy ketone [45-49],  $\alpha$ -alkoxy benzyl [50],  $\alpha$ -amino alkyl phenone [51, 52], Michler's ketone [53, 54], acyl phosphine oxide [55-60], polysilane [61, 62], thioxanthone [63-81], benzophenone [82-95], camphorquinone [96-98], benzil [99, 100], anthraquinone [101] which are generally synthesised via incorporation of photoinitiator unit as a pendant group or directly into the polymer chain, have been studied widely by many researchers in literature (Figure 1.11) [102].

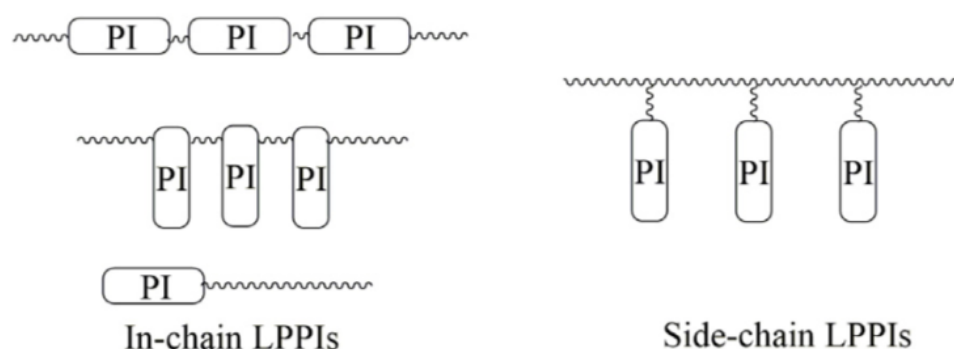


Figure 1.11. Structural characteristics of different types of polymeric photoinitiators; In-chain linear polymeric PPIs (LPPIs) or side-chain LPPIs. Reproduced with permission from [102] Elsevier, Copyright (2019), (Figure A.8).

Type II polymeric photoinitiating systems can be attained in two different ways. As a one option, a polymeric Type II photoinitiator and a polymeric amine can be used together. However, polymeric photoinitiators or coinitiators has poor mobility which decreases their photoreactivity. As a second alternative, one component polymeric photoinitiators [63, 72-75, 77, 78, 80, 82, 84, 87, 93-100] can be synthesized via covalently substitution of a coinitiator into the polymeric photoinitiator structure which improves the photoinitiation efficiency with improving the energy migration or intramolecular interactions between initiator and coinitiator units.

Three different PU (Polyurethane)-type polymeric photoinitiators containing side-chain benzophenone and coinitiator amine units were synthesized [89] (Figure 1.12). The photopolymerization behaviors of these photoinitiators were tested in the photopolymerization of TMPTA. Whereas PUSBA-h and PUSBA-i show similar results,

PUSBA-t displays the most effective performance in the photocuring of TMPTA. This result may be ascribed to the higher efficiency of PUSBA-t in the proton transfer process rather than PUSBA-h and PUSBA-i.

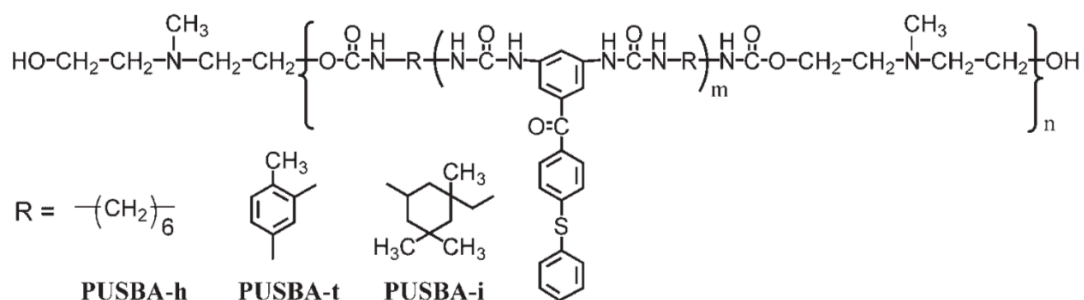


Figure 1.12. PU-Type one component polymeric photoinitiators containing side chain benzophenone and coinitiator amine. Reproduced with permission from [89] John Wiley and Sons, Copyright (2007), (Figure A.9).

Two different one component polymeric photoinitiators were synthesized in some of the previous works of our group [18, 68] (Figure 1.13). PPI(TX1-*co*-DMAEM) and PPI(PI1-*co*-DMAEM) were synthesized through a copolymerization reaction between tert-butyl  $\alpha$ -hydroxymethacrylate (TBHMA)-based TX functionalized photoinitiator or 2-(chloromethyl)acryloyl chloride (CMAC) based benzophenone functionalized photoinitiator and *N,N*-dimethylaminoethyl methacrylate (DMAEM), respectively. DMAEM was functionalized as a coinitiator. The reactivities of the PPI(TX1-*co*-DMAEM) and PPI(PI1-*co*-DMAEM) were investigated in the photocuring of HDDA and TMPTA, respectively. The photopoefficiency of both photoinitiators were found more efficient than their low molecular commercial analogs BP and TX.

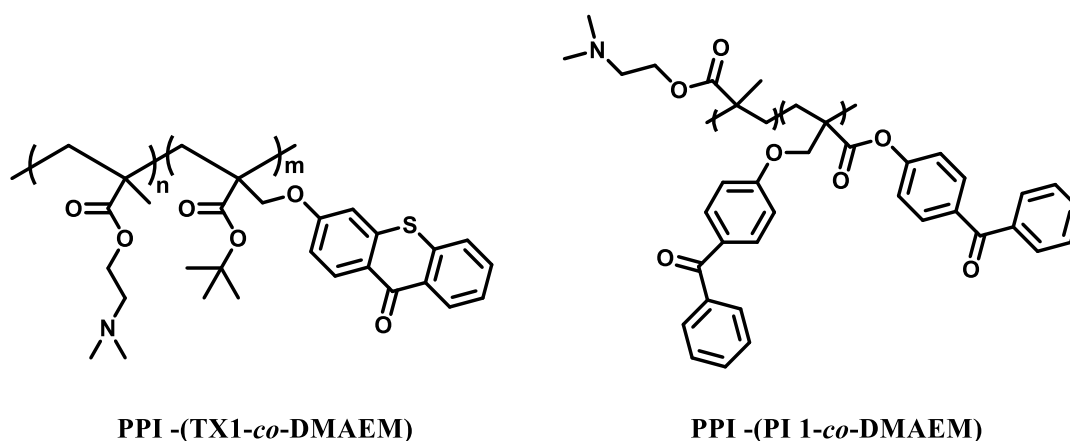


Figure 1.13. One component TX or BP functionalized polymeric photoinitiators [18, 68].

### 1.4.3. Hyperbranched/Dendrimeric Photoinitiators

Polymeric photoinitiators having a hyperbranched or dendrimeric core have a lower viscosity compared to linear polymers making them more soluble and compatible in the photocuring formulations. Also, hyperbranched or dendrimeric polymers have multifunctional active groups enabling the attachment of more chromophoric units which could improve the reactivity of a photoinitiator [102-104]. These advantages of hyperbranched PPIs over linear PPIs make them preferable in many research fields. The general structure of dendrimeric/hyperbranched photoinitiators can be seen in Figure 1.14.

Hyperbranched or dendrimeric PPIs including Type I or Type II chromophoric units, such as,  $\alpha$ -hydroxy ketones [105], acyl phosphine oxides [106], polysilane [107], [108], thioxanthone [109-117], benzophenone [118-126] and xanthene dyes (as a sensitizer) [127, 128] have already been a subject in many studies in literature so far.



Four different thioxanthone derivatives (ATX, CTX, MATX and ABP) were incorporated as guest photoinitiators into various host molecules; hyperbranched poly(ether amine)s with different hydrophilicity through hydrophilic/hydrophobic and hydrogen bonding interactions between the amino groups of polymers and carboxyl units of the thioxanthone derivatives to synthesize the novel supramolecular hyperbranched photoinitiators [114] (Figure 1.15). The novel photoinitiators exhibit amphiphilic property, so, they are both soluble in aqueous and organic solutions. They are highly photoreactive in the photopolymerization of water soluble acrylamide (AAm) and oil soluble monomers HDDA and TMPTA.

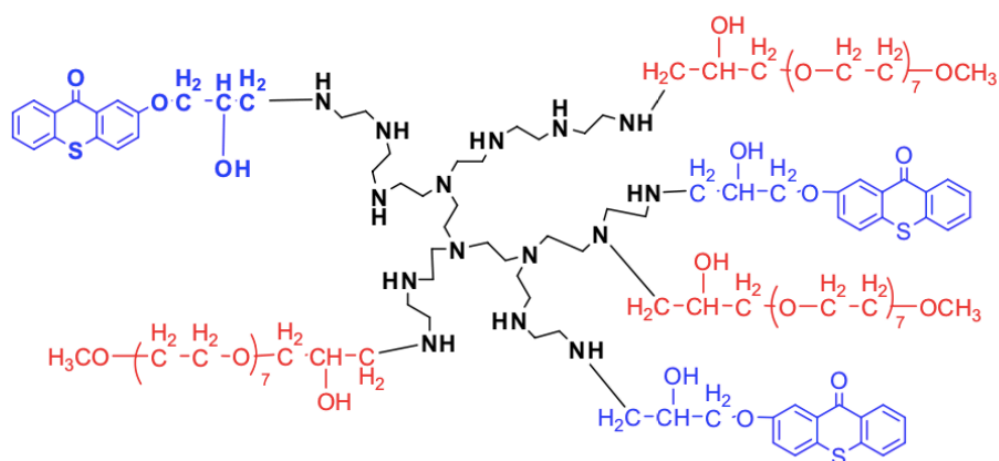


Figure 1.16. Structure of hyperbranched PPI containing TX and PEO chain. Reproduced with permission from [116] Elsevier, Copyright (2009), (Figure A.11).

Two different hyperbranched polymeric photoinitiators (AHPTX1 and AHPTX2) were synthesized with two different amounts of TX and PEO (Figure 1.16) [116]. Beside all the other known advantages of hyperbranched polymers, its polymeric core may also function as a hydrogen donating coinitiator. Photoinitiation efficiency of these novel hyperbranched photoinitiators and a low molecular weight analogues 2-(2-hydroxy-3-(methyl(2,3,4,5,6-pentahydroxyhexyl)amino)propoxy) thioxanthone (MGA-TX)/TEA system as a reference were examined in the photopolymerization of acrylamide (AAm). Both of the hyperbranched photoinitiators displayed a higher reactivity than the low molecular weight reference system

which is attributed to the intramolecular hydrogen abstraction between coinitiator amine and TX units in AHPTXs.

#### 1.4.4. Dual-curable Photoinitiators

Dual-curing process is a method to form interpenetrating polymer networks (IPNs) through two independent polymerization reactions proceeding sequentially. Photoinitiators with dual curing capability gets a part of the cured film through IPN formation which contributes to diminish the migration of the PI [129]. To obtain a good performance in a dual-curing process, the two consecutive curing reactions must be discriminating and occur in harmony with each other to restrain any undesired reaction. Choice of different stimulants triggering the consecutive curing reactions such as UV light, temperature, etc. enable us to control the dual-curing process from a kinetics viewpoint [130, 131]. Hence, the intermediate material will be stable and not cured until the second stimulant triggers the following reaction. The general description of a dual-curing process can be seen in Figure 1.17 [131].

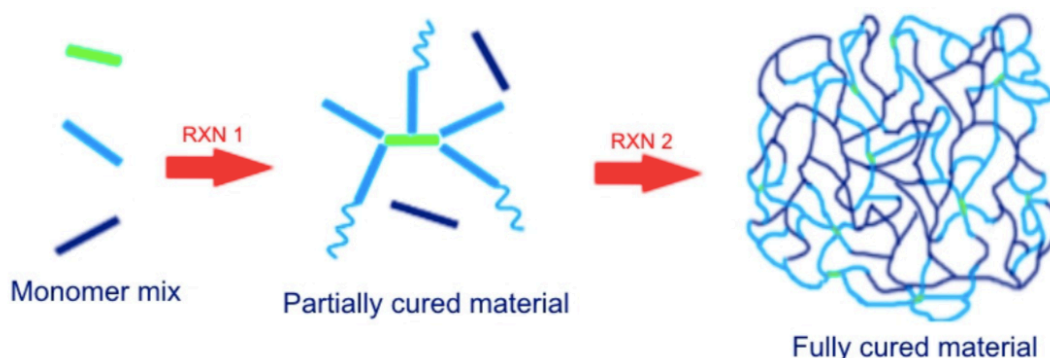


Figure 1.17. Schematic representation of a dual-curing process [131].

To devise dual-curable systems in an efficient and environmentally friendly way, using click chemistry is an effective approach [132, 133]. Michael addition reactions between the click chemistry polymerization reactions are most widely used in dual-curing processes [134, 135]. The conjugate addition of a nucleophile also called “Michael donor” to an activated electrophilic double bond, the “Michael acceptor”, determines the Michael

addition reaction. A base or a nucleophile can be used as a catalyst to trigger the process. Amines, thiols and phosphines are most frequently used as Michael donors in dual curing systems. There are many alternatives for Michael acceptors such as acrylates, methacrylates, sulfones and many other electrophilic groups. When Michael addition reaction is performed in the presence of an amine as a Michael donor which is called as aza-Michael addition, there is no need for a catalyst anymore since amines can serve both as a nucleophile and a base.

Aza-Michael addition followed by a photoinduced polymerization reaction is one of the frequently used combinations of dual-curing processes. The benefit of the dual-curing process is the tunability of the final properties of the obtained polymer through altering the relative contribution of the Michael addition and photopolymerization reactions which makes the product custom-tailorable. These advantages makes dual-curable systems favored in many applications such as holography, surface topology, optical materials, shape-memory materials, lithography and photopatterning [136-142].

There are not many studies on dual curable photoinitiators except a few examples [63, 129]. Piperazine functionalized benzophenone (bis-4-(piperazine-1-yl) methanone) is one of the examples (Figure 1.18) [129]. The free amine units on the piperazines have the capability to give aza-Michael addition reaction with an acrylate or methacrylate. At the same time, the novel piperazine functionalized benzophenone can behave as a one component Type II photoinitiator since the piperazine linkage acts as a hydrogen donating coinitiator which enables the use of it in a photopolymerization reaction as a second chemical reaction under light irradiation. Hence, this photoinitiator has the capability of undergoing two different polymerization reactions.

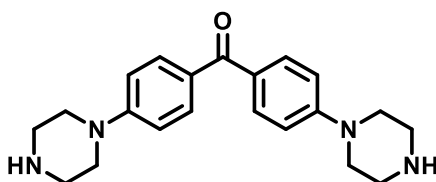


Figure 1.18. Structure of piperazine functionalized benzophenone [129].

### 1.5. Water Soluble Photoinitiators

The ability to use a photoinitiator in an aqueous system paves the way for its use in biomedical applications, as it is referred in Section 1.3. Therefore, development of newly designed water soluble photoinitiators gain importance.

Photoinitiator design plays a crucial role in the aqueous photopolymerization technique. To undergo water-borne photopolymerization, emulsions or dispersions of oil-soluble photoinitiators in water are generally used but they are thermodynamically unstable, since they can be destroyed by time with aggregation or coalescence which affects the final performances of the polymeric products [1]. Therefore, these systems are not applicable in the fields which need long-term stability. Sufficiently water soluble photoinitiators are highly demanded to overcome these problems.

Different strategies have been developed to design truly water compatible photoinitiators. An approach is to attach ionic hydrophilic groups such as quaternary ammonium salts, sulfonates, thiosulfates, carboxylic acids to conventional photoinitiators. Another alternative way to enhance the solubility is to incorporate conventional photoinitiators into hydrophilic oligomeric or polymeric groups such as long ethoxy ether chains (PEGs), poly(ethylene imine)s, poly(propylene imine)s or polyvinyl alcohols. In recent years, many waterborne photoinitiators were synthesized to meet the growing demand in this area, by incorporating ionic or hydrophilic groups into oil-soluble photoinitiators such as hydroxyalkylphenones [46-49, 143-148], mono- and bis-(acyl)phosphane oxides [55-57, 59, 149-152], aliphatic ketones [153], polysilanes [61, 62], benzil [99, 100], anthraquinone [101], Michler's ketone [53, 54], benzophenone [64, 69, 82, 83, 88, 121, 154-157], and thioxanthone [63, 64, 74-80, 113, 114, 116, 158-162]. Water soluble benzylidene cyclanone dyes [163], carboxylated camphorquinone [164], carbazole derivatives [165], naphthalimide derivatives [166], xanthene dyes [127, 167-170], coumarin derivatives [171] have also been designed.

2-hydroxy-4'-(2-hydroxyethoxy)-2-methylpropiophenone (I2959) is a very well-known commercial water soluble PI which has also high reactivity and biocompatibility. However, I2959 suffers from poor solubility in water (5 g L<sup>-1</sup>). In one study, a novel

bifunctional hydroxyketone based PI (Di-PI) with a solubility of 25 g L<sup>-1</sup> in water which is 5 times greater than I2959 was synthesized (Figure 1.19) [148]. The photocuring efficiency of Di-PI was similar with I2959 in the polymerization of dipropylene glycol diacrylate and slightly lower in the polymerization of aqueous *N*-acryl-morpholine solution. However, Di-PI exhibited a diminished migration property compared to I2959.

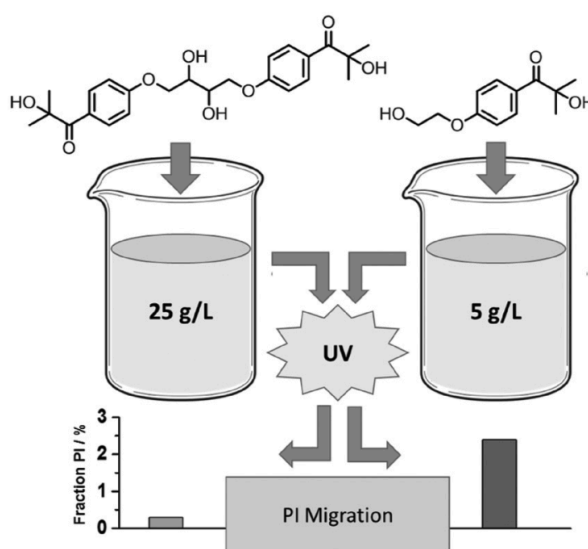


Figure 1.19. Properties of bifunctional hydroxyketone based photoinitiator compared with I2959. Reproduced with permission from [148] John Wiley and Sons, Copyright (2017), (Figure A.12).

Beside its low solubility (5 g/L), I2959 also is not active in visible light curing which is another drawback. In the search for a photoinitiator which will eliminate the drawbacks of I2959, water soluble, visible light and biocompatible PIs, monoacylphosphineoxide (BAPO) and monoacylphosphineoxide (MAPO) salts were analyzed (Figure 1.20) [149]. BAPO-ONa (60 g/L) displayed the best water solubility between these PIs (BAPO-OLi (54 g/L), Li-TPO (47 g/L), Na-TPO (29 g/L)). Best biocompatibility belonged to Li-TPO. As a result of the photo-DSC studies for the polymerization of aqueous *N*-acryl-morpholine solution, MAPO salts (Na-TPO and Li-TPO) exhibited best photoinitiation efficiency under UV light irradiation, BAPO-OLi showed best photoactivity under visible light irradiation.

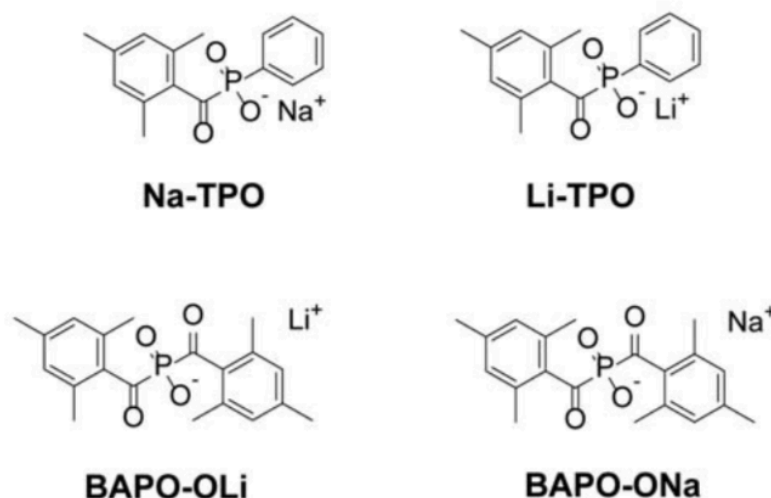


Figure 1.20. Structures of MAPO and BAPO salts. Reproduced with permission from [149] John Wiley and Sons, Copyright (2015), (Figure A.13).

### 1.6. Visible Light Photoinitiators

UV or visible light irradiation is frequently used to activate a free radical photoinitiator for the photoinitiation process. In accordance with the sensitive wavelength region, the free radical photoinitiators can be classified as UV light or visible light photoinitiators. The commercial photoinitiators mostly work in the UV light region, since UV light carries more energy than visible light and affects more chemical bonds which makes UV photoinitiators preferable in many industrial applications such as coating, inks and photoresistors [172]. However, UV light curing is not a radiation safe method which limits its use especially in biomedical applications. Therefore, there is a growing interest for visible light systems with the aim of a greener photopolymerization technology [173–175]. Visible light induced photocuring offers many advantages compared to UV light triggered photopolymerization such as easily accessibility, cost effectivity, safety (no release of ozone, no radiation hazard) and high penetration depth which paves the way for the visible light photoinitiators to be applicable in many significant applications: printing plates [176], integrated circuits [177], dental filling materials [178, 179], photoresists [180], laser-induced 3D curing [181] and holographic recordings [181]. The visible light curing has been first started in 1970s in dentistry using a metal halide lamp [174]. Xe lamps, halogen lamps, laser diodes

(monochromatic light), LEDs (quasi monochromatic light) and sunlight are other light sources adaptable in visible light curing applications [1].

Generally used photoinitiating systems in visible light curing are acylphosphine oxides [56, 57, 149, 182, 183], camphorquinones [96-98, 164, 184-186], anthraquinones [187-192], modified versions of UV sensitive photoinitiators; benzophenones [154, 193-198] or thioxanthenes [33-35, 37, 42, 65, 69, 80, 159, 162, 199-213] germanium based initiating systems [214-223], naphthalimide derivatives [44, 166, 224-227], metal complex and metal based photoinitiating systems [228-232], coumarin derivatives [171] and newly established dyes [43, 127, 167-170, 233-236].

Novel double chromophoric sulfonium salt PI (ITXPhenS) was derived [211]. The charge transfer complex (CTC) between ITXPhenS and *N,N*-dimethyl aniline (DMA) was formed as a visible light photoinitiator with the aim of having higher absorbtivity and red-shifting the absorption maximum to the visible wavelength region (Figure 1.21). ITXPhenS/DMA CTC is very efficient in the initiation of free radical or cationic photopolymerization of many different monomers, isobutyl vinyl ether (IBVE), cyclohexene oxide (CHO), methyl methacrylate (MMA), styrene (St), triethylene glycol divinylether (TEGDVE) and triethyleneglycol dimethacrylate (TEGDMA) under visible or sunlight exposure. According to the proposed photoinitiation mechanism of ITXPhenS/DMA CTC, radical and ionic species are formed through the light triggered cleavage of phenacyl unit which enables the initiation of two different polymerization reactions providing the formation of interpenetrating networks under visible light.

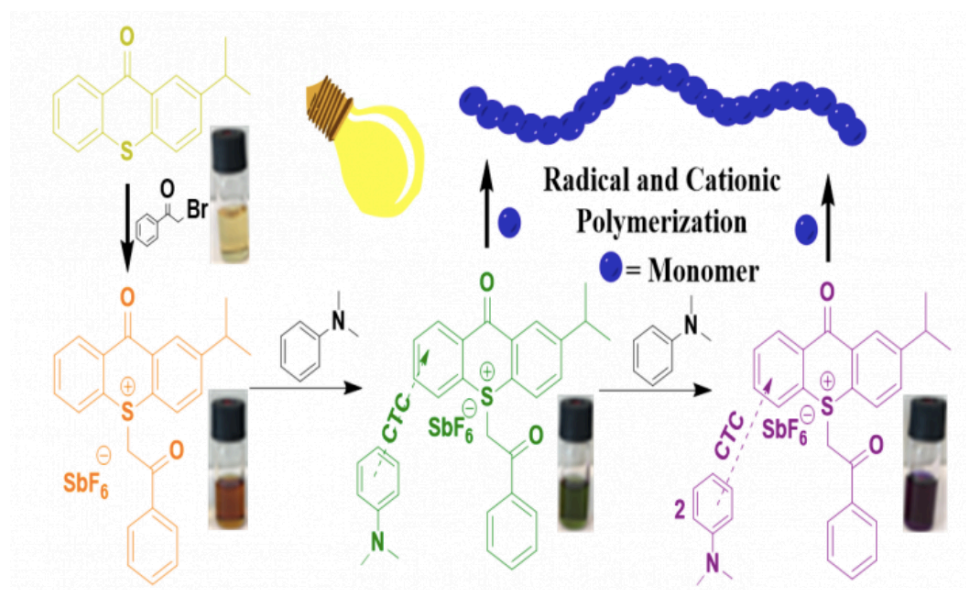


Figure 1.21. Scheme for the synthesis of charge transfer complex of a sulfonium salt as visible light PI. Reproduced with permission from [211] John Wiley and Sons, Copyright (2019), (Appendix A14).

Different tetraacylgermanes which are previously synthesized in literature were used as visible light photoinitiators in dental resins and methacrylate based composites (Figure 1.22) [220, 221]. These photoinitiators exhibited very high visible light absorption characteristics. Photoinitiation mechanism of the tetraacylgermanes are given in Figure 1.22. They undergo an  $\alpha$ -cleavage reaction upon visible light irradiation and form two different radicals; a germanium-centered radical and a benzoyl radical. The photoreactivity of the tetraacylgermanes were tested using different dental monomers such as Bis-[4-(2-hydroxy-3-methacryloyloxypropoxy)phenyl]propane (Bis-GMA) and 6-bis-[2-methacryloyloxyethoxycarbonylamino]-2,4,4-trimethylhexane (UDMA). It was observed that tetrakis(2-methyl-benzoyl)germane (PI 2) displayed highest photoreactivity at very low PI concentration under visible light irradiation.

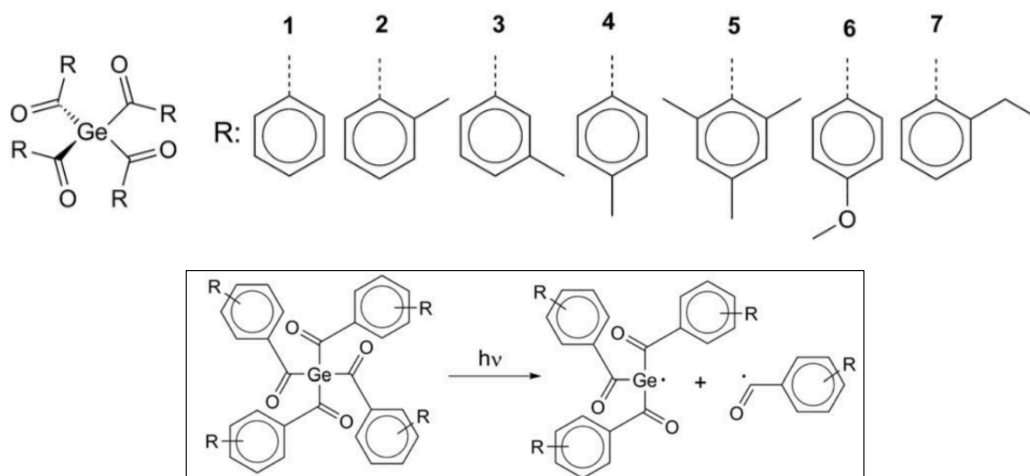


Figure 1.22. Structure of different tetraacylgermanes and their photoinitiation mechanism. Reproduced with permission from [220] John Wiley and Sons, Copyright (2017), (Figure A.15).

### 1.7. Monomers

A monomer can be defined as a molecule having an unsaturation which is able to react another unsaturated molecule to generate a macromolecule called a polymer film [177]. Monomers, oligomers or prepolymers are basic components of a photocurable resin. There are many commercially accessible monomers such as acrylates, methacrylates, vinyl ethers, unsaturated polyesters, styrene and N-vinyl pyrrolidone [237]. The type of the monomer or oligomer used in a photopolymerizable formulation determines the properties of the cured film. The properties such as viscosity, reactivity, shrinkage during polymerization, chemical resistance, flexibility, hardness, adhesion, weathering, cost, shelf life, volatility, odor and toxicity can be anticipated just by looking at the chemical structures of the monomers or oligomers.

The characteristics of acrylates and methacrylates such as high photoreactivity, no yellowing property, optical properties, good adhesion, nontacky coatings make them popular monomers in many curing applications [31]. However, acrylates are more preferable than the methacrylates in many light induced free radical polymerization reactions due to their higher reactivity (acrylic > methacrylic > vinylic > allylic) and also availability of broad

range of functional groups such as monofunctional, difunctional, trifunctional and tetrafunctional [238].

The acrylate monomers which are adaptable to use in light curing applications usually have one to four acrylate groups having a molecular weight range of 150-500 (Figure 1.23). The acrylate monomers are generally light colored liquids with a viscosity range of 5-200 centipoise at 25 °C. Acrylate monomers can be used as reactive diluents which may reduce viscosity similar to a solvent and also are capable of reacting with the crosslinker in the resin and becoming a part of the cured film. However, changes in the functionality of the acrylate can affect the properties of the cured product in different way (Table 1.1).

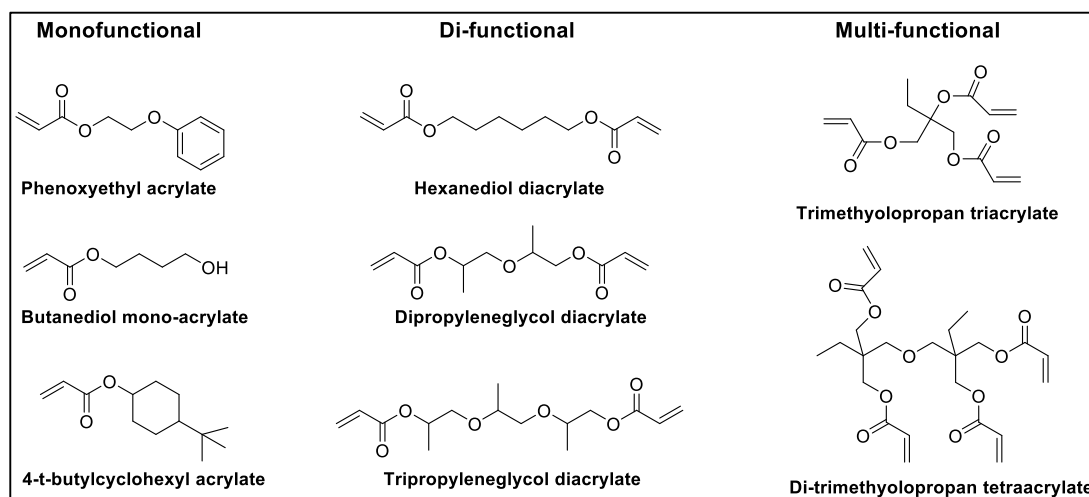


Figure 1.23. Examples of basic acrylate monomers [4].

As seen in Table 1.1, as the functionality of the acrylate monomer increases, the crosslinking density of the photocured material also increases which leads to local viscosity increase and early gelation process. Thus, the “Trommsdorff Effect” which is also known as autoacceleration is seen, since rate of polymerization starts to increase sharply even at the beginning of the polymerization.

Table 1.1. Effects of the functionality of acrylates on their performance [239].

Monomer Type	General Performance Effects
Monofunctional	Reduce crosslinking, lower shrinkage, increase adhesion, best viscosity reduction, can increase residual uncured material; decrease chemical resistance and reactivity
Difunctional	Good compromise between flexibility, hardness, viscosity reduction, chemical resistance and reactivity
Trifunctional and greater	Increase crosslinking, reactivity, hardness, chemical resistance, scratch resistance, shrinkage; decrease flexibility and adhesion; not as effective in reducing viscosity.

### 1.8. Light Sources

Light energy which gives the name to the photopolymerization process plays a crucial role in photocuring applications by triggering the polymerization reaction. The matching between the spectral output of the light source and absorbance wavelength of the photoinitiator is very important for a light cure application to undergo successfully. As the photoinitiator absorbs the light source's emission more intensely, the curing process gets more efficient. Light intensity on the product also affects the rate of the photopolymerization reaction.

There are a wide range of light sources which can have different emission intensity and wavelength properties, thus addressing to the needs of different product properties (cure speed, surface cure, depth of cure etc.) such as xenon lamps, mercury arc lamps, light-emitting diodes (LEDs), laser sources and sun. The light used in photocuring applications generally covers a range of (i) ultraviolet (UV) light (200–400nm range classified as UVA: 320–400nm, UVB: 290–320nm, and UVC: 190–290nm); (ii) visible light (400–700nm); and (iii) near-infrared (IR) light (700–1000nm).

Xenon (Xe) lamps require high electrical power and release a lot of heat but emit photons with high light intensity over a wide spectral range. Mercury arc lamps which are the earliest and the most frequently used UV lamps also emit energy in a broad range of the electromagnetic spectrum from UVC to the IR (blue bars) as shown in Figure 1.24 [239]. Characteristic narrow transitions occur between some of the excited atomic energy levels and ground state. A set of particular wavelengths is thus emitted: 254, 313, 366, 405, 435, 546 and 579 nm. A mercury arc lamp can also be doped with various elements (e.g. xenon, gallium, indium, and iron halides) to modify the emission spectrum, especially to improve the emission intensity in near UV-visible region which are called as doped lamps [1].

LEDs emit energy in the form of photons at specific wavelength range centered at 365 nm (345-385 nm) or 395 nm (380-420 nm) with an intensity about a few 10-100 mW cm<sup>-2</sup>. LEDs have some advantages such as low heat generation (no IR light), energy efficiency, environmental friendliness (no ozone or mercury), low operating costs, less maintenance; a ~50000 h life and portability including possible incorporation in programmed robots that can move the lamps to improve the curing of shadow areas [1].

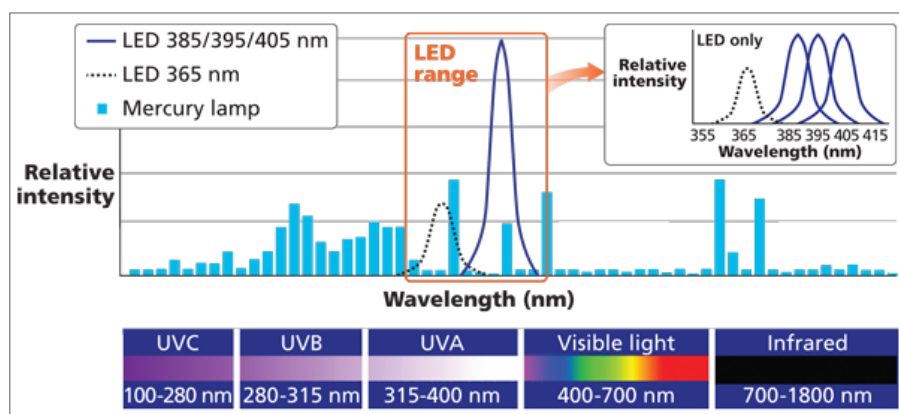


Figure 1.24. Emission spectra of mercury arc lamp and UV LEDs [239].

Lasers also emit energy in the form of photons at specific wavelengths. As in conventional sources, many lasers deliver the light continuously as a function of time. Some lasers can also emit the light as (very) short pulses.

The sun is also very useful and inexpensive light source. It emits photons in the near UV-visible wavelength range but with a low intensity, which of course is also affected by any change in weather, the location or the season of the year.

## 2. OBJECTIVES AND SCOPE

The goal of this study was to create and evaluate novel photoinitiators with “greener” properties: water solubility, migration stability, biocompatibility and visible light operation (no need for UV). For this purpose monomeric, polymeric and mesomolecule (not large enough to be called a macromolecule, but large enough for its diffusion to be negligible) photoinitiators have been designed. The polymerizable/polymeric/large molecule nature is intended to provide the migration stability, the choices of backbone and/or functional groups were made to achieve water solubility, biocompatibility and visible light operation. The photophysical and photochemical properties of the synthesized PIs were investigated, together with the PIs’ effect on some of the properties of the final products.

Different ionic or hydrophilic functional groups (carboxylic acid, bisphosphonate/bisphosphonic acid) and water soluble polymeric backbones (a poly(amido amine) or poly(ethylene imine)) were selected in the design of the new photoinitiators with different aims. In the third chapter, visible light one-component monomeric TX based photoinitiator (TXdMA) with carboxylic acid functionality which may bring surface attachment ability was synthesized. TXdMA can give cyclopolymers upon polymerization, this way it can endow the final polymer with better mechanical properties. In the fourth chapter, water soluble mesomolecule TX and BP based photoinitiators (TXBP and BPBP) having the bisphosphonic acid functionality were synthesized. The incorporation of the bisphosphonic acid group brought hydrophilicity in TX or BP without disturbing their photochemical properties. Besides, the hydroxyl groups on the bisphosphonic acid moiety may act as hydrogen donors which makes them potential one-component PIs. In the fifth chapter, a water soluble photoinitiator (TXBP2) was obtained through incorporation of a bisphosphonate group into TX. The bisphosphonate group will provide biocompatibility and hydrophilicity to the TX photoinitiator. In the six chapter, a water soluble polymeric photoinitiator (PAATX) was synthesized by the introduction of TX functionality into a poly(amido amine) backbone. The PAA backbone not only gives the water solubility and biocompatibility to the novel PI but also the dual curing property which may provide many advantages in terms of product properties.

In the last chapter, water soluble multifunctional PEI based photoinitiators (PEI-I2959 and PEI-I2959-Ts) were fabricated. Enhanced water solubility and better migration stability was attained compared to commercial I2959.

### 3. THIOXANTHONE BASED MONOMERIC PHOTOINITIATOR WITH 1,6-HEPTADIENE STRUCTURE

This chapter is published as: Eren, T. N., B. Graff, J. Lalevee, D. Avci, “Thioxanthone-Functionalized 1,6-Heptadiene as Monomeric Photoinitiator”, *Prog. Org. Coat.*, Vol. 128, pp. 148-156, 2019.

#### 3.1. Introduction

In this chapter, we present a novel PI designed with the considerations of Sect. 1.3 in mind. The photoinitiating ability, including visible-light operation, is given by the TX functionalization, and for migration stability, we have chosen the basic structure of 1,6-heptadiene featuring two active acrylic acid groups, which makes it both polymerizable and crosslinkable; and may bring surface attachment ability due to acid moieties. It also has a hydrogen donating tertiary amine functionality on its structure which can make it a one-component PI. It is well known that polymerization of 1,6-heptadienes proceeds through sequential intermolecular-intramolecular propagation to give cyclopolymers or crosslinked structures depending on concentration and/or temperature [240]. The cyclopolymers or crosslinked polymers obtained have many advantageous properties such as high glass transition temperatures, excellent thermal stabilities, and less shrinkage during polymerization than noncyclic linear analogs; and it might be expected that some of these properties can be carried over to final polymer produced in the photopolymerization reaction.

The photopolymerization efficiency and migration stability along with TX as a reference was studied in the polymerization of trimethylolpropane triacrylate (TMPTA). Photophysical and photochemical properties have also been examined.

## 3.2. Experimental

### 3.2.1. Materials and Methods

2-aminothioxanthone (TXNH<sub>2</sub>) [36] and *tert*-butyl  $\alpha$ -bromomethacrylate (TBBr) [241, 242] were prepared according to literature procedures. Ethyl 4-(dimethylamino)benzoate (EDB), thioxanthone (TX), trimethylolpropane triacrylate (TMPTA), poly(ethylene glycol) diacrylate (PEGDA, M<sub>n</sub> = 250 D) and the other reagents and solvents were purchased from Sigma-Aldrich or Alfa Aesar and used as received without further purification. Di-*tert*-butyldiphenyl iodonium hexafluorophosphate (Iod) was obtained from Lambson.

<sup>1</sup>H and <sup>13</sup>C-NMR spectra were recorded on a Varian Gemini (400 MHz) spectrometer with deuterated methanol (MeOD) as a solvent, and tetramethylsilane as an internal standard. The UV–vis spectra were obtained using a Carry 3 UV/Vis spectrophotometer from Varian. A Nicolet 6700 FT-IR spectrophotometer was used for recording IR spectra. Combi Flash Companion Teledyne ISCO Flash Chromatography with C18 reverse phase column was used for purification of monomers.

### 3.2.2. Synthesis of 2,2'-(((9-oxo-9H-thioxanthen-2-yl)azanediyl)bis(methylene)) diacrylic acid (TXdMA)

To a mixture of 2-aminothioxanthone (0.14 g, 0.6 mmol) and K<sub>2</sub>CO<sub>3</sub> (0.29 g, 2.11 mmol) in dimethylformamide (0.33 mL) and tetrahydrofuran (0.93 mL) under nitrogen, TBBr (0.49 g, 2.22 mmol) was added dropwise in an ice bath. After stirring at 80 °C for 48 h, the solvents were removed under reduced pressure. Dichloromethane (20 mL) was added and the solution was extracted with water (3 × 5 mL). The organic phase was dried over anhydrous sodium sulfate, filtered and the solvent was removed under reduced pressure. The residue was washed with ether and ether was removed under reduced pressure to obtain TXdMA-*t*-Butyl as an orange solid in 75%.

Trifluoroacetic acid (TFA) (0.18 mL, 2.41 mmol) was added dropwise to TXdMA-*t*-Butyl (0.35 g, 0.69 mmol) in an ice bath under nitrogen. The mixture was stirred at room

temperature for 24 h. After removal of excess TFA, the crude product was washed with ether and purified by reverse phase flash chromatography on C18, eluting with MeOH:water (60:40) followed by evaporation of solvents to give pure monomer as a dark orange powder in 25% yield (mp 105 °C). <sup>1</sup>H-NMR (MeOH, 400 MHz, δ): 4.26 (s, 4H, CH<sub>2</sub>-N), 5.51 (s, 2H, CH<sub>2</sub>=C), 6.20 (s, 2H, CH<sub>2</sub>=C), 7.08 (dd, 1H, Ar-CH), 7.39 (m, 1H, Ar-CH), 7.44 (d, 1H, Ar-CH), 7.57 (m, 2H, Ar-CH), 7.66 (d, 1H, Ar-CH), 8.41 (s, 1H, Ar-CH) ppm. <sup>13</sup>C NMR (MeOH, 101 MHz, δ): 52.78 (CH<sub>2</sub>-N), 111.12 (Ar-CH), 120.49 (Ar-CH), 125.75 (CH<sub>2</sub>=C), 126.22 (Ar-C), 127.11 (Ar-CH), 127.51 (Ar-C), 128.42 (Ar-CH), 129.73 (Ar-C), 130.64 (Ar-CH), 130.93 (Ar-CH), 133.48 (Ar-CH), 137.25 (C=CH<sub>2</sub>), 139.64 (Ar-C), 148.24 (Ar-C), 169.54 (C=O acid), 181.65 (C=O ketone) ppm. FTIR (ATR, cm<sup>-1</sup>): 2928 (O-H), 1713 (C=O acid), 1682 (C=O ketone), 1129 (C-N).

### 3.2.3. Computational Procedure

Molecular orbital calculations were carried out by the Gaussian 03 suite of programs. The time dependent density functional theory at B3LYP/6-31+G\* on the relaxed geometries calculated at UB3LYP/6-31G\* level is used to calculate the electronic absorption spectra for the studied PI [243, 244].

### 3.2.4. Photochemical Analyses

3.2.4.1. Steady State Photolysis Experiments. The studied PI was irradiated with the LED@375 nm in the presence and absence of EDB in acetonitrile for predetermined time intervals, and the UV-vis spectra were recorded using a Carry 3 UV/Vis spectrophotometer from Varian spectrophotometer at different irradiation times.

3.2.4.2. Fluorescence Experiments. Fluorescence properties of the PI were investigated in acetonitrile by using JASCO FP-750 Spectrofluorometer. The interaction rate constants between the studied PI and the additives (Iod, EDB) were derived from Stern-Volmer plot using the formula;  $(I_0/I = 1 + k_q\tau_0[Iod])$ , where  $I_0$  and  $I$  symbolize the fluorescence intensity of the photoinitiator in the absence and presence of the quencher (Iod or EDB), respectively and  $\tau_0$  is the singlet excited state lifetime of the PI in the absence of the quencher.

**3.2.4.3. Laser Flash Photolysis.** Nanosecond laser flash photolysis (LFP) experiments were carried out using a Q-switched nanosecond Nd/YAG laser ( $\lambda_{exc} = 355$  nm (9 ns pulses; energy reduced down to 10 mJ; minilite Continuum) and the analyzing system (for absorption measurements) consisted of a ceramic xenon lamp, a monochromator, a fast photomultiplier and a transient digitizer (Luzchem LFP 212) [245].

**3.2.4.4. Cyclic Voltammetry.** The reduction potential ( $E_{red}$  vs SCE) of the studied PI was measured in acetonitrile by cyclic voltammetry. Tetrabutylammonium hexafluorophosphate (0.1 M) was used as a supporting electrolyte (Voltalab 6 Radiometer). The experimental set-up is presented in detail in the literature example [246].

The free energy change  $\Delta G$  for electron transfer between the PI and Iod can be calculated from the classical Rehm-Weller equation:

$$\Delta G = E_{ox} - E_{red} - E_S \text{ (or } E_T) + C \quad (3.1)$$

where  $E_{ox}$ ,  $E_{red}$ ,  $E_S$  (or  $E_T$ ), and  $C$  stand for, respectively, the oxidation potential of the electron donor and the reduction potential of the electron acceptor, the excited singlet (or triplet) state energy of the studied PI, and the electrostatic interaction energy 34hioxan initially formed ion pair, generally considered as negligible in polar solvents) [247].

### 3.2.5. Photopolymerization Experiments

Photo-DSC: Photopolymerization experiments were performed using photo-DSC (Q250, TA Instruments). Monomers (3-4 mg) containing 0.5 mol % photoinitiator were placed on an aluminum DSC pan and equilibrated for 5 min under nitrogen flow to remove oxygen. Then, they were exposed to a light source (Omnicure 2000) (intensity of 200 mW / cm<sup>2</sup>,  $\lambda = 320$ -500 nm) under pure nitrogen flow. All polymerizations were performed at 30 °C for 5 min in duplicate. The heat flow was monitored as a function of time with DSC. The cure speed of polymerization reactions were calculated by using

$$\text{Rate} = \frac{(Q/s)M}{n(\Delta H_p)m} \quad (3.2)$$

where  $Q/s$  is the heat flow per second,  $M$  the molar mass of the monomer,  $n$  the number of double bonds per monomer molecule,  $\Delta H_p$  the heat of reaction evolved and  $m$  the mass of monomer in the sample. The theoretical heat 35hioxan total conversion of an acrylate double bond is 86 kJ/mol [248, 249].

Photopolymerizations were also carried out for a mixture of TMPTA containing 0.5 wt% of TXdMA and 1 wt% of Iod on Al films using a laser diode @405nm (spot size around 50  $\mu$ m) 35hioxan spatially controlled irradiation.

### 3.2.6. Migration Study

PEGDA in the presence of TXdMA/Iod and TX/Iod (1/3 mol%) was photopolymerized under air for 1 hour in glass vials using a photoreactor containing 12 Philips TL 8W BLB lamps ( $\lambda = 365$  nm). The crosslinked polymers were ground into small particles and immersed in 25 mL of methanol for 7 days. The amount of extracted photoinitiators was determined by UV-visible spectroscopy. The concentration of extracted photoinitiator was determined according to the Beer–Lambert law, and the weight ( $m$ ) was calculated by

$$m = M c V_{solution} = MA 10^{-2}/\epsilon l \quad (3.3)$$

where  $\epsilon$  is the molar extinction coefficient of the photoinitiator in acetonitrile,  $l$  is optical path length, and  $M$  is the molecular weight of photoinitiator [24].

## 3.3. Results and Discussion

### 3.3.1. Synthesis and Characterization of TXdMA

A TX-functionalized 1,6-heptadiene (TXdMA) was synthesized as a novel PI in two steps according to Figure 3.1. In the first step, TBBr was reacted 2-aminothioxanthone in the presence of  $K_2CO_3$  to give TXdMA-*t*-Butyl. In the second step, cleavage of *t*-butyl groups of TXdMA-*t*-Butyl using TFA provided TXdMA as a dark orange compound in high yields

(25 %). The crystals of TXdMA melt at 105 °C. This compound's solubility in organic solvents is similar to with TX (Table 3.1), and it has a very good solubility in basic conditions (aq. NaOH) due to formation of salt from its carboxylic acid groups. TXdMA was found to be less compatible with commercial monomers such as TMPTA and HDDA compared to TX which should be taken into consideration when interpreting the photopolymerization results. However, much better compatibility was achieved with PEGDA and HEMA compared to TX.

Table 3.1. Solubilities of TXdMA and TX.

PI	H <sub>2</sub> O	Methanol	Ether	CH <sub>2</sub> Cl <sub>2</sub>	THF	DMF
TX	-	+	-	+	+	+
TXdMA	-	+	-	-	+	+

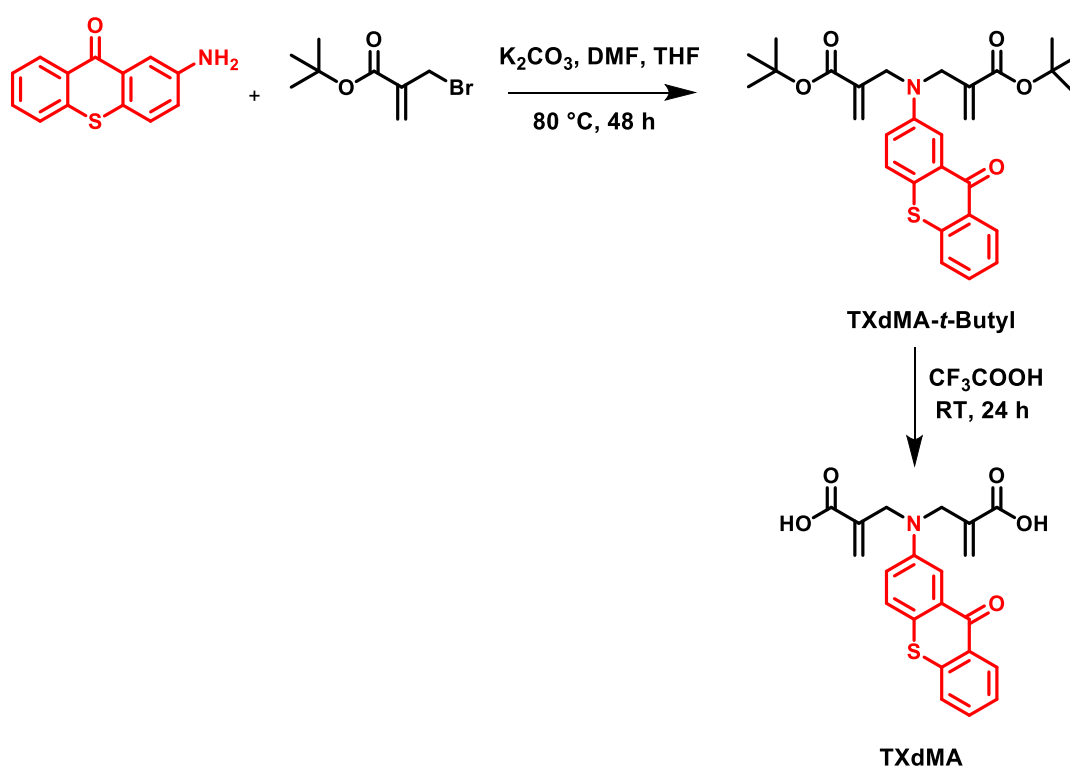


Figure 3.1. Synthesis route for the novel photoinitiator TXdMA.

The structure of the novel photoinitiator TXdMA was confirmed by  $^1\text{H}$ ,  $^{13}\text{C}$  NMR and FTIR spectroscopy (Figure 3.2).  $^1\text{H}$  NMR spectrum shows both the peaks for methylene groups at 4 ppm and the acrylate protons at 5.51, 6.20 ppm as singlets and also the specific signals of the thioxanthone aromatic ring between 7.08 and 8.41 ppm. FTIR spectrum shows two different C=O peaks due to carboxylic acid ( $1713\text{ cm}^{-1}$ ) and ketone ( $1682\text{ cm}^{-1}$ ) groups.

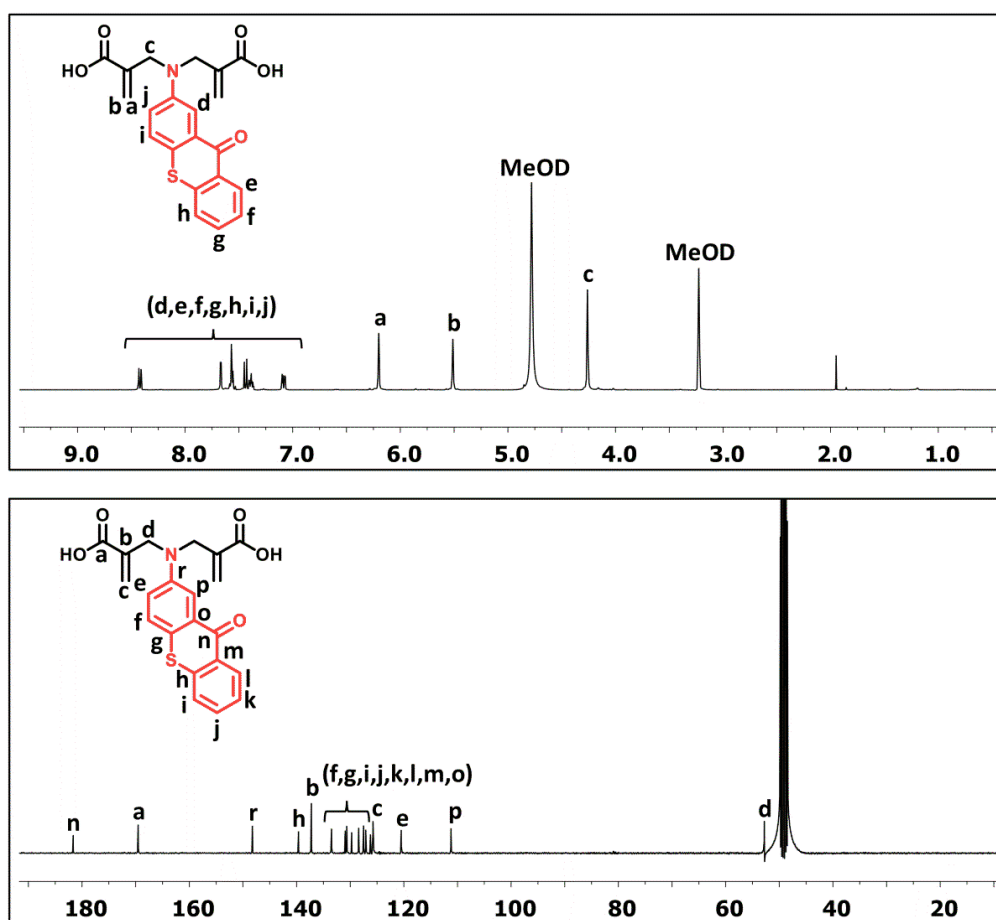


Figure 3.2.  $^1\text{H}$  and  $^{13}\text{C}$  NMR spectra of TXdMA.

### 3.3.2. Light Absorption

UV-Vis absorption spectroscopy of TXdMA in different solvents is given in Figure 3.3. Absorption maximum ( $\lambda_{\text{max}}$ ) and molar extinction coefficient values ( $\epsilon$ ) of TXdMA and TX as reference in different solvents are reported in Table 3.2.  $\lambda_{\text{max}}$  of TXdMA shows significant shifts in different solvents. Maximum absorption wavelength of TXdMA was

found to be 435-439 nm, hence shows a strong bathochromic shift compared to the reference TX with  $\lambda_{\text{max}} = 380$  nm, which may be due to the auxochromic effect of electron donating tertiary amino group attached to TX chromophore [250, 251]. Therefore, TXdMA allows better coverage of the emission spectra of the visible light sources and can be used with different types of lamp.

The optimized geometries and also the frontier orbital (highest occupied molecular orbital (HOMO) and lowest unoccupied molecular orbital (LUMO) calculations were carried out by using time dependant density functional theory (TDDFT) at B3LYP/6-31G\* level (Figure 3.3). Interestingly, a strong participation of the amino substituent is observed in the HOMO but the LUMO remains located on the thioxantone moiety suggesting a charge transfer behavior in agreement with the observed bathochromic shift compared to TX.

TXdMA, bearing strongly electron donating dialkylamino group and electron accepting TX functionality was expected to have a convenient architecture to exhibit fluorescence properties. Its fluorescence emission property in different solvents was examined by a spectrofluorometer after the excitation with the wavelength of 355 nm, as can be seen in Figure 3.4. A notable change was also observed in the fluorescence spectra with solvent polarity. As solvent polarity increases, a red shift (58 nm) is observed in  $\lambda_{\text{max}}$  values;  $\lambda_{\text{max}}$  (in 38hioxan, 0.36 D) = 498 nm,  $\lambda_{\text{max}}$  (in acetonitrile, 3.92 D) = 516 nm due to the change in molecular environment which indicates redistribution of charge upon excitation in agreement with the charge transfer character observed above 38hioxan lowest energy transition [252]. Also, it was observed that in aprotic solvents acetonitrile shows higher fluorescence intensity compared to 38hioxan. In a polar protic solvent, methanol (1.70 D), two bands are seen,  $\lambda_{\text{max}} = 497, 556$  nm, the short wavelength emission may correspond to typical  $\pi-\pi^*$  transition, and the long wavelength emission indicating a CT fluorescence. The absorption and emission spectra of TXdMA in acetonitrile are shown in Figure 3.4. The crossing point of these spectra allows the determination of the first singlet excited state energies ( $E_{S1} = 2.63$  eV). The Stokes shifts ( $123456$   $\text{cm}^{-1}$ ) reported in Table 3.2 were large.

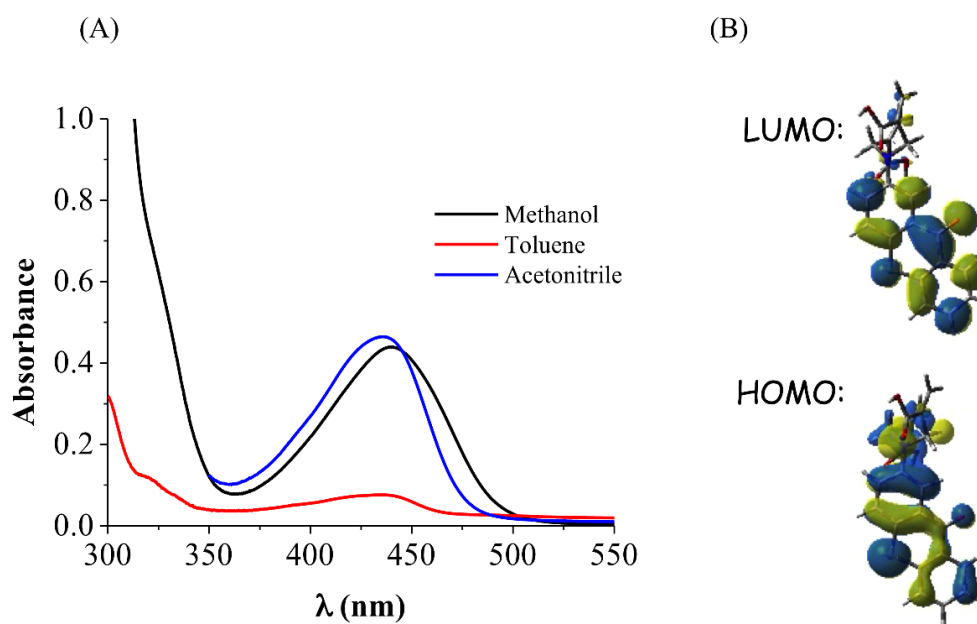


Figure 3.3. (A) UV-visible absorption spectra of TXdMA in different solvents ( $1.3 \times 10^{-4}$  M); (B) Frontier orbitals (HOMO-LUMO) calculated on the B<sub>3</sub>LYP/6-31 G\* level for TXdMA.

Table 3.2. Absorption characteristics of TXdMA in selected solvents.

PI	Solvents	$\lambda_{\text{abs}}$ [nm]	$\lambda_{\text{em}}$ [nm]	Stokes shift [cm <sup>-1</sup> ]	$\epsilon$ (M <sup>-1</sup> cm <sup>-1</sup> )
TX	DMF	380	-	-	5890
TXdMA	Acetonitrile	435	516	123456	3590
TXdMA	MeOH	439	497, 556	-	3380
TXdMA	Toluene	435	498	-	600

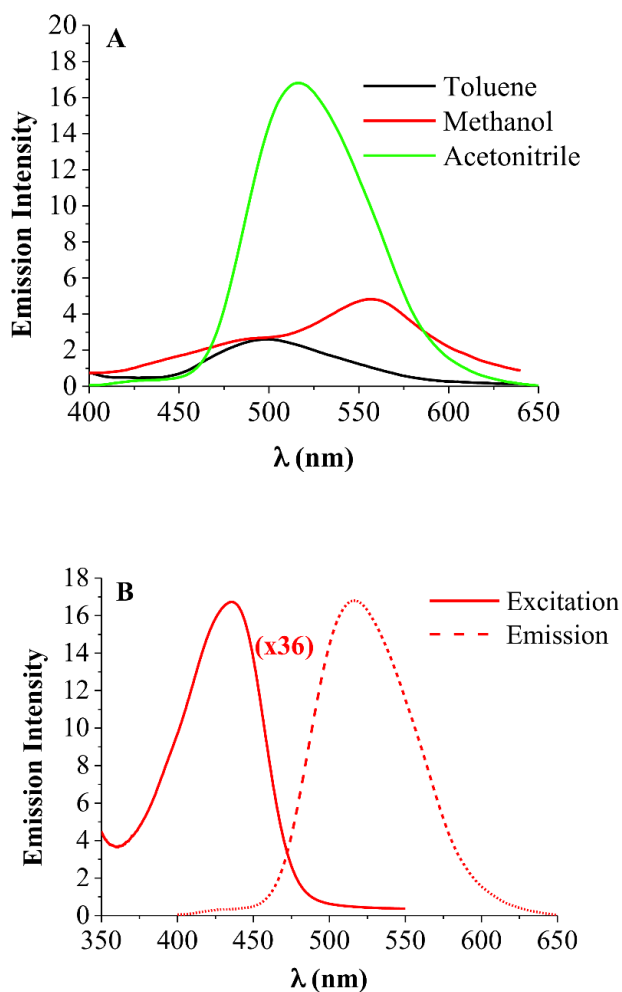


Figure 3.4. (A) Fluorescence spectra of TXdMA in different solvents ( $1.3 \times 10^{-4}$  M)  $\lambda_{\text{exc}} = 355$  nm; (B) Absorption (solid lines) and corrected emission (dashed lines) spectra of TXdMA dissolved in acetonitrile. Solutions were excited at  $\lambda_{\text{exc}} = 355$  nm. Absorption spectrum was multiplied by the indicated factor. The concentration of TXdMA is  $1.3 \times 10^{-4}$  M.

### 3.3.3. Photochemical Mechanisms

3.3.3.1. Steady State Photolysis. TXdMA is expected to undergo photolysis in the absence of hydrogen donors because of a hydrogen-donating tertiary amine group in its structure. The photolysis of TXdMA in acetonitrile at 375 nm in the presence and absence of EDB was investigated (Figure 3.5). In both cases, a decrease with time in absorption maxima was

observed, indicating the efficiency of both TXdMA and TXdMA/EDB in terms of photoreactivity. Although the photolysis of TXdMA/EDB is slightly faster compared to TXdMA, TXdMA has a potential to be used as one-component polymerizable visible light photoinitiator.

In general, during the photolysis of thioxanthone compounds, the PI absorbs photon to produce an excited singlet state which could pass into an excited triplet state  $^3\text{PI}$  through intersystem crossing and interact with the amine group. The electron transfer followed by the proton transfer produce an amino alkyl radical and a thioxanthyl ketyl radical. Actually a small shoulder peak (around 380 nm) observed after 7 (in the presence of EDB) and 17 min (in the absence of EDB) may be due photoproducts associated with aminoalkyl and ketyl radicals. This ketyl radical was reported to absorb around 330–370 nm by Amirzadeh et al. [253]. The thioxanthyl ketyl radicals are not reactive in polymerization reactions due to steric hindrance and delocalization of unpaired electrons, whereas aminoalkyl radicals can initiate polymerizations. The red-shift in our systems may be attributable to the aminoalkyl substituent which could act as electron donors [254].

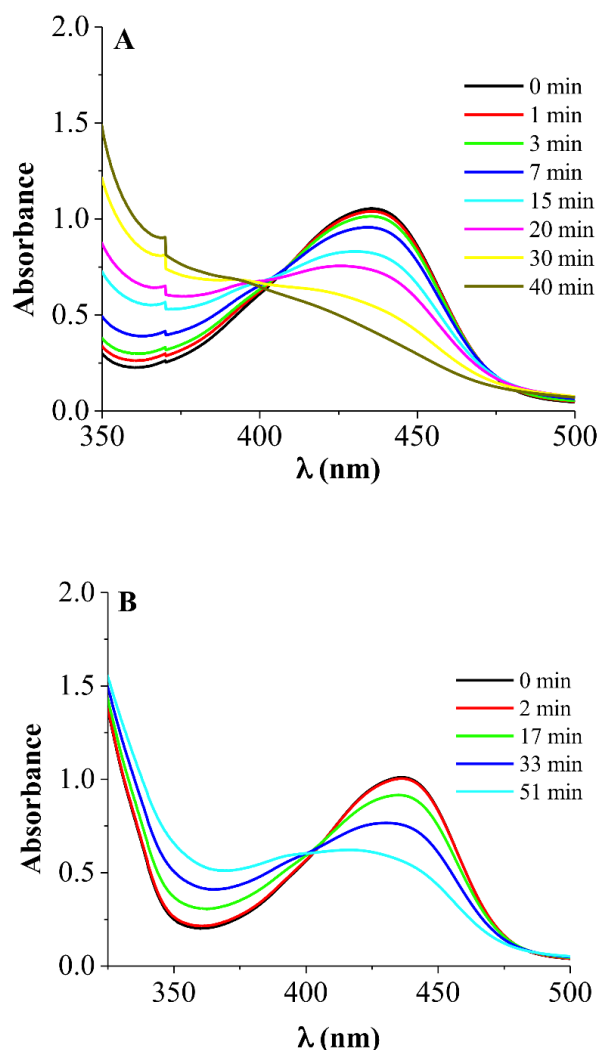


Figure 3.5. Photolysis of TxdMA ( $2.78 \times 10^{-4}$  M) in acetonitrile in the presence (A) and absence (B) of EDB ( $1.38 \times 10^{-3}$  M).

3.3.3.2. Fluorescence Quenching, Laser Flash Photolysis (LFP), Cyclic Voltammetry Experiments. The fluorescence quenching study was carried out to follow the quenching process between the singlet excited state of the photoinitiator and quencher (Iod) at different quencher concentration (Figure 3.6A). A fast fluorescence quenching with a linear Stern–Volmer plot over the used range of Iod concentrations ( $R^2 = 0.99$ ) was observed (Figure 3.6B). Stern–Volmer quenching coefficient,  $K_{sv}$ , obtained from the slope, is  $90.8 \text{ M}^{-1}$ . The fluorescence quenching rate constant ( $k_q$ ) allows evaluation of the interaction of the TX singlet with the Iod in the polymerization medium and is given by the equation of  $k_q = K_{sv}/\tau$ .

Fluorescence lifetime (s) values were measured to be 20 ns in the absence of quencher. And the quenching rate constants ( $k_q$ ) are calculated to be  $4.54 \times 10^9 \text{ s}^{-1} \text{ M}^{-1}$  (Table 3.4). The quenching rate constant  $k_q$  could relate to the energetics of electron transfer between the singlet excited state of photoinitiator and the quencher Iod. This  $k_q$  value is very close to the rate constant of the diffusion-controlled reaction rate. The electron transfer quantum yields in the excited singlet state  $\phi_{\text{et}(S_1)}$  were calculated by

$$\phi_{\text{et}} = K_{\text{sv}}[\text{Iod}]/(1+K_{\text{sv}}[\text{Iod}]). \quad (3.4)$$

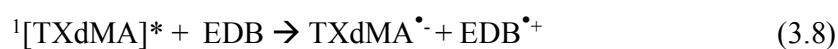
The singlet state pathway is clearly predominant (vs. triplet state) as the electron transfer quantum yield from  $S_1$  is already very high (0.8).

In general, the TXdMA/Iod interaction corresponds to an electron transfer reaction finally leading to an aryl radical  $\text{Ar}\cdot$  which can be seen in



$\text{Ar}\cdot$  and  $\text{TXdMA}^{\bullet+}$  can be considered as the initiating species for the radical polymerization and the cationic polymerization, respectively,

Fluorescence quenching in the presence of EDB was also studied (Figure 7C). In general, the TXdMA/EDB interaction should lead to an electron transfer reaction between EDB and TXdMA followed by the formation of  $\text{EDB}^{\bullet(-\text{H})}$  (8, 9) capable of initiating the free radical polymerization in TXdMA/EDB PIs which can be seen in



Laser flash photolysis experiments show that TXdMA probably reacts through a singlet state pathway i.e. contrary to TX, the triplet state absorption is very weak for TXdMA and the fluorescence quenching for TXdMA is high. The redox potential of TXdMA was measured in acetonitrile by cyclic voltammetry (CV) (Figure 3.6E). The free energy change  $\Delta G_{\text{et}}$  for the electron transfer reaction between TXdMA as electron donor and Iod as an electron acceptor was calculated from the classical Rehm–Weller equation (Equation (3.1)) and using the oxidation potentials  $E_{\text{ox}}$  and the excited state energies  $E_{\text{S1}}$  of TXdMA (Table 3.3 and Table 3.4).

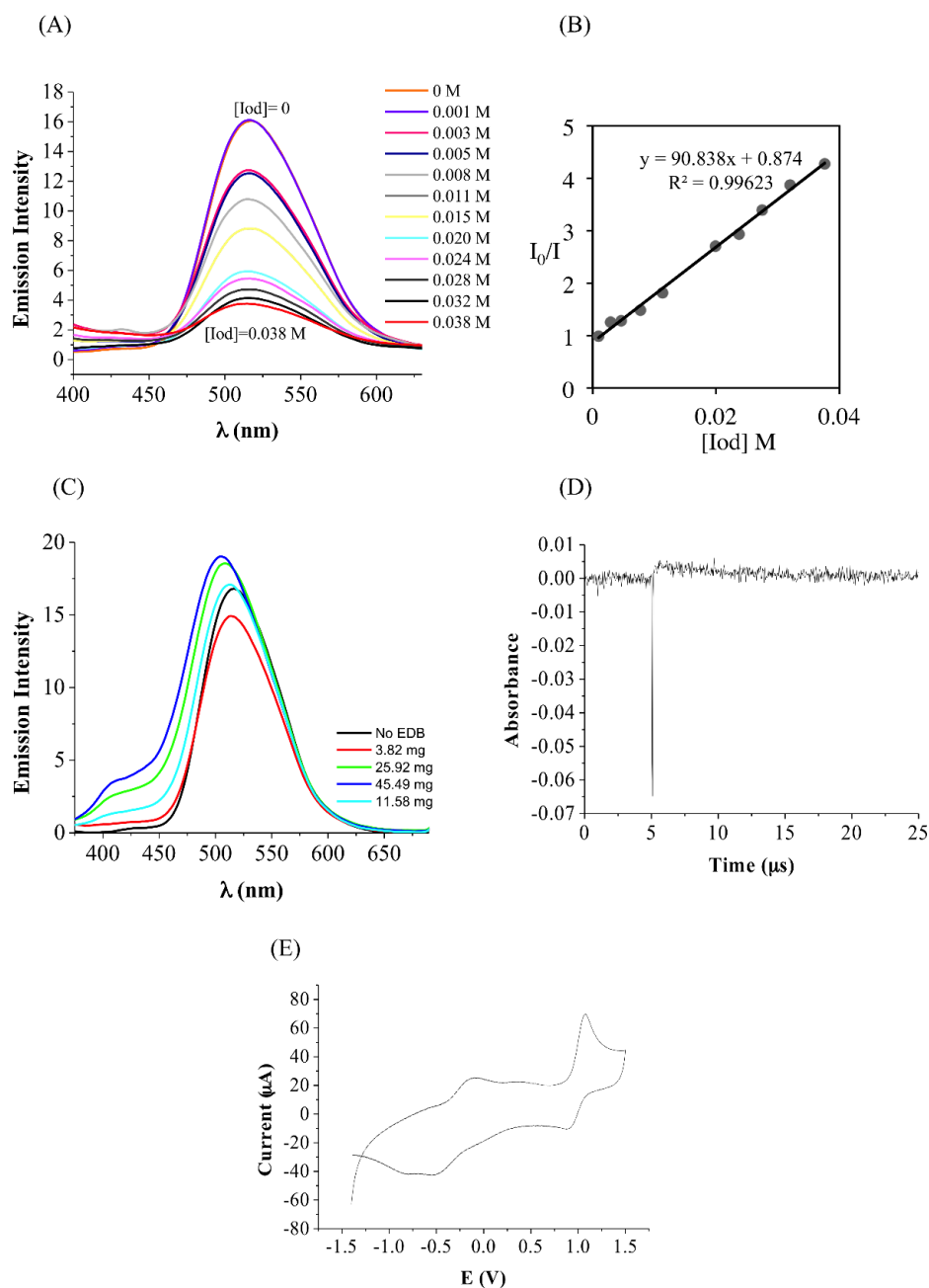


Figure 3.6. (A) The fluorescence quenching of TXdMA in acetonitrile solution ( $1.32 \times 10^{-4}$  M) with different concentration of Iod; (B) Stern-Volmer plot; (C) The fluorescence quenching of TXdMA in acetonitrile solution ( $1.32 \times 10^{-4}$  M) with different concentration of EDB; (D) Kinetic for TXdMA in LFP experiments (laser excitation for  $t = 5 \mu$ s); (E) Oxidation potential determination of TXdMA in acetonitrile.

Table 3.3. Photophysical/photochemical and electrochemical properties of TXdMA.

PI	$E_{ox}$ [eV]	$E_T$ [eV]	$E_{S1}$ [eV]	$\tau^{a(N2)}$ [ns]
TXdMA	0.97	2.41	2.63	20

<sup>a</sup> $\tau$  = fluorescence lifetime.

Table 3.4. Parameters characterizing the chemical mechanisms associated with the TXdMA/Iod system in acetonitrile.

PI	$\Delta G_{S1}^a$ [eV]	$K_{SV}$ [M <sup>-1</sup> ]	$k_q$ [M <sup>-1</sup> s <sup>-1</sup> ]	$\Phi_{(et)}$	$\Delta G_{T1}^a$ [eV]
TXdMA/Iod	-1.46	90.8	4.54x10 <sup>9</sup>	0.8	-1.24

<sup>a</sup>Reduction potential of -0.2 V is used for Iod.

### 3.3.4. Photopolymerization

The photopolymerization efficiency of TXdMA in the polymerization of TMPTA and PEGDA in the presence and absence of additives (EDB, Iod) was tested and TX was used for comparison. Figure 3.7 presents the rate-time and conversion-time plots for the polymerization of TMPTA photoinitiated by TXdMA and TX under the same conditions. TXdMA containing solutions were not clear, unlike the TX containing ones. Insoluble PI particles may decrease the penetration of light (internal filter effect) and decrease performance of TXdMA compared to TX.

According to the results; TXdMA exhibits low photoinitiation activity by itself,  $R_{pmax} = 0.004 \text{ s}^{-1}$ ,  $t_{max} = 0.47 \text{ min}$ , conversion = 31%, indicating that the tertiary amine group of TXdMA is not efficient in producing aminoalkyl radicals.

The addition of an amine (EDB) did not change its photoinitiation activity significantly in agreement with the low quenching of <sup>1</sup>TXdMA observed above ( $R_{pmax} = 0.012 \text{ s}^{-1}$ ,  $t_{max} = 0.16 \text{ min}$ , conversion = 37% for TXdMA/EDB). However, TX/EDB system works

efficiently in the polymerization of TMPTA with  $R_{pmax}$  (final conversions) of  $0.058\text{ s}^{-1}$  (41%). Similar behavior was observed by Yagci et al. when thioxanthone-fluorene carboxylic acid was used as PI and amines as coinitiators. This unexpected behavior was explained by the acid-base salt forming reaction which decreased the electron donating power of the coinitiator [255]. Also, sterically hindered structure of TXdMA may cause a slow intramolecular H-abstraction process.

Photopolymerization of TMPTA in the presence of TXdMA/Iod couple was found to be highly efficient with enhanced  $R_{pmax}$  value of  $0.058\text{ s}^{-1}$ , conversion of 44% and the decreased  $t_{max}$  value of 0.02 min. This system exhibits slightly higher efficiency than TX/EDB and TX/Iod systems. All these results clearly indicate that TXdMA is quite efficient in photooxidation process (electron transfer from TXdMA to Iod) but not in photoreduction process (electron transfer from EDB to TXdMA).

Polymerization of PEGDA in the presence of TXdMA was also carried out in order to investigate performance of TXdMA in a clear solution (Figure 3.8). PEGDA was also selected since it has hydrogen donating properties due to its ether structure. However, a similar trend with TMPTA was observed when TXdMA/Iod or TXdMA/EDB systems were used as PIs. For example, the performances of TXdMA/Iod and TX/Iod couples were found to be very high. Some laser write experiments were also carried out using a laser diode @405 nm to show the good initiating ability of the TXdMA/Iod (0.5/ 1% w/w) system in TMPTA upon visible light (Figure 3.7B).

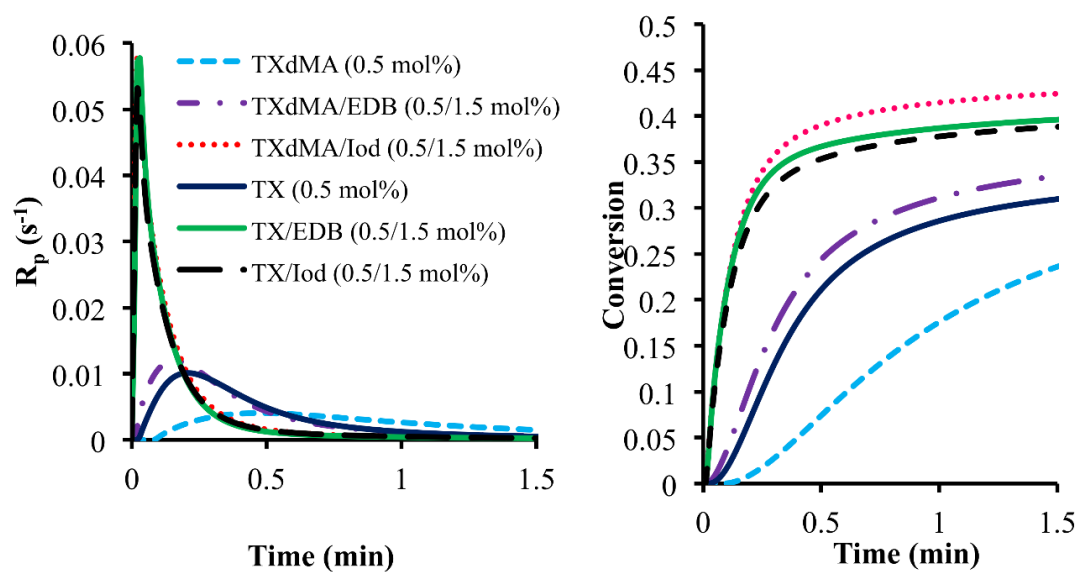


Figure 3.7. (A) Rate-time and conversion-time plots for the photopolymerization of TMPTA under nitrogen at 30 °C,  $\lambda = 320-500$  nm in the presence of TXdMA, TXdMA/EDB, TXdMA/Iod, TX, TX/EDB and TX/Iod and (B) laser write experiments using a laser diode @405 nm.

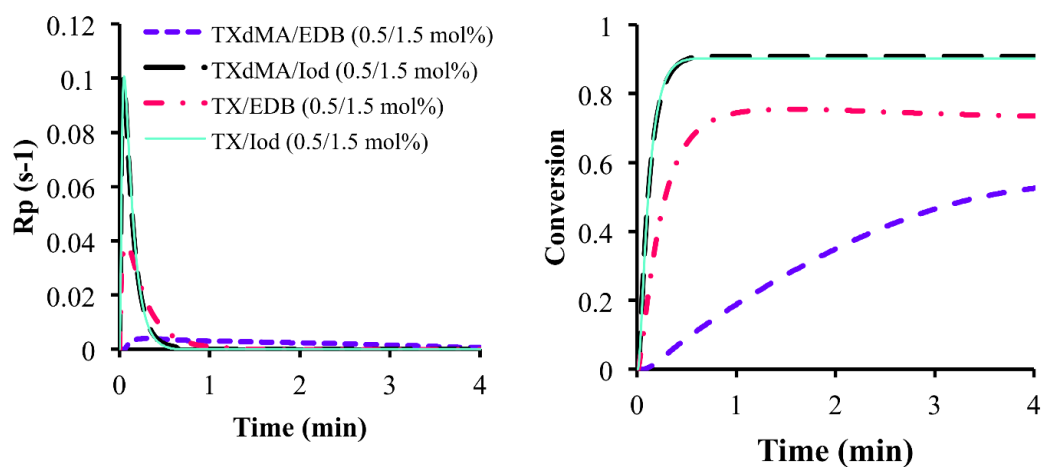


Figure 3.8. Rate-time and conversion-time plots for the photopolymerization of PEGDA under nitrogen at 30 °C,  $\lambda = 320\text{-}500$  nm in the presence of TXdMA/EDB, TXdMA/Iod, TX/EDB and TX/Iod.

### 3.3.5. Migration Stability

To investigate migration stability of TXdMA, PEGDA polymers were prepared with TXdMA and TX and extracted by methanol. The amount of the extracted PIs was determined using UV-vis spectroscopy in methanol. As shown in Figure 3.9, the residual free TXdMA amount is lower than that of TX, with the extracted mass fraction of 58 and 19% for TX and TXdMA, indicating incorporation of TXdMA through copolymerization with PEGDA. Therefore, TXdMA can be used to decrease the toxicity of the cured film.

Incorporation of the PI into the network was further investigated by thermogravimetric analysis of the PEGDA networks produced using 5/10 mol% of TXdMA/Iod, with a similar network produced using TX/Iod as reference. It was observed that the former started to decompose at 370 while the latter at 350 °C. This result is consistent with the expectation of higher thermal stability due to formation of cyclopolymers or crosslinked structures, outlined in the Introduction section.

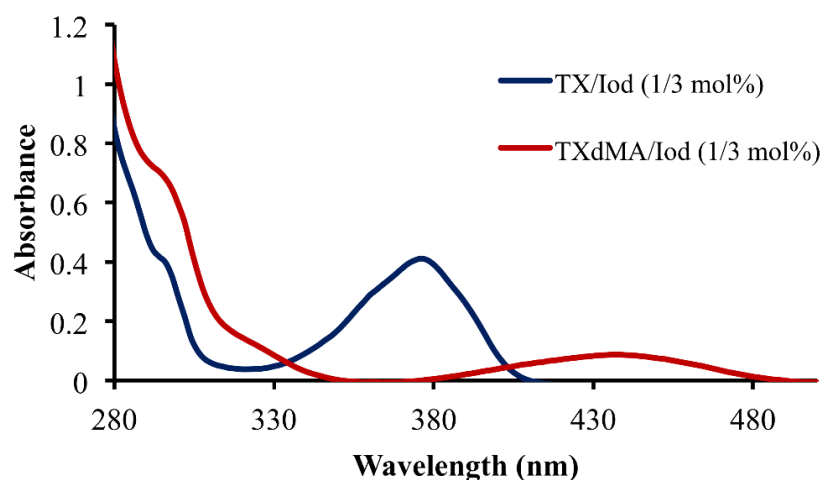


Figure 3.9. UV-vis absorption spectra of TX and TXdMA extracted with MeOH from the PEGDA polymer samples.

### 3.4. Conclusions

The synthesis of TXdMA, the first TX-based monomeric photoinitiator with 1,6-heptadiene structure was reported. It has a maximum absorption wavelength around 435-439 nm which allows better coverage of the emission spectra of the visible light sources compared to TX. TXdMA is fluorescent due to the strongly electron donating dialkylamino group and electron accepting TX functionality and has a singlet state (S1) lifetime of 20 ns and efficiently initiates free radical polymerization of acrylates (PEGDA and TMPTA) in the presence of an iodonium salt. Its photoinitiating efficiency was found to be similar to that of TX, but has a very good migration stability compared to TX and a bathochromic shift for longer wavelength excitation. TXdMA does not just catalyze a polymerization reaction, but may also influence the properties of the final polymer they get incorporated into.

## 4. WATER-SOLUBLE BISPHOSPHONIC ACID-FUNCTIONALIZED TYPE-II PHOTOINITIATORS

This chapter is published as: Eren, T. N., J. Lalevee, D. Avci, “Bisphosphonic Acid-Functionalized Water-Soluble Photoinitiators”, *Macromol. Chem. Phys.*, Vol. 220, pp. 1900268-1900278, 2019.

### 4.1. Introduction

The photoinitiators presented in this chapter, TXBP and BPBP, focus on the water-solubility aspect of the green theme. The introduction of the bisphosphonic acid group has brought water solubility to TX or benzophenone, which themselves lack this property. This was done without disturbing their photochemical properties, including their excellent absorption characteristics [2]. Furthermore, the OH groups on the bisphosphonic acid moiety may act as hydrogen donors, making them potential one-component PIs. The photopolymerization properties of TXBP and BPBP were determined by studying the polymerization of the aqueous solution of poly(ethyleneglycol) diacrylate (PEGDA). The novel photoinitiators were also investigated in terms of photophysical and photochemical aspects.

### 4.2. Experimental

#### 4.2.1. Materials and Methods

2-((9-oxo-9H-thioxanthen-2-yl)oxy)acetic acid (TXCH<sub>2</sub>COOH) was prepared according to a literature procedure [256]. 3-benzoylbenzoic acid, oxalyl chloride, tris(trimethylsilyl) phosphite, ethyl 4-(dimethylamino)benzoate (EDB), thioxanthone (TX), poly(ethylene glycol) diacrylate (PEGDA, Mn = 250 D), I2959, acrylamide (AAm) and the other reagents and solvents were purchased from Sigma-Aldrich or Alfa Aesar and used as

received without further purification. Bis-(4-tert-butylphenyl)-iodonium hexafluorophosphate (SpeedCure938 or Iod) was obtained from Lambson Ltd.

$^1\text{H}$  and  $^{13}\text{C}$ -NMR spectra were recorded on a Varian Gemini (400 MHz) spectrometer with deuterated methanol (MeOD) as a solvent, and tetramethylsilane as an internal standard. A Nicolet 6700 FT-IR spectrophotometer was used for recording IR spectra.

#### 4.2.2. Syntheses of PIs: General Procedure for the Synthesis of BPBP and TXBP

To a solution of 3-benzoylbenzoic acid or 2-((9-oxo-9H-thioxanthen-2-yl)oxy)acetic acid (0.66 mmol) in dry dichloromethane (0.8 mL), oxalyl chloride (0.22 g, 0.15 mL) in dry dichloromethane (1.16 mL) was added dropwise in an ice bath under nitrogen. Then six drops of DMF solution (0.2 mL of DMF in 1 mL of dry dichloromethane) was added and the mixture was stirred for half an hour in an ice bath and three and half hours at room temperature. After removal of the solvent, the crude acid chloride was used in the next step without further purification.

To the acid chloride (0.66 mmol) in dry THF (0.1 mL), tris(trimethylsilyl)phosphite (1.33 mmol, 0.39 mL) was added and the mixture was stirred at room temperature for 1 h. The mixture was evaporated to dryness, followed by methanol (1 mL) addition and stirring of the mixture 1 h at room temperature. After solvent removal, the residue was washed with diethyl ether (2 x 20 mL) to remove  $\text{H}_3\text{PO}_3$  and then the pure product was obtained in 85-88% yield as a white (BPBP) or orange (TXBP) solid after the removal of ether under reduced pressure. BPBP:  $^1\text{H}$ -NMR ( $\text{D}_2\text{O}$ , 400 MHz,  $\delta$ ): 7.58 (m, 3H, Ar-CH), 7.73 (dd,  $J = 15.1, 7.7$  Hz, 2H, Ar-CH), 7.82 (d,  $J = 7.1$  Hz, 2H, Ar-CH), 8.10 (d,  $J = 7.4$  Hz, 1H, Ar-CH), 8.20 (s, 1H, Ar-CH) ppm;  $^{13}\text{C}$  NMR ( $\text{D}_2\text{O}$ , 101 MHz,  $\delta$ ): 75.66 (C-OH), 127.74 (Ar-CH), 127.99 (Ar-CH), 128.29 (Ar-CH), 129.20 (Ar-CH), 130.22 (Ar-CH), 130.72 (Ar-CH), 133.30 (Ar-CH), 136.25 (Ar-C), 136.45 (Ar-C), 137.03 (Ar-C), 200.69 (C=O ketone) ppm; IR (ATR): 3395 (O-H), 1635 (C=O), 1286 (P=O), 916, 951 (P-O)  $\text{cm}^{-1}$ ; UV-vis (MeOH):  $\lambda_{\text{max}}$  ( $\epsilon$ ) = 254 (11740), 338 nm (123); Q-Tof-MS ( $m/z$ ): Calcd for  $\text{C}_{14}\text{H}_{14}\text{O}_8\text{P}_2$ , 372.21. Found: 373.02 [M+H] $^+$ . TXBP:  $^1\text{H}$ -NMR (MeOD, 400 MHz,  $\delta$ ): 4.51 (t,  $J = 10.6$  Hz, 2H,  $\text{CH}_2\text{-O}$ ), 7.39 (dd,  $J = 8.7, 2.7$  Hz, 2H, Ar-CH), 7.50 (d,  $J = 8.7$  Hz, 1H, Ar-CH), 7.56 (d,  $J$

= 4.4 Hz, 2H, Ar-CH), 7.97 (s, 1H, Ar-CH), 8.40 (d,  $J = 8.1$  Hz, 1H, Ar-CH) ppm;  $^{13}\text{C}$  NMR (MeOD, 101 MHz,  $\delta$ ): 72.15 (CH<sub>2</sub>-C-OH), 113.08 (C-OH), 124.78 (Ar-CH), 126.76 (Ar-CH), 127.54 (Ar-CH), 128.82 (Ar-CH), 129.67 (Ar-C), 130.63 (Ar-C), 131.32 (Ar-CH), 133.83 (Ar-C), 135.71 (Ar-CH), 139.27 (Ar-CH), 159.34 (Ar-C), 181.22 (C=O ketone) ppm; IR (ATR): 3385 (O-H), 1632 (C=O), 1216 (P=O), 930, 1001 (P-O) cm<sup>-1</sup>; UV-vis (MeOH):  $\lambda_{\text{max}}$  ( $\epsilon$ ) = 395 (4393); Q-ToF-MS (m/z): Calcd for C<sub>15</sub>H<sub>14</sub>O<sub>9</sub>P<sub>2</sub>S, 432.28. Found: 432.99 [M+H]<sup>+</sup>.

### 4.2.3. Photochemical Analyses

4.2.3.1. UV-vis Spectroscopy Experiments. UV-vis measurements of the PIs in water, THF and methanol were carried out on a Carry 3 UV/vis spectrophotometer from Varian. For steady-state photolysis experiments, solutions of PIs were irradiated with a LED (385 nm) in the presence and absence of co-initiators (EDB, Iod). Samples were taken at predetermined time intervals, and the UV-vis spectra were recorded.

4.2.3.2. Fluorescence Experiments. Fluorescence properties of TXBP were investigated in methanol using JASCO FP-6200 Spectrofluorometer. The interaction rate constants between PI and the additives (Iod, EDB) were derived from the Stern-Volmer plot using the formula; ( $I_0/I = 1 + k_q\tau_0[\text{Iod}]$ ), where  $I_0$  and  $I$  symbolize the fluorescence intensity of the photoinitiator in the absence and presence of the quencher (Iod or EDB), respectively and  $\tau_0$  is the singlet excited state lifetime of the PI in the absence of the quencher.

4.2.3.3. Laser Flash Photolysis. Q-switched nanosecond Nd/YAG laser ( $\lambda_{\text{exc}} = 355$  nm (9 ns pulses; energy reduced down to 10 mJ; minilite Continuum) and the analyzing system (for absorption measurements) consisted of a ceramic xenon lamp, a monochromator, a fast photomultiplier and a transient digitizer (Luzchem LFP 212) were used to perform nanosecond laser flash photolysis (LFP) experiments [245].

4.2.3.4. ESR Spin Trapping (ESR-ST) Experiments. ESR-ST experiments were carried out using a Bruker EMX-plus spectrometer (X-band). The radicals were generated at room temperature upon irradiation by LED at 365 nm under N<sub>2</sub>. The radicals generated were trapped by phenyl-N-*tert*-butylnitron (PBN) according to a procedure described in detail in

the literature [257]. The ESR spectra simulations were carried out using the WINSIM software.

#### 4.2.4. Photoinitiating Activity Measurements

Photo-DSC: Photo-DSC analysis was performed with a TA Instruments DSC 250 differential photo calorimeter using an Omnicure 2000 mercury lamp light source with a 320-500 nm filter. PEGDA-water (80-20 wt%) mixtures (4-5 mg) containing 0.5 mol% PI and 1.5 mol% co-initiator (EDB or Iod) were irradiated at 25 °C under nitrogen for 5 min. The heat flow was monitored as a function of time with DSC. The cure speed of polymerization reactions was calculated by

$$\text{Rate} = \frac{(Q/s)M}{n(\Delta H_p)m} \quad (4.1)$$

where  $Q/s$  is the heat flow per second,  $M$  the molar mass of the monomer,  $n$  the number of double bonds per monomer molecule,  $\Delta H_p$  the heat of reaction evolved and  $m$  the mass of monomer in the sample. The theoretical heat for the total conversion of an acrylate double bond is 86 kJ/mol [248, 249].

Photoreactor: A solution of BPBP or TXBP (0.0015 mmol) in 0.5 mL of water was added to AAm (0.5 mmol). The solution was placed into a Pyrex tube and irradiated in a photoreactor containing 12 Philips TL 8W BLB lamps, exposing it to UV light (365 nm) for 15-30 min in the presence and absence of co-initiators (TEA and sesamol, 0.0045 mmol) in an air atmosphere. Poly(acrylamide) formed was precipitated in 10-fold excess acetone and dried in vacuum. Conversions were calculated gravimetrically.

### 4.3. Results and Discussion

#### 4.3.1. Syntheses of BPBP and TXBP

Two new photoinitiators (BPBP and TXBP) were synthesized in two steps as shown in Figure 4.1. In the first step, 3-benzoylbenzoyl chloride or 2-((9-oxo-9H-thioxanthen-2-

yl)oxy)acetyl chloride was synthesized from the reaction of 3-benzoyl benzoic acid or 2-((9-oxo-9H-thioxanthen-2-yl)oxy)acetic acid and oxalyl chloride. The acid chloride derivatives were then reacted with tris(trimethylsilyl)phosphite using a procedure described by Guenin et al and Egorov et al [258, 259]. BPBP and TXBP were obtained in 85 to 88 % yield after purification. They are soluble in water, which is a very important property for water-based formulations (Table 4.1). BPBP shows excellent solubility (28 g/L) in water at ambient temperature, compared to TXBP (0.05 g/L) and also the commercial PI I2959 (5 g/L) [148]. They also have a very good solubility in basic conditions (aq. NaOH) due to the formation of bisphosphonic acid salts. For example, solubility of BPBP increased to 53 g/L in 1.25 M NaOH. PIs are not compatible with commercial monomers such as TMPTA and HDDA. However, much better compatibility was achieved with PEGDA and HEMA.

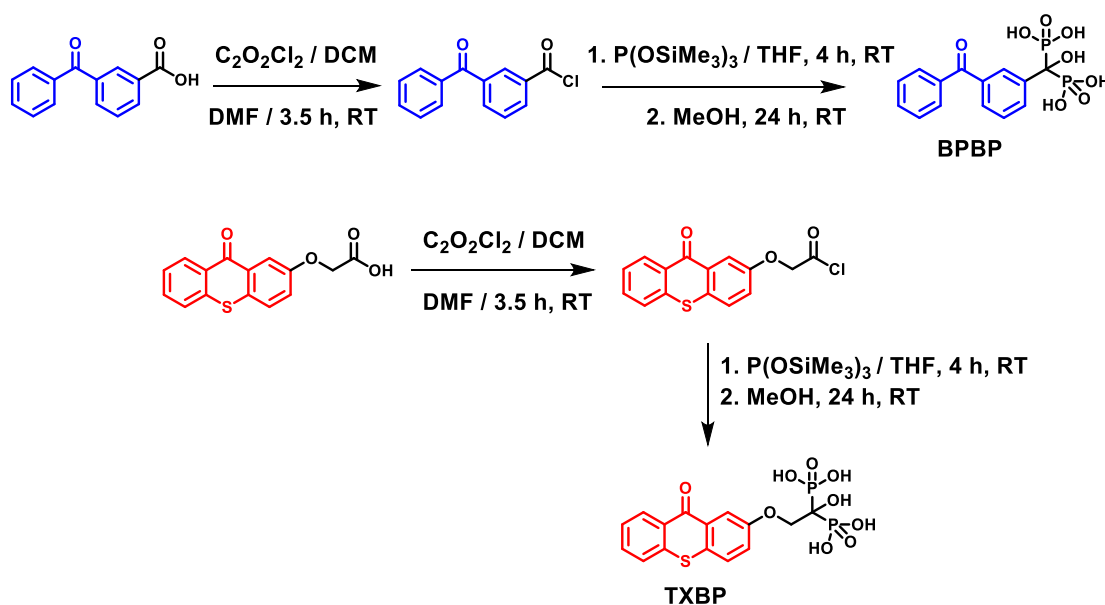


Figure 4.1. Syntheses of BPBP and TXBP.

Table 4.1. The solubility of BPBP and TXBP.

PI	H <sub>2</sub> O	DMF	THF	MeOH	DCM	Acetone	Diethyl Ether
BPBP	+	+	+	+	-	+	-
TXBP	+	+	+	+	-	-	-

The structures of monomers were confirmed by <sup>1</sup>H, <sup>13</sup>C NMR, and FTIR spectroscopies. In the <sup>1</sup>H NMR spectrum of TXBP, we observed a triplet peak for methylene protons at 4.5 ppm due to phosphorus-proton coupling (Figure 4.2). In the <sup>13</sup>C NMR spectrum of BPBP, the triplet seen at around 75.66 ppm is due to carbon attached to two phosphorus. The FTIR spectra of PIs show broad peaks in the region of 3500-2100 cm<sup>-1</sup> due to OH stretching, weak peaks at 1632 (TXBP) or 1635 cm<sup>-1</sup> (BPBP) due to C=O, and the bands at around 916 and 951 cm<sup>-1</sup> correspond to the symmetric and asymmetric vibration of P-O.

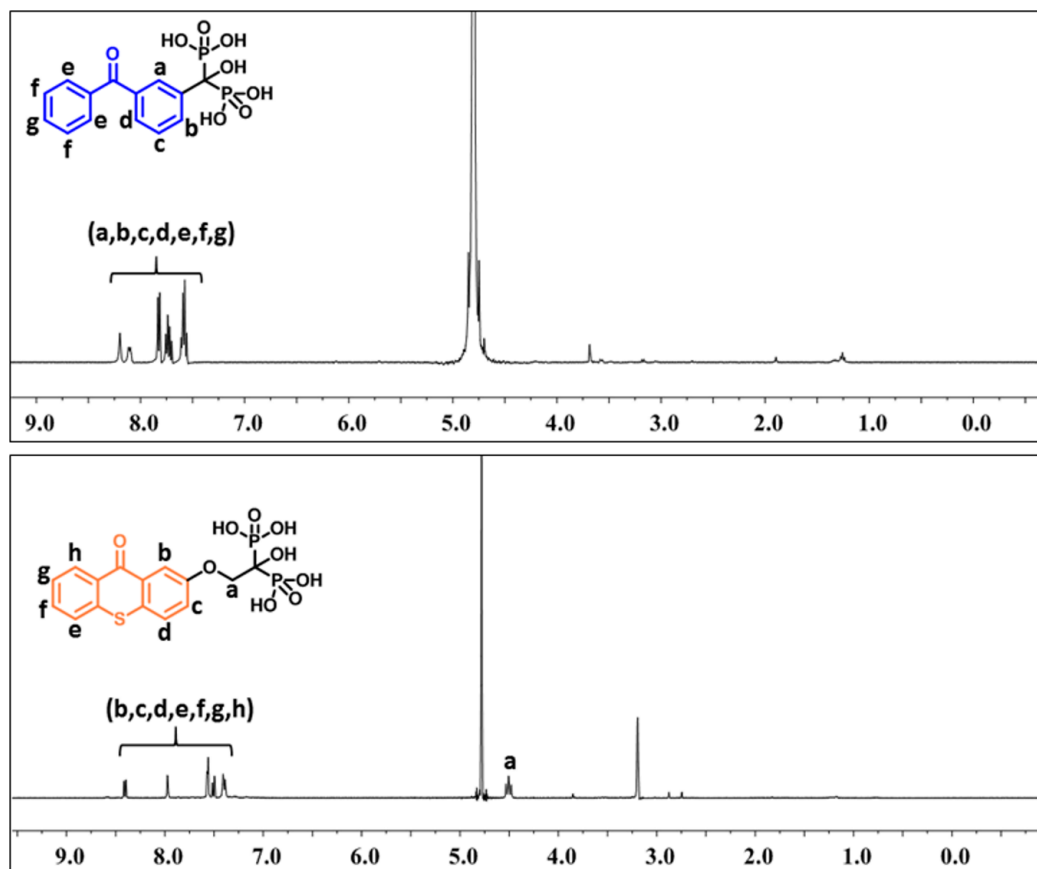


Figure 4.2.  $^1\text{H}$  NMR spectra of BPBP and TXBP.

#### 4.3.2. Light Absorption Properties

The UV-vis absorption spectra of BPBP and TXBP in different solvents are shown in Figure 4.3. As expected, BPBP absorbs light in the UV-region and has maxima of  $\pi\text{-}\pi^*$  transitions between 252 to 260 nm ( $\sim\varepsilon = 12000\text{-}14000$ ) in different solvents. Its  $n\text{-}\pi^*$  transition, “forbidden” by symmetry considerations and has more reactive excited states than those of  $\pi\text{-}\pi^*$  towards hydrogen abstraction, was observed at 338 nm. The same transitions are observed for commercial PI BP at 250 ( $\sim\varepsilon = 17775$ ) and 340 nm. For TXBP, a transition is observed in the visible region from 395 to 405 nm ( $\sim\varepsilon = 3300\text{-}4500$ ) which enables photopolymerization of aqueous formulations under visible light. This PI shows a bathochromic shift compared to the commercial TX ( $\lambda_{\text{max}} = 380$  nm). The introduction of an electron-donating oxygen atom gave this 15-20 nm shift to a longer wavelength.

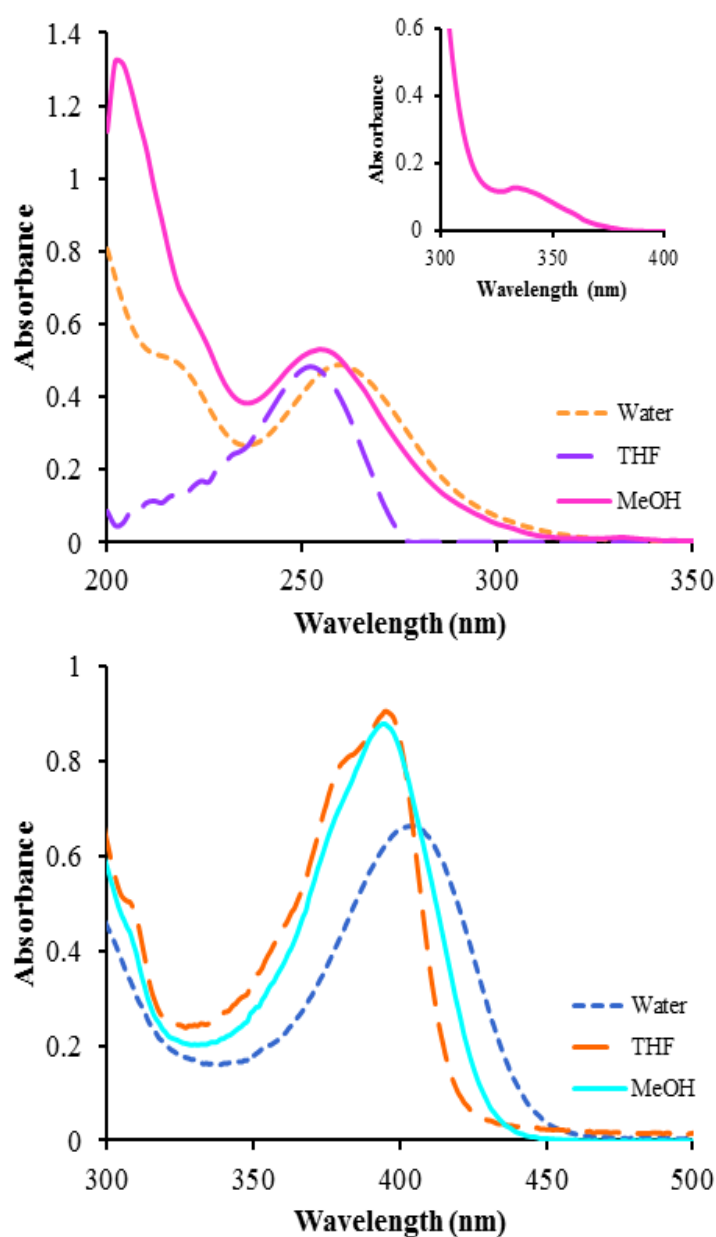


Figure 4.3. A) UV–Vis absorption spectra of BPBP ( $4 \times 10^{-5}$  M) (inset:  $2 \times 10^{-3}$  M in methanol) and B) TXBP ( $2 \times 10^{-4}$  M) in different solvents.

It was observed that the maximum absorption wavelength of the PIs depends on the solvent. A slight shift in absorption maximum (6–8, 10 nm for BPBP and TXBP) was observed in going from methanol or toluene to water. In general, an increase in the dielectric constant of the solvent destroys the intermolecular hydrogen bonding, resulting in a change

of the absorption behavior of the PIs [80]. THF and methanol have approximately similar dielectric constants, therefore,  $\lambda_{\text{max}}$  values are similar in these solvents for both of the PIs (252 and 254 nm for BPBP and 395 nm for TXBP) (Figure 4.3). However, water, which has a higher dielectric constant creates a redshift compared to the other solvents for both of the PIs by forming hydrogen bonds between solvent and PI molecules, lowering the energy of the excited state.

TXBP has an auxochrome group and a  $\pi$ -electron system which enable it to fluoresce in the visible range. Its fluorescence property, which may provide information on the nature of the excited state, was examined by a spectrofluorometer after excitation with a wavelength of 355 nm, as can be seen in Figure 4.4. The maximum emission wavelength value was found to be  $\lambda_{\text{em}} = 474$  nm. The absorption and emission spectra of TXBP in methanol showed almost a mirror image (Figure 4.4), showing its singlet excited state. The first singlet state energy ( $E_{S1}$ ) of TXBP is estimated from the intersection of absorbance and emission spectra as 2.92 eV. The Stokes shift ( $126582 \text{ cm}^{-1}$ ) was large.

### 4.3.3. Photochemical Mechanisms

4.3.3.1. Steady-state Photolysis. To investigate the photobleaching behavior of the PIs, steady-state photolysis of TXBP was performed. When the solution of TXBP is exposed to radiation at  $\lambda = 385$  nm in methanol, it undergoes fast photobleaching indicating the possibility of intra- or intermolecular hydrogen abstraction reactions (Figure 4.5B). A faster decrease in the maximum absorbance of TXBP in the presence of Iod is presented in Figure 4.5A. A small shoulder (around 320-330 nm) which appears after 20 min (TXBP/Iod) or 25 min (TXBP) irradiation may be attributed to the absorption of coupling products with an aryl radical as photodecomposition products of the PI [253]. During the irradiation of TXBP/EDB system in methanol, it was observed that the absorption of TXBP at 396 nm did not decrease, as shown in Figure 4.5C. These results indicate that EDB is not efficient in the photolysis of TXBP probably due to the formation of a quaternary ammonium salt. Similar behavior was observed in BPBP/EDB system in acetonitrile solution: no change in absorbance at around 275 nm due to the same reason. These results are in good agreement with the photopolymerization efficiency of TXBP/Iod or BPBP/Iod systems for the free radical polymerization of PEGDA compared to TXBP/EDB or BPBP/EDB systems.

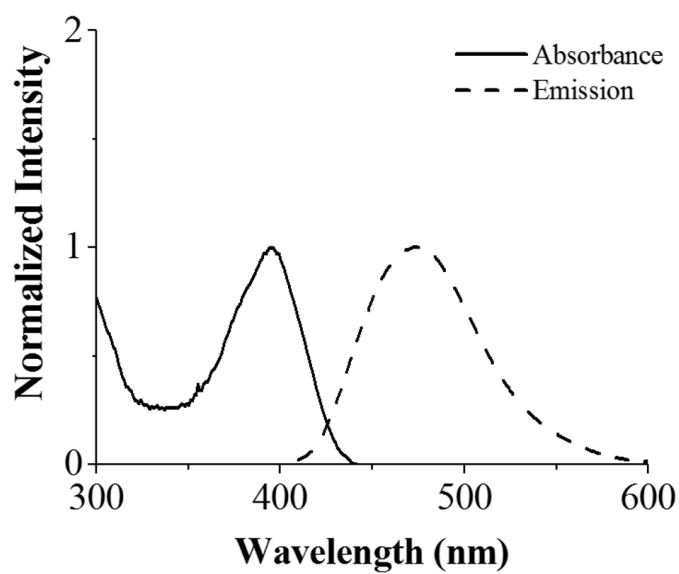


Figure 4.4. Corrected absorption (black line) and emission (dashed line) spectra of TXBP in methanol. The solution was excited at  $\lambda_{\text{exc}} = 396$  nm.

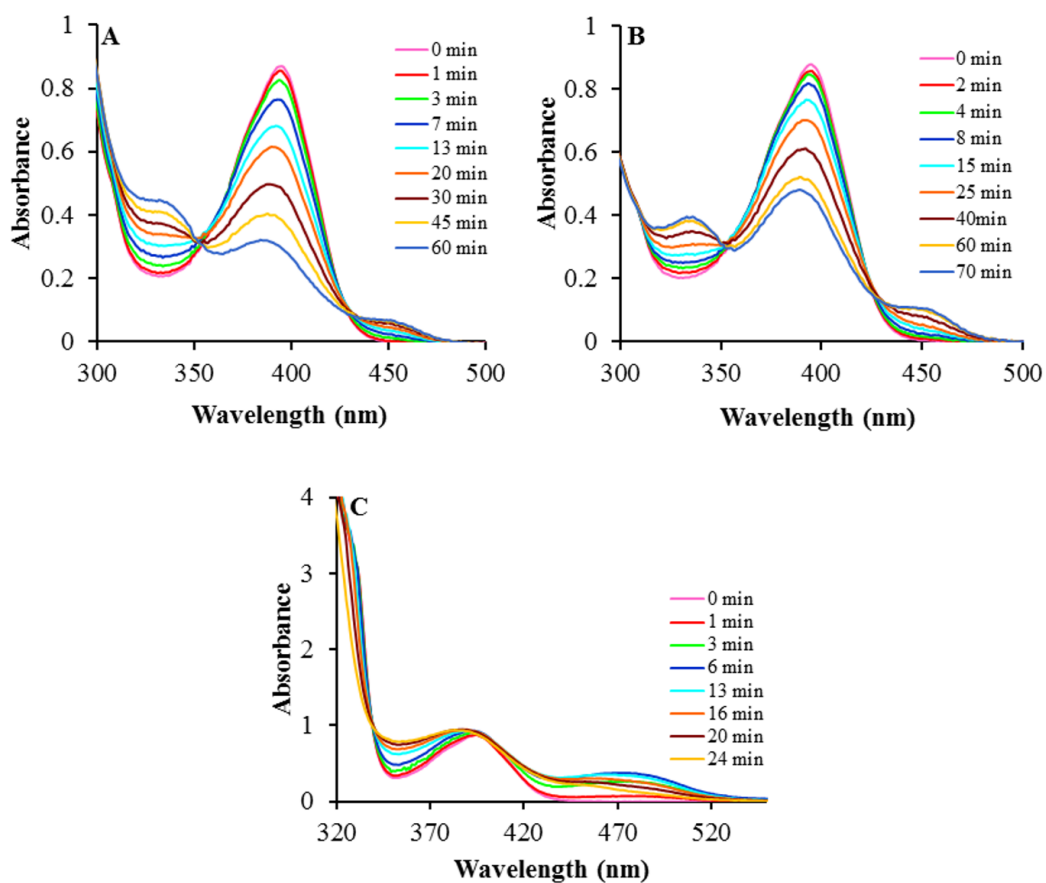


Figure 4.5. Photolysis of TXBP in methanol ( $2 \times 10^{-4}$  M) in the presence A) and absence B) of Iod ( $1 \times 10^{-3}$  M), and in the presence of EDB ( $1 \times 10^{-3}$  M) C) using a 385 nm LED.

**4.3.3.2. Fluorescence Quenching, Laser Flash Photolysis (LFP), Electron Spin Resonance (ESR).** The fluorescence quenching properties of TXBP were investigated to understand the singlet excited state reactivity of the PI in the presence of Iod or EDB as quenchers (Figure 4.6). The fluorescence lifetime of TXBP could be found as 9.3 ns from Figure 4.6. The Stern-Volmer plots for both TXBP/Iod and TX/EDB show fast fluorescence quenching property of TXBP (Figure 4.6B and Figure 4.6D). The Stern-Volmer quenching constants,  $K_{sv}$ , calculated from the slope of the Stern-Volmer plots are  $57.5 \text{ M}^{-1}$  and  $79.2 \text{ M}^{-1}$  in the presence of Iod and EDB, respectively. Then, the quenching rate constant  $k_q$  in the presence of Iod and EDB can be determined as  $6.19 \times 10^9 \text{ s}^{-1} \text{ M}^{-1}$  and  $8.52 \times 10^9 \text{ s}^{-1} \text{ M}^{-1}$ , respectively, by using the formula  $k_q = K_{sv}/\tau$  (Figure 4.6E).  $k_q$  represents the rate of the reaction between the singlet excited state of the PI and the quencher.

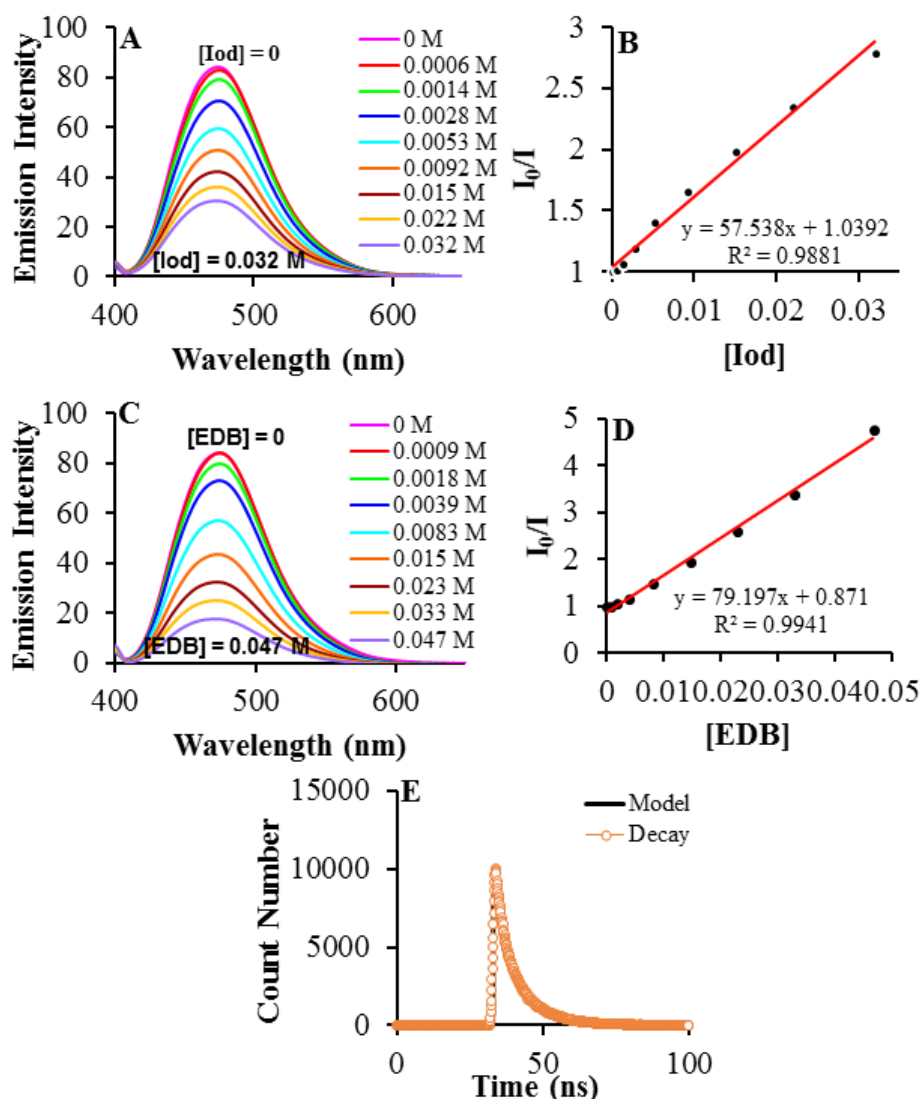


Figure 4.6. A) The fluorescence quenching of TXBP in methanol solution ( $4.5 \times 10^{-5}$  M) with different concentrations of Iod; B) The Stern-Volmer plot of A; C) The fluorescence quenching of TXBP in methanol solution ( $4.5 \times 10^{-5}$  M) with different concentrations of EDB; D) The Stern-Volmer plot of C; E) Fluorescence lifetime measurement of TXBP dissolved in methanol.

Photoinitiation of TXBP occurs from its singlet excited state rather than triplet state which is evidenced from the fact that the electron transfer quantum yields of the PI in the presence of Iod and EDB are very high, 0.6 and 0.8, respectively, found by using the formula  $\phi_{et} = K_{sv}[Iod]/(1+K_{sv}[Iod])$  (Figure 4.7).

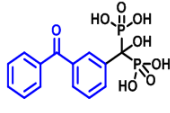
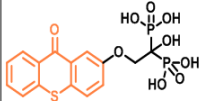
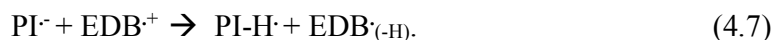
Chemical Structures of PIs	Singlet								Triplet		
	$E_{S1}$ [eV]	Iod				EDB				$k_{q(O2)}$ [ $M^{-1}s^{-1}$ ]	$\tau$ [ns]
		$K_{sv}$ [ $M^{-1}$ ]	$k_q$ [ $M^{-1}s^{-1}$ ]	$\Phi_{(et)}$	$K_{sv}$ [ $M^{-1}$ ]	$k_q$ [ $M^{-1}s^{-1}$ ]	$\Phi_{(et)}$	$\tau$ [ns]			
 <b>BPBP</b>	-	-	-	-	-	-	-	-	$3.2 \times 10^9$	156	
 <b>TXBP</b>	2.92	57.5	$6.19 \times 10^9$	0.6	79.2	$8.52 \times 10^9$	0.8	9.3	-	-	

Figure 4.7. Parameters characterizing the reactivity of the PIs.

The electron transfer photosensitization between BPBP or TXBP and Iod works in a photooxidative pathway which means an electron is transferred from the photoinitiator to Iod giving rise to the formation of the  $Ar\cdot$  radical and  $TXBP\bullet+$  or  $BPBP\bullet+$  which can be used in the radical and cationic polymerization, respectively [260], as these are given in



The initiation mechanism of BPBP/EDB or TXBP/EDB also occurs in a photoreductive pathway, however electron is transferred from hydrogen donor EDB to the PI, in contrast to TXBP/Iod or BPBP/Iod which can be seen in



The aminoalkyl radical formed  $\text{EDB}^{\cdot(-\text{H})}$  is capable of initiating the radical polymerization.

Laser flash photolysis experiments were performed to characterize the triplet excited state properties of the photoinitiators (Figure 4.8), in particular showing that, TXBP does not have significant triplet excited state reactivity (Figure 4.8B).

In the case of BPBP, to verify the triplet state reactivity, oxygen quenching experiments were conducted and it is clearly seen that BPBP was quenched by oxygen at its triplet excited state with a rate constant,  $k_q$ , of  $3.2 \times 10^9 \text{ s}^{-1} \text{ M}^{-1}$  and the triplet state lifetime was measured as 156 ns from the triplet state decays (Figure 4.8A).

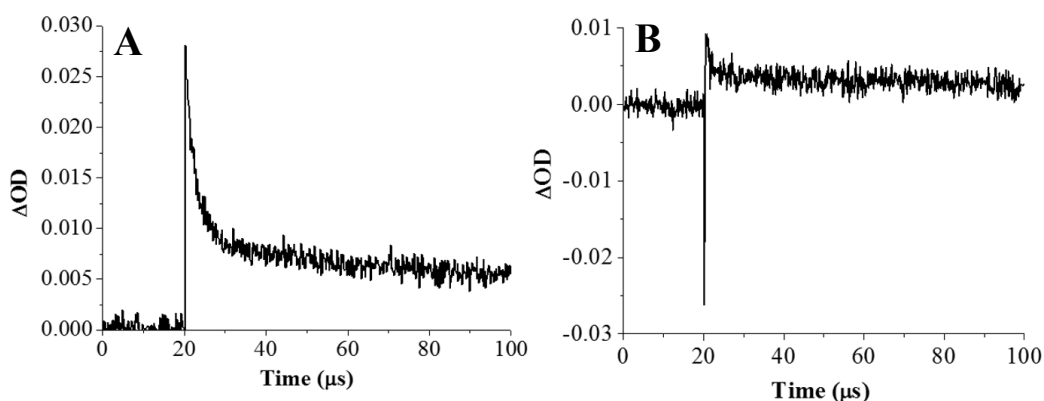


Figure 4.8. Triplet state decay traces observed after laser excitation of A) BPBP and B) TXBP at 355 nm. Laser excitation for  $t = 20 \mu\text{s}$ .

ESR-ST spin trapping experiments were carried out to detect the radicals formed from BPBP alone under LED irradiation. The results obtained show that BPBP generates free radical upon light excitation suggesting a monomolecular Type II photoinitiator behavior (Figure 4.9).

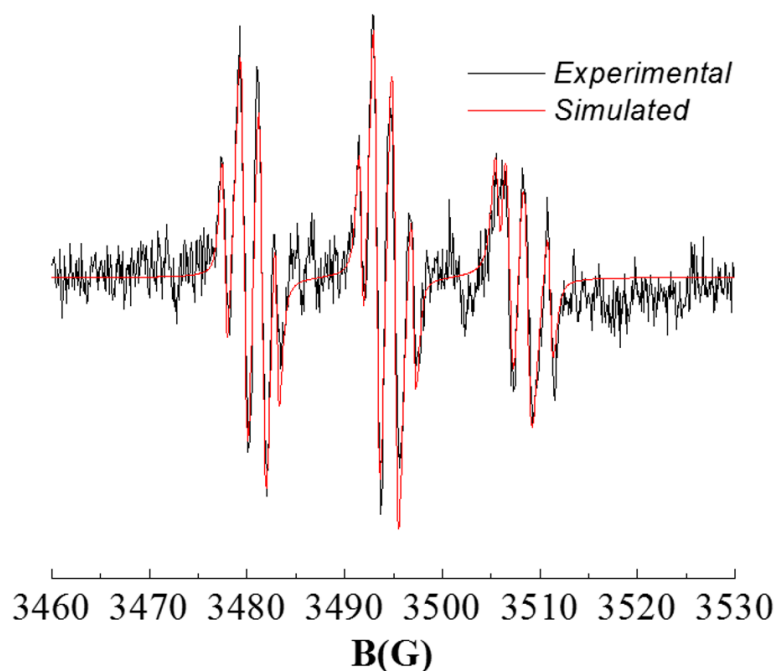


Figure 4.9. ESR spectra of the radicals generated in BPBP irradiated by LED@365 nm exposure and trapped by PBN in tert-butylbenzene. PBN radical adducts obtained are:  $a_N = 13.6$  G,  $a_H = 1.9$  G; and  $a_N = 14.0$  G,  $a_H = 5.3$  G.

#### 4.3.4. Photopolymerization

The novel PIs were used in the free radical polymerization of a PEGDA-water (80:20 wt%) mixture in the absence and presence of additives (EDB, Iod) upon irradiation with light at 320-500 nm to evaluate their photoinitiating performances. BPBP and TXBP have good compatibility with PEGDA and PEGDA-water mixture, forming clear solutions.

It was observed that BPBP can initiate polymerization of PEGDA-water (80:20 wt%) mixture in the absence of hydrogen donors,  $R_{pmax} = 0.036$  s<sup>-1</sup>,  $t_{max} = 0.08$  min, conversion = 81% (Figure 4.10). In the literature, thiol [79], hydroxy [116], amine [162], aldehyde [80], and carboxylic acid [121] derivatives of TX were reported as effective one-component photoinitiating systems. Therefore, we can expect the hydroxyl proton can function as a hydrogen donor in the BPBP structure. The two-component system BPBP and EDB (a tertiary amine co-initiator for type II PIs), exhibited a lower photopolymerization rate ( $R_{pmax}$

=  $0.029 \text{ s}^{-1}$ ), higher  $t_{\text{max}}$  (0.12 min) and lower conversion (72%) for polymerization of the same formulation than the system with BPBP. However, upon the addition of Iod to BPBP, the polymerization is significantly enhanced,  $R_{\text{pmax}} = 0.13 \text{ s}^{-1}$ ,  $t_{\text{max}} = 0.4 \text{ min}$  and conversion = 98%; in line with the fluorescence quenching experiment.

The photopolymerization profiles of PEGDA-water (80:20 wt%) mixture using TXBP are given in Figure 4.11. It was observed that photopolymerization in the absence of hydrogen donor was very slow, ( $R_{\text{pmax}} = 0.005 \text{ s}^{-1}$ ,  $t_{\text{max}} = 1.52 \text{ min}$ , conversion = 84%). The addition of a co-initiator (EDB) improves the performance, increasing  $R_{\text{pmax}} = 0.013 \text{ s}^{-1}$  and decreasing  $t_{\text{max}} = 0.24 \text{ min}$ . However, the final conversions were lower (76%). This can be attributed to fast gelation, leading to a decrease in the flexibility of the system and the mobilities of reactive species. However, the TXBP/Iod system has a very high rate of polymerization ( $R_{\text{pmax}} = 0.056 \text{ s}^{-1}$ ,  $t_{\text{max}} = 0.08 \text{ min}$ ). The reason why both BPBP and TXBP have low photoinitiation capability with EDB may be ascribed to an acid-base reaction between EDB and bisphosphonic acid group of the PIs which lowers the hydrogen donating efficacy of EDB [261].

The efficiency of the synthesized PIs has been also investigated for the photopolymerization of AAm in aqueous solution at  $\lambda = 365 \text{ nm}$  (Table 4.2). The influence of different parameters such as co-initiators (TEA and sesamol), monomer, initiator/co-initiator concentrations and time of irradiation on conversion have been evaluated. As it is seen in Table 4.2, the polymerizations can proceed without a coinitiator and the conversions are nearly proportional to the amount of the photoinitiator. For example, an increase in conversion from 36 to 46% was observed with an increase in BPBP concentration from 1 to  $3 \times 10^{-3} \text{ M}$ . However, no polymerization was observed upon the addition of  $3 \times 10^{-3} \text{ M}$  TEA to BPBP ( $1 \times 10^{-3} \text{ M}$ ). After this critical concentration of TEA, polymerization proceeds at a slower rate, giving a conversion of 24% at  $9 \times 10^{-3} \text{ M}$  TEA concentration. The lower conversions obtained for BPBP/TEA and TXBP/TEA systems may be attributed again to the acid-base reaction between TEA and bisphosphonic acid units, decreasing the hydrogen donating ability of the amine. In recent years, benzodioxole derivatives which are natural components from dietary plants were used to replace conventional amine co-initiators [24, 262, 263]. The photochemical mechanism involves methine radical formation from the interaction with Type II photoinitiators such as benzophenone. In order to avoid

complications resulting from interactions of our photoinitiators with the amine, we tried to use sesamol as co-initiator with our PIs. The formulations containing sesamol showed improved yield compared to that of TEA under the same conditions, proving our assumption.

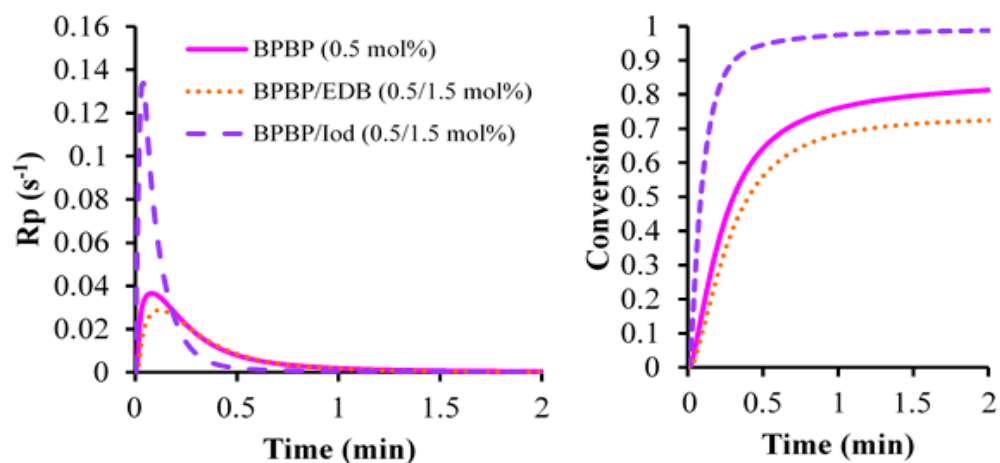


Figure 4.10. Rate-time and conversion-time plots for the photopolymerization of PEGDA-Water (80:20 wt%) under nitrogen at 25 °C,  $\lambda = 320-500$  nm in the presence of BPBP, BPBP/EDB, BPBP/Iod.

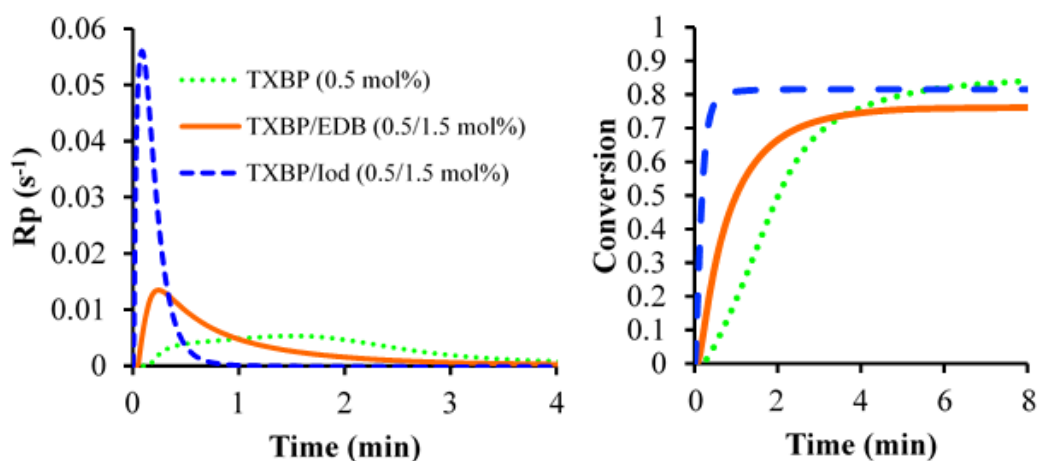


Figure 4.11. Rate-time and conversion-time plots for the photopolymerization of PEGDA-Water (80:20 wt%) under nitrogen at 25 °C,  $\lambda = 320-500$  nm in the presence of TXBP, TXBP/EDB, TXBP/Iod.

Table 4.2. Photoinitiated polymerization of AAm at room temperature at  $\lambda=365$  nm

<b>Monomer [M]</b>	<b>PI</b>	<b>[PI] (<math>10^{-3}</math>)</b>	<b>[Co-initiator] (<math>10^{-3}</math>)</b>	<b>Time [min]</b>	<b>Conversion (%)</b>
<b>3</b>	BPBP	5	-	30	72
<b>1</b>	BPBP	3	-	15	46
<b>1</b>	BPBP	1	-	15	36
<b>1</b>	BPBP/TEA	3	9	15	24
<b>1</b>	BPBP/TEA	1	3	15	-
<b>1</b>	BPBP/Sesamol	3	9	15	60
<b>1</b>	BPBP/Sesamol	1	3	15	42
<b>1</b>	TXBP	3	-	15	57
<b>1</b>	TXBP/TEA	3	9	15	40
<b>1</b>	TXBP/Sesamol	3	9	15	49

#### 4.4. Conclusions

Two new water-soluble (BPBP and TXBP) BP and TX-based radical photoinitiators having bisphosphonic acid groups have been synthesized. TXBP enables photopolymerization of aqueous formulations under visible light. BPBP works under UV but shows higher water solubility compared to both TXBP and the commonly used commercial PI, I2959. The performance of these novel PIs in aqueous solutions was demonstrated for photopolymerizations of poly(ethyleneglycol) diacrylate and acrylamide. Furthermore, these photoinitiators can work as one-component PIs, albeit at a low rate.

Furthermore, the use of BPBP to photosensitively prepare PEGDA hydrogels by utilizing both the polymerizing and the crosslinking ability of benzophenone is continuing. The result will be a hydrogel with bisphosphonic acid functionality.

## 5. A WATERBORNE BISPHOSPHONATE FUNCTIONALIZED THIOXANTHONE-BASED PHOTOINITIATOR

This chapter is published as: Eren, T. N., T. Gencoglu, M. Abdallah, J. Lalevee, D. Avcı, “A Water Soluble and Highly Reactive Bisphosphonate Functionalized Thioxanthone-Based Photoinitiator”, *Eur. Polym. J.*, Vol. 135, 109906, 2020.

### 5.1. Introduction

The design of TXBP2, the novel photoinitiator introduced in the present chapter, focuses on achieving the water solubility and biocompatibility aspects of the green theme. This synthesized bisphosphonate functionalized thioxanthone photoinitiator absorbs in the UV-Vis region (~400 nm) (Figure 5.1). The bisphosphonate group was particularly selected to provide hydrophilic property to the oil-soluble thioxanthone photoinitiator due to its high polarity and biocompatibility. The structure of the PI was confirmed by characterization studies and photochemical mechanism and photopolymerization activity of the novel PI were investigated.

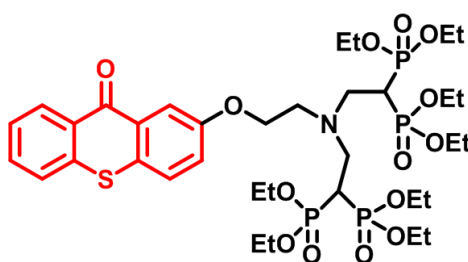


Figure 5.1. Structure of the novel photoinitiator TXBP2.

## 5.2. Experimental

### 5.2.1. Materials and Methods

2-(2-aminoethoxy)-9H-thioxanthen-9-one (TXOCH<sub>2</sub>CH<sub>2</sub>NH<sub>2</sub>) was synthesized according to literature procedure [264]. Tetraethyl vinylidene bisphosphonate was prepared from tetraethyl methylene bis(phosphonate) by the method of Degenhardt and Burdsall [265]. Thiosalicylic acid, phenol, 2-(Boc-amino)ethyl bromide, tetraethyl methylenebis(phosphonate), paraformaldehyde, diethyl amine, p-toluenesulfonic acid, ethyl 4-(dimethylamino)benzoate (EDB), thioxanthone (TX), trimethylolpropane triacrylate (TMPTA), poly(ethylene glycol) diacrylate (PEGDA, M<sub>n</sub> = 575 D), and the other reagents and solvents were purchased from Sigma-Aldrich or Alfa Aesar and used as received without further purification. Bis-(4-*tert*-butylphenyl)-iodonium hexafluorophosphate (Iod or Speedcure 938) was obtained from Lambson Ltd.

<sup>1</sup>H NMR spectra were recorded on a Varian Gemini (400 MHz) spectrometer at ambient temperature with deuterated methanol (MeOD) as a solvent. Nicolet 6700 FT-IR spectrophotometer was used for recording IR spectra.

### 5.2.2. Synthesis of TXBP2

2-(2-aminoethoxy)-9H-thioxanthen-9-one (0.015 g, 0.055 mmol) and tetraethyl vinylidene bisphosphonate (0.05 g, 0.166 mmol) were stirred in chloroform (0.5 mL) at room temperature for 48 hours. After removal of the solvent, the product was washed with diethyl ether/petroleum ether (1/1 v/v) mixture to remove excess tetraethyl vinylidene bisphosphonate. The product was obtained as a yellow colored viscous oil in 25% yield. <sup>1</sup>H-NMR (CDCl<sub>3</sub>, 400 MHz, δ): 1.30 (td, *J* = 7.1, 2.3 Hz, 24H, CH<sub>3</sub>-CH<sub>2</sub>), 2.89 (tt, *J* = 24.6, 4.8 Hz, 2H, CH-P), 3.07 (t, *J* = 5.3 Hz, 2H, TX-O-CH<sub>2</sub>-CH<sub>2</sub>-N), 3.23 (td, *J* = 15.4, 4.8 Hz, 4H, N-CH<sub>2</sub>-CH-P=O), 4.16 (m, 18H, TX-O-CH<sub>2</sub> & CH<sub>3</sub>-CH<sub>2</sub>), 7.28 (dd, *J* = 8.8, 2.9 Hz, 1H, Ar-CH), 7.46 (m, 2H, Ar-CH), 7.58 (m, 2H, Ar-CH), 8.03 (d, *J* = 2.8 Hz, 1H, Ar-CH), 8.60 (d, *J* = 8.8 Hz, 1H, Ar-CH) ppm. FTIR (ATR): 2981 (C-H), 1692 (C=O), 1243 (P=O), 1014, 961 (P-O-C) cm<sup>-1</sup>.

### 5.2.3. Photochemical Analyses

5.2.3.1. UV-vis Spectroscopy Experiments. UV-vis spectra were recorded using a Carry 3 UV/vis spectrophotometer (Varian). For steady state photolysis experiments, chloroform solutions of PI with or without the additives (EDB, Iod) were irradiated with LED@385 nm and UV-vis spectra were taken at different irradiation times.

5.2.3.2. Fluorescence Experiments. Fluorescence characteristics of the PI were investigated in chloroform with a JASCO FP-6200 spectrofluorometer. The formula  $I_0/I = 1 + k_q\tau_0[\text{additive}]$  which is acquired from classical Stern-Volmer treatments was used to obtain the interaction rate constant  $k_q$  between PI and the additive (Iod, EDB), where  $I_0$  and  $I$  are the fluorescence intensity of PI in the absence and the presence of the additive, respectively, and  $\tau_0$  is the lifetime of the excited PI in the absence of the additive ( $\tau_0$  is measured using laser flash photolysis experiments).

5.2.3.3. Laser Flash Photolysis Experiments. A Q-switched nanosecond Nd/YAG laser ( $\lambda_{\text{exc}} = 355$  nm, 9 ns pulse width; energy reduced down to 10 mJ) obtained from Continuum and an analyzing system consisting of a ceramic xenon lamp, a monochromator, a fast photomultiplier and a transient digitizer (Luzchem LFP 212) were used to carry out nanosecond laser flash photolysis (LFP) experiments [245].

### 5.2.4. Photoinitiating Activity Measurements

5.2.4.1. Photo-DSC. TA Instruments DSC 250 differential photocalorimeter using an Omnicure 2000 mercury lamp light source with a 320-500 nm filter was used for photopolymerization experiments. PEGDA and TMPTA monomers (3-4 mg) containing 0.5 wt% TXBP2 in the presence and absence of 1.5 wt% coinitiator (EDB or Iod) were exposed to irradiation at 25 °C under nitrogen for 5 min. The heat flow was monitored as a function of time with DSC. The polymerization rate was calculated by

$$\text{Rate} = \frac{(Q/s)M}{n(\Delta H_p)m} \quad (5.1)$$

where  $Q/s$  is the heat flow per second,  $M$  the molar mass of the monomer,  $n$  the number of double bonds per monomer molecule,  $\Delta H_p$  the heat of reaction evolved and  $m$  the mass of monomer in the sample. The theoretical heat for the total conversion of an acrylate double bond is 86 kJ/mol.

**5.2.4.2. Photoreactor.** A solution of TXBP2 (0.0015 mmol) in 0.5 mL of water was added to acrylamide (AAm) (1 mmol). The solution in pyrex tube was irradiated in a photoreactor containing 12 Philips TL 8W BLB lamps, under exposure to UV light (365 nm) for 15 min in the presence and absence of the co-initiator (TEA, 0.0045 mmol) in an air depleted or aerated atmosphere. Poly(acrylamide) formed was precipitated in tenfold excess acetone and dried in vacuum. Conversions were calculated gravimetrically.

### 5.2.5. 3D Printing Experiments

For 3D printing experiments, a computer controlled laser diode @405 nm (spot size around 50  $\mu\text{m}$ ) was used for the spatially controlled irradiation. The photosensitive resin was polymerized under air and the generated 3D patterns were analyzed using a numerical optical microscope (DSX-HRSU from OLYMPUS Corporation) as presented in ref. [266].

## 5.3. Results and Discussion

### 5.3.1. Synthesis of TXBP2

The synthesis of TXBP2 was carried out through the aza-Michael addition reaction between tetraethyl vinylidene bisphosphonate and 2-(2-aminoethoxy)-9H-thioxanthen-9-one as shown in Figure 5.2. Selective formation of the bisadduct was obtained by using excess tetraethyl vinylidene bisphosphonate (tetraethyl vinylidene bisphosphonate:2-(2-aminoethoxy)-9H-thioxanthen-9-one mol ratio is 3:1). TXBP2 was obtained as a yellow viscous liquid in 25% yield. This PI showed excellent water-solubility of 86  $\text{g L}^{-1}$  compared to the water-borne commercial PI, Irgacure 2959 (5  $\text{g L}^{-1}$ ). The water solubility of this PI also exceeds the solubility of our previously synthesized bisphosphonic acid functionalized PIs (28  $\text{g L}^{-1}$  for BPBP and 0.05  $\text{g L}^{-1}$  for TXBP) [267]. Two polar bisphosphonate

functional groups play an important role on the water solubility of this PI. It is soluble in common organic solvents such as acetone, methanol, THF, DMF and dichloromethane, insoluble in diethyl ether and compatible with commercial monomers such as TMPTA and PEGDA.  $^1\text{H-NMR}$  spectrum of TXBP2 features characteristic peaks of methyl protons at 1.30 (triplet of doublets), ethyl protons at 3.07 (triplet) and 4.16 ppm (multiplet), methine protons (triplets of triplet) at 2.89 ppm and methylene protons attached to methine (triplet of doublets) at 3.23 ppm (Figure 5.3). The formation of the bisadduct structure was verified by the integration of the aromatic protons with respect to methine or ethyl protons. In the FTIR spectrum, the peaks at  $1692\text{ cm}^{-1}$  and  $1243\text{ cm}^{-1}$  are attributed to the stretching vibration of the carbonyl and P=O functional groups.

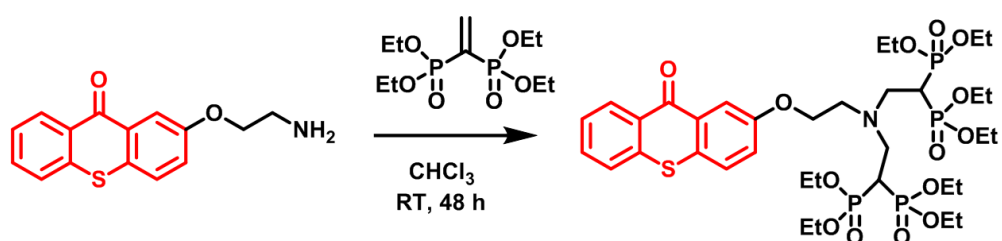


Figure 5.2. Synthesis scheme of TXBP2.

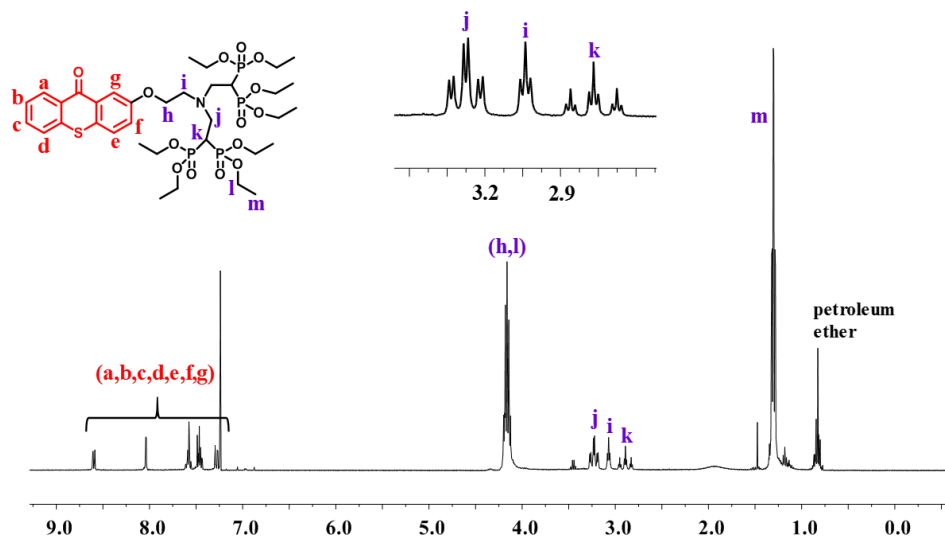


Figure 5.3.  $^1\text{H}$  NMR spectrum of TXBP2.

### 5.3.2. Light Absorption Properties

The UV-Vis spectrum of TXBP2 in different solvents is shown in Figure 5.4A (see also Table 5.1). TXBP2 has a clear bathochromic shifted absorption characteristic compared to the commercial TX ( $\lambda_{\text{max}} = 380$  nm), resulting from the electron-rich oxygen atom in its structure. It exhibits slight solvatochromism, the absorption spectrum being slightly affected by solvents, with  $\lambda_{\text{max}}$  values of 395 (in methanol), 398 (in THF) and 402 nm (in  $\text{CHCl}_3$ ) and 404 nm (in  $\text{H}_2\text{O}$ ).

TXBP2 exhibits fluorescence property which may be attributed to the possession of both an electron donating tertiary amine and electron withdrawing TX units in its structure. The fluorescence properties of tertiary aliphatic amines have already been disclosed by previous studies in literature [268], [269]. Fluorescence emission properties of TXBP2 after excitation at 396 nm are given in Figure 5.4B which may supply information about the singlet excited state properties of the photoinitiator. The mirror image like relationship between absorption and emission graphs verifies its singlet excited state reactivity. The Stokes shift value was determined as  $138888\text{ cm}^{-1}$  (Table 5.1). The intersection point of the

absorption and fluorescence spectra allows the identification of the first singlet excited state energies ( $E_{S1}$ ) as 2.92 eV.

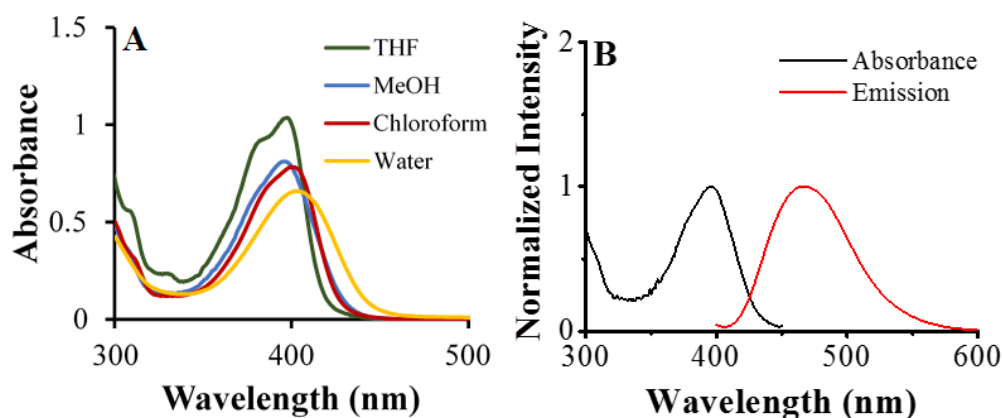


Figure 5.4. (A) UV–Vis absorption spectra of TXBP2 ( $1.5 \times 10^{-4}$  M) in THF, MeOH,  $\text{CHCl}_3$  and  $\text{H}_2\text{O}$ . (B) Corrected absorption (black line) and emission (red line) spectra of TXBP2 in  $\text{CHCl}_3$ . The solution was excited at  $\lambda_{\text{exc}} = 396$  nm.

Table 5.1. Absorption characteristics of TXBP2 ( $1.5 \times 10^{-4}$  M) in different solvents.

Solvents	$\lambda_{\text{abs}}$ [nm]	$\lambda_{\text{em}}$ [nm]	Stokes Shift [ $\text{cm}^{-1}$ ]	$\epsilon$ ( $\text{M}^{-1} \text{cm}^{-1}$ )
$\text{CHCl}_3$	402	-	-	5200
THF	398	-	-	6820
MeOH	395	467	138888	5400
Water	404	-	-	4509

### 5.3.3. Photochemical Mechanisms

**5.3.3.1. Steady-State Photolysis.** The photobleaching experiments were carried out in the presence and absence of additives (EDB & Iod) in chloroform upon 385 nm LED irradiation (Figure 5.5). The steady state photolysis of TXBP2/Iod system is the fastest of all, more specifically, the absorbance of the peak at 402 nm decreased very fast in only 6 minutes

(Figure 5.5C). Addition of EDB also slightly improves the photodecomposition of TXBP2 (Figure 5.5B) whereas TXBP2 alone is highly photostable (Figure 5.5A). The faster photodegradation property of TXBP2/Iod compared to TXBP2/EDB implies that the higher susceptibility of TXBP2 to react through a photooxidation mechanism rather than a photoreduction.

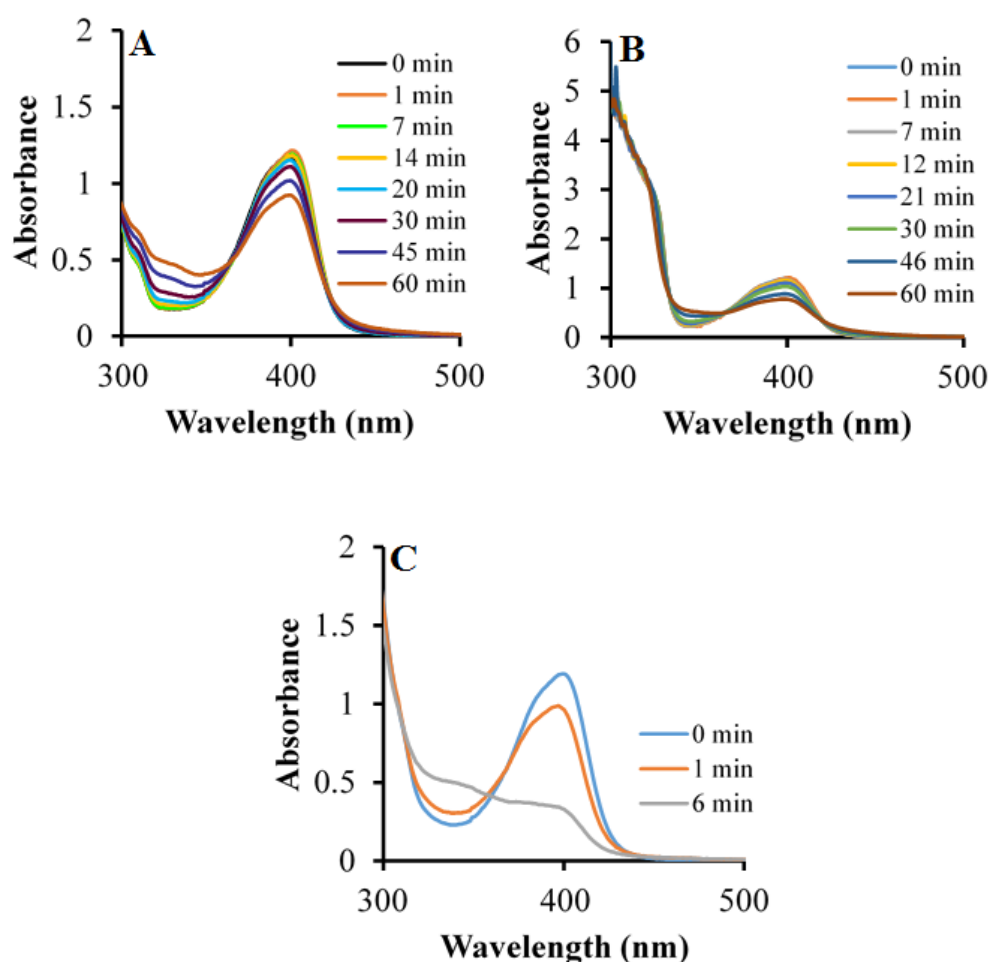


Figure 5.5. Photolysis of TXBP2 in chloroform ( $2 \times 10^{-4}$  M) in the absence (A) and presence (B) of EDB ( $1 \times 10^{-3}$  M), and in the presence of Iod ( $1 \times 10^{-3}$  M) (C) using a 385 nm LED.

Fluorescence quenching for the TXBP2/Iod and TXBP2/EDB systems were investigated by adding EDB or Iod at different concentrations in chloroform to understand the singlet excited state features of the PI better (Figure 5.6). Fast fluorescence quenching

process of TXBP2 is seen in the presence of EDB which is indicated by the high  $K_{sv}$ , Stern Volmer coefficient of TXBP2/EDB interaction,  $81.1 \text{ M}^{-1}$ . However,  $K_{sv}$  value for the TXBP2/Iod interaction was determined as  $2.6 \text{ M}^{-1}$  (Table 5.2). The interaction rate constants of  $^1\text{TXBP2/Iod}$  and  $^1\text{TXBP2/EDB}$  were calculated using the formula  $k_q = K_{sv}/\tau$  as  $2.8 \times 10^8 \text{ s}^{-1} \text{ M}^{-1}$  and  $9 \times 10^9 \text{ s}^{-1} \text{ M}^{-1}$ , respectively (Table 5.2). In addition, the electron transfer quantum yields of TXBP2 in the presence of EDB and Iod from the excited singlet state  $\phi_{et(S1)}$  were estimated (according to the formula  $\phi_{et} = K_{sv}[\text{Iod}]/(1+K_{sv}[\text{Iod}])$ ) as 0.8 and 0.1, respectively (Table 5.2). The fluorescence lifetime of TXBP2 is reported as 9 ns (Table 5.2). The higher quenching rate constant for EDB in contrast to Iod associated with slower photolysis for EDB suggest a back electron transfer in the presence of this amine that regenerates the starting materials (decreasing the initiation efficiency). For Iod, such a back electron transfer is not possible as the dissociation of iodonium after its reduction is very fast in agreement with better initiating ability (Figure 5.7).

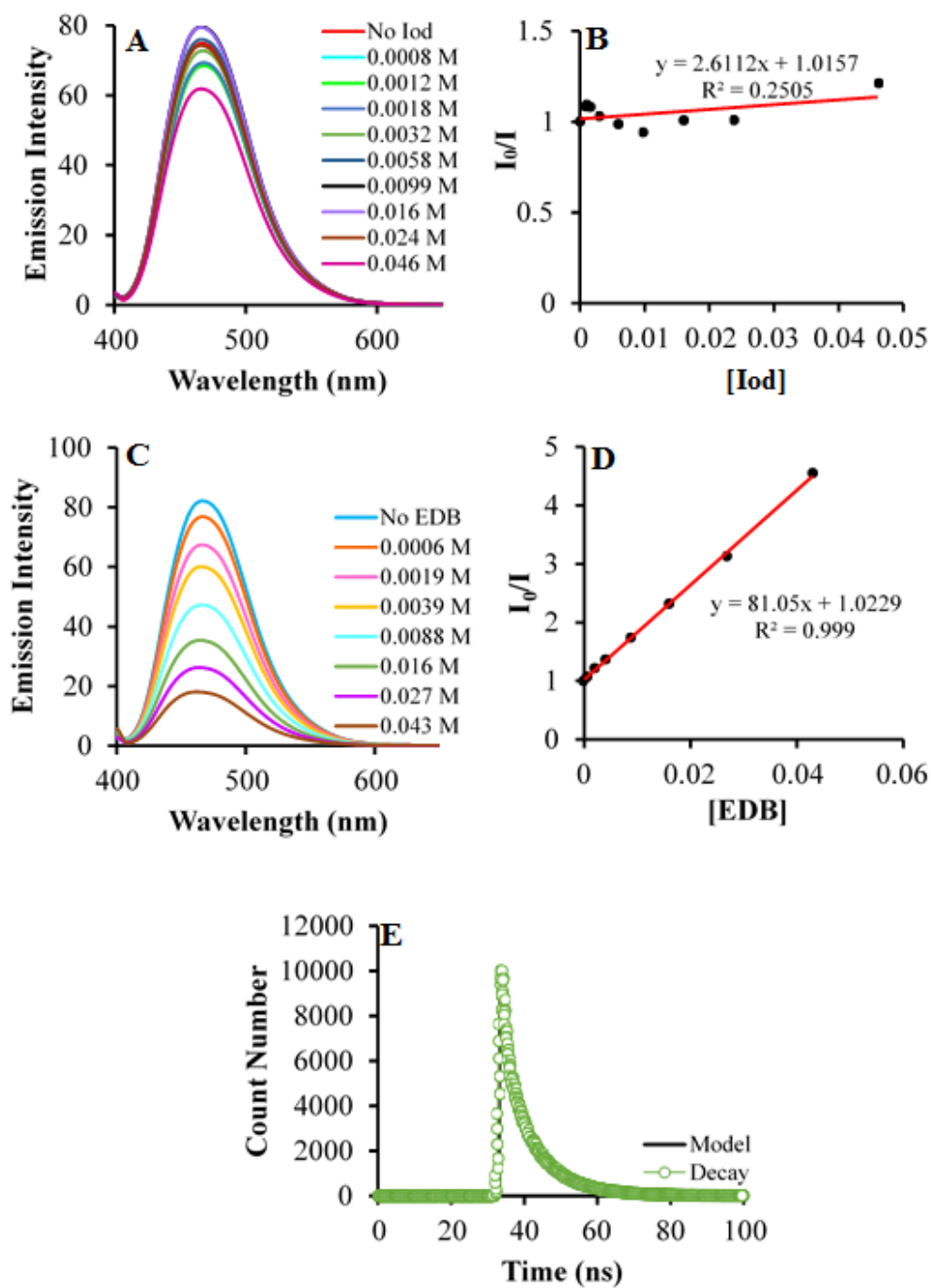


Figure 5.6. The fluorescence quenching of TXBP2 in chloroform solution with different concentrations of Iod (A) and EDB (C). The Stern-Volmer plot of TXBP2/Iod (B) of TXBP2/EDB (D). Fluorescence life time measurement of TXBP2 in chloroform.

The TXBP2/Iod interaction corresponds to a photooxidative redox reaction between TXBP2 and Iod (which involves the oxidation of the PI by Iod) forming  $\text{Ar}^\bullet$  phenyl radical and  $\text{TXBP2}^{+\bullet}$  radical cation which are capable of initiating free radical or cationic photopolymerization reactions, respectively (Figure 5.7) [260].

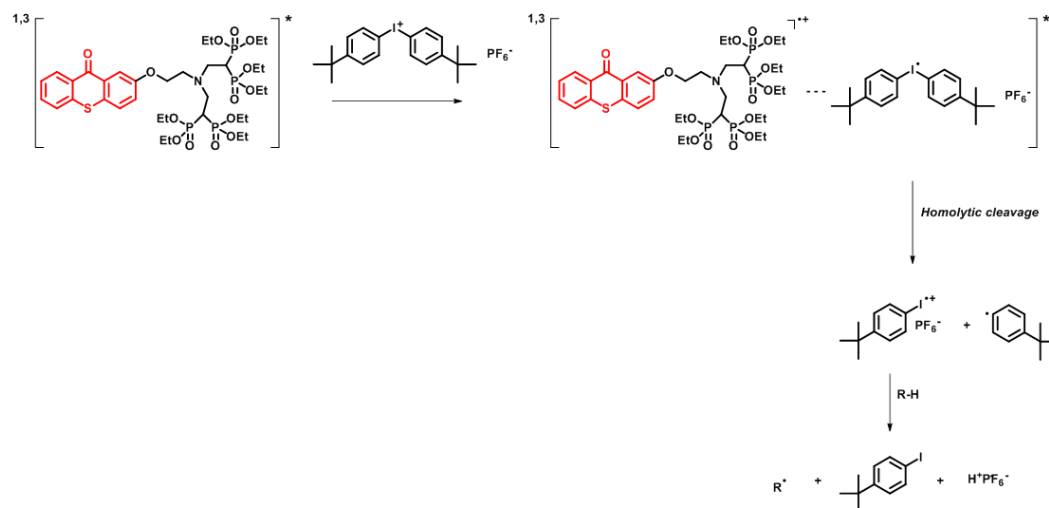


Figure 5.7. Photooxidation mechanism of TXBP2 with Iod.

The TXBP2/EDB interaction consists of an electron transfer reaction between EDB and TXBP2 through a photoreduction mechanism (which involves the reduction of the PI by EDB with an electron abstraction) resulting in the formation of  $\text{EDB}_{(-\text{H})}^\bullet$  which enables the initiation of the free radical photopolymerization in TXBP2/EDB photoinitiating system (Figure 5.8).

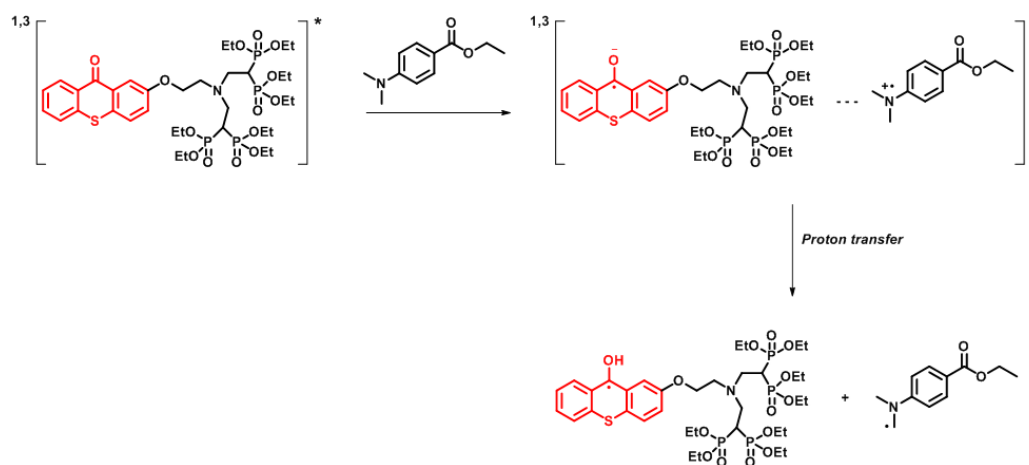


Figure 5.8. Photoreduction mechanism of TXBP2 with EDB.

In order to get insight about the triplet excited state characteristics of TXBP2, the laser flash experiments were also performed. The change in the transient absorption spectrum was recorded after irradiation with 9 ns pulses at 355 nm in different Iod and EDB concentrations (Figure 5.9A and 5.9B). The inverse lifetimes of these decays were plotted against the concentration of the quenchers; Iod and EDB (Figure 5.9C, 5.9D). As the concentration of the Iod and EDB was increased, the shortening in the triplet state decays can easily be noticed which shows the quenching of the triplet excited state of the Pis by Iod and EDB. The bimolecular quenching rate constants belonging to the interactions of  $^3[\text{TXBP2}]^*/\text{Iod}$  and  $^3[\text{TXBP2}]^*/\text{EDB}$  were calculated as  $9 \times 10^7$  and  $1 \times 10^9 \text{ M}^{-1}\text{s}^{-1}$  utilizing the slope of Stern-Volmer plots (Table 5.3). The high quenching rate constant values were ascribed to the efficiency of the initiator radical formation in TXBP2/EDB and TXBP2/Iod photoinitiating systems. The triplet excited state lifetime of the photoinitiator was estimated as  $9.3 \mu\text{s}$  (Table 5.3).

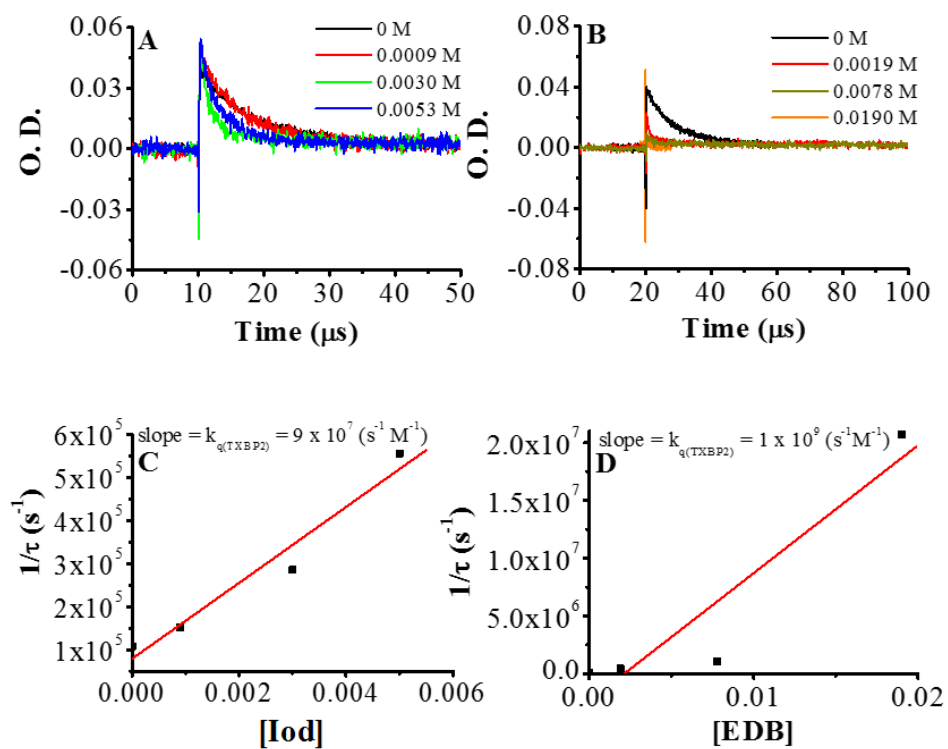


Figure 5.9. Triplet state decay traces observed after laser excitation of TXBP2 in chloroform at 355 nm, kinetic traces recorded at 600 nm under  $\text{N}_2$ : A) in different Iod concentrations; B) in different EDB concentrations, Stern–Volmer plot for quenching of  $^3[\text{TXBP2}]^*$  C) by Iod and D) by EDB.  $\lambda_{\text{exc}} = 355 \text{ nm}$ .

Table 5.2. Parameters characterizing the singlet excited state reactivity of the TXBP2.

Singlet							
	Iod			EDB			
$E_{S1}$	$K_{SV}$	$k_q$	$\Phi_{(et)}$	$K_{SV}$	$k_q$	$\Phi_{(et)}$	$\tau^a$
[eV]	[M <sup>-1</sup> ]	[M <sup>-1</sup> s <sup>-1</sup> ]		[M <sup>-1</sup> ]	[M <sup>-1</sup> s <sup>-1</sup> ]		[ns]
2.92	2.6	2.8 x 10 <sup>8</sup>	0.1	81.1	9 x 10 <sup>9</sup>	0.8	9

<sup>a</sup> fluorescence lifetime

Table 5.3. Parameters characterizing the triplet excited state reactivity of the TXBP2.

Triplet		
Iod	EDB	
$k_q$	$k_q$	$\tau^a$
[M <sup>-1</sup> s <sup>-1</sup> ]	[M <sup>-1</sup> s <sup>-1</sup> ]	[ $\mu$ s]
9 x 10 <sup>7</sup>	1 x 10 <sup>9</sup>	9.3

<sup>a</sup> triplet excited state life-time

#### 5.3.4. Photopolymerization

To understand the photoinitiation efficiency of the novel photoinitiator TXBP2 in commercial acrylate crosslinkers, the free radical photopolymerization of hydrophobic TMPTA and hydrophilic PEGDA by TXBP2 in the presence and absence of the additives Iod and EDB upon a visible light irradiation (between 320-500 nm) were studied. Bare TX

was also tested in the free radical photopolymerization of TMPTA for comparison. However, TX could not be used in PEGDA formulations, since they were not compatible. TXBP2 was compatible with both of the crosslinkers used.

The photo-DSC profiles belonging to the free radical photopolymerization of TMPTA are given in Figure 5.10. It is obvious that TXBP2/Iod system has the fastest rate of polymerization ( $R_{pmax} = 0.065 \text{ s}^{-1}$ ,  $t_{max} = 0.02 \text{ min}$ ) and highest conversion (42 %). TXBP2/EDB also shows similar results ( $R_{pmax} = 0.059 \text{ s}^{-1}$ ,  $t_{max} = 0.02 \text{ min}$ , conversion = 41%). As it can be seen clearly from Figure 5.10, TXBP2/EDB and TXBP2/Iod are more efficient systems than TX/EDB ( $R_{pmax} = 0.046 \text{ s}^{-1}$ ,  $t_{max} = 0.03 \text{ min}$ , conversion = 40%) and TX/Iod ( $R_{pmax} = 0.033 \text{ s}^{-1}$ ,  $t_{max} = 0.03 \text{ min}$ , conversion = 36%). TXBP2 alone can initiate polymerization very slowly ( $R_{pmax} = 0.014 \text{ s}^{-1}$ ,  $t_{max} = 0.12 \text{ min}$ , conversion = 39%) which is still better than TX alone ( $R_{pmax} = 0.009 \text{ s}^{-1}$ ,  $t_{max} = 0.21 \text{ min}$ , conversion = 31%).

Figure 5.11 displays rate vs time and conversion vs time plots belonging to the photopolymerization of PEGDA by TXBP2 alone or in combination with Iod and EDB. TXBP2/Iod is the most efficient system ( $R_{pmax} = 0.14 \text{ s}^{-1}$ ,  $t_{max} = 0.03 \text{ min}$ , conversion = 93%) of all the formulations as in the polymerization of TMPTA. TXBP2/EDB system has a good performance in the initiation of the polymerization of PEGDA having a high rate of polymerization and conversion value ( $R_{pmax} = 0.062 \text{ s}^{-1}$ ,  $t_{max} = 0.07 \text{ min}$ , conversion = 85%). However, TXBP2 alone is not sufficient to initiate the polymerization of PEGDA ( $R_{pmax} = 0.006 \text{ s}^{-1}$ ,  $t_{max} = 0.29 \text{ min}$ , conversion = 70%). TXBP2 alone system has a very low photoreactivity in both the polymerization of TMPTA and PEGDA since the intramolecular reaction between the ketone and the H-donating moiety is low (due to poor overlap) and intermolecular reactions probably predominate as in usual mono-component Type II photoinitiator behavior [270]. Moreover, the stability of these initiating radicals may be decreased because of the electronic (electron withdrawing effect of phosphonates) and steric effect of biphosphonate groups which also reduces the reactivity of TXBP2 alone in a photocurable matrix.

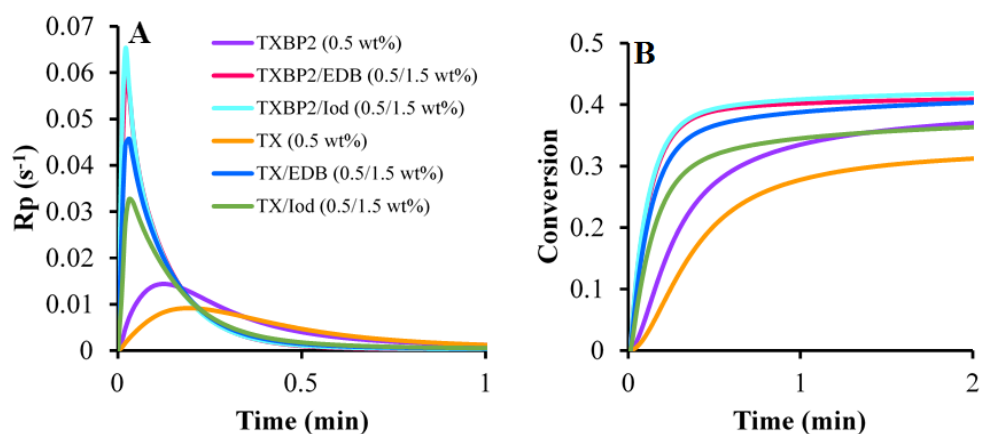


Figure 5.10. Rate-time and conversion-time plots for the photopolymerization of TMPTA under nitrogen at 25 °C,  $\lambda = 320\text{-}500$  nm in the presence of TX, TX/EDB, TX/Iod and TXBP2, TXBP2/EDB, TXBP2/Iod.

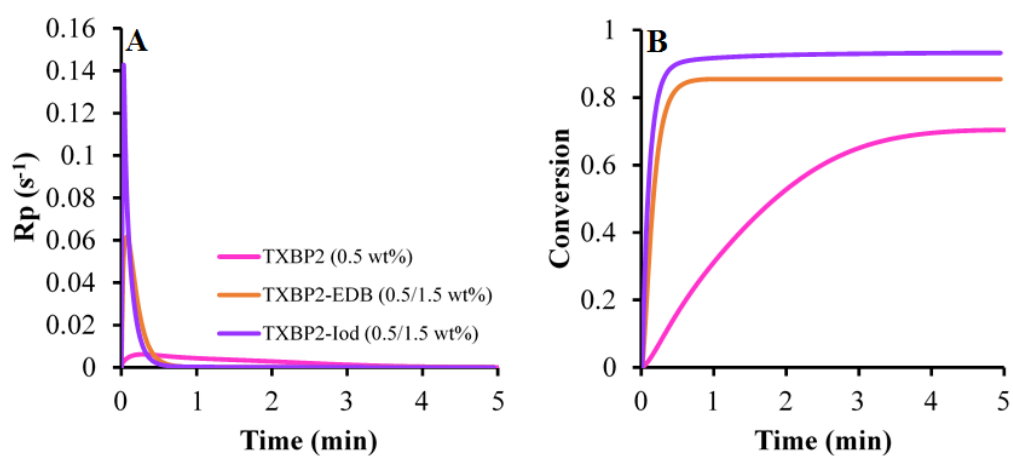


Figure 5.11. Rate-time and conversion-time plots for the photopolymerization of PEGDA under nitrogen at 25 °C,  $\lambda = 320\text{-}500$  nm in the presence of TXBP2, TXBP2/EDB, TXBP2/Iod.

The photopolymerization performance of TXBP2 in aqueous environment was also tested in the polymerization of Aam monomer at  $\lambda = 365$  nm (Table 5.4). Two different photoinitiating systems (TXBP2 and TXBP2/TEA) were studied. The influence of air on the efficiency of the polymerization was also considered. As it can be seen from Table 5.4, the photopolymerization reaction can take place without a co-initiator in air depleted

atmosphere. However, TXBP2 alone can not photoinitiate Aam in aerated atmosphere, even if the concentration of Aam was kept higher. As we can observe, the conversions of the polymerizations were higher in the presence of TXBP2/TEA system both in air depleted (35%) and aerated atmosphere (30%) than TXBP2 in air depleted atmosphere (16%).

Table 5.4. Photoinitiated polymerization of Aam in aqueous media at 25 °C at  $\lambda=365$  nm for 15 minutes.

[Aam]	[TXBP2] (10 <sup>-3</sup> )	[TEA] (10 <sup>-3</sup> )	Conversion [%]
3	3	-	0 <sup>b</sup>
2	3	-	16 <sup>a</sup>
2	3	9	35 <sup>a</sup>
2	3	9	30 <sup>b</sup>

<sup>a</sup>air depleted atmosphere

<sup>b</sup>aerated atmosphere

### 5.3.5. Laser Write Experiments using TXBP2/Iod

To produce printing of 3D patterns easily, laser write 3D polymerization experiments were performed. Some examples of 3D printing were obtained as a result of the 3D printing experiments upon laser diode irradiation at 405 nm under air using TXBP2/Iod (0.1/1 wt%) system in PEGDA (Figure 5.12). Thick polymer samples were acquired with high spatial resolution and short writing time (~ 1-2 min). Numerical optical microscopy was used to characterize the 3D written samples.

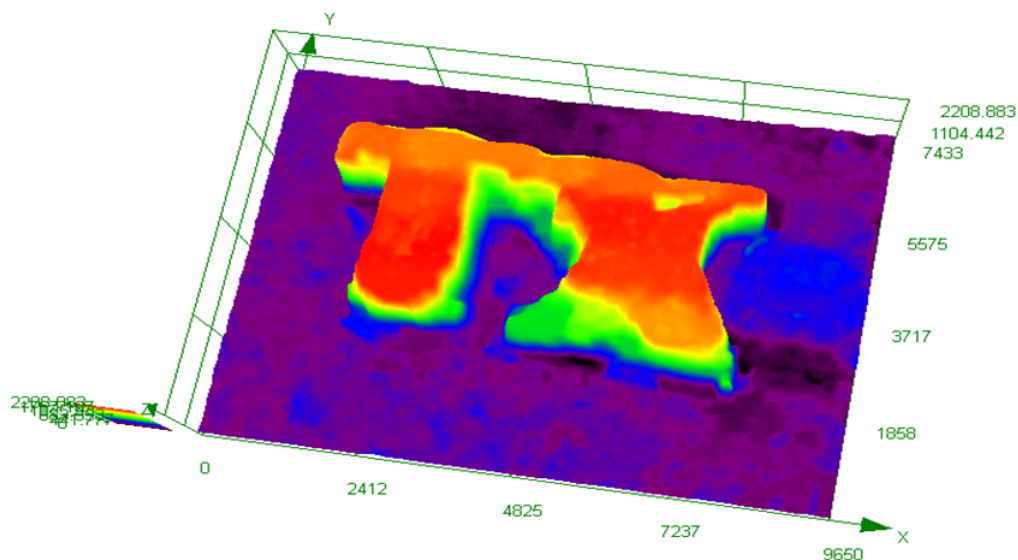


Figure 5.12. Free radical photopolymerization experiments for 3D printing upon laser diode irradiation @405 nm: characterization of the patterns by numerical optical microscopy; TXBP2/Iod (0.1/1 wt%) in PEGDA.

#### 5.4. Conclusions

In this study, synthesis of a novel water-borne photoinitiator (TXBP2) containing a bisphosphonate functional group was reported. In addition to having a high water solubility, TXBP2 was also compatible with multifunctional crosslinkers such as TMPTA and PEGDA which facilitates its use in oil- and water-based UV-Vis curing formulations. From fluorescence and laser flash photolysis experiments, it is found that TXBP2 exhibits both triplet and singlet state reactivity. TXBP2 is efficient in the photopolymerization of TMPTA and PEGDA, but necessity of a coinitiator such as Iod or EDB for a better initiation performance is obvious. It is expected that TXBP2 will have calcium binding ability due to the bisphosphonate group and can initiate mineralization of hydrogels where it is used as photoinitiator during their synthesis. Hence, TXBP2 is expected to be useful for biomedical applications.

## **6. A WATER SOLUBLE THIOXANTHONE FUNCTIONALIZED POLYMERIC PHOTOINITIATOR WITH A DUAL CURING ABILITY**

This chapter is published as: Eren, T. N., J. Lalevee, D. Avci, “Water Soluble Polymeric Photoinitiator for Dual-curing of Acrylates and Methacrylates”, *J. Photochem. Photobiol. A*, Vol. 389, pp. 112288-112298, 2020.

### **6.1. Introduction**

The photoinitiator presented in this chapter, PAATX, features many aspects of green PIs: water solubility, biocompatibility, visible light activation and migration stability. This PI was synthesized by aza-Michael addition reaction between acrylate functionalized 87lycol87e87one and linear poly(amido amine) (PAA) (Figure 6.1). It also has dual-curing ability, in the first stage as the nucleophile and 87lycol87e an aza-Michael reaction, in the second stage as a photoinitiator in conjunction with Iod. Hence, unlike other dual curing processes reported in the literature so far, this process does not need the addition of an amine during the first stage and/or a PI during the second.

The novel photoinitiator PAATX was examined in photophysical and photochemical aspects. Curing properties of PAATX were investigated in the Michael addition reaction with an acrylate in the presence of a methacrylate as the first stage, and in the photoinduced free radical polymerization of methacrylate as the second stage.



Alfa Aesar and used as received without further purification. Bis-(4-*tert*-butylphenyl)-iodonium hexafluorophosphate (SpeedCure938 or Iod) was obtained from Lambson Ltd.

<sup>1</sup>H NMR spectra were recorded on a Varian Gemini (400 MHz) spectrometer at ambient temperature with deuterated methanol (MeOD) as a solvent. Nicolet 6700 FT-IR spectrophotometer was used for recording IR spectra. Gel Permeation Chromatography (GPC) experiments were carried out by Agilent 1260 Series Instrument using polyethyleneoxide standards.

### 6.2.2. Synthesis of PAATX

*N,N'*-methylene bisacrylamide (2.6 mmol, 400 mg) and 1,4-diamino butane (2.9 mmol, 256 mg) were dissolved in MeOH (1.5 mL) and stirred for 12 h at 40 °C. Then the pure polymer was isolated by precipitating into diethyl ether, filtered and dried under vacuum. Linear PAA (0.1 g, 0.02 mmol) and 9-oxo-9H-thioxanthen-2-yl acrylate (0.028 g, 0.01 mmol) were dissolved in MeOH (2.5 mL) and stirred at 70 °C for 48 hours under nitrogen. When the solution was added to excess diethyl ether, pure polymer was isolated as an orange solid in 50% yield.

### 6.2.3. Photochemical Analyses

6.2.3.1. UV-vis Spectroscopy Experiments. Carry 3 UV/vis spectrophotometer from Varian was used to take UV-vis measurements of the PI in methanol. PAATX in the presence and absence of the additives (Iod, EDB) in methanol were irradiated with a LED (385 nm) and the UV-Vis spectra were recorded at different irradiation times for steady state photolysis experiments.

6.2.3.2. Fluorescence Experiments. Fluorescence properties of the PI were examined in methanol using JASCO FP-6200 Spectrofluorometer. The interaction rate constants  $k_q$  between PI and the additives (Iod, EDB) were calculated from the Stern-Volmer treatments by using the formula;  $(I_0/I = 1 + k_q\tau_0[Iod])$ , where  $I_0$  and  $I$  symbolize the fluorescence intensity of the photoinitiator in the absence and presence of the quencher (Iod or EDB), respectively and  $\tau_0$  represents the singlet excited state lifetime of the PI in the absence of the

quencher. Time-resolved experiments (Jobin-Yvon Fluoromax 4) were applied to determine the fluorescence lifetimes.

**6.2.3.3. Laser Flash Photolysis.** Nanosecond laser flash photolysis (LFP) experiments were carried out by using Q-switched nanosecond Nd/YAG laser ( $\lambda_{\text{exc}} = 355 \text{ nm}$  (9 ns pulses; energy reduced down to 10 mJ; minilite Continuum) and the analyzing system (for absorption measurements) consisted of a ceramic xenon lamp, a monochromator, a fast photomultiplier and a transient digitizer (Luzchem LFP 212) [245].

#### **6.2.4. Photopolymerization Experiments**

Four HEMA/PEGDA/PAATX/Iod (1-4) and one HEMA/PEGDA/PAATX (6) formulations shown in Table 3 were prepared by first mixing PAATX (0.5 or 1.5 wt%) (the amount of TX in the PAATX was calculated to be as 0.5 wt%) with HEMA, then adding Iod (1 wt%) (for the formulations 1-4) and finally adding the required amount of PEGDA by quick stirring; and the reaction was analyzed immediately to catch also the prepolymerization (by aza-Michael addition) of the resin. To compare the efficiency of the novel photoinitiator PAATX, formulation 5 containing commercial TX (0.5 wt%) instead was also prepared and analyzed. Photopolymerization efficiency of all the formulations were tested in Photo-DSC. Formulation 1 was also used in FTIR experiments to follow the aza-Michael addition and photopolymerization reactions consecutively.

**6.2.4.1. FTIR.** Nicolet 6700 FTIR spectrometer equipped with an attenuated total reflection (ATR) accessory (GoldenGate™, Specac Ltd.) which is temperature controlled was used to monitor the degree of cure of the samples during the aza-Michael reaction and photocuring. Real time spectra were taken in absorbance mode with a resolution of  $2 \text{ cm}^{-1}$  in the wavelength range from  $4000$  to  $400 \text{ cm}^{-1}$  averaging 4 scans for each spectrum. Scans were carried out with duration time of 1.5 sec. A drop of sample (Formulation 1; given in Table 5.3) was covered with a Mylar polyester film to prevent the inhibition effect of oxygen during photoinduced free radical polymerization. The aza-Michael addition reaction was followed by 10 minutes and then 5 minutes of UV-irradiation was applied to monitor the photopolymerization reaction at  $30 \text{ }^\circ\text{C}$ . The conversion of functional groups was determined using

$$\text{Conversion (\%)} = \left(1 - \frac{A_t(815)}{A_0(815)}\right) \times 100 \quad (6.1)$$

where  $A_t$  is taken as the area under the absorbance peak at  $815 \text{ cm}^{-1}$  (C=C deformation) at time  $t$  (curing time) and  $A_0$  is the area under the absorbance peak at  $815 \text{ cm}^{-1}$  at time 0 (beginning of the curing). Hence, overall acrylate and methacrylate conversion was estimated using the peak at  $815 \text{ cm}^{-1}$ .

**6.2.4.2. Photo-DSC.** Photo-DSC analyses were conducted on a DSC 250 (TA Instruments) equipped with a UV-vis light (320-500 nm) source, Omnicure 2000 with dual-quartz light guide. Formulations (1-5) which are given in Table 3 (3-4 mg) were irradiated for 5 min at  $30 \text{ }^\circ\text{C}$  and under nitrogen flow of  $50 \text{ mL min}^{-1}$ . The heat flow of the polymerization reaction was monitored as a function of time. All measurements were performed in duplicate. The cure speed of polymerization reactions were calculated by

$$\text{Rate} = \frac{(Q/s)M}{n(\Delta H_p)m} \quad (6.2)$$

where  $Q/s$  is the heat flow per second,  $M$  is the molar mass of the monomer,  $n$  is the number of double bonds per monomer molecule,  $\Delta H_p$  is the heat of reaction evolved and  $m$  is the mass of monomer in the sample. The theoretical heat for the total conversion of an acrylate and methacrylate double bond is  $86 \text{ kJ/mol}$  and  $55 \text{ kJ/mol}$ , respectively [248], [249].

**6.2.4.3. Photoreactor.** (HEMA/PEGDA(75/25 wt%)-water (70-30 wt%) or (HEMA/PEGDA(50/50 wt%)-water (70-30 wt%) mixtures in the presence of PAATX (0.5 wt%) and Iod (1 wt%) were placed into glass vials (diameter: 9 mm, thickness: 5 mm). The mixtures were then exposed to UV light (365 nm) for 30 min in a photoreactor containing 12 Philips TL 8 W BLB lamps in an air atmosphere. Then the gels were washed with methanol for 5 days and dried under vacuum and weighed. The conversions were calculated gravimetrically.

### 6.2.5. Migration Study

HEMA/PEGDA(75/25 wt%) in the presence of PAATX or TX (0.5 wt%) and Iod (1 wt%) was photopolymerized (365 nm) for 1.5 h in glass vials under air. The crosslinked polymers were soaked in 25 ml of methanol for 7 days. The percent of extracted photoinitiator was determined by UV-vis spectroscopy [24].

## 6.3. Results and Discussion

### 6.3.1. Synthesis of PAATX

The novel polymeric photoinitiator PAATX was synthesized in two steps as seen in Figure 6.2. In the first step a linear PAA was synthesized via an aza-Michael addition reaction between *N,N'*-methylene bisacrylamide and 1,4-diamino butane. The molecular weight of the polymer was determined by GPC as  $M_n = 2400$  g/mol. Then the PAA was coupled with acrylate functionalized thioxanthone through again an aza-Michael addition reaction. The light-sensitive TX group is thus attached to a water soluble polymer. This synthesis method which enables specific design of different photoinitiating systems has many advantages. First, it allows introduction of different light-sensitive groups to the PAA backbone. Secondly, the concentration of the light-sensitive group can be controlled by adjusting the initial mole ratio of PAA to the light-sensitive compound. This way the solubility of the resulting polymeric photoinitiator can also be tuned. Thirdly, other functional groups can be attached to the backbone by nucleophilic substitution reactions of the residual secondary amines. Lastly, Michael addition reactions with multifunctional acrylates or acrylamides result in crosslinked network formation.

The amount of TX units in PAATX was determined as 10 wt% according to UV-Vis absorption studies by the use of the extinction coefficient of pure TX ( $\lambda_{max} = 380$  nm,  $\epsilon_{380} = 5890$  M<sup>-1</sup> cm<sup>-1</sup>). To find out the molecular weight of PAATX, the amount of TX in PAATX (10 wt%) was added to the molecular weight of the linear PAA and calculated as 2700 g/mol. The novel photoinitiator PAATX is soluble in water (3 g/L) which makes it suitable for water-based applications (Table 6.1). It is stable at 4 °C for at least 60 days. However, in the presence of monomers it immediately gives crosslinked networks.

PAATX shows good compatibility with the methacrylate HEMA. However, PAATX is not miscible with acrylates (PEGDA, TMPTA) alone, because the PI gives reaction with acrylates through Michael addition. Thus, HEMA behaves as a reactive solvent to prepare acrylate:methacrylate mixtures.

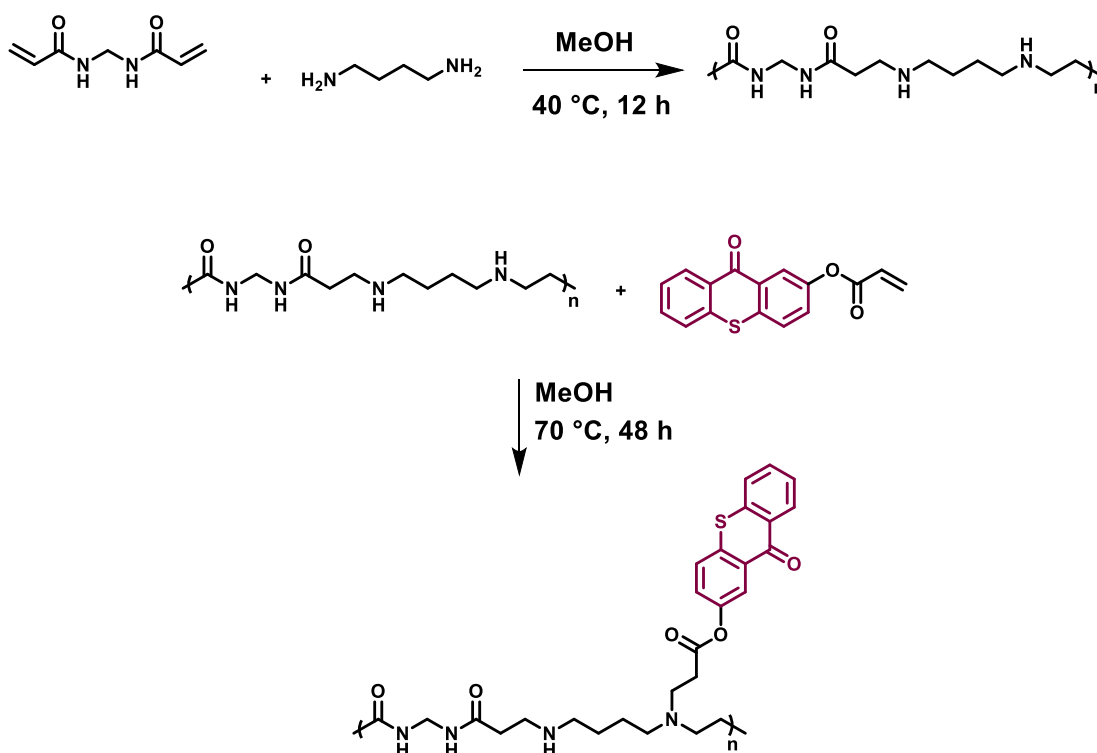


Figure 6.2. The synthesis of PAATX.

Table 6.1. The solubility of PAATX.

PI	H <sub>2</sub> O	DMF	THF	MeOH	DCM	Acetone	Diethyl Ether
PAATX	+	±	-	+	-	-	-

The structure of the polymer was proven by  $^1\text{H}$  and FTIR spectroscopies. In the  $^1\text{H}$  NMR spectrum of PAATX, the peaks between 7.17-8.42 ppm show the aromatic protons of TX which verifies its substitution into the linear PAA (Figure 6.3). The peaks due to the methylenes attached to carbonyls (2.27 ppm and 2.31 ppm) and amide (4.48 ppm) nitrogens were observed. In the FTIR spectrum, the polymer showed characteristic peaks at  $3272\text{ cm}^{-1}$  (NH stretching) and  $1533\text{ cm}^{-1}$  (NH bending). PAATX also showed three different carbonyl peaks due to TX and PAA structures, both ketone carbonyl of TX and amide carbonyl of PAA at  $1636\text{ cm}^{-1}$  and an ester carbonyl at  $1729\text{ cm}^{-1}$  (Figure 6.3).

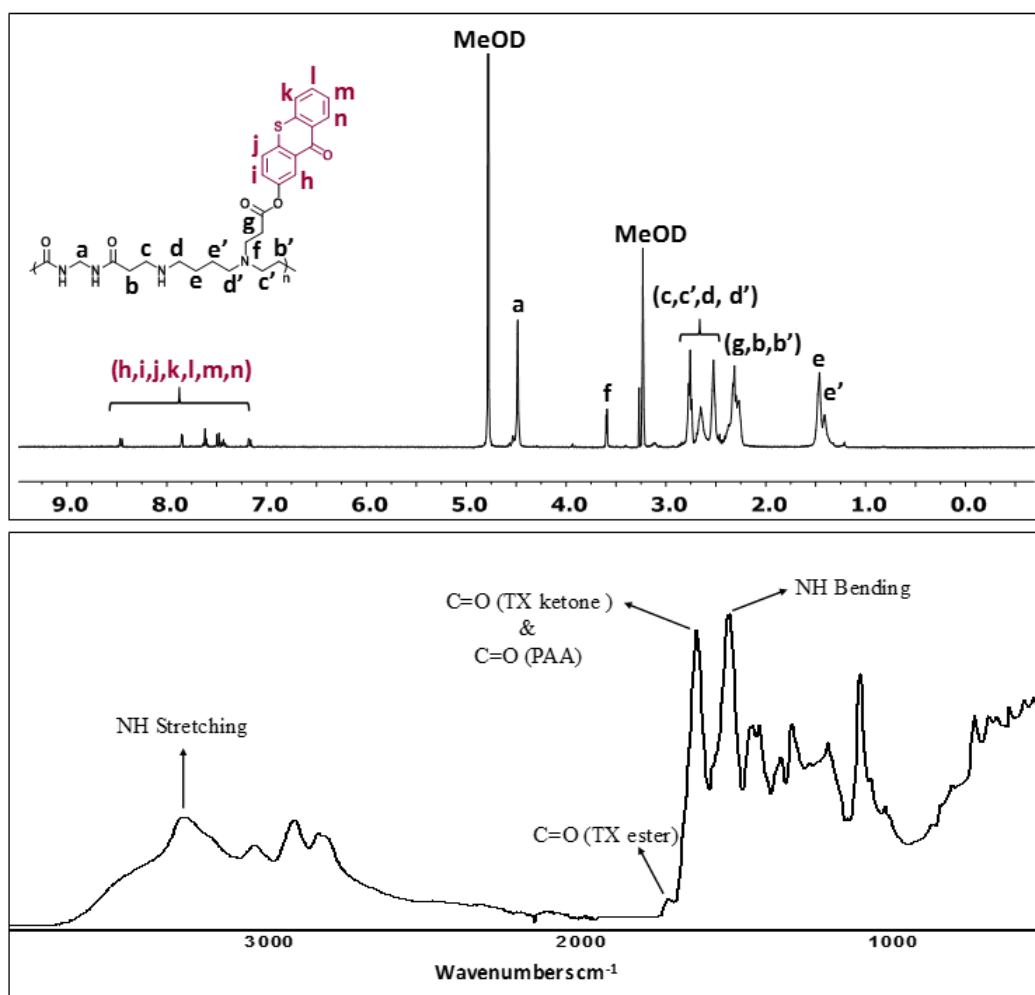


Figure 6.3.  $^1\text{H}$  NMR and FTIR spectrum of PAATX.

### 6.3.2. Light Absorption Properties

Absorption characteristics of PAATX in MeOH ( $9.4 \times 10^{-5}$  M) was investigated by UV-vis spectroscopy (Figure 6.4A). The maximum absorption wavelength of PAATX is located at the edge of the visible region at 400 nm ( $\sim \epsilon = 11.5 \times 10^3 \text{ M}^{-1} \text{ cm}^{-1}$ ), a slightly red-shifted compared to the commercial TX ( $\lambda_{\text{max}} = 380 \text{ nm}$ ), probably due to the electron donating oxygen group attached to TX.

PAATX was found to fluoresce when investigated with a spectrofluorometer. This is consistent with the fluorescence properties of tertiary aliphatic amines and linear polymers with a tertiary amine in their backbone or as a side group, revealed by previous studies in literature [268, 269, 273]. The fluorescence properties of PAATX upon excitation at 402 nm were determined, giving information about the excited state characteristics, as seen in Figure 6.4B. Mirror-image like relationship of absorbance and emission graphs confirms the singlet state reactivity of PAATX. The first singlet excited energy ( $E_{S1}$ ) was calculated as 2.81 eV from the intersection point of the absorbance and emission plots. The Stokes shift was found as  $119047 \text{ cm}^{-1}$ .

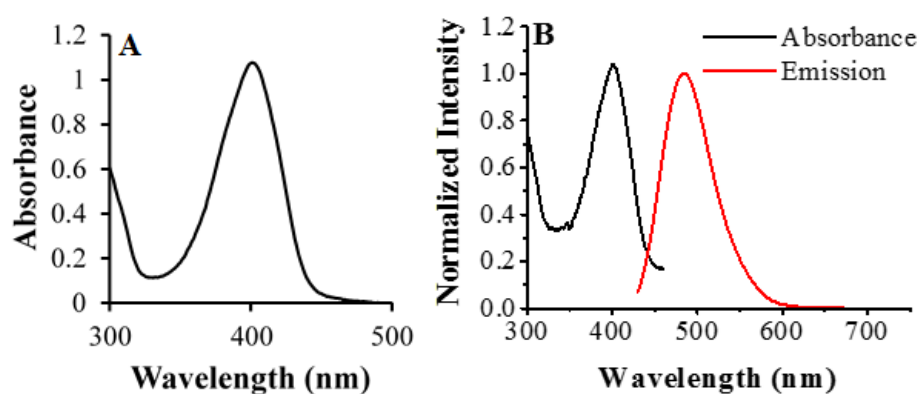


Figure 6.4. (A) UV-vis absorption spectrum of PAATX ( $9.4 \times 10^{-5}$  M) in MeOH. (B) Absorption (black line) and emission (red line) spectra of PAATX in methanol. The solution was excited at  $\lambda_{\text{exc}} = 402 \text{ nm}$ .

### 6.3.3. Photochemical Mechanisms

**6.3.3.1. Steady-State Photolysis.** Steady state photolysis experiments were performed to understand the photochemical mechanism of the novel photoinitiator (Figure 6.5). The PAATX/Iod system shows a very fast photobleaching compared to photostable PAATX and PAATX/EDB systems as seen in Figure 6.5C. This behavior can be attributed to the better efficiency of PAATX in a photooxidation mechanism rather than a photoreduction mechanism. New photoproducts can be identified by the shoulders at  $\lambda \sim 450\text{--}460\text{ nm}$  for all the systems, which is due to the formation of new radicals in photooxidation (with Iod, reactions 4,5 and 6 below) or photoreduction (with EDB, reactions 7 and 8 below) or intramolecular H-abstraction (PAATX alone). The two isosbestic points were noticed in all the systems which implies that there is no side reaction.

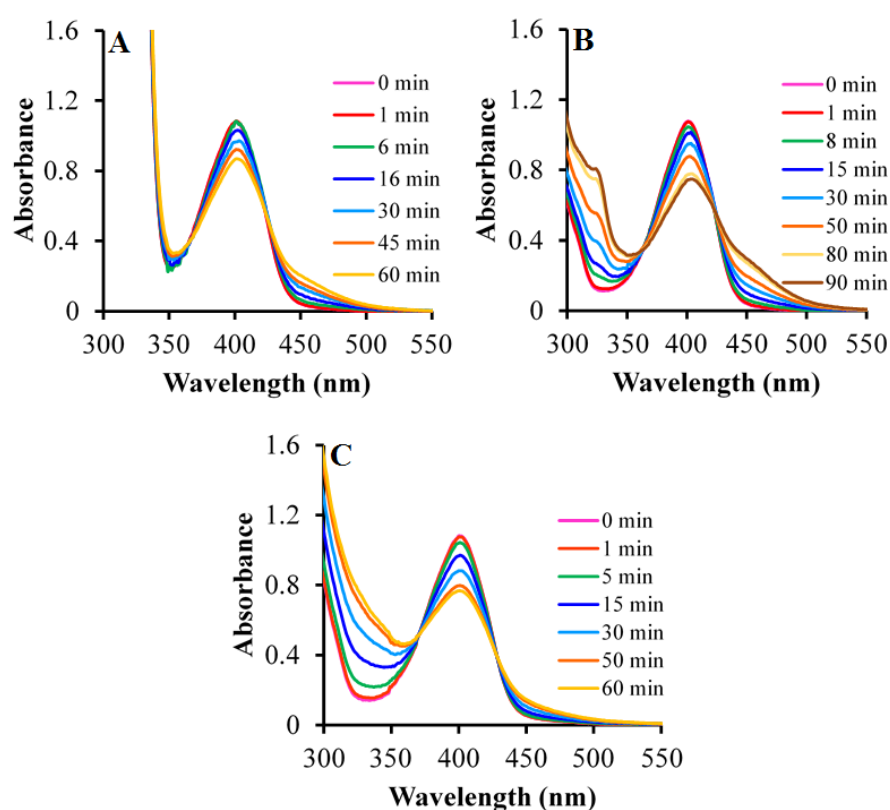


Figure 6.5. Photolysis of PAATX in methanol ( $9.4 \times 10^{-5}\text{ M}$ ) in the presence (A) and absence (B) of EDB ( $1 \times 10^{-3}\text{ M}$ ), and in the presence of Iod ( $1 \times 10^{-3}\text{ M}$ ) (C) using a 385 nm LED.

6.3.3.2. Fluorescence Quenching, Laser Flash Photolysis (LFP). Fluorescence quenching experiments were performed, adding EDB or Iod at different concentrations and the change in the emission spectrum of PAATX in MeOH was followed to figure out the singlet excited state reactivity of the PI (Figure 6.6). The fluorescence lifetime of PAATX was reported as 7.7 ns in Table 6.2. The Stern-Volmer plots for both PAATX/Iod and PAATX/EDB show fast fluorescence quenching property of PAATX. It is important that Stern-Volmer plots show a straight line with reasonable point scattering. Stern-Volmer quenching constants,  $K_{sv}$ , were calculated from the slopes as  $23.3 \text{ M}^{-1}$  and  $69 \text{ M}^{-1}$  for PAATX/Iod and PAATX/EDB, respectively. The interaction rate constants of  $^1\text{PAATX}/\text{Ph}_2\text{I}^+$  and  $^1\text{PAATX}/\text{EDB}$  were very high and mainly diffusion controlled ( $3 \times 10^9 \text{ s}^{-1} \text{ M}^{-1}$  and  $8.9 \times 10^9 \text{ s}^{-1} \text{ M}^{-1}$ ) by using the formula  $k_q = K_{sv}/\tau$ , respectively (Table 6.2). The electron transfer quantum yields of PAATX in the presence of Iod and EDB were derived by using the formula  $\phi_{et} = K_{sv}[\text{Iod}]/(1+K_{sv}[\text{Iod}])$  as 0.4 and 0.5 respectively, which are very high. This result shows that photoactive radicals that take part in the photopolymerization reactions are generated from singlet excited state rather than triplet excited state (Table 6.2).

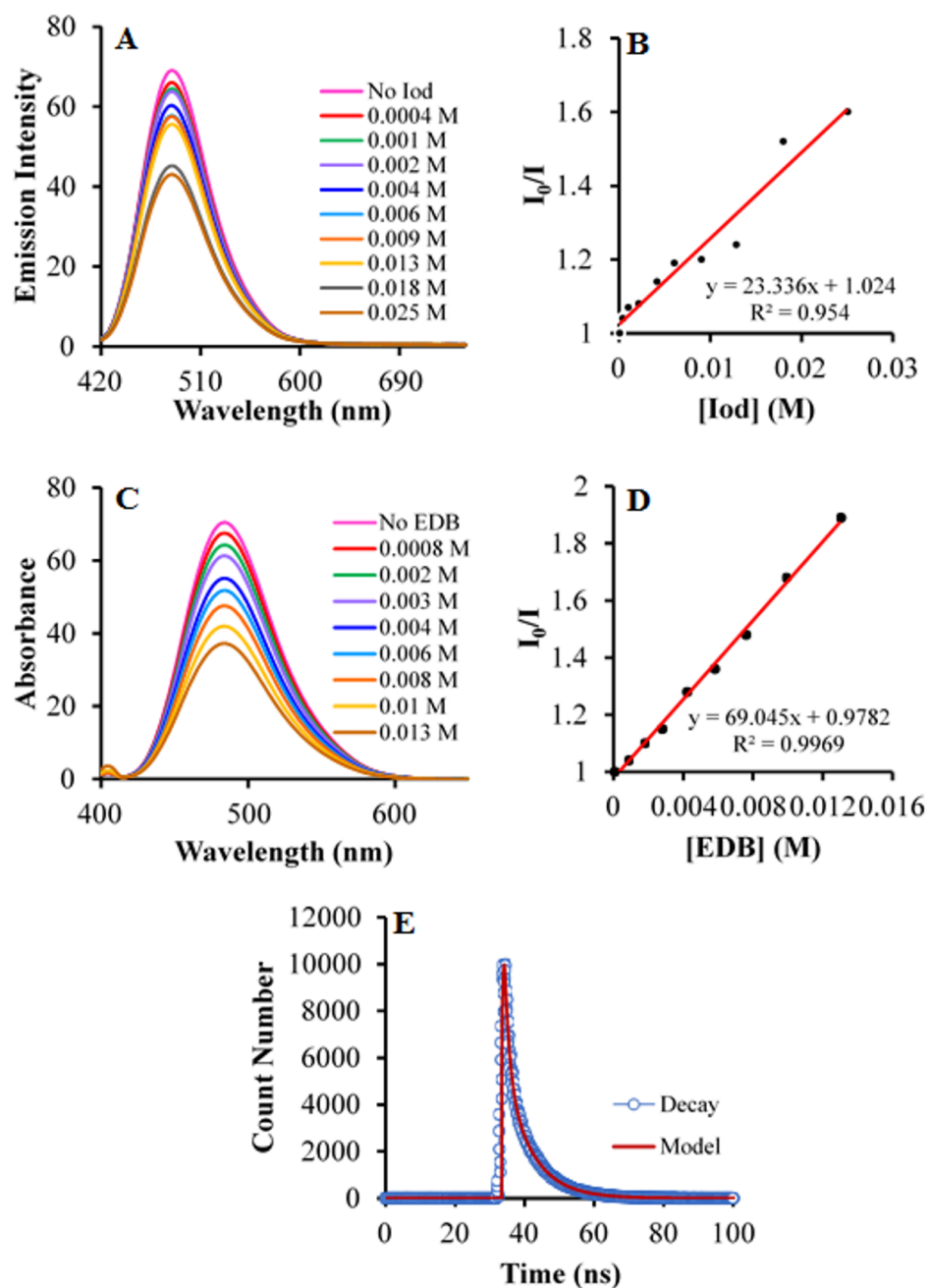


Figure 6.6. (A) The fluorescence quenching of PAATX in methanol solution with different concentrations of Iod; (B) The Stern-Volmer plot of A; (C) The fluorescence quenching of PAATX in methanol solution with different concentrations of EDB; (D) The Stern-Volmer plot of C, (E) Fluorescence life-time measurement of PAATX dissolved in methanol.

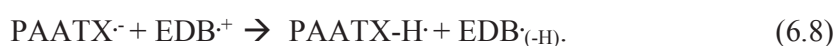
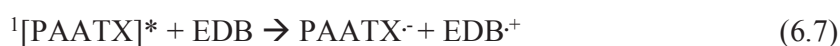
Table 6.2. Parameters characterizing the reactivity of the PAATX.

	<b>Iod</b>				<b>EDB</b>			
<b>PI</b>	<b>E<sub>S1</sub></b> [Ev]	<b>K<sub>SV</sub></b> [M <sup>-1</sup> ]	<b>k<sub>q</sub></b> [M <sup>-1</sup> s <sup>-1</sup> ]	<b>Φ<sub>(et)</sub></b>	<b>K<sub>SV</sub></b> [M <sup>-1</sup> ]	<b>k<sub>q</sub></b> [M <sup>-1</sup> s <sup>-1</sup> ]	<b>Φ<sub>(et)</sub></b>	<b>τ</b> [ns]
<b>PAATX</b>	2.81	23.3	3 x 10 <sup>9</sup>	0.4	69	8.9 x 10 <sup>9</sup>	0.5	7.7

The decomposition mechanism of Iod by PAATX through photooxidative redox reaction is given below. In this reaction, the photoinitiator is oxidized by Iod giving an electron to form Ar• radical and PAATX<sup>•+</sup> which can be utilized as initiating species in the radical and cationic photopolymerization, respectively [260], which can be seen in



The photoreductive redox reaction occurs between singlet state of PAATX and EDB. This reaction occurs through the reduction of the photoinitiator by EDB with an electron abstraction and the aminoalkyl radical EDB<sup>•(-H)</sup> forms which can be used in the free radical photopolymerization reactions as given by



Laser flash experiments were also performed to clarify the excited state reactivity issues (Figure 6.7). According to the results there is no significant triplet state reactivity which confirms the dominance of singlet excited state reactivity over triplet excited state, found by fluorescence quenching experiments, once more.

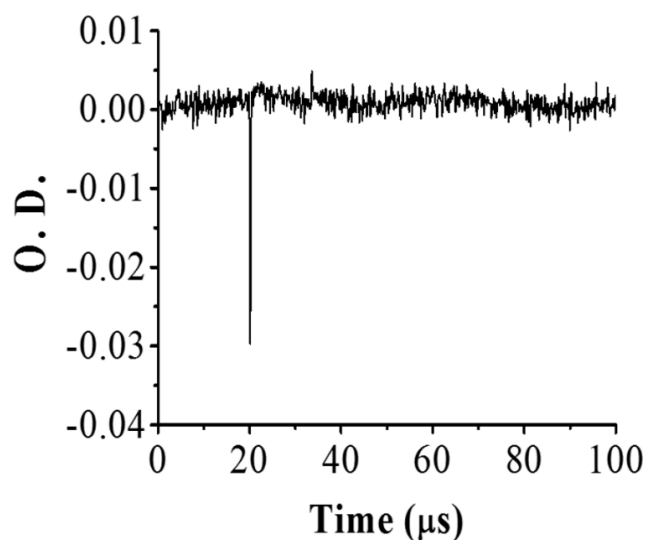


Figure 6.7. Triplet state decay trace observed after laser excitation of PAATX. Laser excitation was for  $t = 20 \mu\text{s}$ .

#### 6.3.4. Photopolymerization

The efficiency of PAATX during sequential dual curing reactions was evaluated using FTIR and photo-DSC. We used PEGDA ( $M_n = 575 \text{ g/mol}$ ) as an acrylate for the aza-Michael addition of our nucleophile/base (no catalyst is required), PAATX, for the first stage of curing process. HEMA was used as a methacrylate to increase conversion during photopolymerization reaction for the second stage of curing (methacrylates are known to be poor Michael acceptors, hence HEMA does not affect the first reaction much). We expect the tertiary amines formed during aza-Michael addition to act as co-initiators for TX and also overcome the inhibitory effect of oxygen during free radical polymerization. Four HEMA/PEGDA/PAATX/Iod formulations (Table 6.3) were prepared. HEMA/PEGDA/TX/Iod (formulation 5) and HEMA/PEGDA/PAATX (formulation 6) were also prepared for comparison (Table 6.3).

Table 6.3. Compositions of the formulations.

Formulations	HEMA (wt%)	PEGDA (wt%)	PI (wt%)	Iod (wt%)
1	75	25	0.5 <sup>a</sup>	1
2	75	25	1.5 <sup>a</sup>	1
3	50	50	0.5 <sup>a</sup>	1
4	50	50	1.5 <sup>a</sup>	1
5	75	25	0.5 <sup>b</sup>	1
6	75	25	0.5 <sup>a</sup>	-

<sup>a</sup>PAATX<sup>b</sup>TX

Figure 6.8A shows the FTIR spectra collected to monitor the polymerization of formulation 1 during both stages of the curing processes. Although a reduction in the intensities of peaks at 1636 (C=C stretching) and 815 (C=C bending)  $\text{cm}^{-1}$  was observed, we used only the peak at 815  $\text{cm}^{-1}$  to investigate the conversion of the aza-Michael reaction towards acrylates, and overall conversion. As it can be seen from Figure 6.8A, the absorbance peak at 815  $\text{cm}^{-1}$  decreases during aza-Michael addition (no UV light) for the first 10 minutes and then after exposure to UV-curing for 5 minutes the peak disappears almost completely. The conversion (%) during aza-Michael addition reaction/photocuring of the formulation 1 is given in Fig. 6.8B. In the first curing stage, the acrylate conversion was observed to be 36% by the Michael addition reaction between PEGDA and PAATX, in the second stage, the conversion increased to 83% through photopolymerization of both HEMA and excess PEGDA. Polymerization results of the formulation 6 demonstrate that although PAATX can successfully initiate polymerization of PEGDA, it does not initiate photopolymerization of HEMA effectively in the absence of Iod (Figure 6.8B). Iod reacts with PAATX through photooxidation mechanism through the singlet excited state to initiate photopolymerization. EDB, reacting with PAATX through photoreduction mechanism was also used, but did not give significant polymerization, showing the difference between oxidative and reductive mechanisms.

Photo-DSC profiles of all the formulations are represented in Figure 6.9A and 6.9B. According to the results, formulation 4 has the highest rate of polymerization and lowest  $t_{\text{max}}$  value ( $R_{\text{pmax}} = 0.011 \text{ s}^{-1}$ ,  $t_{\text{max}} = 0.57 \text{ min}$ , conversion = 66%). Formulation 2 and formulation

3 show similar reactivity; ( $R_{\text{pmax}} = 0.0093 \text{ s}^{-1}$ ,  $t_{\text{max}} = 0.83 \text{ min}$ , conversion = 70%) and ( $R_{\text{pmax}} = 0.009 \text{ s}^{-1}$ ,  $t_{\text{max}} = 0.77 \text{ min}$ , conversion = 66%), respectively. Formulation 1 is the slowest system between the PAATX containing formulations ( $R_{\text{pmax}} = 0.008 \text{ s}^{-1}$ ,  $t_{\text{max}} = 1.14 \text{ min}$ , conversion = 70%). We can see that, formulations containing higher proportion of acrylate (PEGDA) and/or higher amount of photoinitiator (PAATX) exhibit slightly higher photopolymerization efficiency. Commercial TX has lower polymerization rate ( $R_{\text{pmax}} = 0.0027 \text{ s}^{-1}$ ), higher  $t_{\text{max}}$  (2.45 min) and lower conversion (50 %) for the polymerization of the same formulation HEMA/PEGDA(75/25 wt%) than the system containing PAATX (Formulation 1).

The efficiency of PAATX in the photopolymerization of the formulations 1 and 3 in aqueous environment has also been tested at  $\lambda = 365 \text{ nm}$ , and the conversions were found as 72% and 85%, respectively.

### 6.3.5. Migration Stability

The migration stability of PAATX was examined and compared with commercial TX. The photoinitiator concentrations leaching to methanol from the crosslinked HEMA/PEGDA (75/25 wt%) polymer samples were determined by UV-vis absorption spectroscopy. According to the results, extractability of PAATX was found nearly 3 times lower than TX (Figure 6.10). Hence, it can be concluded that PAATX has a higher migration stability compared to small molecule TX because of its incorporation into polymer structure through formation of an interpenetrated network.

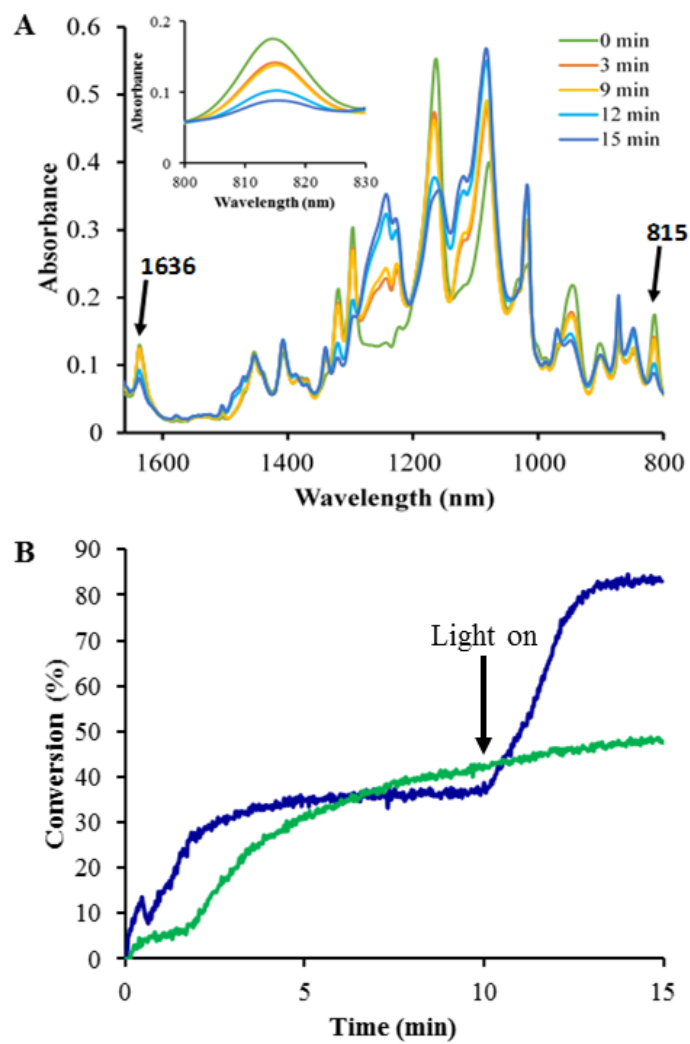


Figure 6.8. A) FTIR spectra for formulation 1 and B) Conversion (%) for formulations 1 and 6 monitored during the aza-Michael (10 min) and photopolymerization (5 min) reactions.

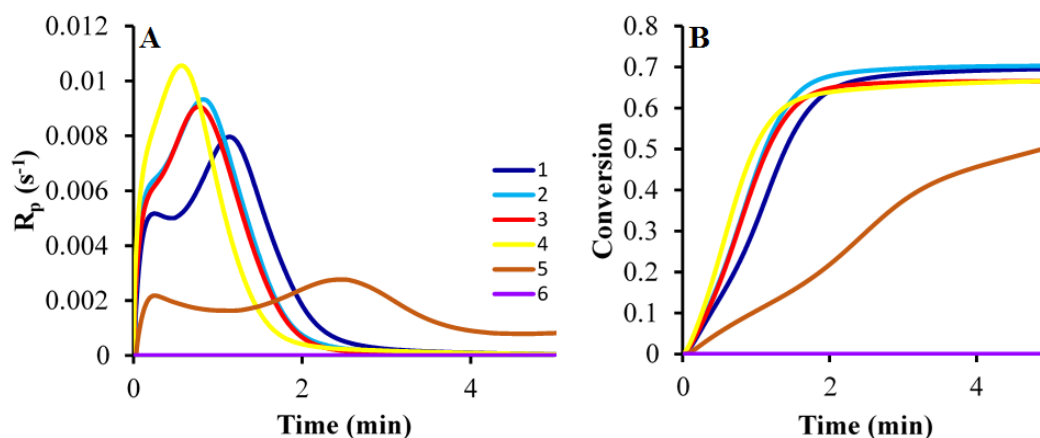


Figure 6.9. A) Rate-time and B) Conversion-time plots of formulations 1-6 in Photo-DSC.

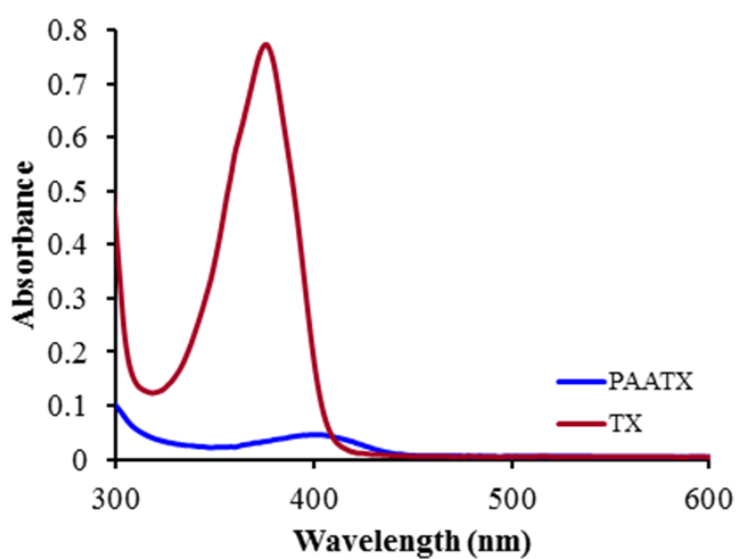


Figure 6.10. UV-vis absorption spectra of PAATX and TX extracted with methanol from the HEMA/PEGDA (75/25 wt%) polymer samples.

#### 6.4. Conclusions

The synthesis of a TX-based polymeric water soluble (photo)initiator, PAATX, for dual curing applications was reported. It has a maximum absorption wavelength at 400 nm and fluorescent due to the strongly electron donating tertiary amine groups and electron

accepting TX functionality and has a singlet state (S1) lifetime of 7.7 ns. Remarkably, compared to the thioxanthone derivatives that usually exhibit triplet state reactivity and for low singlet state reactivity, it is found here that PAATX is mainly characterized by a singlet state pathway. It efficiently initiates the aza-Michael addition of PEGDA, followed by visible-light-initiated radical photopolymerization of HEMA and remaining PEGDA in the presence of an iodonium salt. Taking the advantage of the dual-curing processing, custom-tailorable products can be developed for different industrial applications. PAATX can be used in aqueous formulations which makes it environmentally-friendly.

## 7. BRANCHED POLY(ETHYLENEIMINE) AND I2959 BASED WATER SOLUBLE POLYMERIC PHOTOINITIATORS

This chapter is published as: Eren, T. N., N. Kariksiz, G. Demirci, D. Tuncel, N. Okte, H. Yagci Acar, D. Avci, “Irgacure 2959-Functionalized Poly(ethyleneimine)s as Improved Photoinitiators: Enhanced Water Solubility, Migration Stability and Visible-Light Operation”, *Polym. Chem.*, Vol. 12, pp. 2772-2785, 2021.

### 7.1. Introduction

Photopolymerization as a green technology has many usages in biomedical applications such as dental curing, encapsulation of cells, drug delivery systems and 3D hydrogels for tissue engineering scaffolds [274-278]. Aqueous photopolymerization is especially preferred for biomedical applications. Irgacure 2959 is the most popular commercial photoinitiator for the fabrication of water-borne photocured biomaterials due to its high reactivity, biocompatibility and water solubility, even though the latter is quite limited, less than 2 wt%; furthermore, I2959 has a high migration of the photolysis fragments due to its low molecular weight [148, 279].

In this work, novel water-borne, low migration, non-toxic and multifunctional polymeric photoinitiators (PEI-I2959 and PEI-I2959-Ts) based on branched poly(ethyleneimine) (bPEI,  $M_w = 1800$ ) and I2959 were produced to address the shortcomings of I2959 while keeping the advantages. bPEI also plays two important roles: increasing solubility of the PI and acting as a crosslinker. The latter can be due to aza-Michael addition reaction between the unreacted primary and secondary amines on bPEI and acrylates. This property brings these photoinitiators a dual curing ability, aza-Michael addition reaction followed by photopolymerization (Figure 7.1) [131, 136-138, 142].

The dual curing kinetics of the novel PEI-I2959 and PEI-I2959-Ts PPIs were investigated in the Michael addition reaction with an acrylate (PEGDA) in the presence of a methacrylate (HEMA) as the first stage and in the free radical photopolymerization (FRP)

of both kinds of monomers as the second stage, by Real-Time Fourier Transform Infrared spectroscopy (RT-FTIR) and photo differential scanning calorimetry (photo-DSC). This dual-curability of the new photoinitiators incorporates them into the interpenetrating network too, which may also contribute to reduce the migration of the PPIs. The reactivity of the novel photoinitiators was also studied in aqueous solution during polymerization of acrylamide (AAm) by RT-FTIR. Their solubility in water, UV absorption, thermal, migration and cytotoxicity properties were also analyzed.

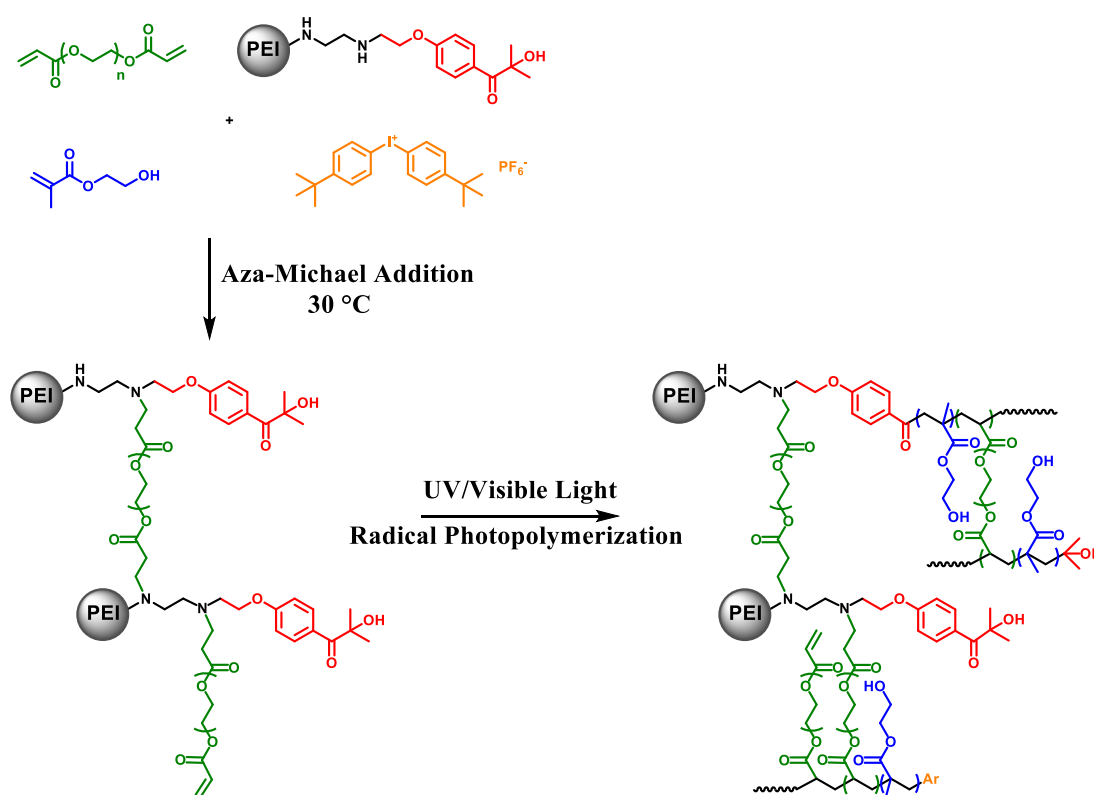


Figure 7.1. Dual Curing of HEMA/PEGDA formulations using PEI-12959.

## 7.2. Experimental

### 7.2.1. Materials and Methods

2-(4-(2-hydroxy-2-methylpropanoyl)phenoxy)ethyl 4-methylbenzenesulfonate (I2959-Ts) was synthesized according to a literature procedure [20]. Branched poly(ethylene imine) (bPEI) ( $M_w = 1800$  g/mol) was purchased from Polysciences Inc. Irgacure 2959 (I2959), 1-hydroxycyclohexyl phenyl ketone (Irgacure 184 or I184), phenylbis (2,4,6-trimethylbenzoyl)-phosphine oxide (BAPO), p-toluenesulfonyl chloride (tosyl chloride, TsCl), 2-hydroxyethyl methacrylate (HEMA), poly(ethylene glycol) diacrylate (PEGDA,  $M_n = 575$  D), acrylamide (AAm) and the other reagents and solvents were purchased from Sigma-Aldrich or Alfa Aesar and used as received without further purification. Bis-(4-tert-butylphenyl)-iodonium hexafluorophosphate (Iod or Speedcure 938) was obtained from Lambson Ltd. Dulbecco's Modified Eagle Medium (DMEM) (with l-glutamine and high glucose (4.5 g/L), penicillin/streptomycin (pen-strep), fetal bovine serum (FBS) and trypsin-EDTA were purchased from Diagnostovum, Ebsdorfergrund (Germany). Thiazolyl blue tetrazolium bromide (MTT) was provided by Gold Biotechnology (USA) and phosphate buffered saline (PBS) tablets were provided by BBI Life Sciences (China). 96-Well plates were obtained from Nest Biotechnology (China). NIH/3T3 mouse embryonic fibroblast cells were a kind gift of Prof. Dr. Halil Kavakli (Department of Molecular Biology and Genetics, Koc University, Istanbul, Turkey). L929 cells were purchased from ATCC (USA).

### 7.2.2. Characterization and Methods

NMR spectra were recorded in deuterated water (D<sub>2</sub>O) at ambient temperature on a Varian Gemini (400 MHz) spectrometer. IR spectra were obtained by using a Nicolet 6700 FT-IR spectrophotometer. UV-vis spectra were recorded on a Varian® Cary 3 spectrometer. Differential scanning calorimetric (DSC) measurements were performed on a TA Instruments Q250 with a heating rate of 10 °C/min. Thermogravimetric analysis (TGA) was performed by using TA Instruments Q500 under nitrogen atmosphere. The samples were heated from room temperature to 100 °C at a rate of 10 °C/min, held at this temperature for 20 min and then heated again from 100 °C to 600 °C at a rate of 10 °C/min.

### 7.2.3. Syntheses of Photoinitiators

7.2.3.1. PEI-I2959. I2959-Ts (0.12 g, 0.31 mmol) and bPEI (0.14 g, 0.078 mmol) were stirred in dimethyl formamide (DMF) (3 mL) in the presence of  $K_2CO_3$  (0.155 g, 1.12 mmol) at 100 °C for 24 h. After removal of the solvent under reduced pressure, the residue was washed with diethyl ether (3x 25 mL) to remove any unreacted I2959-Ts and then dialyzed in water for 6 days using a membrane with a molecular weight cut-off of 1000 Da to discard any salts of 4-toluenesulfonic acid formed during the reaction. The pure product was obtained as a white-yellow solid in 15% yield.

7.2.3.2. PEI-I2959-Ts. I2959-Ts (0.15 g, 0.39 mmol) and bPEI (0.14 g, 0.078 mmol) were stirred in DMF (3 mL) at 100 °C for 24 h. After removal of the solvent under reduced pressure, the residue was dissolved in methanol (0.3 mL) and precipitated into diethyl ether (500 mL). The crude product was washed with diethyl ether:dichloromethane (DCM) (1:3) mixture to give the title product as a yellow-orange solid in 90% yield.

### 7.2.4. RT-FTIR Measurements

A Nicolet 6700 FTIR spectrometer equipped with an attenuated total reflection (ATR) accessory (GoldenGate™, Specac Ltd.) and a UV-vis light (320-500 nm) source, Omnicure 1000 with a quartz light guide, was used to monitor the degree of curing of the samples during the aza-Michael reaction and photocuring. Real time spectra were taken in absorbance mode with a resolution of  $2\text{ cm}^{-1}$  in the wavelength range from 4000 to  $400\text{ cm}^{-1}$  averaging 4 scans for each spectrum. Scans were carried out with a duration time of 1.5 sec.

7.2.4.1. Michael Addition/Photo Studies. HEMA/PEGDA (50/50 wt%) mixtures containing 0.3 I2959-equivalent wt% of either PI (the amount of I2959 in PEI-I2959 or PEI-I2959-Ts was adjusted to be as 0.3 wt%, so the molar concentrations of the PPIs are also the same) were prepared by first mixing the PI with HEMA, then adding Iod, finally adding PEGDA by quick stirring. Then, 5  $\mu\text{L}$  of formulation was covered with a Mylar polyester film to prevent the inhibition effect of oxygen during photoinduced FRP and the reaction was analyzed as fast as possible to detect the aza-Michael addition of the formulation. The aza-

Michael addition reaction was performed for 20 minutes and then 15 minutes of UV-irradiation was applied to monitor the photopolymerization reaction at 30 °C. The conversion of functional groups was determined using

$$\text{Conversion (\%)} = \left(1 - \frac{A_t(815)}{A_0(815)}\right) \times 100 \quad (7.1)$$

where  $A_t$  is taken as the area under the absorbance peak at 815  $\text{cm}^{-1}$  (C=C deformation) at time  $t$  (curing time) and  $A_0$  is the area under the absorbance peak at 815  $\text{cm}^{-1}$  at time 0 (beginning of the curing). Hence, the overall acrylate and methacrylate conversions were estimated using the peak at 815  $\text{cm}^{-1}$ .

7.2.4.2. Aqueous Photopolymerization. UV-irradiation was applied to monitor the aqueous photopolymerization reaction of AAm/water (40/60 wt%) mixture in the presence of 0.1 mol% PEI-I2959-Ts or PEI-I2959 and 0.1 or 0.3 mol% I2959 for 10 minutes in air depleted medium at 30 °C. The conversion of functional groups was determined using

$$\text{Conversion (\%)} = \left(1 - \frac{H_t(985)}{H_0(985)}\right) \times 100 \quad (7.2)$$

where  $H_t$  is taken as the peak height of the absorbance peak at 985  $\text{cm}^{-1}$  (C=C deformation) at time  $t$  (curing time) and  $H_0$  is the peak height of the absorbance peak at 985  $\text{cm}^{-1}$  at time 0 (beginning of the curing). Hence, conversions of AAm/water (40/60 wt%) mixtures were estimated using the peak at 985  $\text{cm}^{-1}$ .

### 7.2.5. Photo-DSC Measurements

A TA Instruments DSC 250 differential photocalorimeter using an Omnicure 2000 mercury lamp light source with a 320-500 nm or 400-500 nm filter was used for photopolymerization experiments. The HEMA monomer (3-4 mg) containing 0.1 or 0.5 I2959-equivalent wt% of either PI or the references (so molar concentrations of the PPIs are also the same); 0.1 wt% I2959 or 0.3 wt% bPEI (since each of the 0.1 wt% novel PI formulations contains 0.3 wt% bPEI) in the presence and absence of 1 wt% coinitiator (Iod)

were exposed to irradiation at 25 °C under nitrogen for 5 min. The heat flow was monitored as a function of time, and the polymerization rate was calculated using

$$\text{Rate} = \frac{(Q/s)M}{n(\Delta H_p)m} \quad (7.3)$$

where  $Q/s$  is the heat flow per second,  $M$  the molar mass of the monomer,  $n$  the number of double bonds per monomer molecule,  $\Delta H_p$  the heat evolved in the reaction and  $m$  the mass of monomer in the sample. The theoretical heat for the total conversion of a methacrylate double bond is 55 kJ/mol.

#### 7.2.6. Migration Study

HEMA/PEGDA (50/50 wt%) mixture in the presence of PEI-I2959-Ts (0.5 I2959-equivalent wt %) and I2959 (0.5 wt%) was photopolymerized via 365 nm irradiation for 2 h in glass vials under air. The crosslinked polymers were soaked in 25 mL of methanol for 7 days. The percentages of the extracted PIs were determined by UV–vis spectroscopy [24].

#### 7.2.7. Cytotoxicity Studies

The cytotoxicity studies of the novel photoinitiators and I2959 as a reference were performed on NIH/3T3 and L929 cell lines with the standard MTT assay. The cells were cultured in DMEM complete medium, respectively, supplemented with 10% (v/v) FBS and 1% (v/v) pen-strep in a 5% CO<sub>2</sub>-humidified incubator at 37 °C and passaged regularly. For viability test, cells were seeded at a density of 10x10<sup>3</sup> cells in 200 µl of complete medium in each well of a 96 well-plate and incubated at 37 °C in 5% CO<sub>2</sub> atmosphere. The photoinitiator samples were added at different concentrations. After 24 h incubation, the cell viability was assessed using MTT colorimetric assay. First, 50 µl of MTT solution (5 mg/mL in PBS) was added into each well with 150 µL of culture medium and incubated for 4 h. Then, the purple formazan crystals formed as a result of mitochondrial activity in viable cells were dissolved with ethanol:dimethyl sulfoxide (1:1 v/v) mixture. Absorbance at 570 nm with a reference reading at 630 nm was recorded for each well using a Synergy – H1

microplate reader (BioTek Instruments Inc., Winooski, VT, USA). Cells which were not exposed to photoinitiators were used as controls which were assumed to have 100% viability. The relative cell viability was expressed as a percentage viability of the control cells using

$$\text{Cell Viability} = \frac{\text{Absorbance (Sample)}}{\text{Absorbance (Control)}} \times 100. \quad (7.4)$$

### 7.2.8. Statistical Analysis

Statistical analyses of the cell viability studies for I2959, PEI-I2959-Ts and PEI-I2959 were conducted by using an ordinary one-way ANOVA analysis of variance followed by multiple Dunnett's comparison test of GraphPad Prism 8 software. Data were presented as mean values  $\pm$  SD of independent experiments (5 replicas for NIH/3T3 and L929 cells).  $p < 0.05$  was accepted as a statistically significant difference.

## 7.3. Results and Discussion

### 7.3.1. Synthesis and Characterization of PEI-I2959 & PEI-I2959-Ts

Novel branched polymeric photoinitiators PEI-I2959 and PEI-I2959-Ts were synthesized in two steps. First, I2959-Ts was formed by the reaction between I2959 and tosyl chloride [20]. Then, the I2959 groups were attached to the bPEI backbone by nucleophilic substitution reaction with I2959-Ts in the presence or absence of  $K_2CO_3$  to generate PEI-I2959 or PEI-I2959-Ts, respectively (Figure 7.2). In the absence of  $K_2CO_3$ , the Ts groups also get incorporated onto bPEI backbone as counterions due to quaternization of amine groups with p-toluenesulfonic acid (TsOH); however with  $K_2CO_3$ , they form TsOH potassium salts and these salts can be removed by dialysis in 6 days. For the second case, adequate purification can only be achieved in this relatively long dialysis period, which however leads to a low yield of 15%; the similar solubilities of the product (PEI-I2959) and byproduct (TsOH potassium salt) preclude other purification methods. PEI-I2959-Ts can be synthesized with a higher yield of 90% since there is no byproduct to eliminate using dialysis. At the end of the purification steps, PEI-I2959 and PEI-I2959-Ts were obtained as white-yellow and yellow-orange solids, respectively. Although they were attained as solid

products, they are prone to get sticky rapidly since the unreacted amine units in their structure are sensitive to humidity. The synthesized PPIs showed an excellent and similar water solubility of 35-45 g/L which is higher than the solubility of I2959 ( $5 \text{ g L}^{-1}$ ) due to the presence of the water soluble PEI core (Table 7.1) [148]. Thus, they are applicable in water based formulations. PEI-I2959-Ts is soluble in highly polar organic solvents such as water, methanol and DMF, whereas PEI-I2959 is only soluble in polar protic solvents such as water and methanol; however they are both insoluble in low polarity solvents such as acetone, tetrahydrofuran (THF) and diethyl ether (Table 7.1). Additionally, both of the novel PPIs have a good compatibility with the methacrylate monomer HEMA. However, they form crosslinked networks with the acrylates (PEGDA, TMPTA) via aza-Michael addition reaction, the rate of which depends on the concentration of the PPIs. Therefore, HEMA is needed as a reactive diluent to be able to prepare the methacrylate:acrylate mixtures for RT-FTIR studies.

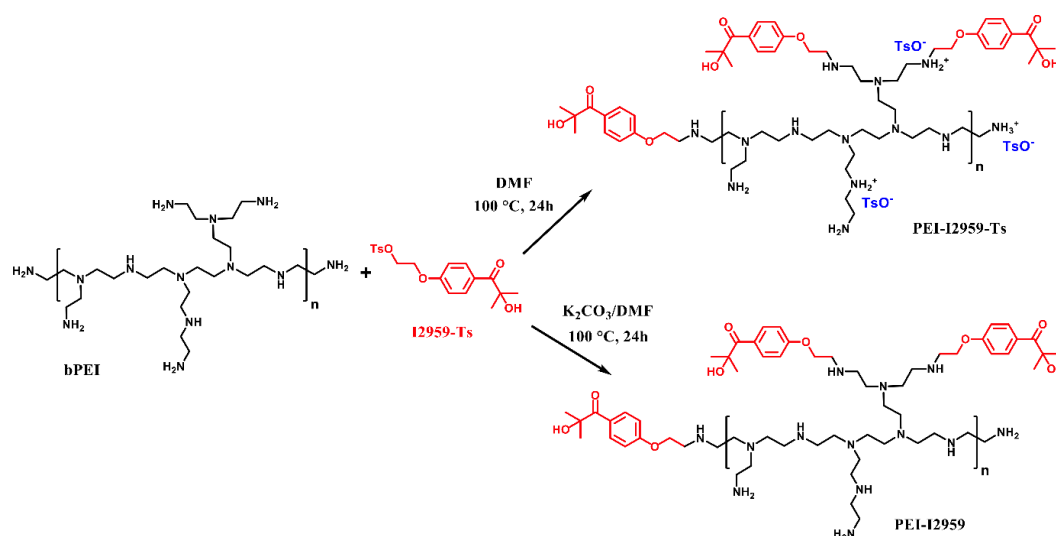


Figure 7.2. Syntheses scheme of PEI-I2959-Ts and PEI-I2959.

Table 7.1. The solubilities of PEI-I2959 and PEI-I2959-Ts.

PI	H <sub>2</sub> O	DMF	THF	MeOH	DCM	Acetone	Diethyl ether
PEI-I2959	+	-	-	+	-	-	-
PEI-I2959-Ts	+	+	-	+	-	-	-

The structures of the novel PPIs were confirmed by <sup>1</sup>H-NMR and FTIR spectroscopies. <sup>13</sup>C-NMR was also taken for PEI-I2959-Ts. In the <sup>1</sup>H-NMR spectra of the both PPIs, the peaks around 1.5 ppm (methyl protons of I2959) and 7-8 ppm (aromatic protons of I2959) prove the incorporation of the I2959 unit into bPEI structure (Figure 7.3). Additionally, in the <sup>1</sup>H-NMR spectrum of PEI-I2959-Ts, the sharp peaks at 2.34 ppm (methyl protons of Ts) and 7.32 and 7.62 ppm (aromatic protons of Ts) verify that Ts acts as a counter anion on PEI core.

It was also observed that PEI protons are more downfield in PEI-I2959-Ts (2.4 – 4.5 ppm) compared to PEI-I2959 (2.3 – 3.6 ppm) which can be explained by the deshielding effect of positively charged ammonium ions relative to neutral amine. The broad peaks in <sup>13</sup>C-NMR spectrum correspond to the bPEI chain (Figure 7.4). The amount of I2959 units in the PPIs was calculated by comparing the integrals of the aromatic protons of I2959 and PEI protons. The average number of moles of I2959 substitution on bPEI was determined as 3 moles per PEI for both of the PPIs. The average degree of substitution was kept similar for both PPIs which gives them comparability in all studies. In the FTIR spectra, both PEI-I2959 and PEI-I2959-Ts show NH and OH-stretching (3272 and 3292 cm<sup>-1</sup>, respectively), carbonyl stretching (1651 cm<sup>-1</sup>) and NH-bending (1598 cm<sup>-1</sup>) peaks (Figure 7.5). In the FTIR spectrum of PEI-I2959-Ts, an additional peak at 1119 cm<sup>-1</sup> (SO<sub>2</sub>) belonging to the Ts counter anion is also seen.

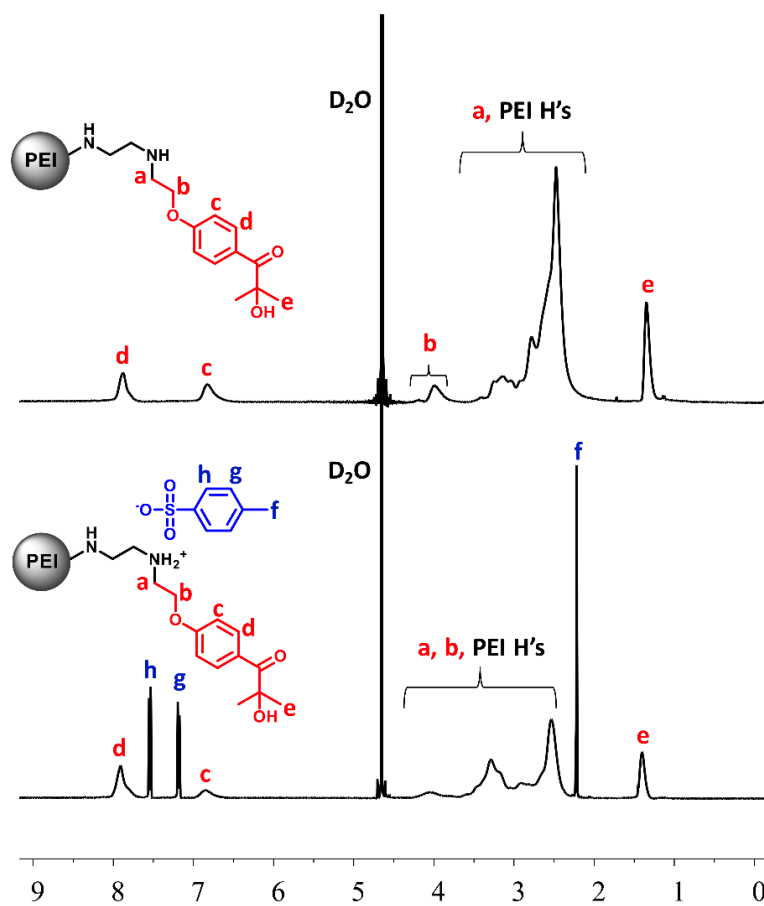


Figure 7.3.  $^1\text{H-NMR}$  spectra of PEI-I2959 and PEI-I2959-Ts.

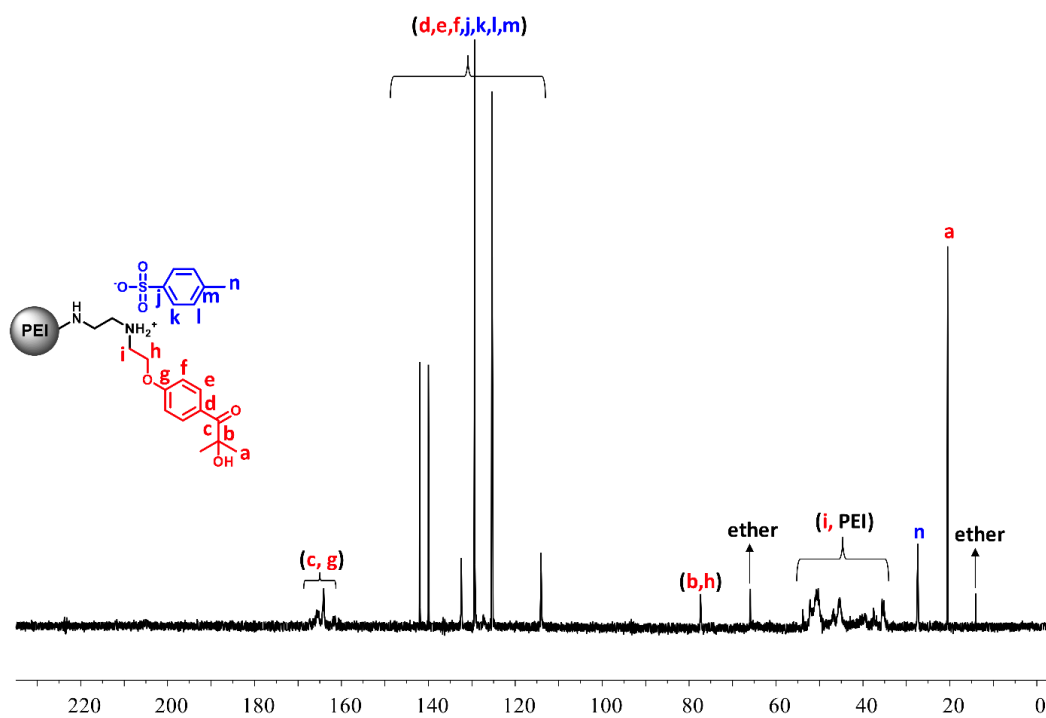
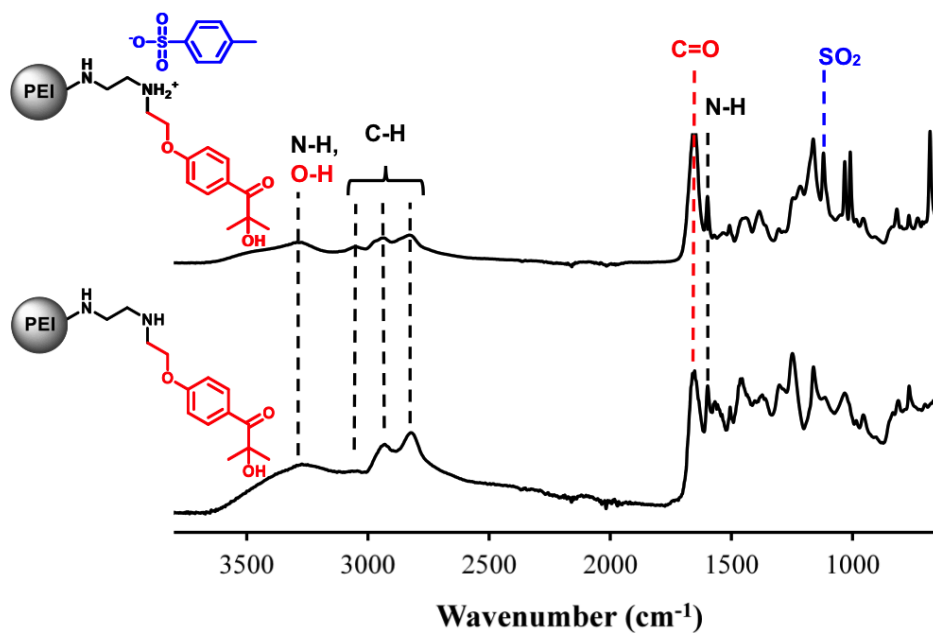
Figure 7.4.  $^{13}\text{C}$ -NMR spectrum of PEI-I2959-Ts.

Figure 7.5. FTIR spectra of PEI-I2959-Ts and PEI-I2959.

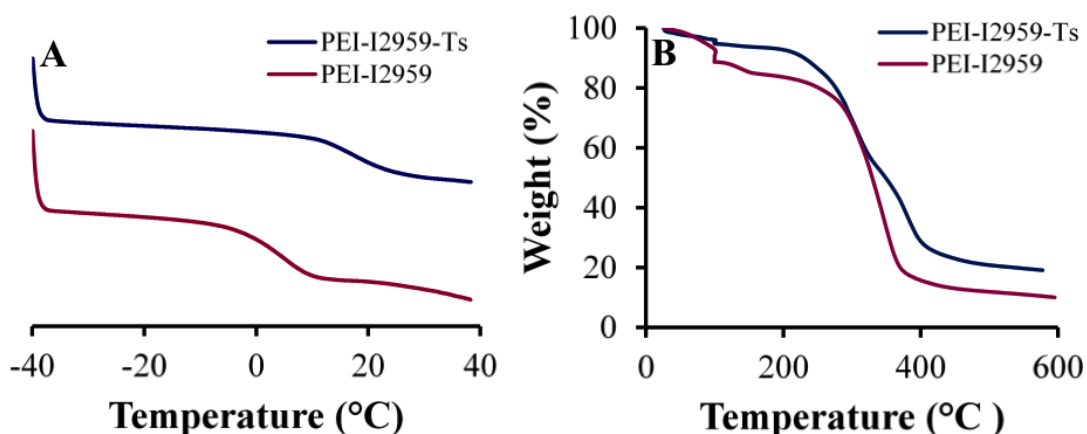


Figure 7.6. A)  $T_g$  and B) TGA spectra of PEI-I2959-Ts and PEI-I2959.

Glass transition temperatures ( $T_g$ ) of the novel PPIs were evaluated using DSC (Figure 7.6A). Branched poly(ethyleneimine) ( $M_w = 1800$  g/mol) has a  $T_g$  value of  $-58$  °C [280]. Addition of I2959 only or together with the Ts counter anion in PEI-I2959 and PEI-I2959-Ts respectively, onto the PEI core generates a restriction in the mobility (steric effect and electrostatic interactions of Ts groups with amine groups of bPEI) of the polymers which causes an increase in their  $T_g$  values compared to bPEI. Hence, PEI-I2959 and PEI-I2959-Ts show  $T_g$  values of  $4$  °C and  $17$  °C, respectively.

Thermogravimetric analyses of the synthesized PPIs were also performed to investigate their thermal stability and degradation behaviour under nitrogen atmosphere (Figure 7.6B). For both polymers, the first weight loss was observed at  $100$  °C due to the loss of water (11 and 5% for PEI-I2959 and PEI-I2959-Ts, respectively). The main degradation of PEI-I2959 occurs at one stage starting from  $239$  °C. However, in contrast to PEI-I2959, PEI-I2959-Ts degraded in two steps in the temperature ranges between  $218$ - $344$  and  $344$ - $600$  °C. The first stage of degradation is due to the decomposition of the quaternary ammonium groups, and the second stage is related to the PEI chain degradation [281]. The char yields also differ for PEI-I2959 (10%) and PEI-I2959-Ts (19%) according to the structure of the PPIs. The higher char yield of PEI-I2959-Ts may be ascribed to the aromatic structure of the additional Ts counter anions.

### 7.3.2. Light Absorption Properties

Absorption characteristics of both of the novel PPIs ( $2 \times 10^{-5}$  M) in different solvents were examined by UV-vis spectroscopy (Figure 7.7). PEI-I2959 and PEI-I2959-Ts show a maximum absorption wavelength in the UV region at 274 nm in water, which is similar to the maximum absorption wavelength of I2959 (276 nm) in water, corresponding to  $\pi$ - $\pi^*$  transition. A slight red shift was observed as the dielectric constant of the solvent increases. An increase in the solvent polarity disrupts the intermolecular hydrogen bonding and enhances the PPIs to interact with the solvent which causes a change in the absorption trend of the PPIs, a phenomenon known as solvatochromism [80]. As the concentration ( $1 \times 10^{-4}$  M) of the solutions were increased, a shoulder peak having a maximum around 320 nm and in the range of 340-380 nm depending on the solvent was also observed for PEI-I2959 and PEI-I2959-Ts, respectively. The larger  $\lambda_{\max}$  value of PEI-I2959-Ts compared to PEI-I2959 may be due to the extended  $\pi$ -conjugation created by the aromatic Ts anions and the electrostatic interaction between Ts anions and bPEI. These peaks are indicating an n- $\pi^*$  transition; however, they overlap with the intense  $\pi$ - $\pi^*$  transition peaks, strong due to their high extinction coefficients (No n- $\pi^*$  transition peak was observed for I2959). This indicates that the synthesized PPIs lead to a more efficient photopolymerizations of formulations using visible light sources compared to I2959 which only absorbs light in the UV-region. The extinction coefficients of the new PPIs are much higher than that of I2959 because they contained 3 photosensitive groups at the same concentration. The extinction coefficient of PEI-I2959-Ts is even higher than that of PEI-I2959 which may result from its ionic nature [144]. The high water solubility and high molar extinction coefficients make these PPIs good candidates for photopolymerizations in aqueous solutions, which will be shown in the following results (Table 7.2).

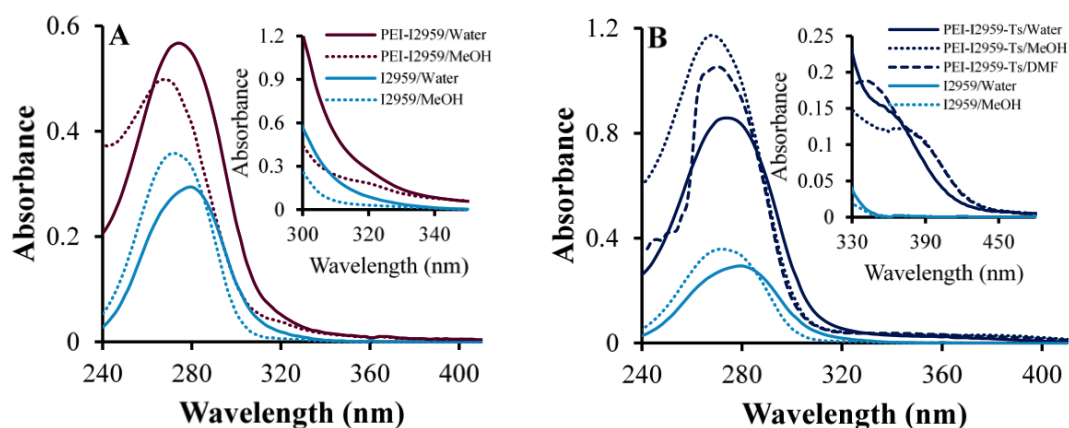


Figure 7.7. UV-vis absorption spectra of A) PEI-I2959 ( $2 \times 10^{-5}$  M) (inset: ( $1 \times 10^{-4}$  M)) and B) PEI-I2959-Ts ( $2 \times 10^{-5}$  M) (inset: ( $1 \times 10^{-4}$  M)) in different solvents.

Table 7.2. Absorption characteristics of PEI-I2959 and PEI-I2959-Ts in different solvents.

PI	Solvents	$\lambda_{\max}$ (nm)	$\epsilon$ ( $\text{M}^{-1} \text{cm}^{-1}$ )
PEI-I2959	Water	274	30384
PEI-I2959	MeOH	268	23036
PEI-I2959-Ts	Water	274	41864
PEI-I2959-Ts	MeOH	268	45936
PEI-I2959-Ts	DMF	272	46595
I2959	Water	276	15150
I2959	MeOH	272	16538

### 7.3.3. Michael Addition and Photopolymerization

The dual-curing abilities (aza-Michael addition followed by FRP) of the novel PPIs were tested in the polymerization of HEMA/PEGDA (50/50 wt%) monomer mixtures. Because PEGDA is one of the important monomers used for fabrication of hydrogels for tissue engineering scaffolds due to its nontoxicity, non-immunogenicity, and water solubility, it was chosen as an acrylate to follow the aza-Michael addition behavior of the PPIs [282]. No catalyst is required for this step since the PEI core of the PPIs having primary

and secondary amine units acts as both a base and a nucleophile. The methacrylate used was HEMA (poor Michael acceptor) for the photoinduced FRP due to the fact that poly-HEMA based hydrogels have bio- and blood-compatibility and have micro porous structure suitable for tissue engineering scaffold [283, 284].

RT-FTIR was used to monitor the aza-Michael addition reaction (20 min) and then photopolymerization (15 min) of HEMA/PEGDA (50/50 wt%) mixtures containing PEI-I2959-Ts (0.3 wt%) or PEI-I2959 (0.3 wt%) (Figure 7.8). In the first curing stage, the acrylate conversion reached about 10% in 20 minutes. The low acrylate conversion as a result of aza-Michael addition is the consequence of the limited accessibility to N-H bonds of PEI due to steric effect of densely branched structure with the considerable amount of tertiary amines which diminishes the reactivity of the primary and secondary amines [285-287]. A sharp increase in the conversion is seen beginning in the 20<sup>th</sup> minute when the UV-light is turned on and the second curing step (FRP) begins. The overall methacrylate-acrylate conversions were found to be about 69 and 81% for mixtures containing PEI-I2959 and PEI-I2959-Ts, respectively, indicating that PEI-I2959-Ts is more reactive towards FRP compared to PEI-I2959. This result can be explained by the higher extinction coefficient of the latter.

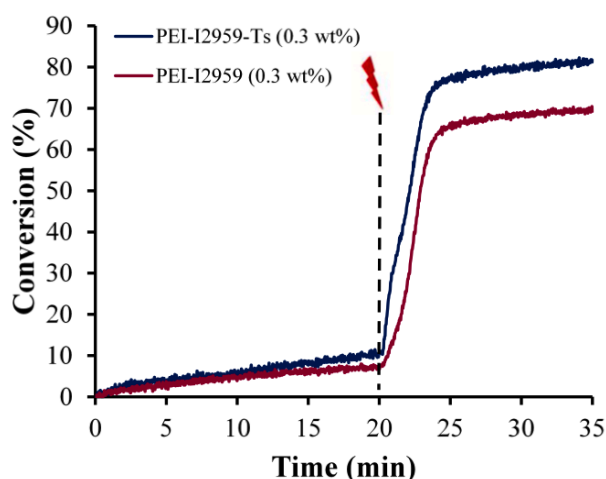


Figure 7.8. Conversion-time plots for HEMA:PEGDA (50:50 wt%) mixtures containing 0.3 wt% PEI-I2959-Ts or PEI-I2959 monitored during the aza-Michael (20 min) and photopolymerization (15 min) reactions.

Beside the RT-FTIR experiments that show the dual curing properties of the PPIs, photocuring experiments were also performed using photo-DSC. The methacrylate HEMA as a poor Michael acceptor was chosen to just clarify the photoreactivity of the PPIs by preventing the interference of aza-Michael addition which is selective towards acrylates. First HEMA containing PEI-I2959-Ts (0.1 wt%), PEI-I2959 (0.1 wt%), Irgacure 2959 (0.1 wt%), I184 (0.1 wt%) and PEI (0.3 wt%) systems were photopolymerized using UV-vis irradiation (320-500 nm) at 25 °C. The amount of PEI used as reference was equalized to the amount of PEI inside each 0.1 wt% PPI formulation which is 0.3 wt%, for reasonable comparison. Photo-DSC plots of all the formulations are given in Figure 7.9A and 7.9B. It was observed that, PEI-I2959-Ts (1,  $R_{pmax} = 0.017 \text{ s}^{-1}$ ,  $t_{max} = 1.67 \text{ min}$ , conversion = 97%) has a shorter induction time of photopolymerization than PEI-I2959 (2,  $R_{pmax} = 0.016 \text{ s}^{-1}$ ,  $t_{max} = 2.05 \text{ min}$ , conversion = 95%) which is similar to the results of I2959 (3,  $R_{pmax} = 0.014 \text{ s}^{-1}$ ,  $t_{max} = 2.05 \text{ min}$ , conversion = 90%). Commercial water soluble photoinitiator I184 (0.1 wt%) ( $R_{pmax} = 0.0043 \text{ s}^{-1}$ ,  $t_{max} = 3.14 \text{ min}$ , conversion = 84%) shows a slower photopolymerization kinetics than both of the PPIs (Figure 7.10). The observed trend in the reactivity of the novel PPIs in photo-DSC studies correlates well with RT-FTIR experiments independent of the monomers. It is obviously seen that PEI alone (4) does not have a photoreactivity.

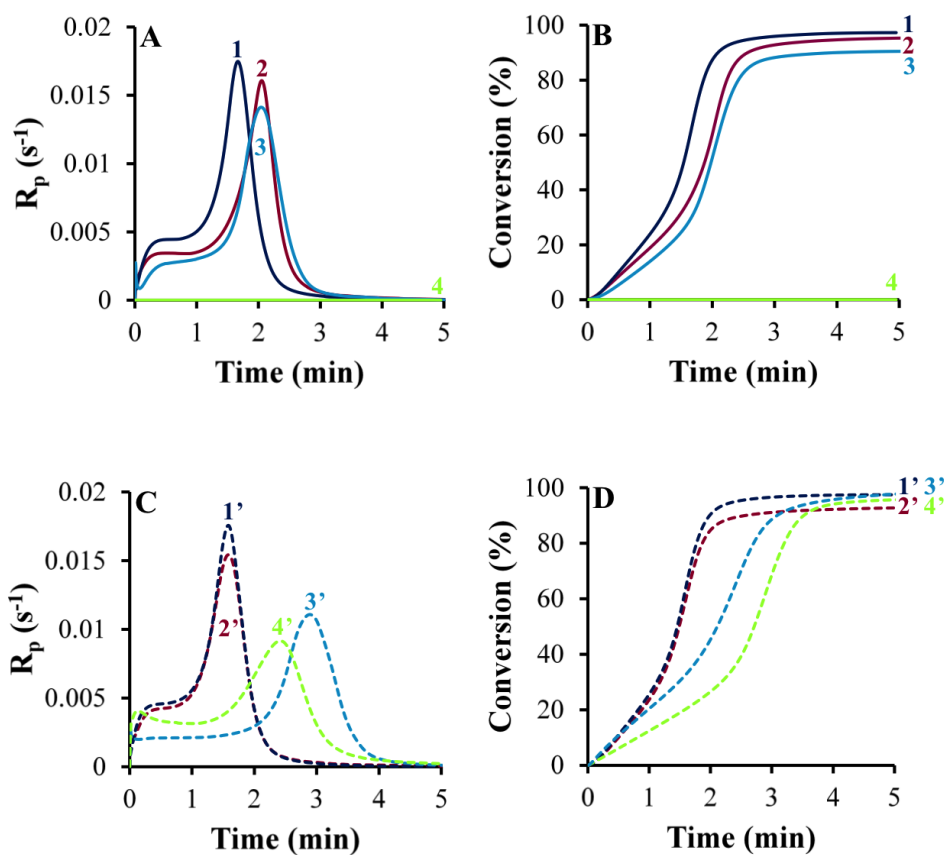


Figure 7.9. A) Rate-time and B) Conversion-time plots for HEMA containing PEI-I2959-Ts (0.1 wt%) (1), PEI-I2959 (0.1 wt%) (2), I2959 (0.1 wt%) (3), PEI (0.3 wt%) (4), C) Rate-time and D) Conversion-time plots for HEMA containing PEI-I2959-Ts/Iod (0.1/1 wt%) (1'), PEI-I2959/Iod (0.1/1 wt%) (2'), I2959/Iod (0.1/1 wt%) (3'), PEI/Iod (0.3/1 wt%) (4'). All photopolymerizations under UV-vis light (320-500 nm) irradiation in photo-DSC.

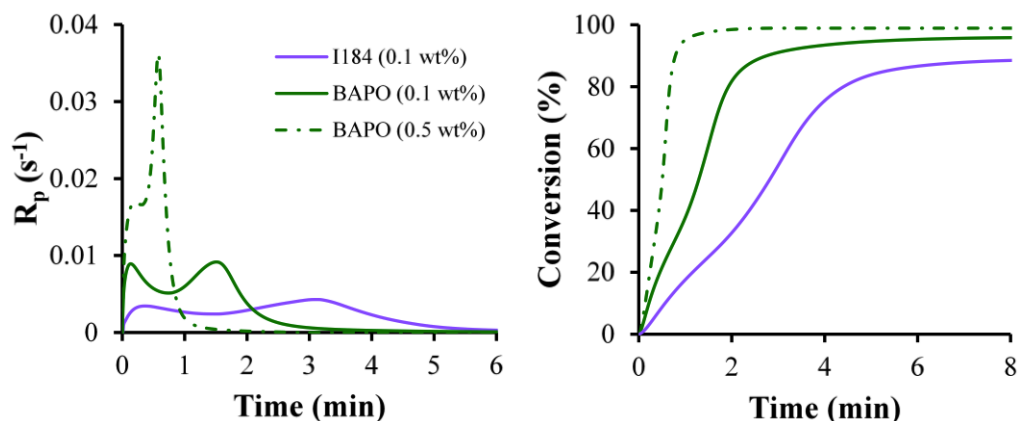


Figure 7.10.  $R_p$  vs time and Conversion (%) vs time plots of BAPO (0.1 wt%) and BAPO (0.5 wt%) under visible light irradiation, I184 (0.1 wt%) under UV light irradiation at 25 °C.

It is known that amine compounds (donor) and iodonium salts (acceptor) form CTC systems for radical and cationic polymerizations [288]. CTC is an association which is formed through an electronic charge transfer between the lowest unoccupied molecular orbital (LUMO) of an electron acceptor and the highest occupied molecular orbital (HOMO) of an electron donor leading to a structure having a lower HOMO-LUMO energy gap than the initial electron donor and acceptor molecules. CTC's have the capability to generate radicals under near-UV or visible light irradiation which can initiate a photoinduced FRP [289]. Our PPIs (donors) containing different types of amines (primary, secondary and tertiary) due to PEI core are expected to form CTCs with Iod (acceptor). Therefore, the photoactivity of the PPIs was also examined in the presence of Iod under UV and visible light irradiation to evaluate the contribution of the radicals produced through the photolysis of the formed CTCs to the polymerization efficiency.

The addition of Iod makes the photopolymerization induction time shorter for both of the PPIs under UV light irradiation; PEI-I2959-Ts/Iod (1',  $R_{pmax} = 0.017 s^{-1}$ ,  $t_{max} = 1.58$  min, conversion = 97%), PEI-I2959/Iod (2',  $R_{pmax} = 0.015 s^{-1}$ ,  $t_{max} = 1.58$  min, conversion = 93%) (Figure 7.9C and 7.9D). It is evident that the change in the  $t_{max}$  value of PEI-I2959/Iod (2') was more dramatic compared to PEI-I2959-Ts (1') which stems from the higher steric hindrance of PEI-I2959-Ts created by tosylate anions, and a small amount of neutral PEI-

amines (donors) available for CTC formation since inside the PEI-I2959-Ts structure they also form ionic interactions with Ts anions, unlike the PEI-amines in PEI-I2959 [289]. Addition of Iod to I2959 has adverse effects in the  $R_p$  and induction time of photopolymerization using I2959/Iod (3',  $R_{pmax} = 0.011 \text{ s}^{-1}$ ,  $t_{max} = 2.89 \text{ min}$ , conversion = 96%) compared to I2959 (3). One possible explanation for the lower reactivity of I2959 in the presence of Iod could be the coupling reaction between the benzoyl or alkyl radicals of I2959 and the aryl radical of Iod. While PEI (4) alone can not initiate the polymerization of HEMA, PEI/Iod system (4',  $R_{pmax} = 0.0092 \text{ s}^{-1}$ ,  $t_{max} = 2.4 \text{ min}$ , conversion = 98%) can take part in the initiation of the polymerization which originates from the charge transfer complex (CTC) formation between PEI and Iod. 1' and 2' showed shorter induction times compared to 4', since not only the alkyl and benzoyl radicals formed through homolysis of I2959 but also aryl radicals generated over photolysis of CTCs are capable of initiating the polymerization of HEMA.

To prove CTC formation between novel PPIs and Iod, photoefficiencies of the PEI-I2959-Ts/Iod and PEI-I2959/Iod systems in the polymerization of HEMA were also checked under visible light irradiation. As can be seen in Figure 7.11A and 7.11B, PEI-I2959-Ts (1,  $R_{pmax} = 0.0016 \text{ s}^{-1}$ ,  $t_{max} = 18.14 \text{ min}$ , conversion = 93%) and PEI-I2959 alone (2,  $R_{pmax} = 0.0015 \text{ s}^{-1}$ ,  $t_{max} = 20.42 \text{ min}$ , conversion = 87%) systems show photopolymerization activity under visible light irradiation even if they displayed slower kinetics than BAPO (0.1 wt% or 0.5 wt%) since they have an absorbance tail in the near-UV/visible range, so weaker visible light absorption than BAPO (Figure 7.10). Faster polymerization kinetics were detected with a higher PI concentration; PEI-I2959-Ts (1a,  $R_{pmax} = 0.0021 \text{ s}^{-1}$ ,  $t_{max} = 12.29 \text{ min}$ , conversion = 96%) and PEI-I2959 (2a,  $R_{pmax} = 0.0020 \text{ s}^{-1}$ ,  $t_{max} = 13.22 \text{ min}$ , conversion = 90%). The higher reactivity of PEI-I2959-Ts in both concentrations under visible light irradiation compared to PEI-I2959 is apparent and can be explained by the more red-shifted visible light absorption of PEI-I2959-Ts than PEI-I2959.

An enhanced  $R_p$  value along with a shorter induction time of photopolymerization was noted with the addition of Iod to both of the PPIs; PEI-I2959-Ts/Iod (1',  $R_{pmax} = 0.0021 \text{ s}^{-1}$ ,  $t_{max} = 11.08 \text{ min}$ , conversion = 91%), PEI-I2959/Iod (2',  $R_{pmax} = 0.0024 \text{ s}^{-1}$ ,  $t_{max} = 10.71 \text{ min}$ , conversion = 85%), PEI-I2959-Ts/Iod (1a',  $R_{pmax} = 0.0034 \text{ s}^{-1}$ ,  $t_{max} = 7.43 \text{ min}$ , conversion = 95%) and PEI-I2959/Iod (2a',  $R_{pmax} = 0.0042 \text{ s}^{-1}$ ,  $t_{max} = 5.78 \text{ min}$ , conversion

= 89%) (Figure 7.11C and 7.11D). Iod addition improves reactivity of PEI-I2959 more than PEI-I2959-Ts also under visible light irradiation. The difference in the induction time and  $R_p$  are more significant between 1a' and 2a' compared to 1' and 2' since the CTC effect is more apparent with high concentration of PPI.

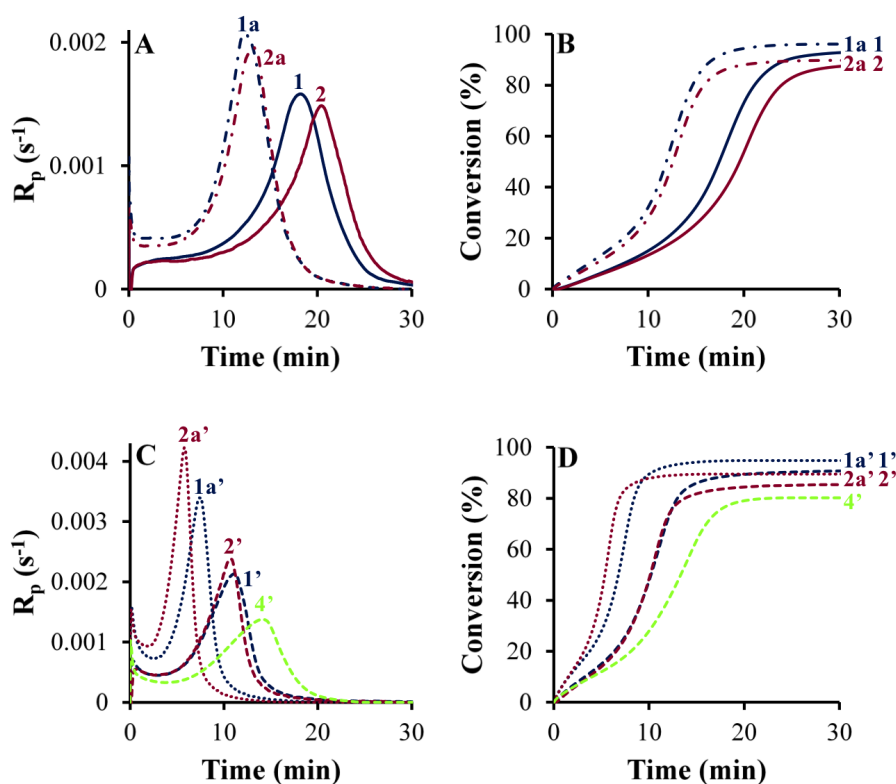


Figure 7.11. A) Rate-time and B) Conversion-time plots for HEMA containing PEI-I2959-Ts (0.1 wt%) (1), PEI-I2959 (0.1 wt%) (2), PEI-I2959-Ts (0.5 wt%) (1a), PEI-I2959 (0.5 wt%) (2a), C) Rate-time and D) Conversion-time plots for HEMA containing PEI-I2959-Ts/Iod (0.1/1 wt%) (1'), PEI-I2959/Iod (0.1/1 wt%) (2'), PEI-I2959-Ts/Iod (0.5/1 wt%) (1a'), PEI-I2959/Iod (0.5/1 wt%) (2a'), PEI/Iod (0.3/1 wt%) (4'). All photopolymerizations under visible light irradiation in photo-DSC.

All the formulations used in Photo-DSC experiments were also kept under observation to determine if any gelation occurs through photolysis of a CTC formed at room temperature and under visible light. Gel formation was observed for the PEI-I2959/Iod (0.1 or 0.5/1 wt%) and PEI/Iod (0.3/1 wt%) systems in HEMA. The observed time for gelation was shorter for PEI-I2959/Iod (0.5/1 wt%) compared to PEI-I2959/Iod (0.1/1 wt%) since the CTC formation

is more efficient with higher PI concentration. The reason why no gelation was detected for the formulation PEI-I2959-Ts/Iod (0.1/1 wt%) in HEMA is explained with the higher steric hindrance and lower free neutral amine content of PEI-I2959-Ts. It is not surprising that no gelation was observed with PEI-I2959 (0.1 or 0.5 wt%) and PEI-I2959-Ts alone (0.1 or 0.5 wt%) systems in HEMA since no CTC formation is expected without Iod.

As a further experimental evidence to show CTC formation between PPIs and Iod, UV-vis absorbance of the photo-DSC formulations of PEI-I2959-Ts and PEI-I2959 were measured. The observed bathochromic shift with the addition of Iod (1 wt%) to the novel PPIs (0.1 wt%) compared to their original spectra is the sign for the formation of the CTC (Figure 7.12A and 7.12B). A higher red shift in PEI-I2959/Iod (0.1/2 wt%) was observed compared to PEI-I2959/Iod (0.1/1 wt%) with an increment in the amount of Iod.

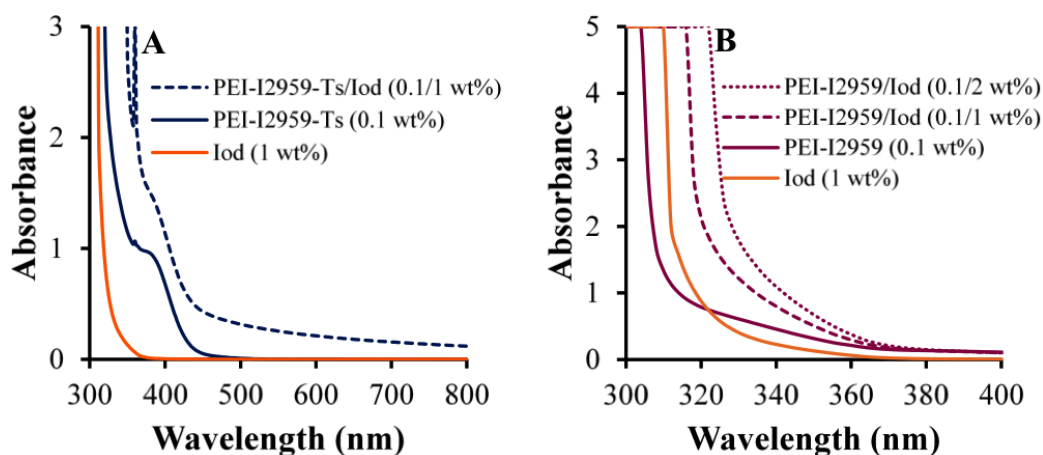


Figure 7.12. Absorption spectra of A) PEI-I2959-Ts/Iod (0.1/1 wt%), PEI-I2959-Ts (0.1 wt%) and Iod (1 wt%) and B) PEI-I2959/Iod (0.1/2 wt%), PEI-I2959/Iod (0.1/1 wt%), PEI-I2959 (0.1 wt%) and Iod (1 wt%) in HEMA.

The photopolymerization performances of the novel PPIs in an aqueous environment were also analyzed in the polymerization of AAm monomer in air depleted atmosphere under UV light irradiation using RT-FTIR (Figure 7.13). PEI-I2959-Ts and PEI-I2959 showed similar conversion values of 98 % and 90 %, respectively. Since the novel PPIs have 3 moles of I2959 in their structure, PEI-I2959-Ts (0.1 mol%) and PEI-I2959 (0.1 mol%)

have higher rates than I2959 (0.1 mol%) but they have similar polymerization kinetics to I2959 (0.3 mol%) which can be seen from the slope of each curve.

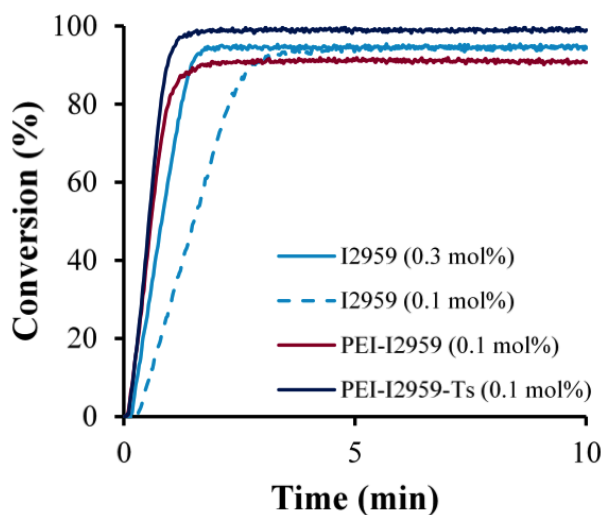


Figure 7.13. Conversion-time plots for AAm:water (40:60 wt%) mixture containing PEI-I2959 (0.1 mol%), PEI-I2959-Ts (0.1 mol%), I2959 (0.3 mol%) or I2959 (0.1 mol%). All photopolymerizations under UV irradiation in air depleted atmosphere in RT-FTIR.

The proposed mechanism for the photoinitiation of (meth)acrylates is presented in Figure 7.14. The PPIs, when irradiated, cleave into benzoyl and alkyl groups, both of which can initiate a polymerization reaction [290]. Also, the amine groups of the PPIs create CTCs with Iod and generate aryl radicals to initiate FRP. The CTC can undergo photolysis and form radicals even without irradiation proving the efficient interaction between the donor and the acceptor.

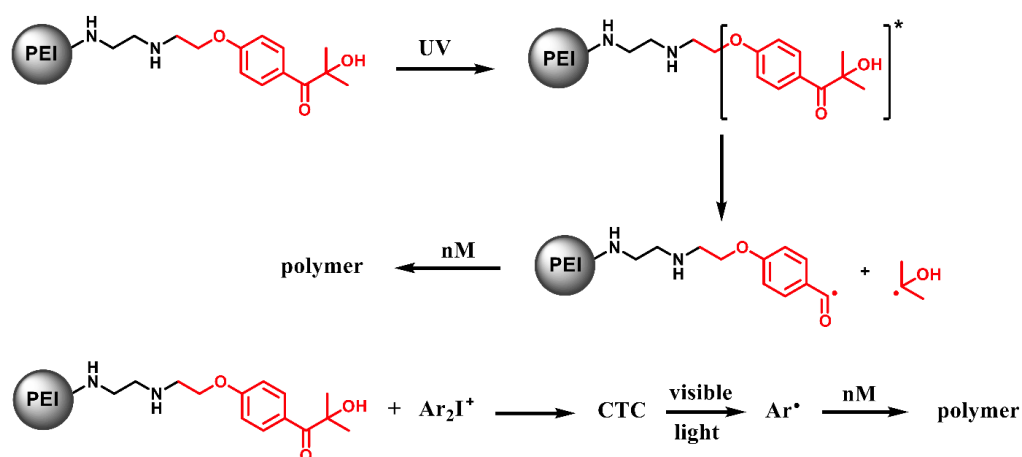


Figure 7.14. Proposed mechanism for the photoinitiation with the PPIs ( $\text{Ar}_2\text{I}^+$  denotes the iodonium salt).

#### 7.3.4. Migration Stability

The migration stability of PEI-I2959-Ts was analyzed and compared with commercial I2959. The migration study was conducted just for PEI-I2959-Ts salt because of its similarity with PEI-I2959 in terms of their substructure and photopolymerization kinetics. UV-vis absorption spectroscopy was used to find out concentrations of the photoinitiators extracted into methanol from the crosslinked HEMA/PEGDA (50/50wt%) polymer samples. The I2959 content of the PEI-I2959-Ts sample was adjusted as 0.5 wt% to be comparable with the reference sample I2959 (0.5 wt%). It was found out that the migration of PEI-I2959-Ts (0.5 wt%) is 8 times lower than that of I2959 (0.5 wt%) (Figure 7.15). As discussed in the Introduction, this was expected due to the higher molecular weight of PEI-I2959-Ts, its branched core and its incorporation into the polymer samples through formation of an interpenetrating network.

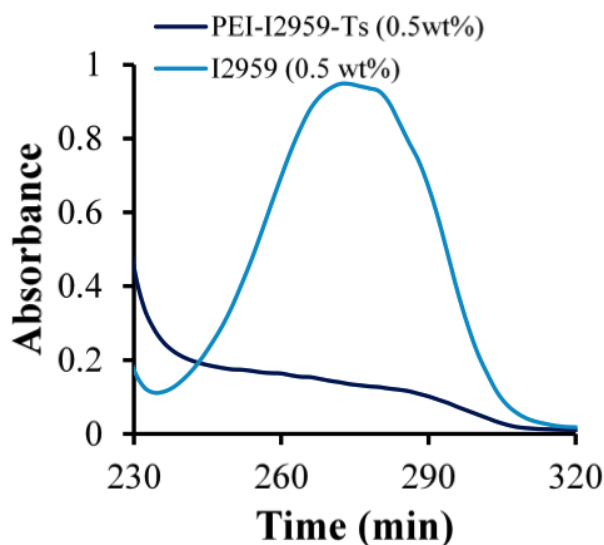


Figure 7.15. UV-vis absorption spectra of PEI-I2959-Ts and I2959 extracted with methanol from the HEMA/PEGDA (50/50 wt%) polymer samples.

### 7.3.5. Cell Viability

Cytotoxicities of the novel PPIs was studied on NIH/3T3 and L929 cell lines to evaluate the usability of the novel water soluble photoinitiators in biological fields or some applications such as inkjet printing, especially when used for labelling in food packaging. I2959 was also studied as a reference. A cell viability above 80% is non-toxic to the cells according to ISO 10993–5 [291]. As can be seen in Figure 7.16, PEI-I2959-Ts shows no cytotoxicity to both of the cells. The cell viability for PEI-I2959-Ts was even higher than that of I2959 on L929 cells. Hence, it seems that PEI-I2959-Ts is a highly biocompatible photoinitiator as with I2959 which paves the way for its use in biological applications. However, PEI-I2959 reduced the cell viability of both of the cells in a dose dependent manner. The cell viability of PEI-I2959 fell below the critical level of 80% at 8  $\mu\text{g}/\text{mL}$  and 20  $\mu\text{g}/\text{mL}$  for NIH/3T3 and L929 cells, respectively. At lower concentrations, PEI-I2959 also shows reasonable cell viability results, especially on the L929 cells.

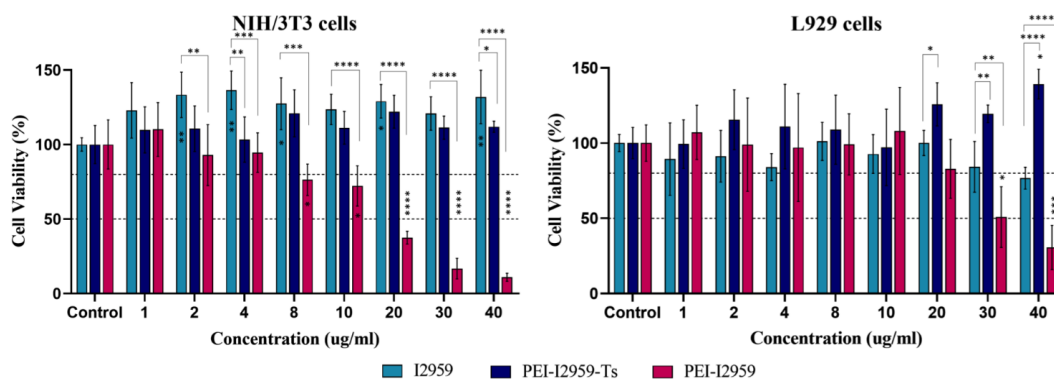


Figure 7.16. Cytotoxicity assay with I2959, PEI-I2959-Ts and PEI-I2959 for 24 hours on NIH/3T3 and L929 cells. Statistical significance:  $p < 0.0332$  (\*),  $p < 0.0021$  (\*\*),  $p < 0.0002$  (\*\*\*), and  $p < 0.0001$  (\*\*\*\*). Dashed lines show the 80% and 50% viabilities.

#### 7.4. Conclusion

In summary, two type I water-borne PPIs were successfully prepared, where the syntheses differ only in the presence or absence of a catalyst ( $K_2CO_3$ ). The introduction of a hydrophilic bPEI skeleton into PPIs enhanced their water solubility, reaching 35-45 g/L, exceeding that of the state-of-the-art PI I2959 7-9-fold. PPIs have an absorption centered at 274 nm and also at 320-380 nm in water. The dual curing abilities of the novel PPIs were shown by aza-Michael addition reaction with PEGDA in the presence of HEMA by the use of their primary and secondary amines, followed by very efficient photopolymerization of (meth)acrylates with the double bond conversions of 90-100%. These PPIs can initiate photopolymerization of only HEMA under both UV and visible light (>90% conversion) through type I photoinitiation. If a PPI/Iod system is used, CTCs form between the amine groups of PPI and Iod, creating a positive difference in the rate and induction time of photopolymerization in comparison with PEI-I2959-Ts and PEI-I2959 alone systems under visible light. The PPIs also have high reactivity in the polymerization of AAm in aqueous environment. The photocured film initiated by one of these PPIs (PEI-I2959-Ts) shows higher migration stability compared to low molecular weight I2959 since PEI-I2959-Ts PPI has higher molecular weight and some of the photolysis fragments are fixed on the PPI. As shown by the cytotoxicity studies, PEI-I2959-Ts has high biocompatibility which allows its

use as a safe photoinitiator in many biological applications. PEI-I2959 also shows a reasonable biocompatibility at lower concentrations especially with L929 cells.

## 8. CONCLUDING REMARKS

Novel photoinitiators were synthesized with various purposes of water solubility, high migration stability, UV-vis light reactivity, biocompatibility and binding functionality. The structures of these PIs were verified via characterization studies, and photoreactivities of the PIs were tested. Their photophysical and photochemical properties were also investigated.

A TX-functionalized PI (TXdMA) with 1,6-heptadiene structure was synthesized. It showed a red-shifted absorption (435-439 nm) compared to commercial TX which makes use with a visible light sources. This PI has surface attachment ability due to the carboxylic acid units in its structure. It has very good migration stability compared to TX thanks to its monomeric nature. Since it is a polymerizable PI, it can also participate in the formed final polymer network, so the PI may influence the mechanical properties of the cured product in a better way.

The first bisphosphonic acid functionalized TX and BP based photoinitiators (TXBP and BPBP) were introduced as water soluble PIs for free radical polymerization. The performance of photoinitiators were examined in aqueous solutions of PEGDA and AAm. Since the OH groups in bisphosphonic acid unit may substitute for a hydrogen donor, the PIs can initiate polymerization without a need for an additive as a one-component PI even though they show a low polymerization rate. These novel PIs can be used in the fabrication of hydrogels with bisphosphonic acid functionality which may endow the hydrogels with calcium binding ability.

A water soluble bisphosphonate functionalized TX-based photoinitiator (TXBP2) was developed. The bisphosphonate moiety was chosen to make the PI hydrophilic and non-toxic. The novel PI is suitable to use in oil-based and aqueous photopolymerization formulations. TXBP2 can initiate free radical polymerization efficiently in the presence of the additives Iod or EDB. The use of TXBP2 in hydrogel production may give hydrogels mineralization ability due to its bisphosphonate units which paves the way for its applicability in biomedical fields.

A polymeric water soluble photoinitiator (PAATX) was produced with a dual curing property. As PAATX can be used in the initiation of a free radical photopolymerization, it can also take part in a sequential dual curing which is an aza-Michael addition followed free radical photopolymerization process. This way, it can be involved in the interpenetrating network by which can help to reduce the leaching of the PI onto surface. The dual curing property of the PI may also be beneficial in the production of custom tailorable materials.

Syntheses of water soluble multifunctional polymeric photoinitiators (PEI-I2959 and PEI-I2959-Ts) were performed. PEI was selected as a core for its hydrophilicity. At the same time, it behaves as a crosslinker, initiating the dual curing of methacrylate:acrylate mixtures due to having unreacted primary and secondary amine units in its structure. The novel PIs have an enhanced water solubility and higher migration stability compared to commercial I2959. Both of the PIs have visible light reactivity. The addition of Iod in the photocuring formulations impacts the rate of polymerization under visible light in a positive way since CTCs form between the amine groups of PPI and Iod. PEI-I2959-Ts shows no cytotoxicity. The novel PIs may find a use for biological applications thanks to their improved properties.

Overall, we have started with the aim of finding ways to shift the already comparatively green process of photopolymerization into the greener direction by designing and synthesizing PIs that do not need carcinogenic UV light or potentially harmful solvents. The PIs we have synthesized also dramatically lower undesired leaching of small molecules, and also are biocompatible and reasonably non-toxic. Hence, we believe that we have made contributions of relevance in the right direction.

## REFERENCES

- [1] Fouassier, J. P. and J. Lalevée, *Photoinitiators for polymer synthesis*, John Wiley & Sons, Inc., Weinheim, Germany, 2012.
- [2] Lalevée, J. and J. P. Fauassier, *Photopolymerisation initiating systems*, Royal Society of Chemistry, United Kingdom, UK, 2018.
- [3] Yagci, Y., S. Jockusch and N. J. Turro, “Photoinitiated polymerization: advances, challenges, and opportunities”, *Macromolecules*, Vol. 43, pp. 6245–6260, 2010.
- [4] Schwalm, R., *UV coatings: Basics, recent developments and new applications*, Elsevier, Amsterdam, The Netherlands, 2007.
- [5] Schwalm, R., “Photoinitiators and photopolymerization”, in *Encyclopedia of Materials: Science and Technology*, Elsevier, 2001.
- [6] Decker, C., “Kinetic study and new applications of UV radiation curing”, *Macromolecular Rapid Communications*, Vol. 23, pp. 1067–1093, 2002.
- [7] Mendes-Felipe, C., J. Oliveira, I. Etxebarria, J. L. Vilas-Vilela and S. Lanceros-Mendez, “State-of-the-art and future challenges of UV curable polymer-based smart materials for printing technologies”, *Advanced Materials Technologies*, Vol. 4. pp. 1800618–1800634, 2019.
- [8] Green, W. A., *Industrial photoinitiators*, CRC Press, United States of America, US, 2010.
- [9] Qin, X. H., A. Ovsianikov, J. Stampfl and R. Liska, “Additive manufacturing of photosensitive hydrogels for tissue engineering applications”, *BioNanoMaterials*, Vol. 15, pp. 49–70, 2014.

- [10] Nesvadba, P., “Radical polymerization in industry”, in *Encyclopedia of Radicals in Chemistry, Biology and Materials*, John Wiley and Sons, Basel, Switzerland, 2012.
- [11] Taschner, R., P. Gauss, P. Knaack and R. Liska, “Biocompatible photoinitiators based on poly- $\alpha$ -ketoesters”, *Journal of Polymer Science*, Vol. 58, pp. 242–253, 2020.
- [12] Lago, M. A., A. Rodríguez-Bernaldo de Quirós, R. Sendón, J. Bustos, M. T. Nieto and P. Paseiro, “Photoinitiators: a food safety review”, *Food Additives and Contaminants - Part A Chemistry, Analysis, Control, Exposure and Risk Assessment*, Vol. 32, pp. 779–798, 2015.
- [13] Snedeker, S. M., “Exposure and health risks to consumers”, in *Toxicants in Food Packaging and Household Plastics*, London, UK, 2014.
- [14] Aparicio, J. L. and M. Elizalde, “Migration of photoinitiators in food packaging: a review”, *Packaging Technology and Science*, Vol. 28, pp. 181–203, 2015.
- [15] *Some chemicals present in industrial and consumer products, food and drinking-water*, International Agency for Research on Cancer Monographs, Lyon, France, 2013.
- [16] Hageman, H. J., “Photoinitiators for free radical polymerization”, *Progress in Organic Coatings*, Vol. 13, pp. 123–150, 1985.
- [17] Magdassi, S., L. Larush, I. Cooperstein and A. A. Pawar, “Particulate photoinitiators and uses thereof”, US Pat. 0348631 A1, 2018.
- [18] Cesur, B., O. Karahan, S. Agopcan, T. N. Eren, N. Okte and D. Avci, “Difunctional monomeric and polymeric photoinitiators: synthesis and photoinitiating behaviors”, *Progress in Organic Coatings*, Vol. 86, pp. 71–78, 2015.

- [19] Liang, S., Y. D. Yang, H. Y. Zhou, Y. Q. Li and J. X. Wang, "Novel polymerizable HMPP-type photoinitiator with carbamate: synthesis and photoinitiating behaviors", *Progress in Organic Coatings*, Vol. 110, pp. 128–133, 2017.
- [20] Sun, F., Y. Li, N. Zhang and J. Nie, "Initiating gradient photopolymerization and migration of a novel polymerizable polysiloxane  $\alpha$ -hydroxy alkylphenones photoinitiator", *Polymer*, Vol. 55, pp. 3656–3665, 2014.
- [21] Cinar, S. A., M. N. Guven, T. N. Eren, B. Cesur, M. Aleksanyan, B. Dedeoglu, N. Okte, V. Aviyente, F. Morlet-Savary, J. Lalevée and D. Avci, "Structure-reactivity relationships of novel monomeric photoinitiators", *Journal of Photochemistry and Photobiology A: Chemistry*, Vol. 329, pp. 77–87, 2016.
- [22] Oesterreicher, A., M. Roth, D. Hennen, F. H. Mostegel, M. Edler, S. Kappaun and T. Griesser, "Low migration type I photoinitiators for biocompatible thiol-ene formulations", *European Polymer Journal*, Vol. 88, pp. 393–402, 2017.
- [23] Karahan, Ö., D. K. Balta, N. Arsu and D. Avci, "Synthesis and evaluations of novel photoinitiators with side-chain benzophenone, derived from alkyl  $\alpha$ -hydroxymethacrylates", *Journal of Photochemistry and Photobiology A: Chemistry*, Vol. 274, pp. 43–49, 2014.
- [24] Yang, J., R. Tang, S. Shi and J. Nie, "Synthesis and characterization of polymerizable one-component photoinitiator based on sesamol", *Photochemical and Photobiological Sciences*, Vol. 12, pp. 923–929, 2013.
- [25] Karaca Balta, D., Ö. Karahan, D. Avci and N. Arsu, "Synthesis, photophysical and photochemical studies of benzophenone based novel monomeric and polymeric photoinitiators", *Progress in Organic Coatings*, Vol. 78, pp. 200–207, 2015.

- [26] Jiang, B., T. Zhang, L. Zhao, Z. Xu and Y. Huang, “Effect of polymerizable photoinitiators on the UV-polymerization behaviors of photosensitive polysiloxane”, *Journal of Polymer Science, Part A: Polymer Chemistry*, Vol. 55, pp. 1696–1705, 2017.
- [27] Sridhar, L., E. N. Silverberg, S. M. Burdzy, A. D. Messana, J. G. Woods and B. Stevens, “Photoinitiators that are polymeric or polymerizable for use in UV curable pressure sensitive adhesives”, US Pat. 10526426 B2, 2020.
- [28] Wei, J. and B. Wang, “A highly efficient polymerizable photoinitiator comprising benzophenone, thio moieties, and N-arylmaleimide”, *Macromolecular Chemistry and Physics*, Vol. 212, pp. 88–95, 2011.
- [29] Roth, M., D. Hennen, A. Oesterreicher, F. H. Mostegel, S. Kappaun, M. Edler and T. Griesser, “Exploring functionalized benzophenones as low-migration photoinitiators for vinyl carbonate/thiol formulations”, *European Polymer Journal*, Vol. 88, pp. 403–411, 2017.
- [30] Wang, H., J. Wei, X. Jiang and J. Yin, “Novel chemical-bonded polymerizable sulfur-containing photoinitiators comprising the structure of planar N-phenylmaleimide and benzophenone for photopolymerization”, *Polymer*, Vol. 47, pp. 4967–4975, 2006.
- [31] Nayak, B. R. and L. J. Mathias, “A novel photoinimer for the polymerization of acrylates and methacrylates”, *Journal of Polymer Science, Part A: Polymer Chemistry*, Vol. 43, pp. 5661–5670, 2005.
- [32] Tang, Y., Y. Zhang, J. Yang and J. Nie, “Synthesis and characteristics of photopolymerized benzophenone”, *Journal of Polymer Science, Part A: Polymer Chemistry*, Vol. 55, pp. 313–320, 2017.
- [33] Wu, Q., Y. Xiong, Q. Liang and H. Tang, “Developing thioxanthone based visible photoinitiators for radical polymerization”, *RSC Advances*, Vol. 4, pp. 52324–52331, 2014.

- [34] Wu, Q., K. Tang, Y. Xiong, X. Wang, J. Yang and H. Tang, “High-performance and low migration one-component thioxanthone visible light photoinitiators”, *Macromolecular Chemistry and Physics*, Vol. 218, pp. 1600484–1600492, 2017.
- [35] Wu, Q., X. Wang, Y. Xiong, J. Yang and H. Tang, “Thioxanthone based one-component polymerizable visible light photoinitiator for free radical polymerization”, *RSC Advances*, Vol. 6, pp. 66098–66107, 2016.
- [36] Qiu, J. and J. Wei, “Thioxanthone photoinitiator containing polymerizable N-aromatic maleimide for photopolymerization”, *Journal of Polymer Research*, Vol. 21, pp. 1–7, 2014.
- [37] Eren, T. N., B. Graff, J. Lalevee and D. Avci, “Thioxanthone-functionalized 1,6-heptadiene as monomeric photoinitiator”, *Progress in Organic Coatings*, Vol. 128, pp. 148–156, 2019.
- [38] Loccufier, J., R. Claes and J. Van Luppen, “Polymerizable photoinitiators and radiation curable compositions”, WO Pat. 029017 A1, 2010.
- [39] Dermaut, W., P. Goris, L. Thomassen and J. Celis, “Polymerizable photoinitiators”, US Pat. 0185689 A1, 2019.
- [40] Loccufier, J., “Polymerizable thioxanthone”, WO Pat. 009194 A1, 2014.
- [41] De Mondt, R. and J. Loccufier, “Radiation curable compositions for food packaging”, US Pat. 9550898 B2, 2017.
- [42] Eren, T. N., N. Yasar, V. Aviyente, F. Morlet-Savary, B. Graff, J. P. Fouassier, J. Lalevee and D. Avci, “Photophysical and photochemical studies of novel thioxanthone-functionalized methacrylates through LED excitation”, *Macromolecular Chemistry and Physics*, Vol. 217, pp. 1501–1512, 2016.

- [43] Huang, X., Y. Zhang, M. Shi, Y. Zhang and Y. Zhao, “Study on a polymerizable visible light initiator for fabrication of biosafety materials”, *Polymer Chemistry*, Vol. 10, pp. 2273–2281, 2019.
- [44] Xiao, P., F. Dumur, M. Frigoli, M. A. Tehfe, B. Graff, J. P. Fouassier, D. Gigmes and J. Lalevée, “Naphthalimide based methacrylated photoinitiators in radical and cationic photopolymerization under visible light”, *Polymer Chemistry*, Vol. 4, pp. 5440–5448, 2013.
- [45] Ma, Z., X. Niu, Z. Xu and J. Guo, “Synthesis of novel macrophotoinitiator for the photopolymerization of acrylate”, *Journal of Applied Polymer Science*, Vol. 131, pp. 40352–40360, 2014.
- [46] Xie, Y. and H. Huang, “Preparation and characterization of an amphiphilic macrophotoinitiator based on 2-hydroxyl-2-methyl-1-phenylpropanone”, *Journal of Applied Polymer Science*, Vol. 133, pp. 43910–43918, 2016.
- [47] Zhang, G., S. Jiang, Y. Gao and F. Sun, “Regulating photochemical behavior and property of imidazolium-based water soluble polysiloxane macromolecular photoinitiators by anions”, *Journal of Photochemistry and Photobiology A: Chemistry*, Vol. 364, pp. 363–372, 2018.
- [48] Liu, Y., X. Huang, K. Han, Y. Dai, X. Zhang and Y. Zhao, “High-performance lignin-based water-soluble macromolecular photoinitiator for the fabrication of hybrid hydrogel”, *ACS Sustainable Chemistry and Engineering*, Vol. 7, pp. 4004–4011, 2019.
- [49] Zhang, G., S. Jiang, Y. Gao and F. Sun, “Initiating the photopolymerization behaviors of water-soluble polymerizable polysiloxane–polyether block imidazolium ionic liquids with antibacterial capability”, *Macromolecular Chemistry and Physics*, Vol. 218, pp. 1700222–1700232, 2017.

- [50] Angiolini, L., D. Caretti, C. Carlini, E. Corelli and E. Salatelli, “Polymeric photoinitiators having benzoin methylether moieties connected to the main chain through the benzyl aromatic ring and their activity for ultraviolet-curable coatings”, *Polymer*, Vol. 40, pp. 7197–7207, 1999.
- [51] Chabreck, P., K. Dietliker and D. Lohmann, “Functionalized photoinitiators, derivatives and macromers therefrom and their use”, US Pat. 6204306 B1, 2001.
- [52] Ye, G., H. Zhou, J. Yang, Z. Zeng and Y. Chen, “Synthesis and characterization of oligomers containing the  $\alpha$ -aminoalkylphenone chromophore as oligomeric photoinitiator”, *Journal of Applied Polymer Science*, Vol. 99, pp. 3417–3424, 2006.
- [53] Wen, Y., X. Jiang, R. Liu and J. Yin, “Amphiphilic polymeric michler’s ketone (MK) photoinitiators (APMKs) containing PEO chain and coinitiator amine”, *Polymers for Advanced Technologies*, Vol. 22, pp. 598–604, 2011.
- [54] Reilly, L. W., “Water soluble michler’s ketone analogs in combined photoinitiator composition and polymerizable composition”, US Pat. 4576975, 1986.
- [55] Yokoi, K. and H. Tsuyama, “Aqueous curable composition and water-soluble photopolymerization initiator”, US Pat. 0362558 A1, 2018.
- [56] Wang, J., S. Stanic, A. A. Altun, M. Schwentenwein, K. Dietliker, L. Jin, J. Stampfl, S. Baudis, R. Liska and H. Grützmacher, “A highly efficient waterborne photoinitiator for visible-light-induced three-dimensional printing of hydrogels”, *Chemical Communications*, Vol. 54, pp. 920–923, 2018.
- [57] De Groot, J. H., K. Dillingham, H. Deuring, H. J. Haitjema, F. J. Van Beijma, K. Hodd and S. Norrby, “Hydrophilic polymeric acylphosphine oxide photoinitiators/crosslinkers for in vivo blue-light photopolymerization”, *Biomacromolecules*, Vol. 2, pp. 1271–1278, 2001.

- [58] Castelvetro, V., M. Molesti and P. Rolla, "UV-curing of acrylic formulations by means of polymeric photoinitiators with the active 2,6-dimethylbenzoylphosphine oxide moieties pendant from a tetramethylene side chain", *Macromolecular Chemistry and Physics*, Vol. 203, pp. 1486–1496, 2002.
- [59] Moszner, N., I. Lamparth, J. Angermann, U. K. Fischer, F. Zeuner, T. Bock, R. Liska and V. Rheinberger, "Synthesis of bis(3-{[2-(allyloxy)ethoxy]methyl}-2,4,6-trimethylbenzoyl) (phenyl)phosphine oxide - a tailormade photoinitiator for dental adhesives", *Beilstein Journal of Organic Chemistry*, Vol. 6, pp. 1–9, 2010.
- [60] Grützmacher, H., T. Ott and K. Dietliker, "Polymer-bound bisacylphosphine oxides", US Pat. 8883872 B2, 2014.
- [61] Liang, Q., L. Zhang, Y. Xiong, Q. Wu and H. Tang, "A facile method to prepare a polyethylene glycol modified polysilane as a waterborne photoinitiator", *Journal of Photochemistry and Photobiology A: Chemistry*, Vol. 299, pp. 9–17, 2015.
- [62] Kminek, I., Y. Yagci and W. Schnabel, "A water-soluble poly(methylphenylsilylene) derivative as a photoinitiator of radical polymerization of hydrophilic vinyl monomers", *Polymer Bulletin*, Vol. 29, pp. 277–282, 1992.
- [63] Eren, T. N., J. Lalevée and D. Avci, "Water soluble polymeric photoinitiator for dual-curing of acrylates and methacrylates", *Journal of Photochemistry and Photobiology A: Chemistry*, Vol. 389, pp. 112288–112298, 2020.
- [64] Curtis, J. R., "Water soluble photoinitiator benzophenone and thioxanthone ethoxy-ether derivatives", US Pat. 4602097, 1986.
- [65] Dadashi-Silab, S., H. Bildirir, R. Dawson, A. Thomas and Y. Yagci, "Microporous thioxanthone polymers as heterogeneous photoinitiators for visible light induced free radical and cationic polymerizations", *Macromolecules*, Vol. 47, pp. 4607–4614, 2014.

- [66] Dadashi-Silab, S., C. Aydogan and Y. Yagci, “Shining a light on an adaptable photoinitiator: advances in photopolymerizations initiated by thioxanthenes”, *Polymer Chemistry*, Vol. 6, pp. 6595–6615, 2015.
- [67] Jiang, X. and J. Yin, “Study of macrophotoinitiator containing in-chain thioxanthone and coinitiator amines”, *Polymer*, Vol. 45, pp. 5057–5063, 2004.
- [68] Eren, T. N., N. Okte, F. Morlet-Savary, J. P. Fouassier, J. Lalevee and D. Avci, “One-component thioxanthone-based polymeric photoinitiators”, *Journal of Polymer Science, Part A: Polymer Chemistry*, Vol. 54, pp. 3370–3378, 2016.
- [69] Madsen, N. J., P. Sehnal, D. G. Anderson and B. R. Nielsen, “Polymeric photoinitiators and photoinitiator monomers”, US Pat. 10040893 B2, 2018.
- [70] Kandirmaz, E. A., N. Kayaman Apohan and E. N. Gençoğlu, “Preparation of novel thioxanthone based polymeric photoinitiator for flexographic varnish and determination of their migration behaviour”, *Progress in Organic Coatings*, Vol. 119, pp. 36–43, 2018.
- [71] Corrales, T., F. Catalina, C. Peinado and N. S. Allen, “Free radical macrophotoinitiators: an overview on recent advances”, *Journal of Photochemistry and Photobiology A: Chemistry*, Vol. 159, pp. 103–114, 2003.
- [72] Luo, A., X. Jiang and J. Yin, “Thioxanthone-containing renewable vegetable oil as photoinitiators”, *Polymer*, Vol. 53, pp. 2183–2189, 2012.
- [73] Gacal, B., H. Akat, D. K. Balta, N. Arsu and Y. Yagci, “Synthesis and characterization of polymeric thioxanthone photoinitiators via double click reactions”, *Macromolecules*, Vol. 41, pp. 2401–2405, 2008.

- [74] Kork, S., G. Yilmaz and Y. Yagci, "Poly(vinyl alcohol)-thioxanthone as one-component type II photoinitiator for free radical polymerization in organic and aqueous media", *Macromolecular Rapid Communications*, Vol. 36, pp. 923–928, 2015.
- [75] Akat, H., B. Gacal, D. Karaca Balta, N. Arsu and Y. Yagci, "Poly(ethylene glycol)-thioxanthone prepared by diels–alder click chemistry as one-component polymeric photoinitiator for aqueous free-radical polymerization", *Polymer*, Vol. 48, pp. 2109–2114, 2010.
- [76] Corrales, T., F. Catalina, N. S. Allen and C. Peinado, "Novel water soluble copolymers based on thioxanthone: photochemistry and photoinitiation activity", *Journal of Photochemistry and Photobiology A: Chemistry*, Vol. 169, pp. 95–100, 2005.
- [77] Jiang, X. and J. Yin, "Water-soluble polymeric thioxanthone photoinitiator containing glucamine as coinitiator", *Macromolecular Chemistry and Physics*, Vol. 209, pp. 1593–1600, 2008.
- [78] Jiang, X., J. Luo and J. Yin, "A novel amphipathic polymeric thioxanthone photoinitiator", *Polymer*, Vol. 50, pp. 37–41, 2009.
- [79] Temel, G. and N. Arsu, "One-pot synthesis of water-soluble polymeric photoinitiator via thioxanthone and sulfonation process", *Journal of Photochemistry and Photobiology A: Chemistry*, Vol. 202, pp. 63–66, 2009.
- [80] Yilmaz, G., G. Acik and Y. Yagci, "Counteranion sensitization approach to photoinitiated free radical polymerization", *Macromolecules*, Vol. 45, pp. 2219–2224, 2012.
- [81] Corrales, T., F. Catalina, C. Peinado, N. S. Allen, A. M. Rufs, C. Bueno and M. V. Encinas, "Photochemical study and photoinitiation activity of macroinitiators based on thioxanthone", *Polymer*, Vol. 43, pp. 4591–4597, 2002.

- [82] Wang, J., J. Cheng, J. Liu, Y. Gao and F. Sun, "Self-floating ability and initiating gradient photopolymerization of acrylamide aqueous solution of a water-soluble polysiloxane benzophenone photoinitiator", *Green Chemistry*, Vol. 15, pp. 2457–2465, 2013.
- [83] Wang, K., Y. Lu, P. Chen, J. Shi, H. Wang and Q. Yu, "Novel one-component polymeric benzophenone photoinitiator containing poly (ethylene glycol) as hydrogen donor", *Materials Chemistry and Physics*, Vol. 143, pp. 1391–1395, 2014.
- [84] Wang, H., J. Wei, X. Jiang and J. Yin, "Highly efficient sulfur-containing polymeric photoinitiators bearing side-chain benzophenone and coinitiator amine for photopolymerization", *Journal of Photochemistry and Photobiology A: Chemistry*, Vol. 186, pp. 106–114, 2007.
- [85] Zhang, N., M. Li, J. Nie and F. Sun, "Microstructure and surface property of macroscopic gradient polymer initiated by polysiloxane benzophenone photoinitiators with different silicone chain lengths", *Journal of Materials Chemistry*, Vol. 22, pp. 9166–9172, 2012.
- [86] Cheng, L. and W. Shi, "Synthesis and photoinitiating behavior of benzophenone-based polymeric photoinitiators used for UV curing coatings", *Progress in Organic Coatings*, Vol. 71, pp. 355–361, 2011.
- [87] Nielsen, C. B., N. J. Madsen and C. M. Joergensen, "Polymeric photoinitiators", US Pat. 10040902 B2, 2018.
- [88] Zhang, G., Y. Cao, J. Yu and F. Sun, "Photoinitiability of a water-borne polysiloxane-modified benzophenone macromolecular photoinitiator", *Journal of Adhesion Science and Technology*, Vol. 30, pp. 2289–2300, 2016.

- [89] Wei, J., H. Wang, X. Jiang and J. Yin, "Study of novel PU-type polymeric photoinitiators comprising of side-chain benzophenone and coinitiator amine: effect of macromolecular structure on photopolymerization", *Macromolecular Chemistry and Physics*, Vol. 208, pp. 287–294, 2007.
- [90] Van Den Bergen, H., P. Gevaert and S. Capele, "Polymeric photoinitiators", US Pat. 10189930 B2, 2019.
- [91] Wei, J., R. Lu and F. Liu, "Effect of photosensitive groups on the photoefficiency of polymeric photoinitiators", *Journal of Polymer Research*, Vol. 18, pp. 1001–1008, 2011.
- [92] Wei, J., H. Wang, X. Jiang and J. Yin, "A highly efficient polyurethane-type polymeric photoinitiator containing In-chain benzophenone and coinitiator amine for photopolymerization of pu prepolymers", *Macromolecular Chemistry and Physics*, Vol. 207, pp. 2321–2328, 2006.
- [93] Wei, J., F. Liu, Z. Lu, L. Song and D. Cai, "Novel PU-type polymeric photoinitiator comprising side-chain benzophenone and coinitiator amine for photopolymerization of PU acrylate", *Polymers for Advanced Technologies*, Vol. 19, pp. 1763–1770, 2008.
- [94] Shi, J., P. Chen, K. Wang, J. Lu and J. Nie, "A novel high efficiency benzophenone based polymeric photoinitiator from ring-opening polymerization of benzoxazine", *Polymer Science Series B*, Vol. 56, pp. 632–638, 2014.
- [95] Jiang, X., X. Luo and J. Yin, "Polymeric photoinitiators containing in-chain benzophenone and coinitiators amine: effect of the structure of coinitiator amine on photopolymerization", *Journal of Photochemistry and Photobiology A: Chemistry*, Vol. 174, pp. 165–170, 2005.
- [96] Angiolini, L., D. Caretti and E. Salatelli, "Synthesis and photoinitiation activity of radical polymeric photoinitiators bearing side-chain camphorquinone moieties", *Macromolecular Chemistry and Physics*, Vol. 201, pp. 2646–2653, 2000.

- [97] Allonas, X., J. P. Fouassier, L. Angiolini and D. Caretti, “Excited-state properties of camphorquinone based monomeric and polymeric photoinitiators”, *Helvetica Chimica Acta*, Vol. 84, pp. 2577–2588, 2001.
- [98] Angiolini, L., D. Caretti, S. Rossetti, E. Salatelli and M. Scoconi, “Radical polymeric photoinitiators bearing side-chain camphorquinone moieties linked to the main chain through a flexible spacer”, *Journal of Polymer Science, Part A: Polymer Chemistry*, Vol. 43, pp. 5879–5888, 2005.
- [99] Catalina, F., C. Peinado, M. Blanco, N. S. Allen, T. Corrales and I. Lukác, “Synthesis, photochemical and photoinitiation activity of water soluble copolymers with pendent benzil chromophores”, *Polymer*, Vol. 39, pp. 4399–4408, 1998.
- [100] Catalina, F., C. Peinado, M. Blanco, A. Alonso and N. S. Allen, “Photocalorimetric study on the photoinitiation activity of water soluble copolymers with pendent benzil moieties”, *Journal of Photochemistry and Photobiology A: Chemistry*, Vol. 131, pp. 141–146, 2000.
- [101] Catalina, F., C. Peinado, M. Blanco, T. Corrales and N. S. Allen, “Synthesis, photochemical and photoinitiation activity of water-soluble copolymers with anthraquinone chromophores as side-chain groups”, *Polymer*, Vol. 42, pp. 1825–1832, 2001.
- [102] Zhou, J., X. Allonas, A. Ibrahim and X. Liu, “Progress in the development of polymeric and multifunctional photoinitiators”, *Progress in Polymer Science*, Vol. 99, pp. 101165–101181, 2019.
- [103] Mishra, M. and S. Kobayashi, *Star and hyperbranched polymers*, CRC Press, United States of America, US, 1999.
- [104] Yates, C. R. and W. Hayes, “Synthesis and applications of hyperbranched polymers”, *European Polymer Journal*, Vol. 40, pp. 1257–1281, 2004.

- [105] Han, W., B. Lin, Y. Zhou and J. Song, "Synthesis and properties of UV-curable hyperbranched polyurethane acrylate oligomers containing photoinitiator", *Polymer Bulletin*, Vol. 68, pp. 729–743, 2012.
- [106] Norcini, G., M. Morone, A. Bernini Freddi, G. Floridi and G. Li Bassi, "Multifunctional acylphosphine oxide photoinitiators", EP 3149013 B1, 2018.
- [107] Si, Q. F., X. D. Fan, Y. Y. Liu, J. Kong, S. J. Wang and W. Q. Qiao, "Synthesis and characterization of hyperbranched-poly(siloxysilane)-based polymeric photoinitiators", *Journal of Polymer Science: Part A: Polymer Chemistry*, Vol. 44, pp. 3261–3270, 2006.
- [108] Si, Q. F., X. Wang, X. D. Fan and S. J. Wang, "Synthesis and characterization of ultraviolet-curable hyperbranched poly(siloxysilane)s", *Journal of Polymer Science, Part A: Polymer Chemistry*, Vol. 43, pp. 1883–1894, 2005.
- [109] Loccufier, J., L. Vanmaele, J. Van Luppen, R. Claes, Y. Chen and H. Frey, "Novel radiation curable compositions", EP 1616921 B1, 2006.
- [110] Jiang, X., H. Xu and J. Yin, "Polymeric amine bearing side-chain thioxanthone as a novel photoinitiator for photopolymerization", *Polymer*, Vol. 45, pp. 133–140, 2004.
- [111] Jiang, X. and J. Yin, "Dendritic macrophotoinitiator containing thioxanthone and coinitiator amine", *Macromolecules*, Vol. 37, pp. 7850–7853, 2004.
- [112] Jiang, X., H. Xu and J. Yin, "Copolymeric dendritic macrophotoinitiators", *Polymer*, Vol. 46, pp. 11079–11084, 2005.
- [113] Jiang, X., W. Wang, H. Xu and J. Yin, "Water-compatible dendritic macrophotoinitiator containing thioxanthone", *Journal of Photochemistry and Photobiology A: Chemistry*, Vol. 181, pp. 233–237, 2006.

- [114] Li, T., Z. Su, H. Xu, X. Ma, J. Yin and X. Jiang, “A supramolecular polymeric photoinitiator with enhanced dispersion in photo-curing systems”, *Polymer Chemistry*, Vol. 11, pp. 1885–1893, 2020.
- [115] Loccufier, J., L. Vanmaele, H. Docx and N. Willems, “Polymerizable polymeric photoinitiators and radiation curable compositions”, US Pat. 8883873 B2, 2014.
- [116] Wen, Y., X. Jiang, R. Liu and J. Yin, “Amphipathic hyperbranched polymeric thioxanthone photoinitiators (AHPTXs): synthesis, characterization and photoinitiated polymerization”, *Polymer*, Vol. 50, pp. 3917–3923, 2009.
- [117] Nehlig, E., R. Schneider, L. Vidal, G. Clavier and L. Balan, “Silver nanoparticles coated with thioxanthone derivative as hybrid photoinitiating systems for free radical polymerization”, *Langmuir*, Vol. 28, pp. 17795–17802, 2012.
- [118] Chen, Y., J. Loccufier, L. Vanmaele, E. Barriau and H. Frey, “Novel multifunctional polymeric photoinitiators and photo-coinitiators derived from hyperbranched polyglycerol”, *Macromolecular Chemistry and Physics*, Vol. 208, pp. 1694–1706, 2007.
- [119] Chen, Y., J. Loccufier, L. Vanmaele and H. Frey, “Novel multifunctional hyperbranched polymeric photoinitiators with built-in amine coinitiators for UV curing”, *Journal of Materials Chemistry*, Vol. 17, pp. 3389–3392, 2007.
- [120] Hu, L., A. Asif, J. Xie and W. Shi, “Synthesis and photoinitiating behavior of hyperbranched polymeric photoinitiators bearing coinitorator amine”, *Polymers for Advanced Technologies*, Vol. 22, pp. 1673–1680, 2011.
- [121] Li, T., Z. Su, H. Xu, X. Jiang, X. Ma and J. Yin, “Hyperbranched poly(ether amine) (hPEA) as novel backbone for amphiphilic one-component type-II polymeric photoinitiators”, *Chinese Chemical Letters*, Vol. 29, pp. 451–455, 2018.

- [122] Temel, G., T. Parali, M. Tulu and N. Arsu, "Photopolymerization of acrylamide with benzophenone/methylated- $\beta$ -cyclodextrin inclusion complex in the presence of jeffamine based dendrimers as coiniciators in aqueous media", *Journal of Photochemistry and Photobiology A: Chemistry*, Vol. 213, pp. 46–51, 2010.
- [123] Wang, K., K. Yang and Q. Yu, "Novel polymeric photoinitiators with side-chain benzophenone: facile synthesis and photopolymerization properties without coiniciator", *Progress in Organic Coatings*, Vol. 77, pp. 1929–1934, 2014.
- [124] Xie, H., L. Hu and W. Shi, "Synthesis and photoinitiating activity study of polymeric photoinitiators bearing BP moiety based on hyperbranched poly(ester-amine) via thiol-ene click reaction", *Journal of Applied Polymer Science*, Vol. 123, pp. 1494–1501, 2012.
- [125] Xie, H., L. Hu, Y. Zhang and W. Shi, "Sulfur-containing hyperbranched polymeric photoinitiator end-capped with benzophenone and tertiary amine moieties prepared via simultaneous double thiol-ene click reactions used for UV curing coatings", *Progress in Organic Coatings*, Vol. 72, pp. 572–578, 2011.
- [126] Jędrzejewska, B., M. Pietrzak, F. Ścigalski, Ż. Tomczyk and J. Pączkowski, "Silver-nanoparticles immobilized initiator and co-initiators for free radical polymerization", *Materials Letters*, Vol. 62, pp. 4260–4262, 2008.
- [127] Arbeloa, E. M., C. M. Previtali and S. G. Bertolotti, "A comparative study on the photophysics and photochemistry of xanthene dyes in the presence of polyamidoamine (PAMAM) dendrimers", *ChemPhysChem*, Vol. 19, pp. 934–942, 2018.
- [128] Kaastrup, K. and H. D. Sikes, "Investigation of dendrimers functionalized with eosin as macrophotoinitiators for polymerization-based signal amplification reactions", *RSC Advances*, Vol. 5, pp. 15652–15659, 2015.

- [129] Share, P., “LED-curable low migration photoinitiators”, US Pat. 0233550 A1, 2019.
- [130] Guo, Q., *Thermosets: structure, properties, and applications*. Cornwall, UK: Elsevier, 2017.
- [131] Konuray, O., X. Fernández-Francos, X. Ramis and À. Serra, “State of the art in dual-curing acrylate systems”, *Polymers*, Vol. 10, pp. 178–202, 2018.
- [132] Tunca, U., “Orthogonal multiple click reactions in synthetic polymer chemistry”, *Journal of Polymer Science, Part A: Polymer Chemistry*, Vol. 52, pp. 3147–3165, 2014.
- [133] Kolb, H. C., M. G. Finn and K. B. Sharpless, “Click chemistry: diverse chemical function from a few good reactions”, *Angewandte Chemie - International Edition*, Vol. 40, pp. 2004–2021, 2001.
- [134] Mather, B. D., K. Viswanathan, K. M. Miller and T. E. Long, “Michael addition reactions in macromolecular design for emerging technologies”, *Progress in Polymer Science*, Vol. 31, pp. 487–531, 2006.
- [135] Konuray, O., X. Fernández-Francos, X. Ramis and À. Serra, “Acetoacetate based thermosets prepared by dual-Michael addition reactions”, *Polymers*, Vol. 11, pp. 1408–1421, 2019.
- [136] Konuray, A. O., X. Fernández-Francos, À. Serra and X. Ramis, “Sequential curing of amine-acrylate-methacrylate mixtures based on selective aza-Michael addition followed by radical photopolymerization”, *European Polymer Journal*, Vol. 84, pp. 256–267, 2016.
- [137] Konuray, A. O., A. Ruiz, J. M. Morancho, J. M. Salla, X. Fernández-Francos, À. Serra and X. Ramis, “Sequential dual curing by selective Michael addition and free radical polymerization of acetoacetate-acrylate-methacrylate mixtures”, *European Polymer Journal*, Vol. 98, pp. 39–46, 2018.

- [138] González, G., X. Fernández-Francos, À. Serra, M. Sangermano and X. Ramis, “Environmentally-friendly processing of thermosets by two-stage sequential aza-Michael addition and free-radical polymerization of amine-acrylate mixtures”, *Polymer Chemistry*, Vol. 6, pp. 6987–6997, 2015.
- [139] Nair, D. P., N. B. Cramer, J. C. Gaipa, M. K. McBride, E. M. Matherly, R. R. McLeod, R. Shandas and C. N. Bowman, “Two-stage reactive polymer network forming systems”, *Advanced Functional Materials*, Vol. 22, pp. 1502–1510, 2012.
- [140] Retailleau, M., A. Ibrahim, C. Croutxé-Barghorn, X. Allonas, C. Ley and D. Le Nouen, “One-pot three-step polymerization system using double click Michael addition and radical photopolymerization”, *ACS Macro Letters*, Vol. 4, pp. 1327–1331, 2015.
- [141] Retailleau, M., A. Ibrahim, C. Croutxé-Barghorn and X. Allonas, “New design of highly homogeneous photopolymer networks for shape memory materials”, *RSC Advances*, Vol. 6, pp. 47130–47133, 2016.
- [142] Retailleau, M., J. Pierrel, A. Ibrahim, C. Croutxé-Barghorn and X. Allonas, “Sequenced click chemistry and photopolymerization: a new approach toward semi-interpenetrating polymer networks”, *Polymers for Advanced Technologies*, Vol. 28, pp. 491–495, 2017.
- [143] Visconti, M. and M. Cattaneo, “Highly efficient photoinitiator for water-borne UV-curable systems”, *Progress in Organic Coatings*, Vol. 40, pp. 243–251, 2000.
- [144] Zhang, G., S. Jiang, Y. Gao and F. Sun, “Design of green hydrophilic polysiloxane-polyether-modified macromolecular photoinitiators with ionic liquid character”, *Journal of Materials Science*, Vol. 52, pp. 9931–9945, 2017.
- [145] Knaus, S. and H. F. Gruber, “Photoinitiators with functional groups. III. water-soluble photoinitiators containing carbohydrate residues”, *Journal of Polymer Science Part A: Polymer Chemistry*, Vol. 33, pp. 929–939, 1995.

- [146] Knaus, S. and H. F. Gruber, "Photoinitiators with functional groups. Part IV. water-soluble photoinitiators containing quaternary ammonium groups", *Journal of Macromolecular Science - Pure and Applied Chemistry*, Vol. 33, pp. 869–881, 1996.
- [147] Liska, R., "Photoinitiators with functional groups. V. new water-soluble photoinitiators containing carbohydrate residues and copolymerizable derivatives thereof", *Journal of Polymer Science, Part A: Polymer Chemistry*, Vol. 40, pp. 1504–1518, 2002.
- [148] Roth, M., D. Hennen, A. Oesterreicher, F. Mostegel, A. Samusjew, M. Edler, E. Maier and T. Griesser, "Highly water-soluble alpha-hydroxyalkylphenone based photoinitiator for low-migration applications", *Macromolecular Chemistry and Physics*, Vol. 218, pp. 1700022–1700028, 2017.
- [149] Benedikt, S., J. Wang, M. Markovic, N. Moszner, K. Dietliker, A. Ovsianikov, H. Grützmacher and R. Liska, "Highly efficient water-soluble visible light photoinitiators", *Journal of Polymer Science, Part A: Polymer Chemistry*, Vol. 54, pp. 473–479, 2016.
- [150] Müller, G., M. Zalibera, G. Gescheidt, A. Rosenthal, G. Santiso-Quinones, K. Dietliker and H. Grützmacher, "Simple one-pot syntheses of water-soluble Bis(acyl)phosphane oxide photoinitiators and their application in surfactant-free emulsion polymerization", *Macromolecular Rapid Communications*, Vol. 36, pp. 553–557, 2015.
- [151] Ullrich, G., B. Ganster, U. Salz, N. Moszner and R. Liska, "Photoinitiators with functional groups. IX. hydrophilic bisacylphosphine oxides for acidic aqueous formulations", *Journal of Polymer Science, Part A: Polymer Chemistry*, Vol. 44, pp. 1686–1700, 2006.
- [152] Henne, A., A. Hesse, M. Jacobi, G. Wallbillich and B. Bronstert, "Acylphosphine compounds and their use as photoinitiators", US Pat. 4719297, 1988.

- [153] Guo, R., Y. Gao, M. Wu and H. Wang, "Aliphatic ketones and aldehydes as water-soluble photoinitiators for the photopolymerization of methacrylic acid", *Polymer*, Vol. 54, pp. 4940–4947, 2013.
- [154] Gaudl, K. U. W. and J. Dieker, "LED photoinitiators", US Pat. 9938232 B2, 2018.
- [155] Chang, F., R. Desousa, T. V. Holland and W. R. Laredo, "Water-soluble UV-absorbing compounds and uses thereof", US Pat. 10322993 B2, 2019.
- [156] Allen, N. S., W. Chen, F. Catalina, P. N. Green and A. Green, "Photochemistry of novel water-soluble para-substituted benzophenone photoinitiators: a polymerization, spectroscopic and flash photolysis study", *Journal of Photochemistry and Photobiology, A: Chemistry*, Vol. 44, pp. 349–360, 1988.
- [157] Lougnot, D. J. and J. P. Fouassier, "Comparative reactivity of water soluble photoinitiators as viewed in terms of excited states processes", *Journal of Polymer Science Part A: Polymer Chemistry*, Vol. 26, pp. 1021–1033, 1988.
- [158] Balta, D. K., E. Bagdatli, N. Arsu, N. Ocal and Y. Yagci, "Chemical incorporation of thioxanthone into  $\beta$ -cyclodextrin and its use in aqueous photopolymerization of methyl methacrylate", *Journal of Photochemistry and Photobiology A: Chemistry*, Vol. 196, pp. 33–37, 2008.
- [159] Demet, K. B., G. Temel, M. Aydin and N. Arsu, "Thioxanthone based water-soluble photoinitiators for acrylamide photopolymerization", *European Polymer Journal*, Vol. 46, pp. 1374–1379, 2010.
- [160] Catalina, F., T. Corrales, C. Peinado, N. S. Allen, W. A. Green and A. Timms, "Photochemistry and photoinitiation activity of novel I-substituted water soluble derivatives of 4-(2-hydroxy-3-N,N,N-trimethylammoniumpropoxy)thioxanthone chloride salt", *European Polymer Journal*, Vol. 29, pp. 125–130, 1993.

- [161] Curtis, J. R. and P. E. Heaton, “Water soluble thioxanthone photoinitiators”, US Pat. 4459416, 1984.
- [162] Wu, Q., Y. Xiong, J. Yang, H. Tang and S. Chen, “Thioxanthone-based hydrophilic visible photoinitiators for radical polymerization”, *Macromolecular Chemistry and Physics*, Vol. 217, pp. 1569–1578, 2016.
- [163] Huang, X., X. Wang and Y. Zhao, “Study on a series of water-soluble photoinitiators for fabrication of 3D hydrogels by two-photon polymerization”, *Dyes and Pigments*, Vol. 141, pp. 413–419, 2017.
- [164] Kamoun, E. A., A. Winkel, M. Eisenburger and H. Menzel, “Carboxylated camphorquinone as visible-light photoinitiator for biomedical application: synthesis, characterization, and application”, *Arabian Journal of Chemistry*, Vol. 9, pp. 745–754, 2016.
- [165] Zheng, Y. C., Y. Y. Zhao, M. L. Zheng, S. L. Chen, J. Liu, F. Jin, X. Z. Dong, Z. S. Zhao and X. M. Duan, “Cucurbit[7]uril-carbazole two-photon photoinitiators for the fabrication of biocompatible three-dimensional hydrogel scaffolds by laser direct writing in aqueous solutions”, *ACS Applied Materials and Interfaces*, Vol. 11, pp. 1782–1789, 2019.
- [166] Zhang, J., F. Dumur, P. Xiao, B. Graff, D. Bardelang, D. Gigmes, J. P. Fouassier and J. Lalevée, “Structure design of naphthalimide derivatives: toward versatile photoinitiators for near-UV/visible LEDs, 3D printing, and water-soluble photoinitiating systems”, *Macromolecules*, Vol. 48, pp. 2054–2063, 2015.
- [167] Encinas, M. V., A. M. Rufs, S. G. Bertolotti and C. M. Previtali, “Xanthene dyes/amine as photoinitiators of radical polymerization: a comparative and photochemical study in aqueous medium”, *Polymer*, Vol. 50, pp. 2762–2767, 2009.

- [168] Bi, Y. and D. C. Neckers, “A visible light initiating system for free radical promoted cationic polymerization”, *Macromolecules*, Vol. 27, pp. 3683–3693, 1994.
- [169] Arbeloa, E. M., G. V. Porcal, S. G. Bertolotti and C. M. Previtali, “Synthesis and characterization of latex nanoparticles using a visible-light photoinitiating system in reverse micelles”, *Colloid and Polymer Science*, Vol. 293, pp. 625–632, 2014.
- [170] Li, S., F. Wu and E. Wang, “A water-soluble supramolecular structured photosensitive initiation system: Me- $\beta$ -CD complex of xanthene dye/aryliodonium salt”, *Polymer*, Vol. 50, pp. 3932–3937, 2009.
- [171] Abdallah, M., A. Hijazi, B. Graff, J. P. Fouassier, G. Rodeghiero, A. Gualandi, F. Dumur, P. G. Cozzi and J. Lalevée, “Coumarin derivatives as versatile photoinitiators for 3D printing, polymerization in water and photocomposite synthesis”, *Polymer Chemistry*, Vol. 10, pp. 872–884, 2019.
- [172] Zhou, D. and Y. Ito, “Visible light-curable polymers for biomedical applications”, *Science China Chemistry*, Vol. 57, pp. 510–521, 2014.
- [173] Dietlin, C., S. Schweizer, P. Xiao, J. Zhang, F. Morlet-Savary, B. Graff, J. P. Fouassier and J. Lalevée, “Photopolymerization upon LEDs: new photoinitiating systems and strategies”, *Polymer Chemistry*, Vol. 6, pp. 3895–3912, 2015.
- [174] Shao, J., Y. Huang and Q. Fan, “Visible light initiating systems for photopolymerization: status, development and challenges”, *Polymer Chemistry*, Vol. 5, pp. 4195–4210, 2014.
- [175] Zhao, J., J. Lalevée, H. Lu, R. MacQueen, S. H. Kable, T. W. Schmidt, M. H. Stenzel and P. Xiao, “A new role of curcumin: as a multicolor photoinitiator for polymer fabrication under household UV to red LED bulbs”, *Polymer Chemistry*, Vol. 6, pp. 5053–5061, 2015.

- [176] Hiller, J., J. D. Mendelsohn and M. F. Rubner, “Reversibly erasable nanoporous anti-reflection coatings from polyelectrolyte multilayers”, *Nature Materials*, Vol. 1, pp. 59–63, 2002.
- [177] Allen, N. S., “Photoinitiators for UV and visible curing of coatings: mechanisms and properties”, *Journal of Photochemistry and Photobiology A: Chemistry*, Vol. 100, pp. 101–107, 1996.
- [178] Moszner, N. and U. Salz, “Recent developments of new components for dental adhesives and composites”, *Macromolecular Materials and Engineering*, Vol. 292, pp. 245–271, 2007.
- [179] Moszner, N. and U. Salz, “New developments of polymeric dental composites”, *Progress in Polymer Science*, Vol. 26, pp. 535–576, 2001.
- [180] Moon, J. H., J. Ford and S. Yang, “Fabricating three-dimensional polymeric photonic structures by multi-beam interference lithography”, *Polymers for Advanced Technologies*, Vol. 17, pp. 83–93, 2006.
- [181] Fouassier, J. P. and F. Morlet-Savary, “Photopolymers for laser imaging and holographic recording: design and reactivity of photosensitizers”, *Optical Engineering*, Vol. 35, pp. 304–312, 1996.
- [182] Huber, A., A. Kuschel, T. Ott, G. Santiso-Quinones, D. Stein, J. Bräuer, R. Kissner, F. Krumeich, H. Schönberg, J. Levalois-Grützmacher and H. Grützmacher, “Phosphorous-functionalized bis(acyl)phosphane oxides for surface modification”, *Angewandte Chemie*, Vol. 51, pp. 4648–4652, 2012.
- [183] Xie, C., Z. Wang, Y. Liu, L. Song, L. Liu, Z. Wang and Q. Yu, “A novel acyl phosphine compound as difunctional photoinitiator for free radical polymerization”, *Progress in Organic Coatings*, Vol. 135, pp. 34–40, 2019.

- [184] Ikemura, K., K. Ichizawa, Y. Jogetsu and T. Endo, “Synthesis of a novel camphorquinone derivative having acylphosphine oxide group, characterization by UV-Vis spectroscopy and evaluation of photopolymerization performance”, *Dental Materials Journal*, Vol. 29, pp. 122–131, 2010.
- [185] Kucybaa, Z., M. Pietrzak, J. Paczkowski, L. A. Lindén and J. F. Rabek, “Kinetic studies of a new photoinitiator hybrid system based on camphorquinone-N-phenylglycine derivatives for laser polymerization of dental restorative and stereolithographic (3D) formulations”, *Polymer*, Vol. 37, pp. 4585–4591, 1996.
- [186] Zhang, J., P. Xiao, S. Shi and J. Nie, “Preparation and characterization of a water soluble methylated  $\beta$ -cyclodextrin/camphorquinone complex”, *Polymers for Advanced Technologies*, Vol. 20, pp. 723–728, 2009.
- [187] Zhang, J., K. Launay, N. S. Hill, D. Zhu, N. Cox, J. Langley, J. Lalevée, M. H. Stenzel, M. L. Coote and P. Xiao, “Disubstituted aminoanthraquinone-based photoinitiators for free radical polymerization and fast 3D printing under visible light”, *Macromolecules*, Vol. 51, pp. 10104–10112, 2018.
- [188] Xiao, P., F. Dumur, B. Graff, J. P. Fouassier, D. Gigmes and J. Lalevée, “Cationic and thiol-ene photopolymerization upon red lights using anthraquinone derivatives as photoinitiators”, *Macromolecules*, Vol. 46, pp. 6744–6750, 2013.
- [189] Zhang, J., J. Lalevée, F. Morlet-Savary, B. Graff and P. Xiao, “Photopolymerization under various monochromatic UV/visible LEDs and IR lamp: Diaminoanthraquinone derivatives as versatile multicolor photoinitiators”, *European Polymer Journal*, Vol. 112, pp. 591–600, 2019.
- [190] Zhang, J., N. S. Hill, J. Lalevée, J. P. Fouassier, J. Zhao, B. Graff, T. W. Schmidt, S. H. Kable, M. H. Stenzel, M. L. Coote and P. Xiao, “Multihydroxy-anthraquinone derivatives as free radical and cationic photoinitiators of various photopolymerizations under green LED”, *Macromolecular Rapid Communications*, Vol. 39, pp. 1800172–1800178, 2018.

- [191] Breloy, L., V. Brezová, A. Blacha-Grzechnik, M. Presset, M. S. Yildirim, I. Yilmaz, Y. Yagci and D. L. Versace, “Visible light anthraquinone functional phthalocyanine photoinitiator for free-radical and cationic polymerizations”, *Macromolecules*, Vol. 53, pp. 112–124, 2020.
- [192] Wang, G., N. S. Hill, D. Zhu, P. Xiao, M. L. Coote and M. H. Stenzel, “Efficient photoinitiating system based on diaminoanthraquinone for 3D printing of polymer/carbon nanotube nanocomposites under visible light”, *ACS Applied Polymer Materials*, Vol. 1, pp. 1129–1135, 2019.
- [193] Chen, Y., G. Li, H. Zhang and T. Wang, “Visible light curing of bisphenol-A epoxides and acrylates photoinitiated by ( $\eta$  6-benzophenone)( $\eta$  5-cyclopentadienyl) iron hexafluorophosphate”, *Journal of Polymer Research*, Vol. 18, pp. 1425–1429, 2011.
- [194] Lalevée, J., M. A. Tehfe, F. Dumur, D. Gigmes, B. Graff, F. Morlet-Savary and J. P. Fouassier, “Light-harvesting organic photoinitiators of polymerization”, *Macromolecular Rapid Communications*, Vol. 34, pp. 239–245, 2013.
- [195] Qin, X., G. Ding, Y. Gong, C. Jing, G. Peng, S. Liu, L. Niu, S. Zhang, Z. Luo, H. Li and F. Gao, “Stilbene-benzophenone dyads for free radical initiating polymerization of methyl methacrylate under visible light irradiation”, *Dyes and Pigments*, Vol. 132, pp. 27–40, 2016.
- [196] Tehfe, M. A., F. Dumur, B. Graff, F. Morlet-Savary, D. Gigmes, J. P. Fouassier and J. Lalevée, “Design of new type I and type II photoinitiators possessing highly coupled pyrene-ketone moieties”, *Polymer Chemistry*, Vol. 4, pp. 2313–2324, 2013.
- [197] Xiao, P., F. Dumur, B. Graff, D. Gigmes, J. P. Fouassier and J. Lalevée, “Variations on the benzophenone skeleton: novel high performance blue light sensitive photoinitiating systems”, *Macromolecules*, Vol. 46, pp. 7661–7667, 2013.

- [198] Zhang, J., N. Zivic, F. Dumur, P. Xiao, B. Graff, D. Gigmes, J. P. Fouassier and J. Lalevée, “A benzophenone-naphthalimide derivative as versatile photoinitiator of polymerization under near UV and visible lights”, *Journal of Polymer Science, Part A: Polymer Chemistry*, Vol. 53, pp. 445–451, 2015.
- [199] Balta, D. K., N. Arsu, Y. Yagci, S. Jockusch and N. J. Turro, “Thioxanthone-anthracene: a new photoinitiator for free radical polymerization in the presence of oxygen”, *Macromolecules*, Vol. 40, pp. 4138–4141, 2007.
- [200] Balta, D. K., G. Temel, G. Goksu, N. Ocal and N. Arsu, “Thioxanthone-diphenyl anthracene: visible light photoinitiator”, *Macromolecules*, Vol. 45, pp. 119–125, 2012.
- [201] Wu, Q., W. Liao, Y. Xiong, J. Yang, Z. Li and H. Tang, “Silicone-thioxanthone: a multifunctionalized visible light photoinitiator with an ability to modify the cured polymers”, *Polymers*, Vol. 11, pp. 695–710, 2019.
- [202] Chen, G., X. Guan, R. Xu, J. Tian, F. Lu, M. He and J. Yang, “Thioxanthone dicarboxamide derivatives as one-component photoinitiators for near-UV and visible LED (365-405 nm) induced photopolymerizations”, *RSC Advances*, Vol. 6, pp. 77093–77099, 2016.
- [203] Valandro, S. R., A. L. Poli, T. Venâncio, J. Pina, J. S. De Melo, H. D. Burrows and C. C. Schmitt, “A novel biopolymeric photoinitiator based on chitosan and thioxanthone derivative: synthesis, characterization and efficiency in photopolymerization”, *Journal of Photochemistry and Photobiology A: Chemistry*, Vol. 327, pp. 15–20, 2016.
- [204] Yilmaz, G., A. Tuzun and Y. Yagci, “Thioxanthone-carbazole as a visible light photoinitiator for free radical polymerization”, *Journal of Polymer Science, Part A: Polymer Chemistry*, Vol. 48, pp. 5120–5125, 2010.

- [205] Yilmaz, G., B. Aydogan, G. Temel, N. Arsu, N. Moszner and Y. Yagci, “Thioxanthone-fluorenes as visible light photoinitiators for free radical polymerization”, *Macromolecules*, Vol. 43, pp. 4520–4526, 2010.
- [206] Balta, D. K. and N. Arsu, “Thioxanthone-ethyl anthracene”, *Journal of Photochemistry and Photobiology A: Chemistry*, Vol. 257, pp. 54–59, 2013.
- [207] Dogruyol, S. K., Z. Dogruyol and N. Arsu, “A thioxanthone-based visible photoinitiator”, *Journal of Polymer Science, Part A: Polymer Chemistry*, Vol. 49, pp. 4037–4043, 2011.
- [208] Dođruyol, S. K., Z. Dođruyol and N. Arsu, “Thioxanthone based 9-[2-(methyl-phenyl-amino)-acetyl]-thia-naphthacene-12- one as a visible photoinitiator”, *Journal of Luminescence*, Vol. 138, pp. 98–104, 2013.
- [209] Dong, X., W. Shen, P. Hu, Z. Li, R. Liu and X. Liu, “Efficient benzodioxole-based unimolecular photoinitiators: from synthesis to photopolymerization under UV-A and visible LED light irradiation”, *Journal of Applied Polymer Science*, Vol. 133, pp. 43239–43249, 2016.
- [210] Karaca, N., D. K. Balta, N. Ocal and N. Arsu, “Thioxanthone of fluorenone: visible photoinitiator for radical polymerization”, *Journal of Polymer Science, Part A: Polymer Chemistry*, Vol. 54, pp. 1012–1019, 2016.
- [211] Kaya, K., J. Kreutzer and Y. Yagci, “A charge-transfer complex of thioxanthonephenacyl sulfonium salt as a visible-light photoinitiator for free radical and cationic polymerizations”, *ChemPhotoChem*, Vol. 3, pp. 1187–1192, 2019.
- [212] Kreutzer, J. and Y. Yagci, “One-component, double-chromophoric thioxanthone photoinitiators for free radical polymerization”, *Journal of Polymer Science, Part A: Polymer Chemistry*, Vol. 55, pp. 3475–3482, 2017.

- [213] Tar, H., D. Sevinc Esen, M. Aydin, C. Ley, N. Arsu and X. Allonas, “Panchromatic type II photoinitiator for free radical polymerization based on thioxanthone derivative”, *Macromolecules*, Vol. 46, pp. 3266–3272, 2013.
- [214] Durmaz, Y. Y., N. Moszner and Y. Yagci, “Visible light initiated free radical promoted cationic polymerization using acylgermane based photoinitiator in the presence of onium salts”, *Macromolecules*, Vol. 41, pp. 6714–6718, 2008.
- [215] Durmaz, Y. Y., M. Kukut, N. Moszner and Y. Yagci, “Sequential photodecomposition of bisacylgermane type photoinitiator: synthesis of block copolymers by combination of free radical promoted cationic and free radical polymerization mechanisms”, *Journal of Polymer Science Part A: Polymer Chemistry*, Vol. 47, pp. 4793–4799, 2009.
- [216] Ganster, B., U. K. Fischer, N. Moszner and R. Liska, “New photocleavable structures, 4: acylgermane-based photoinitiator for visible light curing”, *Macromolecular Rapid Communications*, Vol. 29, pp. 57–62, 2008.
- [217] Ganster, B., U. K. Fischer, N. Moszner and R. Liska, “New photocleavable structures. diacylgermane-based photoinitiators for visible light curing”, *Macromolecules*, Vol. 41, pp. 2394–2400, 2008.
- [218] Moszner, N., U. K. Fischer, B. Ganster, R. Liska and V. Rheinberger, “Benzoyl germanium derivatives as novel visible light photoinitiators for dental materials”, *Dental Materials*, Vol. 24, pp. 901–907, 2008.
- [219] Moszner, N., F. Zeuner, I. Lamparth and U. K. Fischer, “Benzoylgermanium derivatives as novel visible-light photoinitiators for dental composites”, *Macromolecular Materials and Engineering*, Vol. 294, pp. 877–886, 2009.

- [220] Moszner, N., U. K. Fischer, I. Lamparth, P. Fässler, J. Radebner, A. Eibel, M. Haas, G. Gescheidt and H. Stueger, “Tetraacylgermanes as highly efficient photoinitiators for visible light cured dimethacrylate resins and dental composites”, *Journal of Applied Polymer Science*, Vol. 135, pp. 46115–46122, 2018.
- [221] Radebner, J., A. Eibel, M. Leybold, C. Gorsche, L. Schuh, R. Fischer, A. Torvisco, D. Neshchadin, R. Geier, N. Moszner, R. Liska, G. Gescheidt, M. Haas and H. Stueger, “Tetraacylgermanes: highly efficient photoinitiators for visible-light-induced free-radical polymerization”, *Angewandte Chemie - International Edition*, Vol. 56, pp. 3103–3107, 2017.
- [222] Tehfe, M. A., N. Blanchard, C. Fries, J. Lalevée, X. Allonas and J. P. Fouassier, “Bis (germyl) ketones: toward a new class of type I photoinitiating systems sensitive above 500 nm?”, *Macromolecular Rapid Communications*, Vol. 31, pp. 473–478, 2010.
- [223] Holand, T. V., F. Chang and R. Desousa, “Visible-light photoinitiators and uses thereof”, US Pat. 10324311 B2, 2019.
- [224] Bonardi, A. H., S. Zahouily, C. Dietlin, B. Graff, F. Morlet-Savary, M. Ibrahim-Ouali, D. Gignes, N. Hoffmann, F. Dumur and J. Lalevée, “New 1,8-naphthalimide derivatives as photoinitiators for free-radical polymerization upon visible light”, *Catalysts*, Vol. 9, pp. 637–657, 2019.
- [225] Xiao, P., F. Dumur, J. Zhang, B. Graff, D. Gignes, J. P. Fouassier and J. Lalevée, “New role of aminothiazonaphthalimide derivatives: outstanding photoinitiators for cationic and radical photopolymerizations under visible LEDs”, *RSC Advances*, Vol. 6, pp. 48684–48693, 2016.
- [226] Yang, J., W. Liao, Y. Xiong, X. Wang, Z. Li and H. Tang, “A multifunctionalized macromolecular silicone-naphthalimide visible photoinitiator for free radical polymerization”, *Progress in Organic Coatings*, Vol. 115, pp. 151–158, 2018.

- [227] Yang, J., W. Liao, Y. Xiong, Q. Wu, X. Wang, Z. Li and H. Tang, “Naphthalimide dyes: polymerizable one-component visible light initiators”, *Dyes and Pigments*, Vol. 148, pp. 16–24, 2018.
- [228] Xiao, P., J. Zhang, D. Campolo, F. Dumur, D. Gigmes, J. P. Fouassier and J. Lalevée, “Copper and iron complexes as visible-light-sensitive photoinitiators of polymerization”, *Journal of Polymer Science, Part A: Polymer Chemistry*, Vol. 53, pp. 2673–2684, 2015.
- [229] Xiao, P., F. Dumur, J. Zhang, D. Gigmes, J. P. Fouassier and J. Lalevée, “Copper complexes: the effect of ligands on their photoinitiation efficiencies in radical polymerization reactions under visible light”, *Polymer Chemistry*, Vol. 5, pp. 6350–6357, 2014.
- [230] Lalevée, J., N. Blanchard, M. A. Tehfe, M. Peter, F. Morlet-Savary and J. P. Fouassier, “A novel photopolymerization initiating system based on an iridium complex photocatalyst”, *Macromolecular Rapid Communications*, Vol. 32, pp. 917–920, 2011.
- [231] Lalevée, J., F. Dumur, C. R. Mayer, D. Gigmes, G. Nasr, M. A. Tehfe, S. Telitel, F. Morlet-Savary, B. Graff and J. P. Fouassier, “Photopolymerization of N-vinylcarbazole using visible-light harvesting iridium complexes as photoinitiators”, *Macromolecules*, Vol. 45, pp. 4134–4141, 2012.
- [232] Breloy, L., V. Brezová, J. P. Malval, A. Rios De Anda, J. Bourgon, T. Kurogi, D. J. Mindiola and D. L. Versace, “Well-defined Titanium complex for free-radical and cationic photopolymerizations under visible Light and photoinduction of Ti-based nanoparticles”, *Macromolecules*, Vol. 52, pp. 3716–3729, 2019.
- [233] Shih, H. and C. C. Lin, “Visible-light-mediated thiol-ene hydrogelation using eosin-Y as the only photoinitiator”, *Macromolecular Rapid Communications*, Vol. 34, pp. 269–273, 2013.

- [234] Nan, X., Y. Huang, Q. Fan, J. Shao and Y. Yao, “Efficient visible photoinitiator with high-spectrum stability in an acid medium for free-radical and free-radical-promoted cationic photopolymerization based on erythrosine B derivatives”, *Journal of Applied Polymer Science*, Vol. 133, pp. 43035–43044, 2016.
- [235] Zhang, J., P. Xiao, F. Dumur, C. Guo, W. Hong, Y. Li, D. Gigmes, B. Graff, J. P. Fouassier and J. Lalevée, “Polymeric photoinitiators: a new search toward high performance visible light photoinitiating systems”, *Macromolecular Chemistry and Physics*, Vol. 217, pp. 2145–2153, 2016.
- [236] Xiao, P., J. Zhang, F. Dumur, M. A. Tehfe, F. Morlet-Savary, B. Graff, D. Gigmes, J. P. Fouassier and J. Lalevée, “Visible light sensitive photoinitiating systems: recent progress in cationic and radical photopolymerization reactions under soft conditions”, *Progress in Polymer Science*, Vol. 41, pp. 32–66, 2015.
- [237] Belfield, K. D. and J. V. Crivello, “Photoinitiated polymerization”, ACS symposium series; 847, Washington, DC, 2003.
- [238] Ravve, A., *Light-associated reactions of synthetic polymers*, Springer, United States of America, US, 2006.
- [239] Jo, B., A. Arceneaux and K. Willard, “UV & EB chemistry and technology printer’s guide”, *Radtech*, 2016.
- [240] Butler, G. B., *Cyclopolymerization and cyclocopolymerization*, CRC Press, New York, NY, 1992.
- [241] Warren, S. C. and L. J. Mathias, “Synthesis and polymerization of ethyl  $\alpha$ -chloromethylacrylate and related derivatives”, *Journal of Polymer Science Part A: Polymer Chemistry*, Vol. 28, pp. 1637–1648, 1990.

- [242] Mathias, L. J., R. M. Warren and S. Huang, "Tert-butyl  $\alpha$ -(hydroxymethyl)acrylate and its ether dimer: multifunctional monomers giving polymers with easily cleaved ester groups", *Macromolecules*, Vol. 24, pp. 2036–2042, 1991.
- [243] Foresman, J. B. and A. Frisch, *Exploring chemistry with electronic structure methods, 2nd ed.*, Gaussian Inc., Pittsburg, PA, 2015.
- [244] Frisch, M. J., G.W. Trucks, H. B. Schlegel, G. E. Scuseria, M. A. Robb, J. R. Cheeseman, V. G. Zakrzewski, J. A. Montgomery, J. R. E. Stratmann, J. C. Burant, S. Dapprich, J. M. Millam, A. D. Daniels, K. N. Kudin, M. C. Strain, O. Farkas, J. Tomasi, V. Barone, M. Cossi, R. Cammi, B. Mennucci, C. Pomelli, C. Adamo, S. Clifford, J. Ochterski, G. A. Petersson, P. Y. Ayala, Q. Cui, K. Morokuma, P. Salvador, J. J. Dannenberg, D. K. Malick, A.D. Rabuck, K. Raghavachari, J. B. Foresman, J. Cioslowski, J.V. Ortiz, A. G. Baboul, B. B. Stefanov, G. Liu, A. Liashenko, P. Piskorz, L. Komaromi, R. Gomperts, R. L. Martin, D. J. Fox, T. Keith, M. A. Al-Laham, C. Y. Peng, A. Nanayakkara, M. Challacombe, P. M. W. Gill, B. Johnson, W. Chen, M. W. Wong, J. L. Andres, C. Gonzalez, M. Head-Gordon, E. S. Replogle and J. A. Pople, Gaussian 03, Revision B-2, Gaussian, Inc., Pittsburgh PA, 2003.
- [245] Lalevée, J., N. Blanchard, M. A. Tehfe, M. Peter, F. Morlet-Savary, D. Gigmes and J. P. Fouassier, "Efficient dual radical/cationic photoinitiator under visible light: A new concept", *Polymer Chemistry*, Vol. 2, pp. 1986–1991, 2011.
- [246] Xiao, P., F. Dumur, M. A. Tehfe, B. Graff, J. P. Fouassier, D. Gigmes and J. Lalevée, "Keggin-type polyoxometalate ([PMo<sub>12</sub>O<sub>40</sub>]<sup>3-</sup>) in radical initiating systems: application to radical and cationic photopolymerization reactions", *Macromolecular Chemistry and Physics*, Vol. 214, pp. 1749–1755, 2013.
- [247] Rehm, D. and A. Weller, "Kinetics of fluorescence quenching by electron and H-atom transfer", *Israel Journal of Chemistry*, Vol. 8, pp. 259–271, 1970.

- [248] Anseth, K. S., C. M. Wang and C. N. Bowman, “Kinetic evidence of reaction diffusion during the polymerization of multi(meth)acrylate monomers”, *Macromolecules*, Vol. 27, pp. 650–655, 1994.
- [249] Brandrup, J. and E. H. Immergut, *Polymer handbook*, Wiley-Interscience, New York, US, 1975.
- [250] Al Mousawi, A., F. Dumur, P. Garra, J. Toufaily, T. Hamieh, B. Graff, D. Gigmes, J. P. Fouassier and J. Lalevée, “Carbazole scaffold based photoinitiator/photoredox catalysts: toward new high performance photoinitiating systems and application in LED projector 3D printing resins”, *Macromolecules*, Vol. 50, pp. 2747–2758, 2017.
- [251] Nazir, R., E. Balčiunas, D. Buczyńska, F. Bourquard, D. Kowalska, D. Gray, S. Maćkowski, M. Farsari and D. T. Gryko, “Donor-acceptor type thioxanthenes: synthesis, optical properties, and two-photon induced polymerization”, *Macromolecules*, Vol. 48, pp. 2466–2472, 2015.
- [252] Zhou, H. P., D. M. Li, J. Z. Zhang, Y. M. Zhu, J. Y. Wu, Z. J. Hu, J. X. Yang, G. B. Xu, Y. P. Tian, Y. Xie, X. T. Tao, M. H. Jiang, L. M. Tao, Y. H. Guo and C. K. Wang, “Crystal structures, optical properties and theoretical calculation of novel two-photon polymerization initiators”, *Chemical Physics*, Vol. 322, pp. 459–470, 2006.
- [253] Amirzadeh, G. and W. Schnabel, “On the photoinitiation of free radical polymerization-laser flash photolysis investigations on thioxanthone derivatives”, *Die Makromolekulare Chemie*, Vol. 182, pp. 2821–2835, 1981.
- [254] Polykarpov, A. and A. Tiwari, *Photocured materials*, RSC Publishing, 2015.
- [255] Yilmaz, G., S. Beyazit and Y. Yagci, “Visible light induced free radical promoted cationic polymerization using thioxanthone derivatives”, *Journal of Polymer Science Part A: Polymer Chemistry*, Vol. 49, pp. 1591–1596, 2011.

- [256] Aydin, M., N. Arsu and Y. Yagci, “One-component bimolecular photoinitiating systems, 2”, *Macromolecular Rapid Communications*, Vol. 24, pp. 718–723, 2003.
- [257] Xiao, P., J. Lalevaée, X. Allonas, J. P. Fouassier, C. Ley, M. El-Roz, S. Q. Shi and J. Nie, “Photoinitiation mechanism of free radical photopolymerization in the presence of cyclic acetals and related compounds”, *Journal of Polymer Science, Part A: Polymer Chemistry*, Vol. 48, pp. 5758–5766, 2010.
- [258] Guenin, E., E. Degache, J. Liquier and M. Lecouvey, “Synthesis of 1-hydroxymethylene-1,1-bis(phosphonic acids) from acid anhydrides: Preparation of a new cyclic 1-acyloxymethylene-1,1-bis(phosphonic acid)”, *European Journal of Organic Chemistry*, Vol. 2004, pp. 2983–2987, 2004.
- [259] Egorov, M., S. Aoun, M. Padrines, F. Redini, D. Heymann, J. Lebreton and M. Mathé-Allainmat, “A one-pot synthesis of 1-hydroxy-1,1-bis(phosphonic acid)s starting from the corresponding carboxylic acids”, *European Journal of Organic Chemistry*, Vol. 2011, pp. 7148–7154, 2011.
- [260] Kabatc, J., J. Ortyl and K. Kostrzewska, “New kinetic and mechanistic aspects of photosensitization of iodonium salts in photopolymerization of acrylates”, *RSC Advances*, Vol. 7, pp. 41619–41629, 2017.
- [261] Boyer, C., J. Liu, L. Wong, M. Tippett, V. Bulmus and T. P. Davis, “Stability and utility of pyridyl disulfide functionality in RAFT and conventional radical polymerizations”, *Journal of Polymer Science: Part A: Polymer Chemistry*, Vol. 46, pp. 7207–7224, 2008.
- [262] Yang, J., S. Shi, F. Xu and J. Nie, “Synthesis and photopolymerization kinetics of benzophenone sesamol one-component photoinitiator”, *Photochemical and Photobiological Sciences*, Vol. 12, pp. 323–329, 2013.

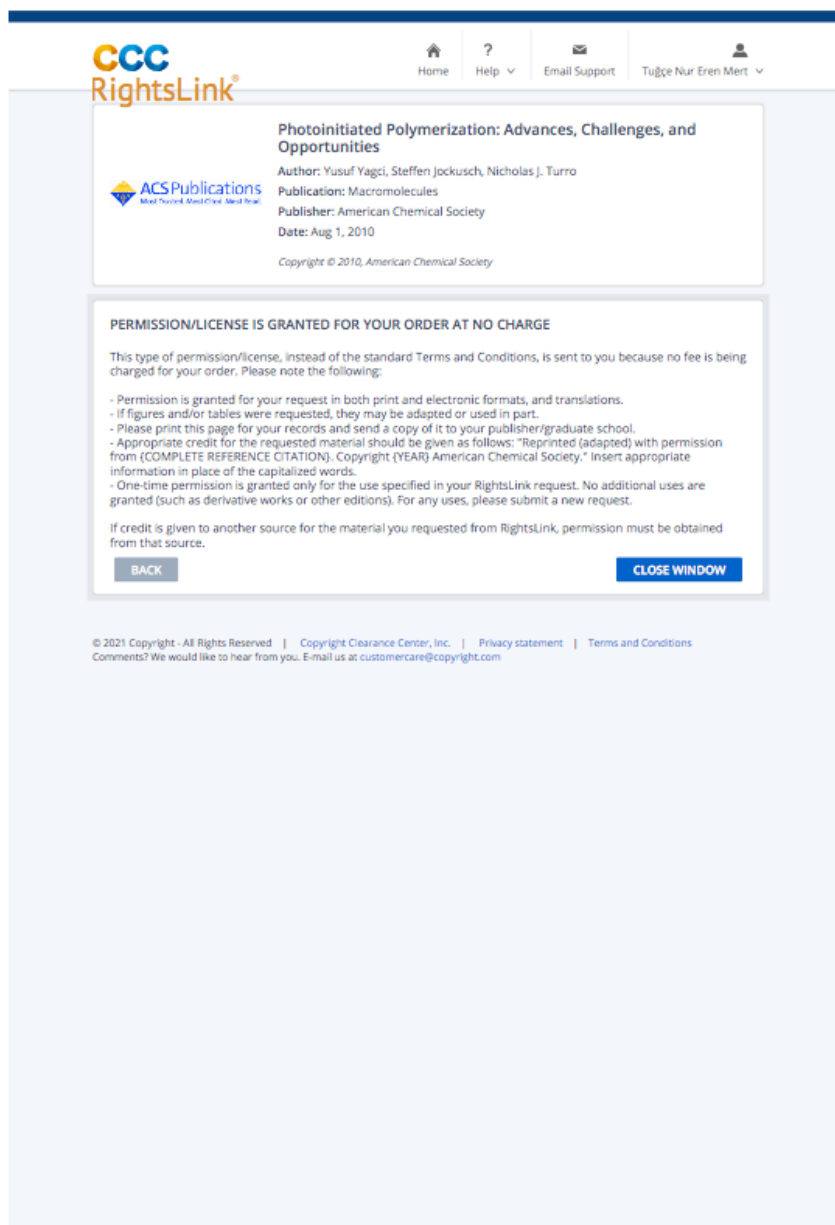
- [263] Yang, J., F. Xu, S. Shi and J. Nie, "Influence of structure of benzodioxole derivatives on photoinitiation efficiency of benzophenone", *Photochemical and Photobiological Sciences*, Vol. 11, pp. 1377–1382, 2012.
- [264] Garofalo, A., A. Parat, C. Bordeianu, C. Ghobril, M. Kueny-Stotz, A. Walter, J. Jouhannaud, S. Begin-Colin and D. Felder-Flesch, "Efficient synthesis of small-sized phosphonated dendrons: potential organic coatings of iron oxide nanoparticles", *New Journal of Chemistry*, Vol. 38, pp. 5226–5239, 2014.
- [265] Degenhardt, C. R. and D. C. Burdsall, "Synthesis of ethenylidenebis(phosphonic acid) and its tetraalkyl esters", *Journal of Organic Chemistry*, Vol. 51, pp. 3488–3490, 1986.
- [266] Xiao, P., F. Dumur, J. Zhang, J. P. Fouassier, D. Gigmes and J. Lalevée, "Copper complexes in radical photoinitiating systems: applications to free radical and cationic polymerization upon visible LEDs", *Macromolecules*, Vol. 47, pp. 3837–3844, 2014.
- [267] Eren, T. N., J. Lalevée and D. Avci, "Bisphosphonic acid-functionalized water-soluble photoinitiators", *Macromolecular Chemistry and Physics*, Vol. 220, pp. 1900268–1900278, 2019.
- [268] Cardoza, J. D., F. M. Rudakov and P. M. Weber, "Electronic spectroscopy and ultrafast energy relaxation pathways in the lowest rydberg states of trimethylamine", *Journal of Physical Chemistry A*, Vol. 112, pp. 10736–10743, 2008.
- [269] Minitti, M. P. and P. M. Weber, "Time-resolved conformational dynamics in hydrocarbon chains", *Physical Review Letters*, Vol. 98, pp. 253004–253008, 2007.
- [270] Liu, S., D. Brunel, K. Sun, Y. Xu, F. Morlet-Savary, B. Graff, P. Xiao, F. Dumur and J. Lalevée, "A monocomponent bifunctional benzophenone-carbazole type II photoinitiator for LED photoinitiating systems", *Polymer Chemistry*, Vol. 11, pp. 3551–3556, 2020.

- [271] Korkut, S. E., G. Temel, D. K. Balta, N. Arsu and M. K. Şener, “Type II photoinitiator substituted zinc phthalocyanine: synthesis, photophysical and photopolymerization studies”, *Journal of Luminescence*, Vol. 136, pp. 389–394, 2013.
- [272] Catalina, F., C. Peinado, E. L. Madruga, R. Sastre, J. L. Mateo and N. S. Allen, “Radical copolymerization of 2-acryloyl thioxanthone with methyl methacrylate”, *Journal of Polymer Science Part A: Polymer Chemistry*, Vol. 28, pp. 967–972, 1990.
- [273] Sun, M., C. Y. Hong and C. Y. Pan, “A unique aliphatic tertiary amine chromophore: fluorescence, polymer structure, and application in cell imaging”, *Journal of the American Chemical Society*, Vol. 134, pp. 20581–20584, 2012.
- [274] Dickens, S. H., J. W. Stansbury, K. M. Choi and C. J. E. Floyd, “Photopolymerization kinetics of methacrylate dental resins”, *Macromolecules*, Vol. 36, pp. 6043–6053, 2003.
- [275] Cruise, G. M., O. D. Hegre, F. V. Lamberti, S. R. Hager, R. Hill, D. S. Scharp and J. A. Hubbell, “In vitro and in vivo performance of porcine islets encapsulated in interfacially photopolymerized poly(ethylene glycol) diacrylate membranes”, *Cell Transplantation*, Vol. 8, pp. 293–306, 1999.
- [276] Lu, S. and K. S. Anseth, “Photopolymerization of multilaminated poly(HEMA) hydrogels for controlled release”, *Journal of Controlled Release*, Vol. 57, pp. 291–300, 1999.
- [277] Ifkovits, J. L. and J. A. Burdick, “Review: photopolymerizable and degradable biomaterials for tissue engineering applications”, *Tissue Engineering*, Vol. 13, pp. 2369–2385, 2007.
- [278] Williams, C. G., A. N. Malik, T. K. Kim, P. N. Manson and J. H. Elisseeff, “Variable cytocompatibility of six cell lines with photoinitiators used for polymerizing hydrogels and cell encapsulation”, *Biomaterials*, Vol. 26, pp. 1211–1218, 2005.

- [279] Tomal, W. and J. Ortyl, “Water-soluble photoinitiators in biomedical applications”, *Polymers*, Vol. 12, pp. 1073–1103, 2020.
- [280] Román, F., P. Colomer, Y. Calventus and J. M. Hutchinson, “Study of hyperbranched poly(ethyleneimine) polymers of different molecular weight and their interaction with epoxy resin”, *Materials*, Vol. 11, pp. 410–436, 2018.
- [281] Cui, X., C. Qiao, S. Wang, Y. Ding, C. Hao and J. Li, “Synthesis, surface properties, and antibacterial activity of polysiloxane quaternary ammonium salts containing epoxy group”, *Colloid and Polymer Science*, Vol. 293, pp. 1971–1981, 2015.
- [282] Zhu, J., “Bioactive modification of poly(ethylene glycol) hydrogels for tissue engineering”, *Biomaterials*, Vol. 31, pp. 4639–4656, 2010.
- [283] Montheard, J. P., M. Chatzopoulos and D. Chappard, “2-Hydroxyethyl methacrylate (HEMA): chemical properties and applications in biomedical fields”, *Journal of Macromolecular Science*, pp. 1–34, 1992.
- [284] Casadio, Y. S., D. H. Brown, T. V. Chirila, H. B. Kraatz and M. V. Baker, “Biodegradation of poly(2-hydroxyethyl methacrylate) (PHEMA) and poly{(2-hydroxyethyl methacrylate)-co-[poly(ethylene glycol) methyl ether methacrylate]} hydrogels containing peptide-based cross-linking agents”, *Biomacromolecules*, Vol. 11, pp. 2949–2959, 2010.
- [285] Kalita, P., C. D. Pegu, P. Dutta and P. K. Baruah, “Room temperature solvent free aza-Michael reactions over nano-cage mesoporous materials”, *Journal of Molecular Catalysis A: Chemical*, Vol. 394, pp. 145–150, 2014.
- [286] Wu, D., Y. Liu, C. He, T. Chung and S. Goh, “Effects of chemistries of trifunctional amines on mechanisms of Michael addition polymerizations with diacrylates”, *Macromolecules*, Vol. 37, pp. 6763–6770, 2004.

- [287] Bosica, G., J. Spiteri and C. Borg, “Aza-Michael reaction: Selective mono- versus bis-addition under environmentally-friendly conditions”, *Tetrahedron*, Vol. 70, pp. 2449–2454, 2014.
- [288] Baralle, A., P. Garra, F. Morlet-Savary, C. Dietlin, J. P. Fouassier and J. Lalevée, “Polymeric iodonium salts to trigger free radical photopolymerization”, *Macromolecular Rapid Communications*, Vol. 41, pp. 1900644–1900650, 2020.
- [289] Garra, P., B. Graff, F. Morlet-Savary, C. Dietlin, J. M. Becht, J. P. Fouassier and J. Lalevée, “Charge transfer complexes as pan-scaled photoinitiating systems: From 50  $\mu\text{m}$  3D printed polymers at 405 nm to extremely deep photopolymerization (31 cm)”, *Macromolecules*, Vol. 51, pp. 57–70, 2018.
- [290] Segurola, J., N. Allen, M. Edge, A. Parrondo and I. Roberts, “Photochemistry and photoinduced chemical crosslinking activity of several type II commercial photoinitiators in acrylated prepolymers”, *Journal of Photochemistry and Photobiology A: Chemistry*, Vol. 122, pp. 115–125, 1999.
- [291] Wallin, R. F. and E. F. Arscott, “A practical guide to ISO 10993-5: cytotoxicity”, *Medical Device and Diagnostic Industry*, Vol. 20, p. 10993, 1998.

## APPENDIX A: COPY RIGHT LICENCES



The screenshot displays the CCC RightsLink interface. At the top, there is a navigation bar with icons for Home, Help, Email Support, and a user profile for Tugçe Nur Eren Mert. The main content area features the ACS Publications logo and the title "Photoinitiated Polymerization: Advances, Challenges, and Opportunities". Below the title, it lists the author (Yusuf Yagci, Steffen Jockusch, Nicholas J. Turro), publication (Macromolecules), publisher (American Chemical Society), and date (Aug 1, 2010). A copyright notice for 2010 American Chemical Society is also present. A prominent message states "PERMISSION/LICENSE IS GRANTED FOR YOUR ORDER AT NO CHARGE" and provides detailed terms of use, including a list of conditions and a note about credit attribution. At the bottom of the message are "BACK" and "CLOSE WINDOW" buttons. The footer contains copyright information for 2021 and contact details for Copyright Clearance Center, Inc.

**CCC RightsLink®**

Home ? Email Support Tugçe Nur Eren Mert

**ACS Publications**  
More Journals More Books More News

**Photoinitiated Polymerization: Advances, Challenges, and Opportunities**

Author: Yusuf Yagci, Steffen Jockusch, Nicholas J. Turro  
Publication: Macromolecules  
Publisher: American Chemical Society  
Date: Aug 1, 2010  
Copyright © 2010, American Chemical Society

**PERMISSION/LICENSE IS GRANTED FOR YOUR ORDER AT NO CHARGE**

This type of permission/license, instead of the standard Terms and Conditions, is sent to you because no fee is being charged for your order. Please note the following:

- Permission is granted for your request in both print and electronic formats, and translations.
- If figures and/or tables were requested, they may be adapted or used in part.
- Please print this page for your records and send a copy of it to your publisher/graduate school.
- Appropriate credit for the requested material should be given as follows: "Reprinted (adapted) with permission from {COMPLETE REFERENCE CITATION}. Copyright {YEAR} American Chemical Society." Insert appropriate information in place of the capitalized words.
- One-time permission is granted only for the use specified in your RightsLink request. No additional uses are granted (such as derivative works or other editions). For any uses, please submit a new request.

If credit is given to another source for the material you requested from RightsLink, permission must be obtained from that source.

[BACK](#) [CLOSE WINDOW](#)

© 2021 Copyright - All Rights Reserved | Copyright Clearance Center, Inc. | Privacy statement | Terms and Conditions  
Comments? We would like to hear from you. E-mail us at [customer@copyright.com](mailto:customer@copyright.com)

Figure A.1. Permission from [3] American Chemical Society, Copyright (2010).

CCC  
RightsLink®

Home ? Help Email Support Tuğçe Nur Eren Mert

**State-of-the-Art and Future Challenges of UV Curable Polymer-Based Smart Materials for Printing Technologies**

Author: Senentxu Lanceros-Mendez, José Luis Vilas-Vilela, Ikerne Etxebarria, et al  
 Publication: Advanced Materials Technologies  
 Publisher: John Wiley and Sons  
 Date: Jan 11, 2019  
 © 2019 WILEY-VCH Verlag GmbH & Co. KGaA, Weinheim

**Order Completed**

Thank you for your order.

This Agreement between Mrs. Tuğçe Nur Eren Mert ("You") and John Wiley and Sons ("John Wiley and Sons") consists of your license details and the terms and conditions provided by John Wiley and Sons and Copyright Clearance Center.

Your confirmation email will contain your order number for future reference.

License Number 5134350792756 [Printable Details](#)

License date Aug 22, 2021

Licensed Content  Order Details

Licensed Content Publisher	John Wiley and Sons	Type of use	Dissertation/Thesis
Licensed Content Publication	Advanced Materials Technologies	Requestor type	University/Academic
Licensed Content Title	State-of-the-Art and Future Challenges of UV Curable Polymer-Based Smart Materials for Printing Technologies	Format	Print and electronic
Licensed Content Author	Senentxu Lanceros-Mendez, José Luis Vilas-Vilela, Ikerne Etxebarria, et al	Portion	Figure/table
Licensed Content Date	Jan 11, 2019	Number of figures/tables	1
Licensed Content Volume	4	Will you be translating?	No
Licensed Content Issue	3		
Licensed Content Pages	16		

About Your Work  Additional Data

Title	Water Soluble, Low Migration and Visible Light Photoinitiators for Greener Photopolymerization	Portions	Figure 2
Institution name	Bogazici University		
Expected presentation date	Sep 2021		

Figure A.2. Permission from [7] John Wiley and Sons, Copyright (2019).

[Home](#)   [?](#) Help   [Email Support](#)   [Tugçe Nur Eren Mert](#)



**ELSEVIER**

Chapter: Photoinitiators and Photopolymerization  
 Book: Encyclopedia of Materials: Science and Technology  
 Author: R. Schwalm  
 Publisher: Elsevier  
 Date: 2001

Copyright © 2001 Elsevier Ltd. All rights reserved.

---

### Order Completed

Thank you for your order.

This Agreement between Mrs. Tuğçe Nur Eren Mert ("You") and Elsevier ("Elsevier") consists of your license details and the terms and conditions provided by Elsevier and Copyright Clearance Center.

Your confirmation email will contain your order number for future reference.

License Number	5134340988542	<a href="#">Printable Details</a>
License date	Aug 22, 2021	

Licensed Content	Order Details
Licensed Content Publisher: Elsevier	Type of Use: reuse in a thesis/dissertation
Licensed Content Publication: Elsevier Books	Portion: figures/tables/illustrations
Licensed Content Title: Encyclopedia of Materials: Science and Technology	Number of figures/tables/illustrations: 1
Licensed Content Author: R. Schwalm	Format: both print and electronic
Licensed Content Date: Jan 1, 2001	Are you the author of this Elsevier chapter?: No
Licensed Content Pages: 6	Will you be translating?: No

About Your Work	Additional Data
Title: Water Soluble, Low Migration and Visible Light Photoinitiators for Greener Photopolymerization	Portions: Figure 2
Institution name: Bogazici University	
Expected presentation date: Sep 2021	

Requestor Location	Tax Details
Requestor Location: Mrs. Tuğçe Nur Eren Mert Etiler district Uçaksavar Site Fuzeciler street Krizantem apartment No:6 D:9 Istanbul, Turkey (TUR) 34337 Turkey Attn: Mrs. Tuğçe Nur Eren Mert	Publisher Tax ID: GB 494 6272 12

\$ Price	
Total	0.00 USD

---

**Total: 0.00 USD**

Figure A.3. Permission from [5] Elsevier, Copyright (2001).

21.08.2021 Rightslink® by Copyright Clearance Center

CCC RightsLink®

Home Help Email Support Tuğçe Nur Eren Mert

**WILEY**

Book: Photoinitiators for Polymer Synthesis: Scope, Reactivity, and Efficiency  
 Author: Jacques Lalevée Jean-Pierre Fouassier  
 Publisher: John Wiley and Sons  
 Date: Aug 1, 2012  
 Copyright © 2012, John Wiley and Sons

**Order Completed**

Thank you for your order.

This Agreement between Mrs. Tuğçe Nur Eren Mert ("You") and John Wiley and Sons ("John Wiley and Sons") consists of your license details and the terms and conditions provided by John Wiley and Sons and Copyright Clearance Center.

Your confirmation email will contain your order number for future reference.

License Number 5133760478480 [Printable Details](#)

License date Aug 21, 2021

Licensed Content		Order Details	
Licensed Content Publisher	John Wiley and Sons	Type of use	Dissertation/Thesis University/Academic
Licensed Content Publication	Wiley Books	Requestor type	Print and electronic
Licensed Content Title	Photoinitiators for Polymer Synthesis: Scope, Reactivity, and Efficiency	Format	Figure/table
Licensed Content Author	Jacques Lalevée Jean-Pierre Fouassier	Portion	3
Licensed Content Date	Aug 1, 2012	Number of figures/tables	No
Licensed Content Pages	1	Will you be translating?	

About Your Work		Additional Data	
Title	Water Soluble, Low Migration and Visible Light Photoinitiators for Greener Photopolymerization	Portions	Scheme 8.2, Image 1-5 on page 199, Image 45 on page 224
Institution name	Bogazici University		
Expected presentation date	Sep 2021		

Requestor Location		Tax Details	
Requestor Location	Mrs. Tuğçe Nur Eren Mert Etiler district Uçaksavar Site Fuzeçiler street Krizantem apartment No:6 D:9 Istanbul, Turkey (TUR) 34337 Turkey Attn: Mrs. Tuğçe Nur Eren Mert	Publisher Tax ID	EU826007151

**Price**

Total	0.00 USD
-------	----------

<https://s100.copyright.com/AppDispatchServlet> 1/2

Figure A.4. Permission from [1] John Wiley and Sons, Copyright (2012).

CCC  
RightsLink®

Home ? Email Support Tuğçe Nur Eren Mert

WILEY

Book: Encyclopedia of Radicals in Chemistry, Biology and Materials  
Chapter: Radical Polymerization in Industry  
Author: Peter Nesvadba  
Publisher: John Wiley and Sons  
Date: Mar 15, 2012  
Copyright © 2012 John Wiley & Sons, Ltd. All rights reserved.

### Order Completed

Thank you for your order.

This Agreement between Mrs. Tuğçe Nur Eren Mert ("You") and John Wiley and Sons ("John Wiley and Sons") consists of your license details and the terms and conditions provided by John Wiley and Sons and Copyright Clearance Center.

Your confirmation email will contain your order number for future reference.

License Number 5134351015190 [Printable Details](#)

License date Aug 22, 2021

Licensed Content		Order Details	
Licensed Content Publisher	John Wiley and Sons	Type of use	Dissertation/Thesis University/Academic
Licensed Content Publication	Wiley Books	Requestor type	Print and electronic
Licensed Content Title	Radical Polymerization in Industry	Format	Figure/table
Licensed Content Author	Peter Nesvadba	Portion	1
Licensed Content Date	Mar 15, 2012	Number of figures/tables	1
Licensed Content Pages	36	Will you be translating?	No

About Your Work		Additional Data	
Title	Water Soluble, Low Migration and Visible Light Photoinitiators for Greener Photopolymerization	Portions	Scheme 12
Institution name	Bogazici University		
Expected presentation date	Sep 2021		

Requestor Location		Tax Details	
Requestor Location	Mrs. Tuğçe Nur Eren Mert Etiler district Uçaksavar Site Fuzeçiler street Krizantem apartment No:5 D:9 Istanbul, Turkey (TUR) 34337 Turkey Attn: Mrs. Tuğçe Nur Eren Mert	Publisher Tax ID	EU826007151

\$ Price

Total 0.00 USD

Figure A.5. Permission from [10] John Wiley and Sons, Copyright (2012).

CCC  
RightsLink®

Home ? Help Email Support Tugçe Nur Eren Mert

**High-Performance and Low Migration One-Component Thioxanthone Visible Light Photoinitiators**  
 Author: Qingqing Wu, Kuangyi Tang, Ying Xiong, et al  
 Publication: Macromolecular Chemistry and Physics  
 Publisher: John Wiley and Sons  
 Date: Jan 18, 2017  
 © 2017 WILEY-VCH Verlag GmbH & Co. KGaA, Weinheim

**Order Completed**

Thank you for your order.

This Agreement between Mrs. Tugçe Nur Eren Mert ("You") and John Wiley and Sons ("John Wiley and Sons") consists of your license details and the terms and conditions provided by John Wiley and Sons and Copyright Clearance Center.

Your confirmation email will contain your order number for future reference.

License Number 5134341139886 [Printable Details](#)

License date Aug 22, 2021

Licensed Content		Order Details	
Licensed Content Publisher	John Wiley and Sons	Type of use	Dissertation/Thesis
Licensed Content Publication	Macromolecular Chemistry and Physics	Requestor type	University/Academic
Licensed Content Title	High-Performance and Low Migration One-Component Thioxanthone Visible Light Photoinitiators	Format	Print and electronic
Licensed Content Author	Qingqing Wu, Kuangyi Tang, Ying Xiong, et al	Portion	Figure/table
Licensed Content Date	Jan 18, 2017	Number of figures/tables	1
Licensed Content Volume	218	Will you be translating?	No
Licensed Content Issue	6		
Licensed Content Pages	8		

About Your Work		Additional Data	
Title	Water Soluble, Low Migration and Visible Light Photoinitiators for Greener Photopolymerization	Portions	Figure 1
Institution name	Bogazici University		
Expected presentation date	Sep 2021		

Figure A.6. Permission from [34] John Wiley and Sons, Copyright (2017).

CCC  
RightsLink®

Home ? Email Support Tuğçe Nur Eren Mert

**Low migration type I photoinitiators for biocompatible thiol-ene formulations**

**Author:** Andreas Oesterreicher, Meinhart Roth, Daniel Hennen, Florian H. Mostegel, Matthias Edler, Stefan Kappau, Thomas Griesser

**Publication:** European Polymer Journal

**Publisher:** Elsevier

**Date:** March 2017

© 2016 Published by Elsevier Ltd.

**Order Completed**

Thank you for your order.

This Agreement between Mrs. Tuğçe Nur Eren Mert ("You") and Elsevier ("Elsevier") consists of your license details and the terms and conditions provided by Elsevier and Copyright Clearance Center.

Your confirmation email will contain your order number for future reference.

**License Number** 5134341351504 [Printable Details](#)

**License date** Aug 22, 2021

Licensed Content		Order Details	
<b>Licensed Content Publisher</b>	Elsevier	<b>Type of Use</b>	reuse in a thesis/dissertation figures/tables/illustrations
<b>Licensed Content Publication</b>	European Polymer Journal	<b>Portion</b>	figures/tables/illustrations
<b>Licensed Content Title</b>	Low migration type I photoinitiators for biocompatible thiol-ene formulations	<b>Number of figures/tables/illustrations</b>	1
<b>Licensed Content Author</b>	Andreas Oesterreicher, Meinhart Roth, Daniel Hennen, Florian H. Mostegel, Matthias Edler, Stefan Kappau, Thomas Griesser	<b>Format</b>	both print and electronic
<b>Licensed Content Date</b>	Mar 1, 2017	<b>Are you the author of this Elsevier article?</b>	No
<b>Licensed Content Volume</b>	88	<b>Will you be translating?</b>	No
<b>Licensed Content Issue</b>	n/a		
<b>Licensed Content Pages</b>	10		

About Your Work		Additional Data	
<b>Title</b>	Water Soluble, Low Migration and Visible Light Photoinitiators for Greener Photopolymerization	<b>Portions</b>	Graphical Abstract
<b>Institution name</b>	Bogazici University		
<b>Expected presentation date</b>	Sep 2021		

Figure A.7. Permission from [22], Elsevier, Copyright (2016).

CCC  
RightsLink®

Home ? Email Support Tuğçe Nur Eren Mert

**Progress in the development of polymeric and multifunctional photoinitiators**  
 Author: Junyi Zhou,Xavier Allonas,Ahmad Ibrahim,Xiaoxuan Liu  
 Publication: Progress in Polymer Science  
 Publisher: Elsevier  
 Date: December 2019  
 © 2019 Elsevier B.V. All rights reserved.

**Order Completed**

Thank you for your order.

This Agreement between Mrs. Tuğçe Nur Eren Mert ("You") and Elsevier ("Elsevier") consists of your license details and the terms and conditions provided by Elsevier and Copyright Clearance Center.

Your confirmation email will contain your order number for future reference.

License Number 5134350030633 [Printable Details](#)

License date Aug 22, 2021

Licensed Content		Order Details	
Licensed Content Publisher	Elsevier	Type of Use	reuse in a thesis/dissertation
Licensed Content Publication	Progress in Polymer Science	Portion	figures/tables/illustrations
Licensed Content Title	Progress in the development of polymeric and multifunctional photoinitiators	Number of figures/tables/illustrations	1
Licensed Content Author	Junyi Zhou,Xavier Allonas,Ahmad Ibrahim,Xiaoxuan Liu	Format	both print and electronic
Licensed Content Date	Dec 1, 2019	Are you the author of this Elsevier article?	No
Licensed Content Volume	99	Will you be translating?	No
Licensed Content Issue	n/a		
Licensed Content Pages	1		

About Your Work		Additional Data	
Title	Water Soluble, Low Migration and Visible Light Photoinitiators for Greener Photopolymerization	Portions	Figure 1
Institution name	Bogazici University		
Expected presentation date	Sep 2021		

Figure A.8. Permission from [102] Elsevier, Copyright (2019).

**CCC RightsLink®** Home Help Email Support Tugçe Nur Eren Mert

**Study of Novel PU-Type Polymeric Photoinitiators Comprising of Side-Chain Benzophenone and Cointiator Amine: Effect of Macromolecular Structure on Photopolymerization**

Author: Jie Yin, Xuesong Jiang, Hongyu Wang, et al  
 Publication: Macromolecular Chemistry and Physics  
 Publisher: John Wiley and Sons  
 Date: Feb 6, 2007  
 Copyright © 2007 WILEY-VCH Verlag GmbH & Co. KGaA, Weinheim

**Order Completed**

Thank you for your order.

This Agreement between Mrs. Tugçe Nur Eren Mert ("You") and John Wiley and Sons ("John Wiley and Sons") consists of your license details and the terms and conditions provided by John Wiley and Sons and Copyright Clearance Center.

Your confirmation email will contain your order number for future reference.

License Number: 5134350112297 [Printable Details](#)

License date: Aug 22, 2021

Licensed Content		Order Details	
Licensed Content Publisher	John Wiley and Sons	Type of use	Dissertation/Thesis
Licensed Content Publication	Macromolecular Chemistry and Physics	Requestor type	University/Academic
Licensed Content Title	Study of Novel PU-Type Polymeric Photoinitiators Comprising of Side-Chain Benzophenone and Cointiator Amine: Effect of Macromolecular Structure on Photopolymerization	Format	Print and electronic
Licensed Content Author	Jie Yin, Xuesong Jiang, Hongyu Wang, et al	Portion	Figure/table
Licensed Content Date	Feb 6, 2007	Number of figures/tables	1
Licensed Content Volume	208	Will you be translating?	No
Licensed Content Issue	3		
Licensed Content Pages	8		
About Your Work		Additional Data	
Title	Water Soluble, Low Migration and Visible Light Photoinitiators for Greener Photopolymerization	Portions	Graphical Abstract Figure
Institution name	Bogazici University		
Expected presentation date	Sep 2021		

Figure A.9. Permission from [89] John Wiley and Sons, Copyright (2007).

Order Number: 1142277

Order Date: 22 Aug 2021

### Payment Information

Tuğçe Nur Eren Mert  
nureren90@gmail.com  
Payment method: Invoice

**Billing Address:**  
Mrs. Tuğçe Nur Eren Mert  
Etiler district Uçaksavar Site  
Fuzeciler street Krizantem  
apartment  
No:6 D:9  
Istanbul, Turkey (TUR) 343  
37  
Turkey  
  
+90 (538)5560425  
nureren90@gmail.com

**Customer Location:**  
Mrs. Tuğçe Nur Eren Mert  
Etiler district Uçaksavar Site  
Fuzeciler street Krizantem  
apartment  
No:6 D:9  
Istanbul, Turkey (TUR) 343  
37  
Turkey

### Order Details

#### 1. Polymer chemistry

Article: Supramolecular Polymeric Photoinitiator with Enhanced Dispersion in Photo-curing Systems

**Billing Status:**  
Open

<b>Order License ID</b>	1142277-1	<b>Type of use</b>	Republish in a thesis/dissertation
<b>Order detail status</b>	Completed	<b>Publisher</b>	Royal Society of Chemistry
<b>ISSN</b>	1759-9962	<b>Portion</b>	Chart/graph/table/figure
			<b>0.00 USD</b> Republication Permission

### LICENSED CONTENT

<b>Publication Title</b>	Polymer chemistry	<b>Publication Type</b>	e-Journal
<b>Article Title</b>	Supramolecular Polymeric Photoinitiator with Enhanced Dispersion in Photo-curing Systems	<b>Start Page</b>	1885
		<b>End Page</b>	1893
		<b>Issue</b>	11
		<b>Volume</b>	11
<b>Author/Editor</b>	Royal Society of Chemistry (Great Britain)	<b>URL</b>	<a href="http://www.rsc.org/Publishing/Journals/PY/Index.asp">http://www.rsc.org/Publishing/Journals/PY/Index.asp</a>
<b>Date</b>	01/01/2010		
<b>Language</b>	English		
<b>Country</b>	United Kingdom of Great Britain and Northern Ireland		
<b>Rightsholder</b>	Royal Society of Chemistry		

Figure A.10. Permission from [114] Royal Society of Chemistry, Copyright (2020).

CCC  
RightsLink®

Home ? Help Email Support Tugçe Nur Eren Mert

**polymer**  
Amphipathic hyperbranched polymeric thioxanthone photoinitiators (AHPTXs): Synthesis, characterization and photoinitiated polymerization  
Author: Yanna Wen,Xuesong Jiang,Rui Liu,Jie Yin  
Publication: Polymer  
Publisher: Elsevier  
Date: 31 July 2009  
Copyright © 2009 Elsevier Ltd. All rights reserved.

**Order Completed**

Thank you for your order.

This Agreement between Mrs. Tugçe Nur Eren Mert ("You") and Elsevier ("Elsevier") consists of your license details and the terms and conditions provided by Elsevier and Copyright Clearance Center.

Your confirmation email will contain your order number for future reference.

License Number 5134350384241 [Printable Details](#)

License date Aug 22, 2021

Licensed Content		Order Details	
Licensed Content Publisher	Elsevier	Type of Use	reuse in a thesis/dissertation figures/tables/illustrations
Licensed Content Publication	Polymer	Portion	figures/tables/illustrations
Licensed Content Title	Amphipathic hyperbranched polymeric thioxanthone photoinitiators (AHPTXs): Synthesis, characterization and photoinitiated polymerization	Number of figures/tables/illustrations	1
Licensed Content Author	Yanna Wen,Xuesong Jiang,Rui Liu,Jie Yin	Format	both print and electronic
Licensed Content Date	Jul 31, 2009	Are you the author of this Elsevier article?	No
Licensed Content Volume	50	Will you be translating?	No
Licensed Content Issue	16		
Licensed Content Pages	7		

About Your Work		Additional Data	
Title	Water Soluble, Low Migration and Visible Light Photoinitiators for Greener Photopolymerization	Portions	Scheme 1
Institution name	Bogazici University		
Expected presentation date	Sep 2021		

Figure A.11. Permission from [116] Elsevier, Copyright (2009).

CCC  
RightsLink®

Home ? Help Email Support Tugçe Nur Eren Mert

 **Highly Water-Soluble Alpha-Hydroxyalkylphenone Based Photoinitiator for Low-Migration Applications**  
 Author: Thomas Griesser, Eugen Maier, Matthias Edler, et al  
 Publication: Macromolecular Chemistry and Physics  
 Publisher: John Wiley and Sons  
 Date: Apr 18, 2017  
 © 2017 WILEY-VCH Verlag GmbH & Co. KGaA, Weinheim

**Order Completed**

Thank you for your order.

This Agreement between Mrs. Tugçe Nur Eren Mert ("You") and John Wiley and Sons ("John Wiley and Sons") consists of your license details and the terms and conditions provided by John Wiley and Sons and Copyright Clearance Center.

Your confirmation email will contain your order number for future reference.

License Number 5134350481934 [Printable Details](#)

License date Aug 22, 2021

Licensed Content		Order Details	
Licensed Content Publisher	John Wiley and Sons	Type of use	Dissertation/Thesis
Licensed Content Publication	Macromolecular Chemistry and Physics	Requestor type	University/Academic
Licensed Content Title	Highly Water-Soluble Alpha-Hydroxyalkylphenone Based Photoinitiator for Low-Migration Applications	Format	Print and electronic
Licensed Content Author	Thomas Griesser, Eugen Maier, Matthias Edler, et al	Portion	Figure/table
Licensed Content Date	Apr 18, 2017	Number of figures/tables	1
Licensed Content Volume	218	Will you be translating?	No
Licensed Content Issue	14		
Licensed Content Pages	6		

About Your Work		Additional Data	
Title	Water Soluble, Low Migration and Visible Light Photoinitiators for Greener Photopolymerization	Portions	Graphical Abstract Figure
Institution name	Bogazici University		
Expected presentation date	Sep 2021		

Figure A.12. Permission from [148] John Wiley and Sons, Copyright (2017).

CCC  
RightsLink®

Home ? Help Email Support Tuğçe Nur Eren Mert

**Highly efficient water-soluble visible light photoinitiators**  
 Author: Stephan Benedikt, Jieping Wang, Marica Markovic, et al  
 Publication: Journal of Polymer Science Part A: Polymer Chemistry  
 Publisher: John Wiley and Sons  
 Date: Oct 5, 2015  
 © 2015 Wiley Periodicals, Inc.

**Order Completed**

Thank you for your order.

This Agreement between Mrs. Tuğçe Nur Eren Mert ("You") and John Wiley and Sons ("John Wiley and Sons") consists of your license details and the terms and conditions provided by John Wiley and Sons and Copyright Clearance Center.

Your confirmation email will contain your order number for future reference.

License Number 5134350546646 [Printable Details](#)

License date Aug 22, 2021

Licensed Content		Order Details	
Licensed Content Publisher	John Wiley and Sons	Type of use	Dissertation/Thesis
Licensed Content Publication	Journal of Polymer Science Part A: Polymer Chemistry	Requestor type	University/Academic
Licensed Content Title	Highly efficient water-soluble visible light photoinitiators	Format	Print and electronic
Licensed Content Author	Stephan Benedikt, Jieping Wang, Marica Markovic, et al	Portion	Figure/table
Licensed Content Date	Oct 5, 2015	Number of figures/tables	1
Licensed Content Volume	54	Will you be translating?	No
Licensed Content Issue	4		
Licensed Content Pages	8		

About Your Work		Additional Data	
Title	Water Soluble, Low Migration and Visible Light Photoinitiators for Greener Photopolymerization	Portions	Figure 1
Institution name	Bogaziçi University		
Expected presentation date	Sep 2021		

Figure A.13. Permission from [149] John Wiley and Sons, Copyright (2015).

CCC  
RightsLink®

Home ? Help Email Support Tugçe Nur Eren Mert

**WILEY**

**A Charge-Transfer Complex of Thioxanthonephenacyl Sulfonium Salt as a Visible-Light Photoinitiator for Free Radical and Cationic Polymerizations**

Author: Yusuf Yagci, Johannes Kreutzer, Kerem Kaya  
 Publication: ChemPhotoChem  
 Publisher: John Wiley and Sons  
 Date: Jan 4, 2019  
 © 2019 Wiley-VCH Verlag GmbH & Co. KGaA, Weinheim

**Order Completed**

Thank you for your order.

This Agreement between Mrs. Tugçe Nur Eren Mert ("You") and John Wiley and Sons ("John Wiley and Sons") consists of your license details and the terms and conditions provided by John Wiley and Sons and Copyright Clearance Center.

Your confirmation email will contain your order number for future reference.

License Number 5134350622147 [Printable Details](#)

License date Aug 22, 2021

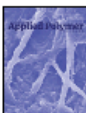
Licensed Content		Order Details	
Licensed Content Publisher	John Wiley and Sons	Type of use	Dissertation/Thesis
Licensed Content Publication	ChemPhotoChem	Requestor type	University/Academic
Licensed Content Title	A Charge-Transfer Complex of Thioxanthonephenacyl Sulfonium Salt as a Visible-Light Photoinitiator for Free Radical and Cationic Polymerizations	Format	Print and electronic
Licensed Content Author	Yusuf Yagci, Johannes Kreutzer, Kerem Kaya	Portion	Figure/table
Licensed Content Date	Jan 4, 2019	Number of figures/tables	1
Licensed Content Volume	3	Will you be translating?	No
Licensed Content Issue	11		
Licensed Content Pages	6		

About Your Work		Additional Data	
Title	Water Soluble, Low Migration and Visible Light Photoinitiators for Greener Photopolymerization	Portions	Graphical Abstract Figure
Institution name	Bogazici University		
Expected presentation date	Sep 2021		

Figure A.14. Permission from [211] John Wiley and Sons, Copyright (2019).

CCC  
RightsLink®

Home ? Email Support Tugçe Nur Eren Mert

 **Tetraacylgermanes as highly efficient photoinitiators for visible light cured dimethacrylate resins and dental composites**  
 Author: Harald Stueger, Georg Gescheidt, Michael Haas, et al  
 Publication: Journal of Applied Polymer Science  
 Publisher: John Wiley and Sons  
 Date: Dec 18, 2017  
 © 2017 Wiley Periodicals, Inc.

**Order Completed**

Thank you for your order.

This Agreement between Mrs. Tugçe Nur Eren Mert ("You") and John Wiley and Sons ("John Wiley and Sons") consists of your license details and the terms and conditions provided by John Wiley and Sons and Copyright Clearance Center.

Your confirmation email will contain your order number for future reference.

License Number 5134350720312 [Printable Details](#)

License date Aug 22, 2021

**Licensed Content**  **Order Details**

Licensed Content Publisher	John Wiley and Sons	Type of use	Dissertation/Thesis
Licensed Content Publication	Journal of Applied Polymer Science	Requestor type	University/Academic
Licensed Content Title	Tetraacylgermanes as highly efficient photoinitiators for visible light cured dimethacrylate resins and dental composites	Format	Print and electronic
Licensed Content Author	Harald Stueger, Georg Gescheidt, Michael Haas, et al	Portion	Figure/table
Licensed Content Date	Dec 18, 2017	Number of figures/tables	2
Licensed Content Volume	135	Will you be translating?	No
Licensed Content Issue	15		
Licensed Content Pages	7		

**About Your Work**  **Additional Data**

Title	Water Soluble, Low Migration and Visible Light Photoinitiators for Greener Photopolymerization	Portions	Scheme 1, Scheme 2
Institution name	Bogazici University		
Expected presentation date	Sep 2021		

Figure A.15. Permission from [220] John Wiley and Sons, Copyright (2017).